



University of Pennsylvania  
**ScholarlyCommons**

---

Publicly Accessible Penn Dissertations

---

2021

## Palladium-Catalyzed Deprotonative Cross-Coupling And Carbonylative Cross-Coupling Processes

Bowen Hu  
*University of Pennsylvania*

Follow this and additional works at: <https://repository.upenn.edu/edissertations>

 Part of the [Inorganic Chemistry Commons](#), and the [Organic Chemistry Commons](#)

---

### Recommended Citation

Hu, Bowen, "Palladium-Catalyzed Deprotonative Cross-Coupling And Carbonylative Cross-Coupling Processes" (2021). *Publicly Accessible Penn Dissertations*. 5330.  
<https://repository.upenn.edu/edissertations/5330>

This paper is posted at ScholarlyCommons. <https://repository.upenn.edu/edissertations/5330>  
For more information, please contact [repository@pobox.upenn.edu](mailto:repository@pobox.upenn.edu).

---

# Palladium-Catalyzed Deprotonative Cross-Coupling And Carbonylative Cross-Coupling Processes

## Abstract

Metal-catalyzed direct C–H bond activation arylation reactions of non- or weakly acidic C–H bonds have recently received much attention. Compared to traditional catalysts that activate C–H bonds, conventional deprotonative cross-coupling processes (DCCP) undergoes an in-situ C–H deprotonation and metalation of the substrate under catalytic cross-coupling conditions. DCCP reactions are generally directing-group-free methods employing simple starting materials under mild reaction conditions. This thesis describes mechanistic study of DCCP-type triarylation of benzylic methyl groups and introduces two novel methods of deprotonative carbonylation of weakly acidic benzylic C(sp<sup>3</sup>)–H bonds.

In Chapter 1, a comprehensive mechanistic study of our palladium-catalyzed deprotonative triarylation of heteroarylmethanes at the benzylic C-H bonds is reported. The reaction works with a variety of aryl halides, enabling the rapid synthesis of triaryl(heteroaryl)methanes. Mechanistic studies point to Pd(cataCXium A)<sub>2</sub> being the resting state of the catalyst and reductive elimination being the turnover-limiting step in the ultimate catalytic cycle.

In Chapter 2, a novel highly selective palladium-catalyzed deprotonative carbonylation of azaarylmethylamines with aryl bromides under 1 atm of CO gas has been achieved. The methods enable access to key components of numerous biologically active natural products and synthetic compounds. The key to success is the presence of a NIXANTPHOS-based palladium catalyst, which efficiently activates aryl bromides and facilitates the deprotonative cross-coupling process under CO.

Chapter 3 presents a novel, selective and high-yielding palladium-catalyzed carbonylative arylation of a variety of weakly acidic (pK<sub>a</sub> 25–35 in DMSO) benzylic and heterobenzylic C(sp<sup>3</sup>)–H bonds with aryl bromides. The Josiphos-based catalytic system, identified by high-throughput experimentation (HTE), solved the selectivity issue in deprotonative carbonylation reactions, providing ketone products without the formation of direct coupling byproducts. Additionally, (Josiphos)Pd(CO)<sub>2</sub> was identified as the catalyst resting state. A kinetic study suggests that the oxidative addition of aryl bromides is the turnover-limiting step. Key catalytic intermediates including (Josiphos)Pd(Ar)(Br) and (Josiphos)Pd(COAr)Br were also isolated.

## Degree Type

Dissertation

## Degree Name

Doctor of Philosophy (PhD)

## Graduate Group

Chemistry

## First Advisor

Patrick J. Walsh

## Second Advisor

Marisa C. Kozlowski

---

**Keywords**

carbonylation, cross-coupling, deprotonation, heterobenzylic, Palladium

**Subject Categories**

Inorganic Chemistry | Organic Chemistry

PALLADIUM-CATALYZED DEPROTONATIVE CROSS-COUPPLING AND CARBONYLATIVE  
CROSS-COUPPLING PROCESSES

Bowen Hu

A DISSERTATION

in

Chemistry

Presented to the Faculties of the University of Pennsylvania

in

Partial Fulfillment of the Requirements for the

Degree of Doctor of Philosophy

2021

Supervisor of Dissertation



Patrick J. Walsh  
Professor of Chemistry

Graduate Group Chairperson



Daniel J. Mindiola

Brush Family Professor of Chemistry

Dissertation Committee

Marisa C. Kozlowski      Professor of Chemistry

Karen I. Goldberg      Vagelos Professor of Energy Research

Neil C. Tomson      Assistant Professor of Chemistry

# ABSTRACT

## PALLADIUM-CATALYZED DEPROTONATIVE CROSS-COUPPLING AND CARBONYLATIVE CROSS-COUPPLING PROCESSES

Bowen Hu

Patrick J. Walsh

Metal-catalyzed direct C–H bond activation arylation reactions of non- or weakly acidic C–H bonds have recently received much attention. Compared to traditional catalysts that activate C–H bonds, conventional deprotonative cross-coupling processes (DCCP) undergoes an in-situ C–H deprotonation and metalation of the substrate under catalytic cross-coupling conditions. DCCP reactions are generally directing-group-free methods employing simple starting materials under mild reaction conditions. This thesis describes mechanistic study of DCCP-type triarylation of benzylic methyl groups and introduces two novel methods of deprotonative carbonylation of weakly acidic benzylic C(sp<sup>3</sup>)–H bonds.

In Chapter 1, a comprehensive mechanistic study of our palladium-catalyzed deprotonative triarylation of heteroarylmethanes at the benzylic C–H bonds is reported. The reaction works with a variety of aryl halides, enabling the rapid synthesis of triaryl(heteroaryl)methanes. Mechanistic studies point to Pd(cataCXium A)<sub>2</sub> being the resting state of the catalyst and reductive elimination being the turnover-limiting step in the ultimate catalytic cycle.

In Chapter 2, a novel highly selective palladium-catalyzed deprotonative carbonylation of azaarylmethylamines with aryl bromides under 1 atm of CO gas has been achieved. The methods enable access to key components of numerous biologically active natural products and synthetic compounds. The key to success is the presence of a NIXANTPHOS-based palladium catalyst, which efficiently activates aryl bromides and facilitates the deprotonative cross-coupling process under CO.

Chapter 3 presents a novel, selective and high-yielding palladium-catalyzed carbonylative arylation of a variety of weakly acidic ( $pK_a$  25–35 in DMSO) benzylic and heterobenzylic  $C(sp^3)-H$  bonds with aryl bromides. The Josiphos-based catalytic system, identified by high-throughput experimentation (HTE), solved the selectivity issue in deprotonative carbonylation reactions, providing ketone products without the formation of direct coupling byproducts. Additionally,  $(Josiphos)Pd(CO)_2$  was identified as the catalyst resting state. A kinetic study suggests that the oxidative addition of aryl bromides is the turnover-limiting step. Key catalytic intermediates including  $(Josiphos)Pd(Ar)(Br)$  and  $(Josiphos)Pd(COAr)Br$  were also isolated.

# TABLE OF CONTENTS

<b>ABSTRACT</b> .....	<b>II</b>
<b>LIST OF TABLES</b> .....	<b>VI</b>
<b>LIST OF ILLUSTRATIONS</b> .....	<b>VII</b>
<b>CHAPTER 1 MECHANISTIC STUDY OF DCCP (DEPROTONATIVE CROSS COUPLING PROCESS) REACTIONS</b> .....	<b>1</b>
<b>1.1 Introduction</b> .....	<b>1</b>
<b>1.2 Results and Discussion</b> .....	<b>4</b>
<b>1.3 Conclusions</b> .....	<b>14</b>
<b>1.4 References</b> .....	<b>15</b>
<b>1.5 Supporting Information</b> .....	<b>18</b>
1.5.1 Reaction study of 2-methylbenzothiazole 1a with chlorobenzene 5a .....	18
1.5.2 Resting state studies .....	22
1.5.3 Reaction of CH(ArHetero)Ph <sub>2</sub> (3a) with chlorobenzene (5a) and NaOt-Bu using Pd(cataCXium A) <sub>2</sub> .....	23
1.5.4 Deuteration reactions .....	26
1.5.5 Impact of the concentration of bases on the reaction time course .....	28
1.5.6 Transmetallation reaction of 7a with 3a .....	30
<b>CHAPTER 2 PALLADIUM-CATALYZED BENZYLIC C(SP<sup>3</sup>)-H CARBOXYLATIVE ARYLATION OF AZAARYLMETHYL AMINES WITH ARYL BROMIDES</b> .....	<b>33</b>
<b>2.1 Introduction</b> .....	<b>33</b>
<b>2.2 Results and Discussion</b> .....	<b>37</b>
<b>2.3 Conclusions</b> .....	<b>46</b>
<b>2.4 References</b> .....	<b>46</b>
<b>2.5 Supporting Information</b> .....	<b>54</b>
2.5.1 General information .....	54
2.5.2 Optimization of the reaction conditions .....	54
2.5.3. General Procedure for DCCC of Azaarylmethyl Amines .....	59

2.5.4 The general procedure for synthetic applications.....	61
2.5.5 Mechanistic studies.....	66
2.5.6 Characterization data for products.....	70
<b>CHAPTER 3 PALLADIUM-CATALYZED BENZYLIC C(SP<sup>3</sup>)-H CARBOXYLATIVE ARYLATION WITH ARYL BROMIDES .....</b>	<b>80</b>
<b>3.1 Introduction .....</b>	<b>80</b>
<b>3.2 Results and Discussion .....</b>	<b>83</b>
3.2.1 Optimization of DCCC with 4-benzylpyridine and Aryl Bromide 2a.....	84
3.2.2 Scope of the carbonylative arylation reaction .....	87
3.2.3 Mechanistic Studies .....	93
3.2.4 Identification of the Catalyst Resting State .....	97
3.2.5 Study of the turnover-limiting step .....	99
3.2.6 Study of key intermediates.....	100
<b>3.3 CONCLUSIONS .....</b>	<b>103</b>
<b>3.4 REFERENCES .....</b>	<b>104</b>
<b>3.5 Experimental.....</b>	<b>108</b>
3.5.1 General Methods.....	108
3.5.2 Representative Microscale High-throughput Experimentation .....	108
3.5.3 Optimization of the Reaction Conditions.....	112
3.5.4 General Procedure for Benzylic Carbonylative Arylation .....	113
3.5.5 Characterization data for $\alpha$ -Aryl ketones .....	115
3.5.6 Mechanistic Study.....	127
<b>APPENDIX A. NMR SPECTRA FOR CHAPTER 2.....</b>	<b>134</b>
<b>APPENDIX B NMR SPECTRA, IR SPECTRA AND X-RAY CRYSTALLOGRAPHIC DATA FOR CHAPTER 3.....</b>	<b>176</b>
<b>NMR SPECTRA.....</b>	<b>176</b>
<b>IR SPECTRUM.....</b>	<b>223</b>
<b>X-RAY CRYSTALLOGRAPHIC DATA .....</b>	<b>223</b>



## LIST OF TABLES

<b>Table 1-S1</b> <sup>1</sup> H NMR monitoring of the reaction of <b>1a</b> with <b>5a</b> (5.0 equiv) at 130°C run 1 .....	19
<b>Table 1-S2</b> <sup>1</sup> H NMR monitoring of the reaction of <b>1a</b> with <b>5a</b> (5.0 equiv) at 130°C run 2 .....	20
<b>Table 1-S3</b> <sup>1</sup> H NMR monitoring of the reaction of <b>3a</b> with different amount of <b>5a</b> using Pd(cataCXium A) <sub>2</sub> at 130°C .....	25
<b>Table 1-S4</b> <sup>1</sup> H NMR monitoring of the reaction of <b>3a</b> or <b>3a-d<sub>1</sub></b> with <b>5a</b> at 130°C .....	27
<b>Table 1-S5</b> <sup>1</sup> H NMR monitoring of the reaction of <b>3a</b> and <b>5a</b> with different amounts of base at 130°C .....	29
<b>Table 2-1.</b> Optimization of reaction conditions for benzylic C–H carbonylative arylation of <b>1a</b> with <b>2a</b> .....	38
<b>Table 2-2.</b> Pd-catalyzed benzylic C–H carbonylative arylation of azaarylmethylamimes <b>1</b> with <b>2a</b> . <sup>a,b</sup> .....	40
<b>Table 2-3.</b> Pd-catalyzed benzylic C–H carbonylative arylation of <b>1a</b> with aryl bromides. <sup>a,b</sup> .....	42
<b>Table 2-S1.</b> Base and solvent screening .....	54
<b>Table 2-S2.</b> Optimization of reaction conditions. <sup>a</sup> .....	56
<b>Table 2-S3.</b> Non effective substrates in the reaction conditions. <sup>a</sup> .....	58
<b>Table 3-1.</b> Examination of different members of the Josiphos family of ligands. <sup>a</sup> .....	85
<b>Table 3-2.</b> Optimization of DCCC with 4-benzylpyridine and Aryl Bromide <b>2a</b> .....	86
<b>Table 3-3.</b> Scope of Aryl Bromides in Pd-Catalyzed Carbonylative Arylation. <sup>a,b</sup> .....	88
<b>Table 3-4.</b> Scope of Pro-nucleophiles in Pd-Catalyzed Carbonylative Arylation. <sup>a,b</sup> .....	91
<b>Table 1-S3.</b> Ligands examined: used in a 4:1 ratio relative to Pd for monodentate ligands and 2:1 ratio for bidentate ligands. ....	110
<b>Table 2-S3.</b> Pd sources examined: Pd(dba) <sub>2</sub> , Pd(OAc) <sub>2</sub> , Pd <sub>2</sub> (dba) <sub>3</sub> and Pd G4 dimer (5 mol % of Pd) were screened with 24 sterically and electronically diverse, mono- and bidentate phosphine (from the Table above) .....	111

## LIST OF ILLUSTRATIONS

<b>Scheme 1-1.</b> Transition metal catalyzed approaches to tetraarylmethanes. ....	2
<b>Scheme 1-2.</b> Palladium catalyzed tandem triarylation reaction of heteroaryl methyl groups to generate tetraarylmethane derivatives.....	4
<b>Scheme 1-3.</b> Conversion data for the reaction of 2-methylbenzothiazole ( <b>1a</b> ) with chlorobenzene ( <b>5a</b> , 5.0 equiv) and NaOt-Bu (5.0 equiv) at 130 °C. Curves are a guide for the eye.....	6
<b>Scheme 1-4.</b> Resting state studies for the reaction of CH(ArHetero)Ph <sub>2</sub> ( <b>3a</b> ) with chlorobenzene ( <b>5a</b> , 5.0 equiv) and NaOt-Bu (2.0 equiv) in <i>o</i> -xylene-d <sub>10</sub> at 130 °C. ....	8
<b>Scheme 1-5.</b> Reaction of CH(Ar <sub>Hetero</sub> )Ph <sub>2</sub> ( <b>3a</b> ) with chlorobenzene ( <b>5a</b> , 5.0 equiv) and NaOt-Bu (2.0 equiv) using Pd(cataCXium A) <sub>2</sub> at 130 °C.....	8
<b>Scheme 1-6.</b> Reaction of CH(ArHetero)Ph <sub>2</sub> ( <b>3a</b> ) with chlorobenzene ( <b>5a</b> , 2.0, 4.0, 6.0, 8.0 or 10.0 equiv) and NaOt-Bu (2.0 equiv) using Pd(cataCXium A) <sub>2</sub> at 130 °C. ....	8
<b>Figure 1-1.</b> Initial rate constant calculated using 2.0–10.0 equiv. chlorobenzene after 3 min at 130 °C. ....	9
<b>Scheme 1-7.</b> Oxidative addition pathways and rate laws proposed by Hartwig <sup>16</sup> .....	10
<b>Scheme 1-8.</b> Comparison of reaction time course of <b>3a</b> (average of 3 runs) and <b>3a-d<sub>1</sub></b> . Curves are a guide for the eye.....	11
<b>Scheme 1-9.</b> Transmetalation reaction of <b>7a</b> with <b>3a</b> .....	13
<b>Scheme 1-10.</b> Proposed catalytic cycle from triarylmethane to tetraarylmethane .....	14
<b>Scheme 1-S1.</b> Conversion data for the reaction of 2-methylbenzothiazole ( <b>1a</b> ) with chlorobenzene ( <b>5a</b> , 5.0 equiv).....	19
<b>Scheme 1-S2.</b> Resting state studies for the reaction of CH(ArHetero)Ph <sub>2</sub> ( <b>3a</b> ) with chlorobenzene ( <b>5a</b> , 5.0 equiv) and NaOt-Bu (2.0 equiv) in <i>o</i> -xylene-d <sub>10</sub> at 130 °C. ....	22
<b>Figure 1-S1</b> <sup>31</sup> P{ <sup>1</sup> H} NMR spectra of the catalyst resting state study. ....	23
<b>Scheme 1-S3.</b> Reaction of CH(Ar <sub>Hetero</sub> )Ph <sub>2</sub> ( <b>3a</b> ) with chlorobenzene ( <b>5a</b> , 5.0 equiv) and NaOt-Bu (2.0 equiv) using Pd(cataCXium A) <sub>2</sub> at 130 °C.....	24
<b>Scheme 1-S3.</b> Reaction of CH(Ar <sub>Hetero</sub> )Ph <sub>2</sub> ( <b>3a</b> ) with chlorobenzene ( <b>5a</b> , 2.0, 4.0, 6.0, 8.0 or 10.0 equiv) and NaOt-Bu (2.0 equiv) using Pd(cataCXium A) <sub>2</sub> at 130 °C. ....	25
<b>Scheme 1-S4.</b> Deprotonation and Deuteration of <b>3a</b> .....	26
<b>Scheme 1-S5.</b> Comparison of reaction time course of <b>3a</b> (average of 3 runs) and <b>3a-d<sub>1</sub></b> .....	27

<b>Chart 1-S1.</b> Conversion data for the reaction of CH(ArHetero)Ph <sub>2</sub> ( <b>3a</b> ) with chlorobenzene ( <b>5a</b> , 2.0 equiv) and NaO <i>t</i> -Bu (1.5, 2.0, 2.5 and 3.0 equiv) at 130 °C. Curves are a guide for the eye. .	30
<b>Scheme 1-6.</b> Transmetallation reaction of <b>7a</b> with <b>3a</b> .....	31
<b>Figure 1-S2</b> <sup>31</sup> P{ <sup>1</sup> H} NMR spectra of transmetallation reaction of <b>7a</b> with <b>3a</b> .....	32
<b>Figure 2-1.</b> Selected pharmacologically active compounds containing α-amino aryl ketones .....	34
<b>Scheme 2-1.</b> Carbene-based approach of Wang and co-workers. ....	35
<b>Scheme 2-2.</b> Deprotonative carbonylative cross-coupling reactions.....	36
<b>Scheme 2-3.</b> Detection of product precursor.....	43
<b>Scheme 2-4.</b> Synthetic Applications.....	45
<b>Scheme 2-5.</b> Plausible Mechanism.....	46
<b>Figure 2-S1:</b> <sup>1</sup> H NMR comparison of standard carbonylation product before aqueous workup, deprotonated <b>3aa</b> , and product <b>3aa</b> in d <sub>8</sub> -THF. These spectra support the contention that the product formed in the carbonylation reaction before workup is the enolate.....	68
<b>Figure 2-S2:</b> <sup>13</sup> C{ <sup>1</sup> H} NMR comparison of standard carbonylation product before aqueous workup, deprotonated <b>3aa</b> , and product <b>3aa</b> in d <sub>8</sub> -THF. These spectra support the contention that the product formed in the carbonylation reaction before workup is the enolate.....	69
<b>Scheme 3-1.</b> Deprotonative carbonylative cross-coupling reactions.....	81
<b>Figure 3-1.</b> Selected pharmacologically active compounds containing α-aryl ketones .....	83
<b>Scheme 3-2.</b> HTE Screen of Pd-Catalyzed Deprotonative Carbonylative Cross-coupling of 4-Benzylpyridine.....	84
<b>Scheme 3-3.</b> Gram-scale synthesis examples .....	93
<b>Scheme 3-4.</b> Synthesis of (Josiphos)Pd(C <sub>2</sub> H <sub>4</sub> ) complex <b>4<sup>a</sup></b> .....	93
<b>Figure 3-2.</b> Crystal structure of <b>4</b> with selected bond lengths (Å): P1–Pd1 = 2.2828(12), P2–Pd1 = 2.3110(12), Pd1–C1 = 2.132(6), Pd1–C2 = 2.133(5), C1–C2 = 1.396(10). Selected bond angles (deg °): P1–Pd1–P2 = 97.52(4), C1–Pd1–P1 = 111.6(2), C2–Pd1–P2 = 112.79(18), C1–Pd1–C2 = 38.2(3).....	94
<b>Scheme 3-5.</b> Synthesis of (Josiphos)Pd(CO) <sub>2</sub> complex <b>5<sup>a</sup></b> .....	95
<b>Figure 3-3.</b> Crystal structure of <b>5</b> with selected bond lengths (Å): P1–Pd1 = 2.3931(17), P2–Pd1 = 2.3735(18), Pd1–C1 = 1.982(8), Pd1–C2 = 1.957(7), C1–O1 = 1.124 (9), C2–O2 = 1.134(9). Selected bond angles (deg °): P1–Pd1–P2 = 93.29(6), C1–Pd1–P1 = 112.3(2), C2–Pd1–P2 = 115.3(2), C1–Pd1–C2 = 117.4(3).....	97
<b>Scheme 3-6.</b> Identification of catalyst resting state. <sup>a</sup> .....	98
<b>Figure 3-4.</b> (a). Room-temperature <sup>31</sup> P{ <sup>1</sup> H} NMR spectra of a catalytic reaction at partial conversion conducted at 80 °C. (b) <sup>31</sup> P{ <sup>1</sup> H} NMR spectra of <b>5</b> . .....	98

<b>Scheme 3-7.</b> Determination of the rate Constants $k_{\text{obs}}$ from the initial rate study. ....	99
<b>Figure 3-5.</b> (a) Dependence of the observed rate constant ( $k_{\text{obs}}$ ) on the concentration of ArBr (0.1–0.8 M) with <b>4</b> as the pre-catalyst, pCO = 1 atm and <b>1a</b> = 0.1 M at 80 °C within 2.5 h, and (b) Time course study of the reaction with <b>4</b> as the pre-catalyst at various pressures of CO (1–4 atm) with <b>2a</b> = 0.15 M, <b>1a</b> = 0.1 M. ....	100
<b>Scheme 3-8.</b> Synthesis of (Josiphos)Pd(Ar)Br Complexes. ....	101
<b>Figure 3-6.</b> Crystal structure of <b>6m'</b> with selected bond lengths (Å): P1–Pd1 = 2.3792(10), P2–Pd1 = 2.2508(10), Pd1–C1 = 2.045(4), Pd1–Br = 2.4792(5). Selected bond angles (deg °): P1–Pd1–P2 = 95.38(3), P1–Pd1–Br = 85.76(3), P2–Pd1–C1 = 84.60(11), C1–Pd1–Br = 84.28(11). ....	102
<b>Scheme 3-9.</b> Proposed mechanism for palladium-catalyzed carbonylative arylation of weakly acid C–H bonds. ....	103
<b>Scheme 1-S3.</b> Ligand screening for carbonylative arylation of <b>1a</b> with <b>2a</b> . ....	110
<b>Chart 1-S3.</b> Reactivity of different ligands and Pd sources. ....	111
<b>Chart 2-S3.</b> Selectivity of different ligands and Pd sources. ....	112
<b>(b) Scheme 2-S3.</b> Gram-scale synthesis. ....	114
<b>Scheme S3.</b> Preliminary reactions were performed to determine the reaction time of initial rate study. ....	130
<b>Chart 3-S3.</b> Reaction time course study results. ....	130
<b>Scheme 4-S3.</b> Dependence of the observed rate constant ( $k_{\text{obs}}$ ) on the concentration ArBr (0.1–0.8 M) with <b>4</b> as the pre-catalyst, pCO = 1 atm and <b>1a</b> = 0.1 M at 80 °C within 2.5 h. ....	131
<b>Chart 4-S3.</b> Reaction rates at different <b>2a</b> concentrations. ....	132
<b>Chart 5-S3.</b> Dependence of the observed rate constant ( $k_{\text{obs}}$ ) on the concentration ArBr. ....	133

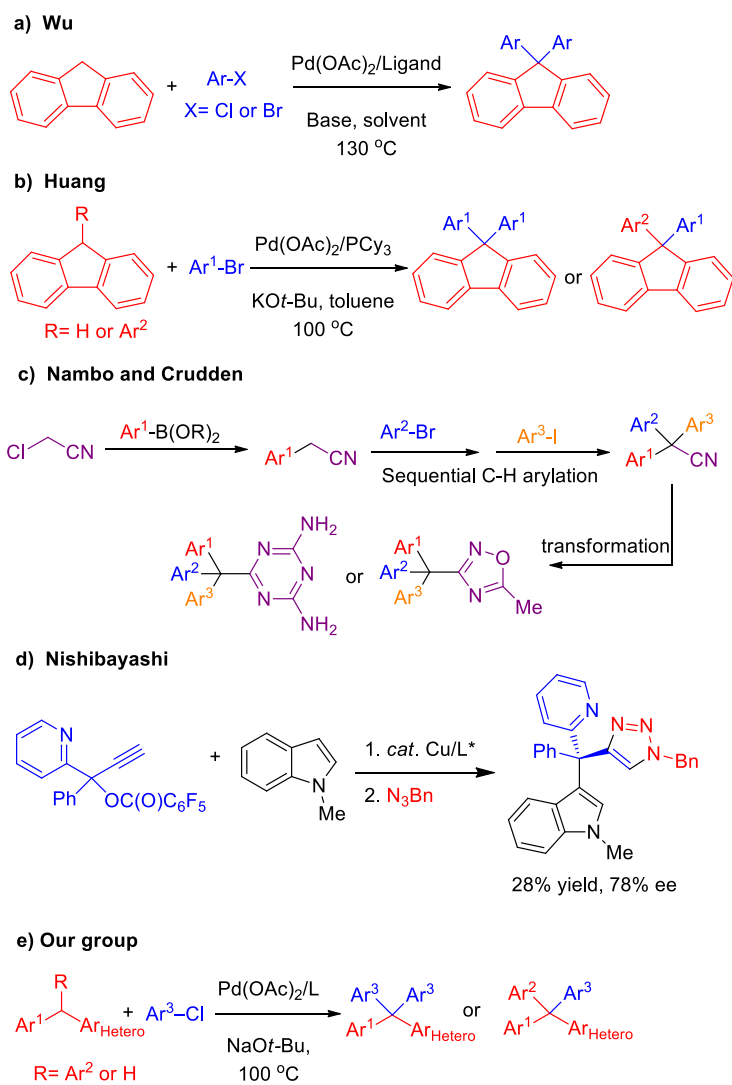
# CHAPTER 1 Mechanistic Study of DCCP (Deprotonative Cross Coupling Process) Reactions

## 1.1 Introduction

Tetraarylmethanes, and related derivatives, are ubiquitous building blocks and exhibit a wide range of applications.<sup>1</sup> Their synthesis, therefore, has attracted much attention. It is surprising, however, that transition metal-catalyzed C–H functionalization reactions, which are among the most versatile methods in organic synthesis, have witnessed only limited success in the synthesis of tetraarylmethanes.<sup>2</sup> We are aware of only a few relevant examples: Wu and Huang (Scheme 1-1, a and b) independently reported palladium-catalyzed arylations of fluorene and monoarylfluorene derivatives with aryl bromides for the synthesis of diarylfluorenes.<sup>3</sup> Nambo and Crudden outlined a sequential palladium-catalyzed arylation to generate triarylacetonitrile products. The triarylacetonitriles were subsequently transformed into triaryl(heteroaryl)methanes (Scheme 1-1, c).<sup>4</sup> Nishibayashi presented a copper-catalyzed enantioselective propargylation of indoles with propargylic esters to construct all carbon quaternary stereocenters bearing an alkyne. Subsequent derivatization of the terminal alkyne with phenylazide generated enantioenriched all carbon substituted tetraarylmethanes with 28% yield and 78% ee (Scheme 1-1, d).<sup>5</sup> Recently, Sun and his coworkers reported an organocatalysis method to construct enantioenriched tetraarylmethanes.<sup>6</sup>

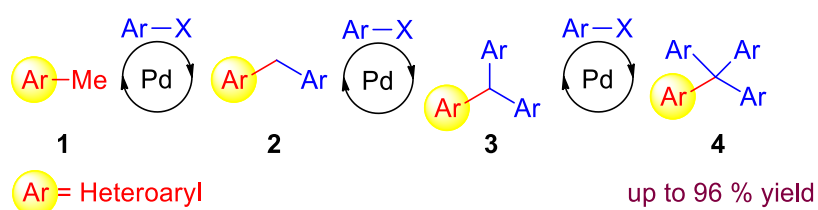
Our research group has been interested in the catalytic functionalization of weakly acidic  $sp^3$ -hybridized C–H bonds through deprotonative cross-coupling processes (DCCP),<sup>7</sup> which are mechanistically similar to carbonyl  $\alpha$ -arylation reactions.<sup>8</sup> DCCP involve

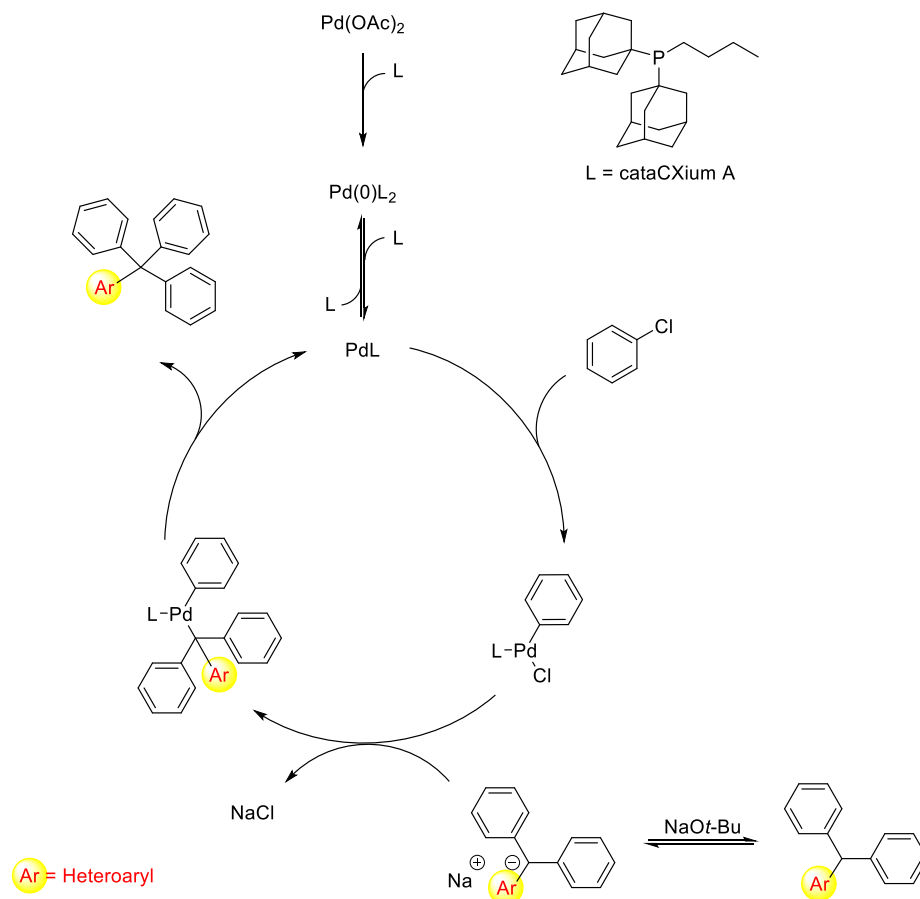
weakly acidic substrates ( $pK_a > 25$ ) that are reversibly deprotonated in the presence of the transition metal catalyst and subsequently functionalized. Based on this approach, we developed a palladium-catalyzed DCCP for direct arylation of aryl(heteroaryl)methanes and diaryl(heteroaryl)methanes with aryl chlorides using palladium catalysts based on tricyclohexyl phosphine (PCy<sub>3</sub>) or cataCXium A (Ad<sub>2</sub>P-*n*-Bu, Ad = adamantyl)<sup>9</sup> to construct triaryl(heteroaryl)methanes in good to excellent yields (Scheme 1-1, e).<sup>10</sup>



**Scheme 1-1.** Transition metal catalyzed approaches to tetraarylmethanes.

General methods for the direct arylation of benzylic methyl groups to construct tetraarylmethanes have not been developed to our knowledge, although the diarylation of benzylic methyl groups to form triarylmethanes has been reported.<sup>2e, 11</sup> Based on our prior studies,<sup>10</sup> we hypothesized that DCCP of benzylic methyl groups in the presence of a palladium catalyst should provide tetraarylmethanes via a tandem triarylation process. The success of this process depends on identifying a catalyst that is able to perform arylations on 3 distinct coupling partners, as shown in Scheme 1-2. With the help of the great work from my coworker Dr. Shuangung Zhang, we developed a novel palladium catalyzed triarylation of heteroaryl methyl groups for the efficient synthesis of tetraarylmethane derivatives (Scheme 1-2). We propose the catalytic cycle of the last arylation step in Scheme 1-2, but several key aspects of the mechanism of the reaction remained unclear. To determine the details of the mechanism of the method, including the resting state of the catalyst and the rate-limiting step, and provide insights for future reaction development, I conducted preliminary mechanistic studies on the tandem sequence.





**Scheme 1-2.** Palladium catalyzed tandem triarylation reaction of heteroaryl methyl groups to generate tetraarylmethane derivatives.

## 1.2 Results and Discussion

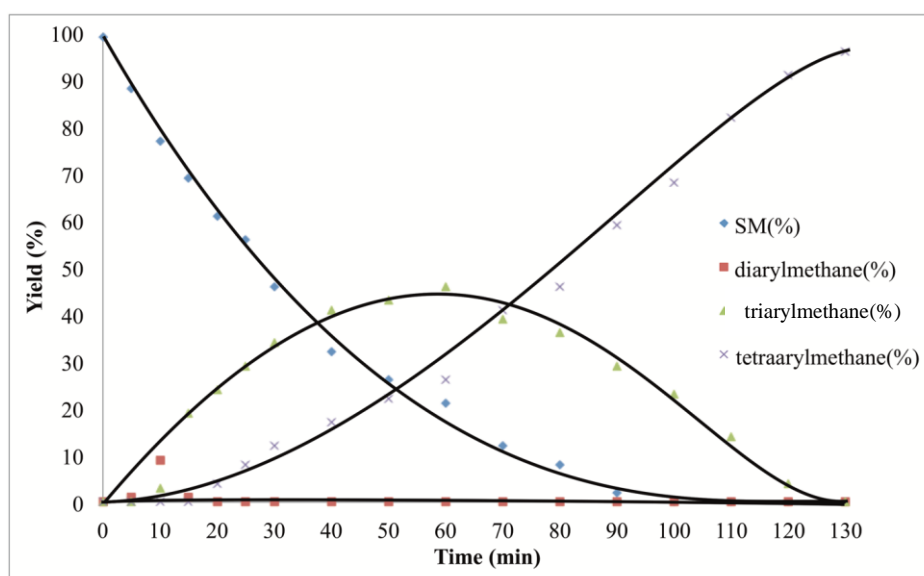
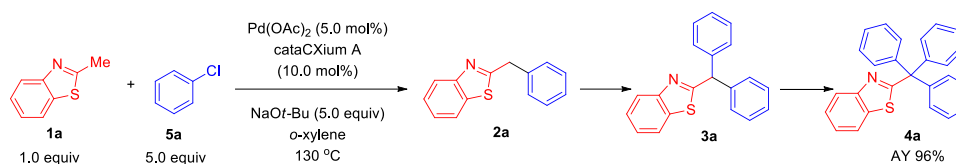
The tandem triarylation process provides us with an opportunity to study the relative reactivity of the arylation of heteroarylmethane derivatives. The catalytic cycles (Scheme 1-2) begin with oxidative addition of the aryl chloride. In general, oxidative addition of aryl chlorides is facile with bulky monodentate phosphine ligands.<sup>15</sup> Hartwig and coworkers<sup>12</sup> have shown that oxidative addition of aryl chlorides to palladium(0) complexes of AdP(*t*-Bu)<sub>2</sub> and CyP(*t*-Bu)<sub>2</sub> proceeds via PdL<sub>1</sub> intermediates. The next step in the catalytic cycle in Scheme 1-2 involve deprotonation of the substrate and transmetalation of the resulting carbanion. The efficiency of the deprotonation



steps depends on both the acidity of the arylmethane substrates and their steric hinderance. Each aryl addition to the heteroarylmethanes (**1**) increases the acidity of the remaining benzylic C–H bonds (by as much as 10 p*K* units).<sup>17</sup> The increase in acidity of the triarylmethane, Ar<sub>Hetero</sub>CHAR<sub>2</sub>, however, will be much less. Deprotonation of Ar<sub>Hetero</sub>CHAR<sub>2</sub> forms a carbanion in which the aryl rings are unable to simultaneously be coplanar with the carbanion, resulting in less stabilization. At the same time, increasing the number of aryl groups on the heteroaryl methane is expected to render deprotonation slower with bulky *tert*-butoxide bases. Likewise, transmetallation of the bulky triarylmethylcarbanion may be slow due to steric clashing with the (cataCXium A)Pd(II)-based catalyst.

To probe the relative reactivity in the tandem arylation, we first studied the reaction of 2-methylbenzothiazole **1a** with chlorobenzene **5a** (5.0 equiv) in the presence of NaO*t*-Bu (5.0 equiv) (Scheme 1-3). This substrate combination was particularly useful, because the relative concentrations of the 2-methylbenzothiazole **1a**, arylated intermediates and tetraarylmethane are all easily determined by <sup>1</sup>H NMR spectrometry. Due to difficulty with in situ NMR monitoring, conversion data was obtained by using stock solutions to set up a series of identical reactions in sealed vials and heating all the vials to 130 °C. One vial was quenched every 5 min for the first 30 min and one every 10 min after that. Samples were quenched (see Experimental **1.5.1** for details) and <sup>1</sup>H NMR spectra of the unpurified mixtures were acquired with integration of 2-methylbenzothiazole **1a**, mono-, di, and triarylated material against an internal standard. The data for the tandem reaction is plotted in Scheme 4. The starting 2-methylbenzothiazole (**1a**) is nearly consumed within 90 min. The monoarylation product, 2-benzylbenzothiazole (**2a**), is consumed nearly as fast as it is produced—its concentration never exceeds a few percent over the course of the tandem reaction. This observation is consistent with the greater acidity of 2-benzylbenzothiazole **2a** (p*K*<sub>a</sub> = 27.6 in DMSO at 25 °C).<sup>17</sup> Presumably transmetallation of the intermediate organosodium, NaCH(Ar<sub>Hetero</sub>)Ph, is facile under these conditions. The

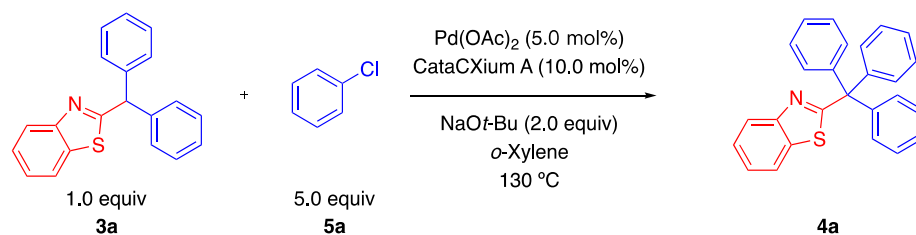
concentration of triarylmethane **3a** builds up with a maximum between 50 and 70 min and is converted to tetraarylmethane **4a** in a similar timeframe. The concentration of tetraarylmethane product increased over the time course of the tandem reaction, reaching 96% AY after 130 min (93% isolated yield).



**Scheme 1-3.** Conversion data for the reaction of 2-methylbenzothiazole (**1a**) with chlorobenzene (**5a**, 5.0 equiv) and NaOt-Bu (5.0 equiv) at 130 °C. Curves are a guide for the eye.

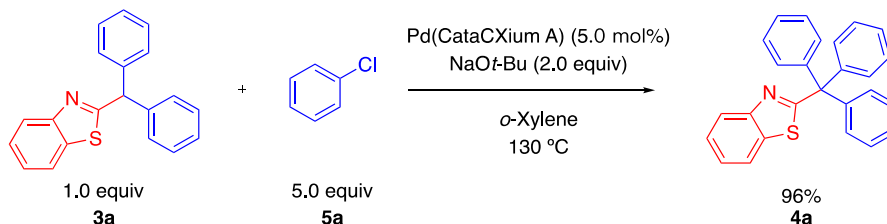
As triarylmethane **3a** builds up, and almost no diarylmethane **2a** is observed during the reaction, the slowest transformation in the tandem reaction is likely the formation of tetraarylmethane **4a** from triarylmethane **3a**. We, therefore, decided to further explore the arylation of **3a** leading to **4a** (Scheme 1-4). To begin the study, we determined the resting state of the catalyst by monitoring the arylation of **3a** with chlorobenzene (5.0 equiv) and

NaOt-Bu (2.0 equiv) at 130 °C in *o*-xylene-*d*<sub>10</sub>. A series of identical reactions were heated, and one vial was removed from the 130 °C bath and cooled to room temperature every 5 min for a total of 25 min. The resulting unpurified reaction mixtures were transferred to NMR tubes in a dry box, sealed and analyzed by <sup>31</sup>P{<sup>1</sup>H} NMR. In samples analyzed at intermediate conversions the <sup>31</sup>P{<sup>1</sup>H} NMR spectra exhibited resonances for three species at 53.1, 49.4 and 24.2 ppm, with peak area ratios of approximately 1.7 : 0.6 : 1.0. Based on Beller's report,<sup>18</sup> and confirmed by our own independent synthesis, we assigned the resonance at 53.1 ppm to the bis-ligand adduct Pd(cataCXium A)<sub>2</sub>. The peak at 24.2 ppm was determined to be free cataCXium A. It is noteworthy that when the reaction reached completion after 25 min at 130 °C, the singlet at 49.4 ppm disappeared from the <sup>31</sup>P{<sup>1</sup>H} NMR spectrum and only Pd(cataCXium A)<sub>2</sub> and free cataCXium A remained (ratio of approximately 2.2 : 1.0). We initially suspected that the peak at 49.4 ppm could be the product of either oxidative addition, (cataCXium A)Pd(Ph)Cl, or of transmetalation, (cataCXium A)Pd(Ph)[C(Ar<sub>Hetero</sub>)Ph<sub>2</sub>]. Based on the integrals, the average ratio of Pd(cataCXium A)<sub>2</sub> to the species at 49.4 ppm (which is assumed to have only one phosphine bound to Pd) was approximately 1.5 : 1.0. Thus, the majority of the phosphine-ligated palladium is found in Pd(cataCXium A)<sub>2</sub>, which is, therefore, the resting state of the catalyst.

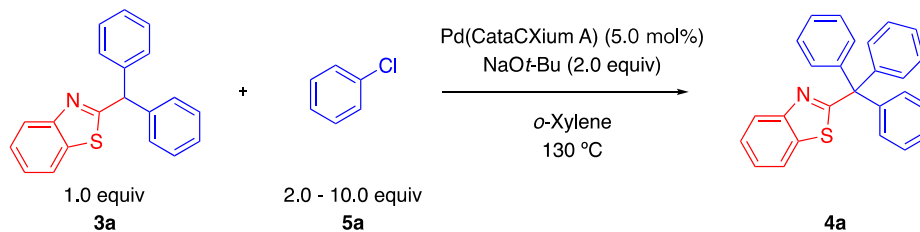


**Scheme 1-4.** Resting state studies for the reaction of  $\text{CH}(\text{ArHetero})\text{Ph}_2$  (**3a**) with chlorobenzene (**5a**, 5.0 equiv) and  $\text{NaOt-Bu}$  (2.0 equiv) in *o*-xylene- $\text{d}_{10}$  at 130 °C.

The resting state species  $\text{Pd}(\text{cataCXium A})_2$  was next synthesized and used for the kinetic study of the oxidative addition step. As expected,  $\text{Pd}(\text{cataCXium A})_2$  was found to be catalytically active under the same conditions (Scheme 1-5). To determine the rate dependency on chlorobenzene, we conducted initial rate studies by varying its concentration (Scheme 1-6). The initial rate constants ( $k_{\text{obs}}$ ) for the formation of tetraarylmethane **4a** at various concentrations of PhCl (2.0, 4.0, 6.0, 8.0, and 10 equiv relative to **3a**) are shown in Figure 1. The initial rates were found to be independent of the concentration of PhCl, suggesting that the oxidative addition step is not turnover limiting.



**Scheme 1-5.** Reaction of  $\text{CH}(\text{ArHetero})\text{Ph}_2$  (**3a**) with chlorobenzene (**5a**, 5.0 equiv) and  $\text{NaOt-Bu}$  (2.0 equiv) using  $\text{Pd}(\text{cataCXium A})_2$  at 130 °C.



**Scheme 1-6.** Reaction of  $\text{CH}(\text{ArHetero})\text{Ph}_2$  (**3a**) with chlorobenzene (**5a**, 2.0, 4.0, 6.0, 8.0 or 10.0 equiv) and  $\text{NaOt-Bu}$  (2.0 equiv) using  $\text{Pd}(\text{cataCXium A})_2$  at 130 °C.

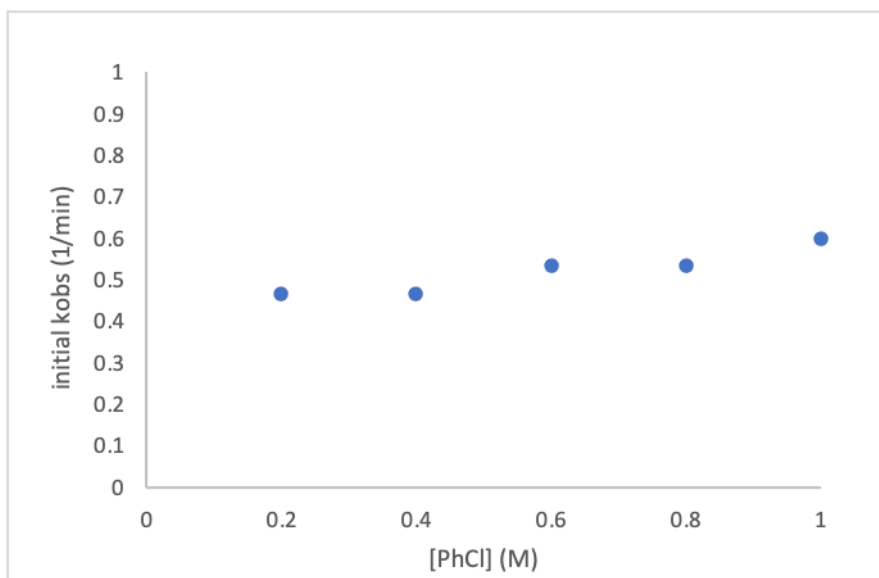
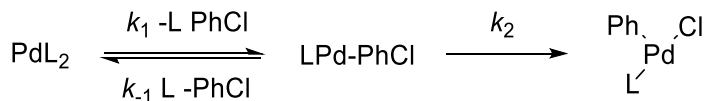


**Figure 1-1.** Initial rate constant calculated using 2.0–10.0 equiv chlorobenzene after 3 min at 130 °C.

Hartwig and coworkers have studied the mechanisms of oxidative addition of aryl halides to PdL<sub>2</sub> complexes with bulky monodentate phosphine ligands.<sup>16</sup> They introduced two possible oxidative addition pathways for chlorobenzene: the associative displacement of the phosphine ligand from PdL<sub>2</sub> followed by oxidative addition (Pathway A, Scheme 1-7), and initial dissociation of a phosphine ligand followed by oxidative addition of the haloarenes (Pathway B, Scheme 1-7).

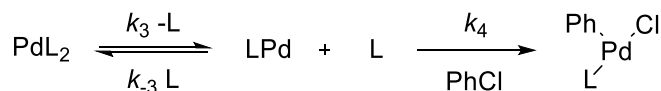
Pathway A



$$\text{if } k_2 \gg k_{-1}[\text{L}] \quad k_{\text{obs}} = k_1[\text{PhCl}]$$

$$\text{if } k_2 \ll k_{-1}[\text{L}] \quad k_{\text{obs}} = k_1 k_2 [\text{PhCl}] / k_{-1}[\text{L}]$$

Pathway B



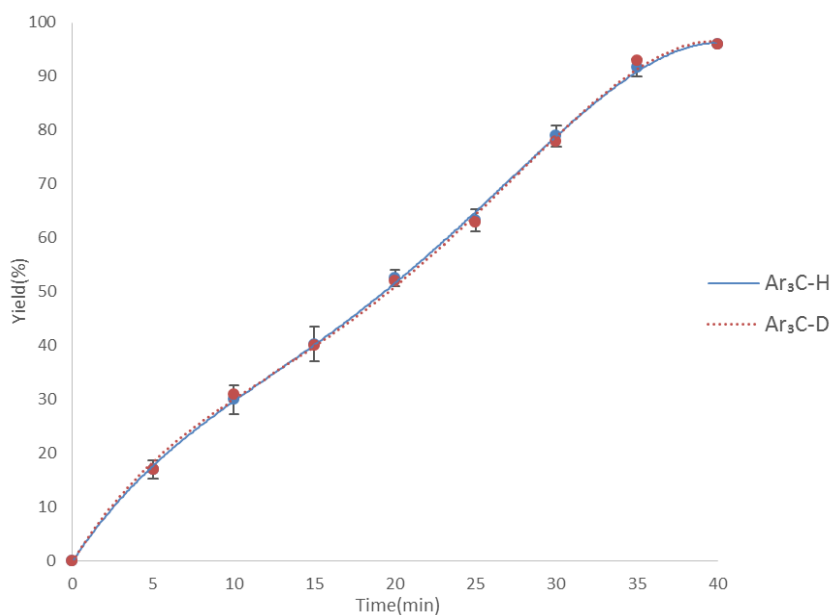
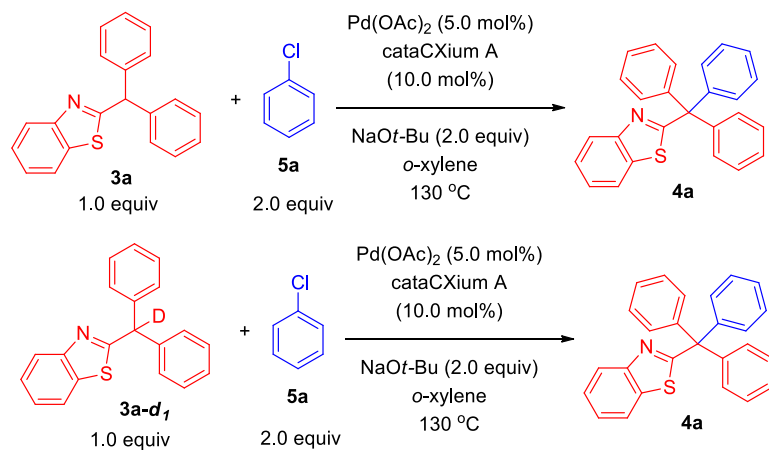
$$\text{if } k_4[\text{PhCl}] \gg k_{-3}[\text{L}] \quad k_{\text{obs}} = k_3$$

$$\text{if } k_4[\text{PhCl}] \ll k_{-3}[\text{L}] \quad k_{\text{obs}} = k_3 k_4 [\text{PhCl}] / k_{-3}[\text{L}]$$

**Scheme 1-7.** Oxidative addition pathways and rate laws proposed by Hartwig<sup>16</sup>

In pathway A, the rate law suggests that  $k_{\text{obs}}$  of the reaction has a positive relationship with the concentration of chlorobenzene. Thus, pathway A can be excluded based on the data in Figure 1. In Pathway B, when  $k_4[\text{PhCl}] \ll k_{-3}[\text{L}]$ , the observed rate constant is proportional to  $[\text{PhCl}]$  too, then it can also be excluded. In the scenario that  $k_4[\text{PhCl}] \gg k_{-3}[\text{L}]$ ,  $k_{\text{obs}}$  can be simplified to  $k_3$  (Scheme 1-7), which is consistent with the initial rate being independent of chlorobenzene concentration.

The next step we probed in the reaction mechanism was deprotonation. There are numerous catalytic arylation processes that convert diarylmethanes to triarylmethanes, but very few report arylation of the triarylmethane products to form tetraarylmethanes<sup>2e</sup>. Based on this observation, it seemed likely that the deprotonation of the triarylmethane or transmetalation of the resulting anion might be difficult. To probe the deprotonation step, we prepared the monodeuterated triarylmethane derivative  $\text{CD}(\text{Ar}_{\text{Hetero}})\text{Ph}_2$  (**3a-d<sub>1</sub>**, 99% based on <sup>1</sup>H NMR analysis). We rationalized that if deprotonation of the triarylmethane was rate determining, the reaction with **3a-d<sub>1</sub>** would exhibit an isotope effect relative to reaction of **3a** (Scheme 1-8). The kinetic data of the arylation of **3a-d<sub>1</sub>** and **3a** with chlorobenzene are compared in Scheme 1-8, which clearly indicate there is no kinetic isotope effect. Furthermore, variation of the equivalents of base from 1.5 to 3.0 had a negligible impact on reaction rate (see Experimental **1.5.4** for details). From these observations, the deprotonation of the triarylmethane substrate is not turnover limiting.

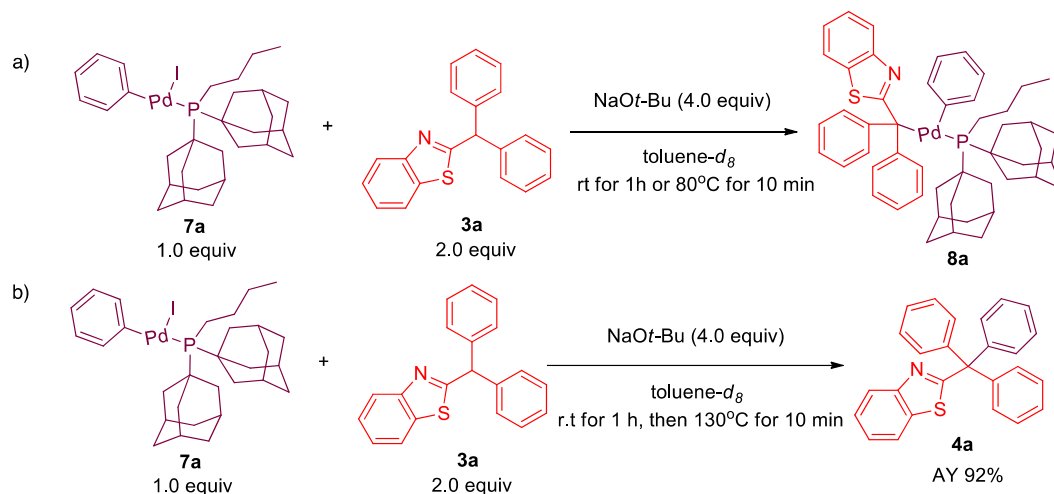


**Scheme 1-8.** Comparison of reaction time course of **3a** (average of 3 runs) and **3a-d<sub>1</sub>**. Curves are a guide for the eye.

To probe the transmetalation and reductive elimination steps, we desired to prepare the corresponding oxidative addition complex, (cataCXium A)Pd(Ph)(Cl). The synthesis, however, proved to be challenging. Similar difficulties were encountered by the Hartwig group in their efforts to prepare LPd(Ph)Cl complexes with bulky ligands via oxidative addition of aryl chlorides. The problems were ascribed to a small equilibrium constant

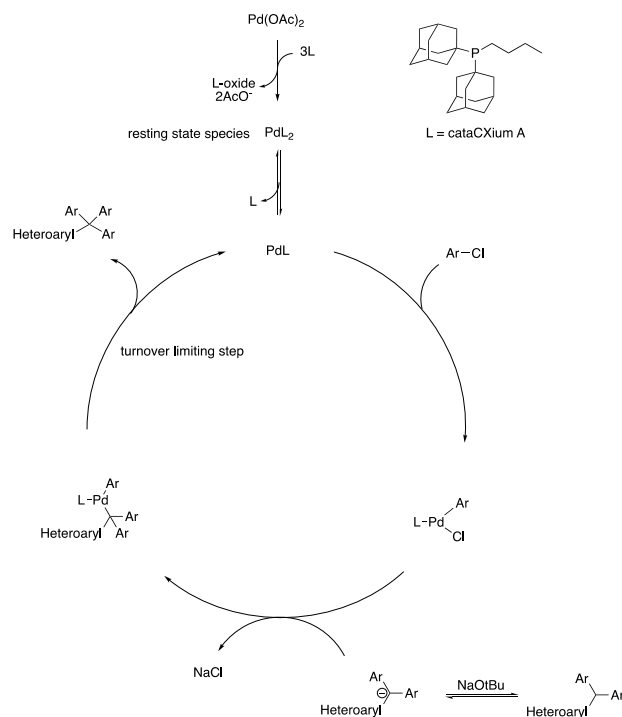
towards the oxidative addition complex and low reaction rate.<sup>19a</sup> We next turned our attention to the synthesis of the oxidative addition complex with iodobenzene, (cataCXium A)Pd(Ph)(I) (**7a**), which was reported by Antoni and Skrydstrup.<sup>20</sup> We expected that the iodobenzene oxidative addition adduct would undergo transmetallation to form the same product as that from (cataCXium A)Pd(Ph)(Cl), positioning us to probe the reductive elimination. Our synthesized (cataCXium A)Pd(Ph)(I) (**7a**) matched the spectral data reported by Antoni and Skrydstrup with a representative broad peak at 41.6 ppm in the  $^{31}\text{P}\{^1\text{H}\}$  NMR spectrum. We investigated the transmetallation by stirring a solution of (cataCXium A)Pd(Ph)(I) (**7a**) and triarylmethane **3a** (2 equiv) with 4 equiv NaOt-Bu at *room temperature* for 1 h (Scheme 1-9, a). The  $^{31}\text{P}\{^1\text{H}\}$  NMR spectrum exhibited a peak at 49.4 ppm with less than 5% Pd(cataCXium A)<sub>2</sub> and no (cataCXium A)Pd(Ph)(I) (**7a**) detected. Note that the resonance at 49.4 ppm observed in this experiment was also detected in the catalyst resting state study described above. When the transmetallation reaction mixture was heated to 130 °C for 10 min (Scheme 1-9, b),  $^1\text{H}$  NMR indicated 92% AY of tetraarylmethane product **4a**. The  $^{31}\text{P}\{^1\text{H}\}$  NMR spectrum of this solution showed that the compound at 49.4 ppm had been completely consumed and new resonances for Pd(cataCXium A)<sub>2</sub> and free cataCXium A were observed. Presumably, Pd(cataCXium A)<sub>2</sub> arises from the disproportionation of the reductive elimination product, which is proposed to be Pd(cataCXium A).





**Scheme 1-9.** Transmetalation reaction of **7a** with **3a**.

In a similar fashion, a second experiment was performed by combining (cataCXium A) $\text{Pd}(\text{Ph})(\text{I})$  (**7a**) (1.0 equiv) with  $\text{CH}(\text{Ar}_{\text{Hetero}})\text{Ph}_2$  (**3a**) (2.0 equiv) and  $\text{NaOt-Bu}$  (4.0 equiv) in toluene- $d_8$  and heated to  $80^\circ\text{C}$  for 10 min (Scheme 10b).  $^1\text{H}$  NMR analysis showed *no tetraarylmethane formation* at this temperature. The  $^{31}\text{P}\{^1\text{H}\}$  NMR spectrum indicated that the (cataCXium A) $\text{Pd}(\text{Ph})(\text{I})$  (**7a**) had been consumed and two resonances had formed: one peak at 53.1 ppm assigned to  $\text{Pd}(\text{cataCXium A})_2$  and the other singlet at 49.4 ppm. We propose that the species at 49.4 ppm is the product of transmetalation, the reductive elimination precursor (cataCXium A) $\text{Pd}(\text{Ph})[\text{C}(\text{Ar}_{\text{Hetero}})\text{Ph}_2]$  (**8a**). Taken together, these results indicate that transmetalation with (cataCXium A) $\text{Pd}(\text{Ph})(\text{I})$  is facile. We propose that transmetalation with the aryl chloride oxidative addition product, (cataCXium A) $\text{Pd}(\text{Ph})(\text{Cl})$  is also likely to be fast. Reductive elimination occurs at much higher temperature and is likely the turnover-limiting step in the formation of tetraarylmethane from  $\text{HC}(\text{Ar}_{\text{Hetero}})\text{Ph}_2$ .



**Scheme 1-10.** Proposed catalytic cycle from triarylmethane to tetraarylmethane

Based on the studies above, we propose the catalytic cycle depicted in Scheme 1-10.  $\text{Pd(OAc)}_2$  is reduced to form phosphine-ligated palladium species, which then loses a ligand to give the  $\text{PdL}_1$ .  $\text{PdL}_1$  complex can then undergo rapid oxidative addition of the aryl chloride. Next, the triarylmethane substrate is deprotonated by  $\text{NaOt-Bu}$  to generate the organosodium,  $\text{NaC(Ar}_{\text{Hetero}})\text{Ph}_2$ . The oxidative addition complex,  $(\text{cataCXium A})\text{Pd(Ph)(Cl)}$ , undergoes transmetalation with  $\text{NaC(Ar}_{\text{Hetero}})\text{Ph}_2$  to generate the reductive elimination precursor. The  $(\text{cataCXium A})\text{Pd(Ph)[C(Ar}_{\text{Hetero}})\text{Ph}_2]$  complex undergoes turnover-limiting reductive elimination to afford the tetraarylmethane product and  $\text{PdL}_1$  to close the cycle.

### 1.3 Conclusions

In summary, we have investigated the triarylation of heteroaryl methyl groups to form tetraarylmethanes. Several key findings were made that shed light on the relative rates of the events in the three catalytic cycles. It is noteworthy that the first arylation in the tandem process with chlorobenzene (Scheme 4) is about 50% complete in 25 min. The actual half-life is shorter, because the deprotonated arylation intermediates, 2-benzylbenzothiazole (**2a**) and  $\text{CH}(\text{Ar}_{\text{Hetero}})\text{Ph}_2$  (**3a**), compete with the deprotonated 2-methylbenzothiazole for the oxidative addition product, (cataCXium A)Pd(Ph)(Cl). Under similar conditions, the arylation of  $\text{CH}(\text{Ar}_{\text{Hetero}})\text{Ph}_2$  (**3a**) with chlorobenzene (2.0 equiv) and NaOt-Bu (2.0 equiv) at 130 °C has a half-life of under 20 min. These results were surprising as they indicate that deprotonation of  $\text{CH}(\text{Ar}_{\text{Hetero}})\text{Ph}_2$  and transmetallation/arylation of the resulting organosodium intermediate  $\text{NaC}(\text{Ar}_{\text{Hetero}})\text{Ph}_2$  take place at similar rates to the arylation of 2-methylbenzothiazole (**1a**), which is consistent with Scheme 1-3. In other words, and contrary to our expectations, the conversion of triarylmethane **3a** to tetraarylmethane product does not appear to be particularly difficult under these conditions with the (cataCXium A)Pd-based catalyst.

#### 1.4 References

1. (a) Ashton, P. R.; Ballardini, R.; Balzani, V.; Credi, A.; Dress, K. R.; Ishow, E.; Kleverlaan, C. J.; Kocian, O.; Preece, J. A.; Spencer, N.; Stoddart, J. F.; Venturi, M.; Wenger, S., *Chem. - Eur. J.* **2000**, *6*, 3558-3574; (b) Bělohradský, M.; Elizarov, A. M.; Stoddart, J. F., *Collect. Czech. Chem. Commun.* **2002**, *67*, 1719-1728; (c) Tseng, H. R.;

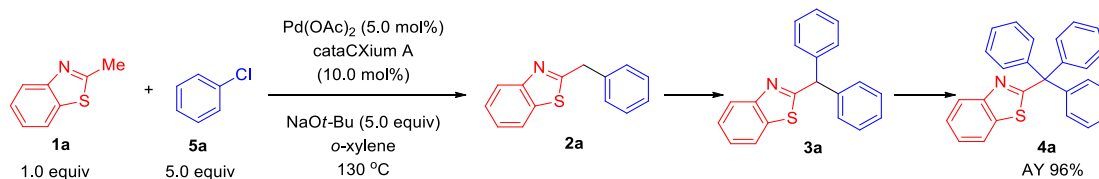
- Vignon, S. A.; Celestre, P. C.; Perkins, J.; Jeppesen, J. O.; Di Fabio, A.; Ballardini, R.; Gandolfi, M. T.; Venturi, M.; Balzani, V., *Chem. - Eur. J.* **2004**, *10*, 155-172; (d) Bonardi, F.; Halza, E.; Walko, M.; Du Plessis, F.; Nouwen, N.; Feringa, B. L.; Driessen, A. J., *Proc. Natl. Acad. Sci. U. S. A.* **2011**, *108*, 7775-7780; (e) Huang, X.; Jeong, Y.-I.; Moon, B. K.; Zhang, L.; Kang, D. H.; Kim, I., *Langmuir* **2013**, *29*, 3223-3233; (f) Dong, J.; Liu, Y.; Cui, Y., *Chem. Commun.* **2014**, *50*, 14949-14952; (g) Lu, J.; Zhang, J., *J. Mater. Chem. A* **2014**, *2*, 13831-13834; (h) Peschko, K.; Schade, A.; Vollrath, S. B.; Schwarz, U.; Luy, B.; Muhle-Goll, C.; Weis, P.; Bräse, S., *Chem. - Eur. J.* **2014**, *20*, 16273-16278; (i) Liao, K.-Y.; Hsu, C.-W.; Chi, Y.; Hsu, M.-K.; Wu, S.-W.; Chang, C.-H.; Liu, S.-H.; Lee, G.-H.; Chou, P.-T.; Hu, Y., *Inorg. Chem.* **2015**, *54*, 4029-4038.
2. (a) Alberico, D.; Scott, M. E.; Lautens, M., *Chem. Rev.* **2007**, *107*, 174-238; (b) Ackermann, L.; Vicente, R.; Kapdi, A. R., *Angew. Chem., Int. Ed.* **2009**, *48*, 9792-9826; (c) Daugulis, O.; Do, H.-Q.; Shabashov, D., *Acc. Chem. Res.* **2009**, *42*, 1074-1086; (d) Lyons, T. W.; Sanford, M. S., *Chem. Rev.* **2010**, *110*, 1147-1169; (e) Nambo, M.; Crudden, C. M., *ACS catal.* **2015**, *5*, 4734-4742; (f) Qiu, G.; Wu, J., *Org. Chem. Front.* **2015**, *2*, 169-178.
3. (a) Chen, J. J.; Onogi, S.; Hsieh, Y. C.; Hsiao, C. C.; Higashibayashi, S.; Sakurai, H.; Wu, Y. T., *Adv. Synth. Catal.* **2012**, *354*, 1551-1558; (b) Cao, X.; Yang, W.; Liu, C.; Wei, F.; Wu, K.; Sun, W.; Song, J.; Xie, L.; Huang, W., *Org. Lett.* **2013**, *15*, 3102-3105.
4. Nambo, M.; Yar, M.; Smith, J. D.; Crudden, C. M., *Org. Lett.* **2014**, *17*, 50-53.
5. Tsuchida, K.; Senda, Y.; Nakajima, K.; Nishibayashi, Y., *Angew. Chem., Int. Ed.* **2016**, *55*, 9728-9732.

6. (a) Zhang, J.; Bellomo, A.; Creamer, A. D.; Dreher, S. D.; Walsh, P. J., *J. Am. Chem. Soc.* **2012**, *134*, 13765-13772; (b) Hussain, N.; Frensch, G.; Zhang, J.; Walsh, P. J., *Angew. Chem., Int. Ed.* **2014**, *53*, 3693-3697; (c) Zhang, J.; Bellomo, A.; Trongsirawat, N.; Jia, T.; Carroll, P. J.; Dreher, S. D.; Tudge, M. T.; Yin, H.; Robinson, J. R.; Schelter, E. J., *J. Am. Chem. Soc.* **2014**, *136*, 6276-6287; (d) Sha, S.-C.; Zhang, J.; Walsh, P. J., *Org. Lett.* **2015**, *17*, 410-413; (e) Kim, B.-S.; Jimenez, J.; Gao, F.; Walsh, P. J., *Org. Lett.* **2015**, *17*, 5788-5791; (f) Li, M.; González-Esguevillas, M.; Berritt, S.; Yang, X.; Bellomo, A.; Walsh, P. J., *Angew. Chem., Int. Ed.* **2016**, *55*, 2825-2829; (g) Yang, X.; Kim, B.-S.; Li, M.; Walsh, P. J., *Org. Lett.* **2016**, *18*, 2371-2374.
7. (a) Hamann, B. C.; Hartwig, J. F., *J. Am. Chem. Soc.* **1997**, *119*, 12382-12383; (b) Palucki, M.; Buchwald, S. L., *J. Am. Chem. Soc.* **1997**, *119*, 11108-11109; (c) Satoh, T.; Kawamura, Y.; Miura, M.; Nomura, M., *Angew. Chem., Int. Ed.* **1997**, *36*, 1740-1742; (d) Novak, P.; Martin, R., *Curr. Org. Chem.* **2011**, *15*, 3233-3262.
8. (a) Zapf, A.; Beller, M., *Chem. Commun.* **2005**, 431-440; (b) Zapf, A.; Ehrentraut, A.; Beller, M., *Angew. Chem., Int. Ed.* **2000**, *39*, 4153-4155.
9. Zhang, S.; Kim, B.-S.; Wu, C.; Mao, J.; Walsh, P. J., *Nat. Commun.* **2017**, *8*, 14641-14649.
10. (a) Burton, P. M.; Morris, J. A., *Org. Lett.* **2010**, *12*, 5359-5361; (b) Song, G.; Su, Y.; Gong, X.; Han, K.; Li, X., *Org. Lett.* **2011**, *13*, 1968-1971.
11. Hatano, T.; Kato, T., *Tetrahedron* **2008**, *64*, 8368-8380.
12. Ablajan, K.; B Panetti, G.; Yang, X.; Kim, B.-S.; Walsh, P. J., *Adv. Synth. Catal.* **2017**, *359*, 1927-1932.

13. (a) Litvinov, V. P., *Adv. Heterocycl. Chem.* **2006**, *91*, 189-300; (b) Joule, J. A.; Mills, K., *Heterocyclic Chemistry 5th ed.*; John Wiley & Sons, 2010.
14. (a) Gao, F.; Kim, B.-S.; Walsh, P. J., *Chem. Commun.* **2014**, *50*, 10661-10664; (b) Gao, F.; Kim, B.-S.; Walsh, P. J., *Chem. Sci.* **2016**, *7*, 976-983.
15. (a) Littke, A. F.; Fu, G. C., *Angew. Chem., Int. Ed.* **2002**, *41*, 4176-4211; (b) Fleckenstein, C. A.; Plenio, H., *Chem. Soc. Rev.* **2010**, *39*, 694-711.
16. Barrios-Landeros, F.; Carrow, B. P.; Hartwig, J. F., *J. Am. Chem. Soc.* **2009**, *131*, 8141-8154.
17. Bordwell, F. G., *Acc. Chem. Res.* **1988**, *21*, 456-463.
18. Segree, A. G.; Spannenberg, A.; Beller, M., *J. Am. Chem. Soc.* **2008**, *130*, 15549-15563.
19. (a) Roy, A. H.; Hartwig, J. F., *J. Am. Chem. Soc.* **2003**, *125*, 13944-13945; (b) Roy, A. H.; Hartwig, J. F., *Organometallics* **2004**, *23*, 1533-1541.
20. Andersen, T. L.; Friis, S. D.; Audrain, H.; Nordeman, P.; Antoni, G.; Skrydstrup, T., *J. Am. Chem. Soc.* **2015**, *137*, 1548-1555.

## 1.5 Supporting Information

### 1.5.1 Reaction study of 2-methylbenzothiazole 1a with chlorobenzene 5a



**Scheme 1-S1.** Conversion data for the reaction of 2-methylbenzothiazole (**1a**) with chlorobenzene (**5a**, 5.0 equiv)

A series of separate parallel reactions were carried out to study the reaction time course. Oven-dried 8 mL reaction vials equipped with stir bars were charged with 2-methylbenzothiazole (**1a**, 12.7  $\mu\text{L}$ , 0.1 mmol, 1.0 equiv) and chlorobenzene (**5a**, 5.0 equiv) in a glove box under a nitrogen atmosphere at room temperature. A stock solution containing Pd(OAc)<sub>2</sub> (1.1 mg, 0.005 mmol, 5.0 mol %) and cataCXium A (3.6 mg, 0.01 mmol, 10.0 mol %) in 1 mL of dry *o*-xylene was taken up by syringe and added to the every reaction vial under nitrogen. Next, NaOt-Bu (48.1 mg, 0.5 mmol, 5.0 equiv) was added to the reaction mixture. The vials were capped, removed from the glove box, and stirred at 130 °C, one vial was cooled in ice bath and quenched with 3 drops of water every 5 min for the first 30 min, and then every 10 min after that, the reaction mixtures were then diluted with 4 mL of ethyl acetate, and filtered over a pad of MgSO<sub>4</sub> and silica. The pad was rinsed with additional ethyl acetate (4 mL) and the solution was concentrated in vacuo. <sup>1</sup>H NMR spectra of the crude material was acquired with integration of SM, mono-, di, and triarylated material against an internal standard (CH<sub>2</sub>Br<sub>2</sub> as the internal standard, one vial added with 7.0  $\mu\text{L}$ , 0.1 mmol). The data are listed in Table 1-S1 and 1-S2.

**Table 1-S1** <sup>1</sup>H NMR monitoring of the reaction of **1a** with **5a** (5.0 equiv) at 130°C run 1

Time (min)	SM (%)	diarylmethane (%)	Triarylmethane (%)	Tetraarylmethane (%)
0	99	0	0	0
5	88	1	0	0
10	77	9	3	0
15	69	1	19	0
20	61	0	24	4
25	56	0	29	8
30	46	0	34	12
40	32	0	41	17
50	26	0	43	22
60	21	0	46	26

70	12	0	39	41
80	8	0	36	46
90	2	0	29	59
100	0	0	23	68
110	0	0	14	82
120	0	0	4	91
130	0	0	0	96

**Table 1-S2**  $^1\text{H}$  NMR monitoring of the reaction of **1a** with **5a** (5.0 equiv) at 130°C run 2

Time (min)	SM (%)	diarylmethane (%)	Triarylmethane (%)	Tetraarylmethane(%)
0	99	0	0	0
5	86	1	1	0
10	76	2	6	0
15	67	1	18	2
20	62	1	23	4
25	57	0	30	7
30	48	0	31	10
40	35	0	39	13
50	29	0	43	19
60	22	0	48	27
70	15	0	41	38
80	10	0	38	42
90	4	0	32	57



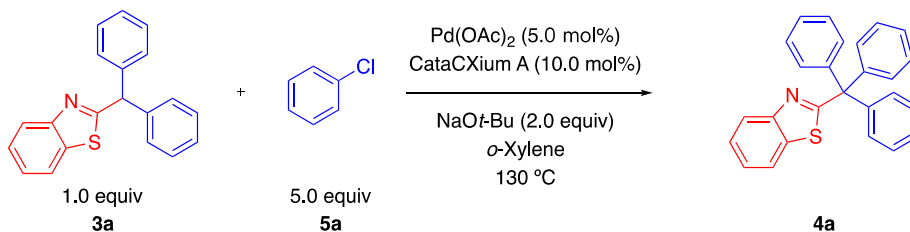
100	1	0	22	69
110	0	0	9	84
120	0	0	3	93
130	0	0	0	96

## 1.5.2 Resting state studies

### (a) Synthesis of **3a**

Compound **3a** was prepared according to literature procedure.<sup>1</sup>

### (b) Resting state studies



**Scheme 1-S2.** Resting state studies for the reaction of CH(ArHetero)Ph<sub>2</sub> (**3a**) with chlorobenzene (**5a**, 5.0 equiv) and NaOt-Bu (2.0 equiv) in *o*-xylene-d<sub>10</sub> at 130 °C.

A stock solution containing Pd(OAc)<sub>2</sub> (1.1 mg, 0.005 mmol, 5.0 mol %) and cataCXium A (3.6 mg, 0.01 mmol, 10.0 mol %) in 0.5 mL of dry *o*-xylene was taken up by syringe and added to the every reaction vial under nitrogen. Next, NaOt-Bu (19.2 mg, 0.2 mmol, 2.0 equiv) was added to the reaction mixtures. The vials were capped, removed from the glove box, and stirred at 130 °C. One vial was cooled in ice bath every 5 min. The resulting unpurified reaction mixtures were transferred to NMR tubes in a dry box, sealed and analyzed by <sup>31</sup>P{<sup>1</sup>H} NMR. The <sup>31</sup>P{<sup>1</sup>H} NMR spectra are showed in Figure S1.

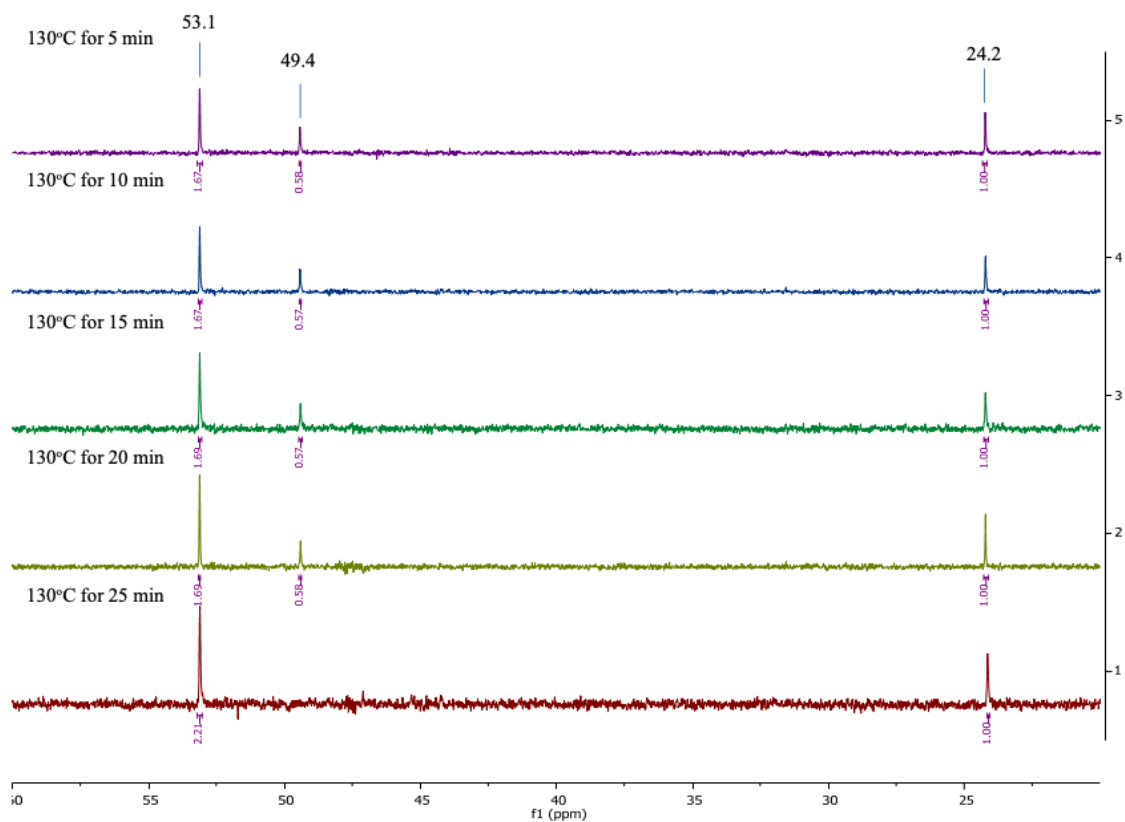


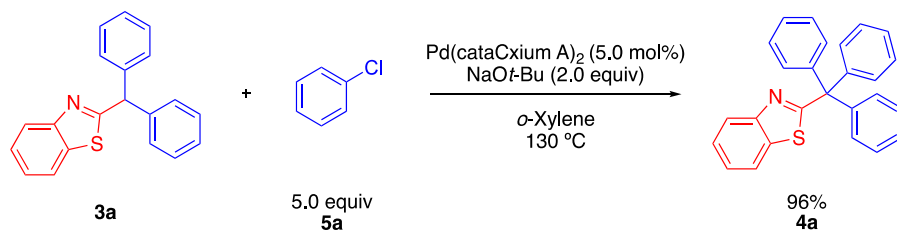
**Figure 1-S1**  $^{31}\text{P}\{^1\text{H}\}$  NMR spectra of the catalyst resting state study.

### 1.5.3 Reaction of $\text{CH}(\text{ArHetero})\text{Ph}_2$ (**3a**) with chlorobenzene (**5a**) and $\text{NaOt-Bu}$ using $\text{Pd}(\text{cataCXium A})_2$

#### (a) Preparation of $\text{Pd}(\text{cataCXium A})_2$

$\text{Pd}(\text{cataCXium A})_2$  was prepared according to literature procedure.<sup>2</sup>

#### (b) Reaction using $\text{Pd}(\text{cataCium A})_2$ as the catalyst

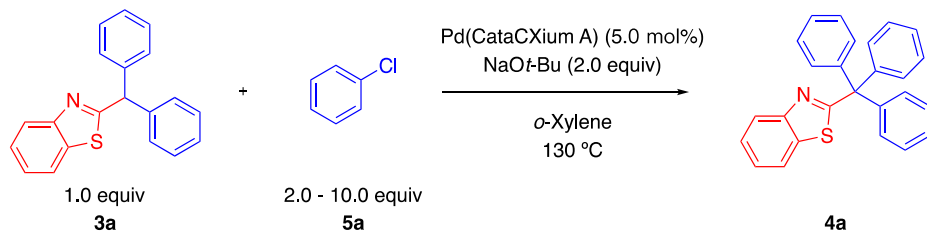


**Scheme 1-S3.** Reaction of  $\text{CH}(\text{Ar}_{\text{Hetero}})\text{Ph}_2$  (**3a**) with chlorobenzene (**5a**, 5.0 equiv) and  $\text{NaOt-Bu}$  (2.0 equiv) using  $\text{Pd}(\text{cataCXium A})_2$  at  $130^\circ\text{C}$ .

Oven-dried 8 mL reaction vials equipped with stir bars were charged with compound **3a** (30.1 mg, 0.1 mmol, 1.0 equiv) and chlorobenzene (**5a**, 5.0 equiv) in a glove box under a nitrogen atmosphere at room temperature.  $\text{Pd}(\text{cataCXium A})_2$  (5.0 mol %) and 0.5 mL of dry *o*-xylene were added to reaction vial under nitrogen. Next,  $\text{NaOt-Bu}$  (19.2 mg, 0.2 mmol, 2.0 equiv) was added to the reaction mixtures. The vials were capped, removed from the glove box, and stirred at  $130^\circ\text{C}$ . The vial was cooled in ice bath and quenched with 3 drops of water, diluted with 4 mL of ethyl acetate, and filtered over a pad of  $\text{MgSO}_4$  and silica. The pad was rinsed with additional ethyl acetate (4 mL) and the solution was concentrated in vacuo.  $^1\text{H}$  NMR spectra of the crude material was acquired with integration of tetraarylmethane against an internal standard ( $\text{CH}_2\text{Br}_2$  as the internal standard, one vial added with 7.0  $\mu\text{L}$ , 0.1 mmol).

**(c) Impact of the concentration of chlorobenzene for the initial rate of the reaction**

Preliminary reactions were performed to determine the reaction time of initial rate study. In order to keep the reaction system simple to study, the reaction time was picked to limit the conversion of each reaction to less than 10%.<sup>3</sup>



**Scheme 1-S3.** Reaction of CH(Ar<sub>Hetero</sub>)Ph<sub>2</sub> (**3a**) with chlorobenzene (**5a**, 2.0, 4.0, 6.0, 8.0 or 10.0 equiv) and NaO*t*-Bu (2.0 equiv) using Pd(cataCXium A)<sub>2</sub> at 130 °C.

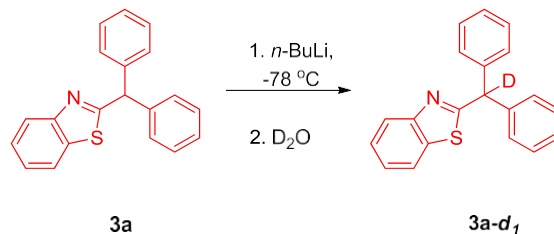
A series of separate parallel reactions were carried out to monitor the conversion rate of the reaction. Oven-dried 8 mL reaction vials equipped with stir bars were charged with compound **3a** (30.1 mg, 0.1 mmol, 1.0 equiv) and chlorobenzene (**5a**, 2.0, 4.0, 6.0, 8.0 or 10.0 equiv) in a glove box under a nitrogen atmosphere at room temperature. Pd(cataCXium A)<sub>2</sub> (5.0 mol %) and 1 mL of dry *o*-xylene were added to every reaction vial under nitrogen. Next, NaO*t*-Bu (2.0 equiv) was added to each vial. The vials were capped, removed from the glove box, and stirred at 130 °C, each vial was cooled in ice and quenched with 3 drops of water, diluted with 4 mL of ethyl acetate, and filtered over a pad of MgSO<sub>4</sub> and silica. The pad was rinsed with additional ethyl acetate (4 mL), and the solution was concentrated in vacuo. <sup>1</sup>H NMR (CDCl<sub>3</sub>) spectra of the crude material was acquired with integration of tetraarylmethane against an internal standard (CH<sub>2</sub>Br<sub>2</sub> as the internal standard, one vial added with 7.0 μL, 0.1 mmol). The data are listed in Table S3.

**Table 1-S3** <sup>1</sup>H NMR monitoring of the reaction of **3a** with different amount of **5a** using Pd(cataCXium A)<sub>2</sub> at 130°C

Time (min)	<b>4a</b> (%) (2.0 equiv <b>5a</b> )	<b>4a</b> (%) (4.0 equiv <b>5a</b> )	<b>4a</b> (%) (6.0 equiv <b>5a</b> )	<b>4a</b> (%) (8.0 equiv <b>5a</b> )	<b>4a</b> (%) (10.0 equiv <b>5a</b> )
0	0	0	0	0	0
3	7	7	8	8	9

## 1.5.4 Deuteration reactions

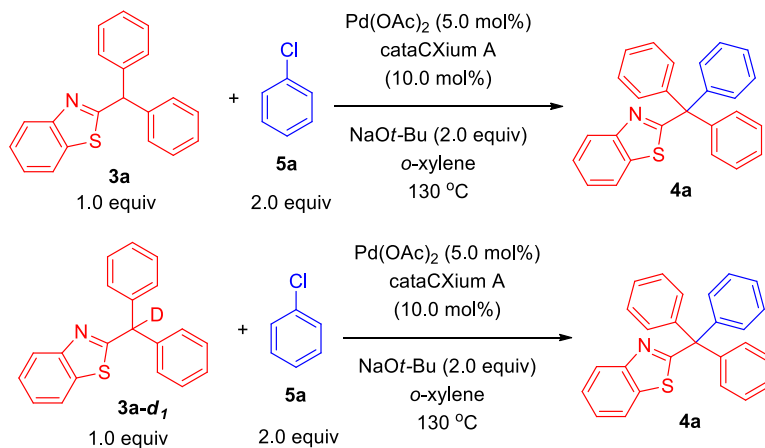
### (a) Synthesis of **3a-d<sub>1</sub>**



### Scheme 1-S4. Deprotonation and Deuteration of **3a**

An oven-dried 100 mL round bottom flask equipped with a stir bar was charged with 2-benzhydrylbenzo[*d*]thiazole (**3a**, 602.1 mg, 2.0 mmol, 1.0 equiv) and dry THF (20 mL) under nitrogen. The flask was capped with a rubber septum and cooled to -78 °C. *n*-BuLi (0.96 mL, 2.4 mmol, 1.2 equiv, 2.5 M in hexanes) was added to the mixture, and the resultant mixture was stirred at -78 °C for 1 h before it was quenched with D<sub>2</sub>O (0.4 mL). The resulting solution was extracted with ethyl acetate (3×40 mL). The combined organic phase was dried over with Na<sub>2</sub>SO<sub>4</sub> and was concentrated in vacuo. The crude material was purified by flash chromatography on silica gel (eluted with hexanes:ethyl acetate = 20:1 to 15:1) to yield the product **3a-d<sub>1</sub>** (584.1 mg, 97% yield, 99% *-d<sub>1</sub>*) as a light yellow solid, mp: 79-81 °C ; R<sub>f</sub> = 0.51 (hexanes:ethyl acetate = 10:1). <sup>1</sup>H NMR (500 MHz, CDCl<sub>3</sub>): δ 8.01 (d, *J* = 8.2 Hz, 1H), 7.77 (d, *J* = 8.0 Hz, 1H), 7.46–7.39 (m, 1H), 7.36–7.29 (m, 9H), 7.26–7.23 (m, 2H) ppm; <sup>13</sup>C {<sup>1</sup>H} NMR (125 MHz, CDCl<sub>3</sub>): δ 174.2, 153.6, 141.4, 135.7, 129.2, 128.8, 127.5, 126.1, 125.0, 123.3, 121.6 ppm; HRMS (TOF MS ES +) *m/z* [M + H]<sup>+</sup> calcd. For C<sub>20</sub>H<sub>15</sub><sup>2</sup>HNS 303.1066, found 303.1080.

### (b) Estimation of kinetic isotopic effect for the conversion rate of the reaction



**Scheme 1-S5.** Comparison of reaction time course of **3a** (average of 3 runs) and **3a-d<sub>1</sub>**.

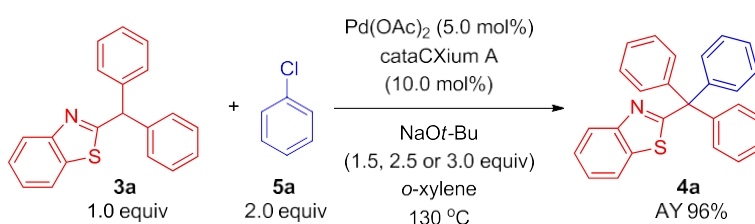
A series of separate parallel reactions were carried out to determine the KIE. Oven-dried 8 mL reaction vials equipped with stir bars were charged with compound **3a** (30.1 mg, 0.1 mmol, 1.0 equiv) (reaction carried out in triplicate) or **3a-d<sub>1</sub>** (30.2 mg, 0.1 mmol, 1.0 equiv) and chlorobenzene (**5a**, 20.3  $\mu$ L, 0.2 mmol, 2.0 equiv) in a glove box under a nitrogen atmosphere at room temperature. A stock solution containing Pd(OAc)<sub>2</sub> (1.1 mg, 0.005 mmol, 5.0 mol %) and cataCXium A (3.6 mg, 0.01 mmol, 10.0 mol %) in 1 mL of dry *o*-xylene was taken up by syringe and added to every reaction vial under nitrogen. Next, NaO*t*-Bu (19.2 mg, 0.2 mmol, 2.0 equiv) was added to the reaction mixtures. The vials were capped, removed from the glove box, and stirred at 130 °C. Every 5 min one vial was removed from the heating bath, cooled in ice bath, quenched with 3 drops of water, diluted with 4 mL of ethyl acetate, and filtered over a pad of MgSO<sub>4</sub> and silica. The pad was rinsed with additional ethyl acetate (4 mL) and the solution was concentrated in vacuo. <sup>1</sup>H NMR (CDCl<sub>3</sub>) spectra of the crude material was acquired with integration of the tetraarylmethane against an internal standard (CH<sub>2</sub>Br<sub>2</sub> as the internal standard, one vial added with 7.0  $\mu$ L, 0.1 mmol). The data are listed in Table S4.

**Table 1-S4** <sup>1</sup>H NMR monitoring of the reaction of **3a** or **3a-d<sub>1</sub>** with **5a** at 130°C

Time (min)	<b>4a</b> (%) (from <b>3a</b> ) first run	<b>4a</b> (%) (from <b>3a</b> ) second run	<b>4a</b> (%) (from <b>3a</b> ) third run	<b>4a</b> (%) average (from <b>3a</b> )	<b>4a</b> average e (%) (from <b>3a-d<sub>1</sub></b> )
0	0	0	0	0	0
5	19	16	16	17	17
10	32	27	31	30	31
15	44	38	39	40	40

20	54	53	51	52.7	52
25	65	64	61	63.3	63
30	81	79	77	79	78
35	93	92	90	91.7	93
40	96	96	96	96	96

### 1.5.5 Impact of the concentration of bases on the reaction time course



A series of separate parallel reactions were carried out to monitor the conversion rate of the reaction. Oven-dried 8 mL reaction vials equipped with stir bars were charged with compound **3a** (30.1 mg, 0.1 mmol, 1.0 equiv) and chlorobenzene (**5a**, 20.3  $\mu$ L, 0.2 mmol, 2.0 equiv) in a glove box under a nitrogen atmosphere at room temperature. A stock solution containing Pd(OAc)<sub>2</sub> (1.1 mg, 0.005 mmol, 5.0 mol %) and cataCXium A (3.6 mg, 0.01 mmol, 10.0 mol %) in 1 mL of dry *o*-xylene was taken up by syringe and added to every reaction vial under nitrogen. Next, NaOt-Bu (1.5, 2.5 or 3.0 equiv) was added to each vial. The vials were capped, removed from the glove box, and stirred at 130 °C. Every 5 min one vial was cooled in ice bath and quenched with 3 drops of water, diluted with 4 mL of ethyl acetate, and filtered over a pad of MgSO<sub>4</sub> and silica. The pad was rinsed with additional ethyl acetate (4 mL) and the solution was concentrated in vacuo. <sup>1</sup>H NMR spectra of the crude material was acquired with integration of the



tetraarylmethane against an internal standard ( $\text{CH}_2\text{Br}_2$  as the internal standard, one vial added with  $7.0 \mu\text{L}$ ,  $0.1 \text{ mmol}$ ). The data are listed in Table S5.

**Table 1-S5**  $^1\text{H}$  NMR monitoring of the reaction of 3a and 5a with different amounts of base at  $130^\circ\text{C}$

Time (min)	4a (%) (1.5 equiv base)	4a (%) (2.5 equiv base)	4a (%) (3.0 equiv base)
0	0	0	0
5	18	18	17
10	31	30	31
15	41	41	45
20	52	54	56
25	63	72	73
30	80	84	86
35	91	94	96
40	96	96	-

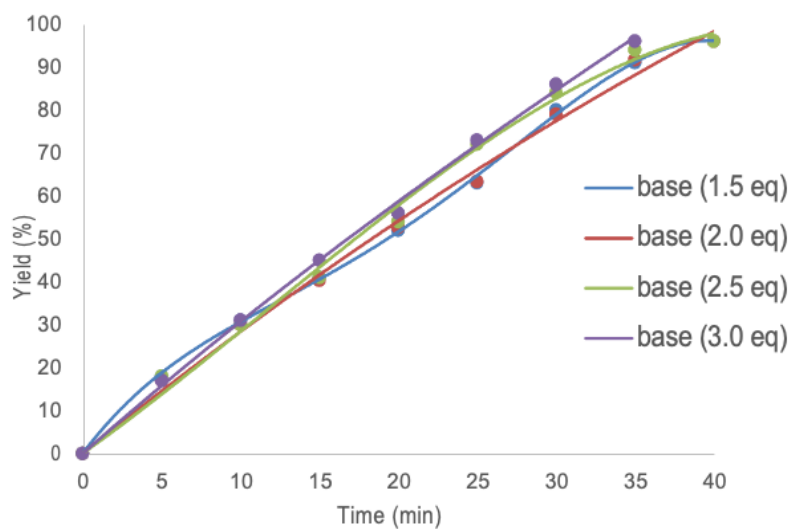


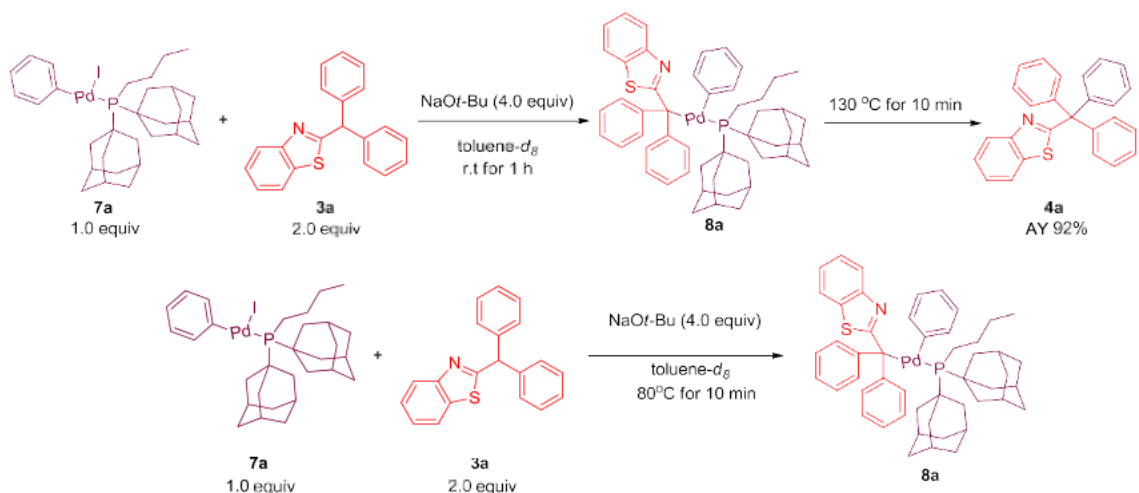
**Chart 1-S1.** Conversion data for the reaction of  $\text{CH}(\text{ArHetero})\text{Ph}_2$  (**3a**) with chlorobenzene (**5a**, 2.0 equiv) and  $\text{NaO}t\text{-Bu}$  (1.5, 2.0, 2.5 and 3.0 equiv) at  $130\text{ }^\circ\text{C}$ . Curves are a guide for the eye.

### 1.5.6 Transmetallation reaction of **7a** with **3a**.

#### (a) Preparation of (cataCXium A)Pd(Ph)(I) (**7a**)

(cataCXium A)Pd(Ph)(I) was prepared according to literature procedure.<sup>4</sup>

#### (b) (cataCXium A)Pd(Ph)(I) (**7a**) for the transmetallation at different temperatures



**Scheme 1-6.** Transmetalation reaction of **7a** with **3a**.

Oven-dried 8 mL reaction vials equipped with stir bars were charged with compound **7a** (6.7 mg, 0.01 mmol, 1.0 equiv) and compound **3a** (2.0 equiv) in a glove box under a nitrogen atmosphere at room temperature. Then 0.5 mL of dry toluene- $d_8$  was added to the reaction vial under nitrogen. Next, NaOt-Bu (2.0 equiv) was added to the reaction mixture. The vials were capped, removed from the glove box, and stirred at room temperature for 1 h then at 130°C for 10 min or at 80 °C for 10 min. Every vial was cooled to room temperature and the resulting unpurified reaction mixtures were transferred to NMR tubes in a dry box, sealed and analyzed by  $^{31}\text{P}\{^1\text{H}\}$  NMR. The  $^{31}\text{P}\{^1\text{H}\}$  NMR spectra are showed in Figure S2.

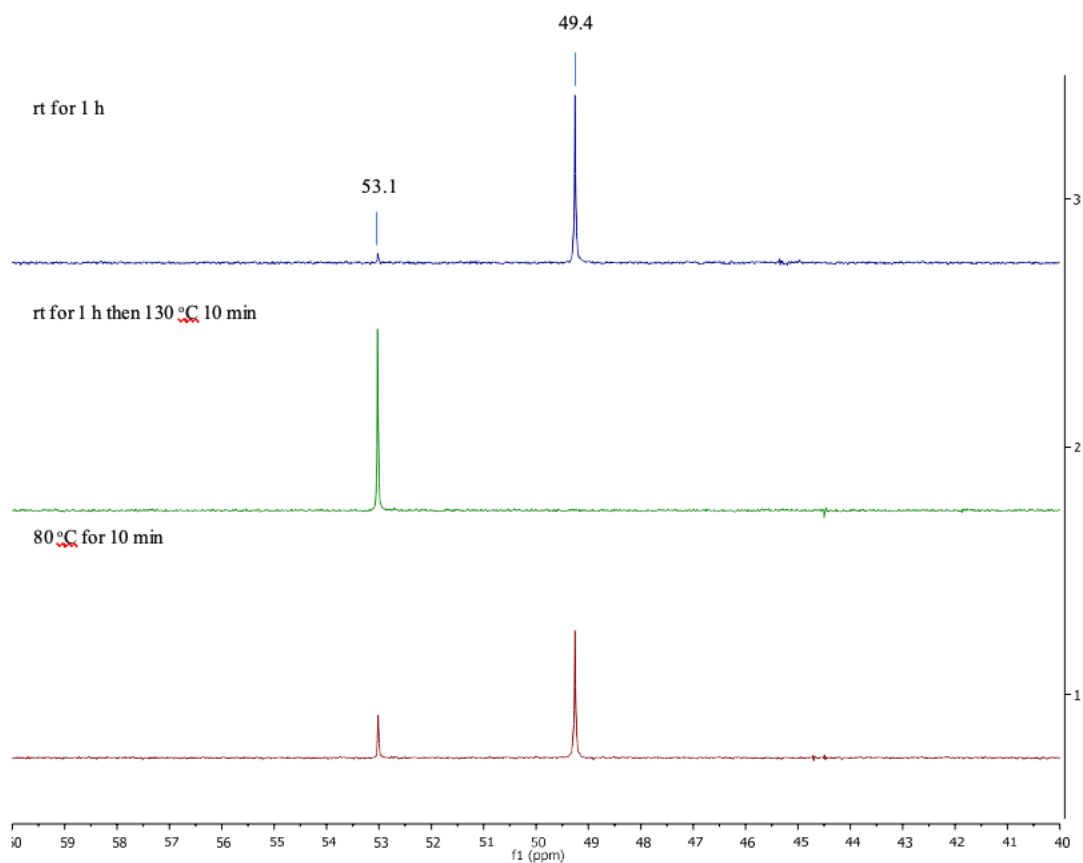


**Figure 1-S2**  $^{31}\text{P}\{^1\text{H}\}$  NMR spectra of transmetalation reaction of **7a** with **3a**

### References

1. Song, G.; Su, Y.; Gong, X.; Han, K.; Li, X., *Org. Lett.* **2011**, *13*, 1968-1971.
2. Sergeev, A. G.; Spannenberg, A.; Beller, M., *J. Am. Chem. Soc.* **2008**, *130*, 15549-15563.
3. Anslyn, E. V.; Dougherty, D. A., *Modern Physical Organic Chemistry.*; University Science Books 2006.
4. Andersen, T. L.; Friis, S. D.; Audrain, H.; Nordeman, P.; Antoni, G.; Skrydstrup, T., *J. Am. Chem. Soc.* **2015**, *137*, 1548-1555.

## CHAPTER 2 Palladium-Catalyzed Benzylic C(sp<sup>3</sup>)-H Carbonylative Arylation of Azaarylmethyl Amines with Aryl Bromides

### 2.1 Introduction

$\alpha$ -Amino ketones are key components of numerous biologically active natural products and synthetic compounds. They display a wide range of medicinal and biological activities, such as anti-depressant, appetite suppressant, and anti-platelet properties (Figure 2-1).<sup>1</sup>  $\alpha$ -Amino ketones also serve as effective synthetic intermediates for the preparation of various heterocycles and 1,2-amino alcohols.<sup>1b, 2</sup> As a result of their widespread utility, there has been substantial and long-standing interest in the efficient construction of  $\alpha$ -amino ketones in the synthetic community.<sup>3</sup> General approaches to construct  $\alpha$ -amino ketones from ketones or their derivatives involve nucleophilic amination,<sup>4</sup> electrophilic amination<sup>5</sup> or oxidative amination.<sup>6</sup> Considerable efforts have also been made to synthesize  $\alpha$ -amino ketones via acylation of imines with aldehydes, acylsilanes or carboxylic acids,<sup>7</sup> Stille reaction of sulfonamides with benzoyl chlorides,<sup>8</sup> cross-coupling of thiol esters with boronic acids or organostannanes,<sup>9</sup> hydrogenation of  $\alpha$ -dehydroamino ketones or  $\alpha$ -ketoketimines,<sup>10</sup> and rearrangement of  $\alpha$ -hydroxyl imines or enamines.<sup>11</sup> Moreover, recent years have witnessed the preparation of  $\alpha$ -amino ketones starting from alkenes,<sup>12</sup> alkynes<sup>13</sup> and sulfonium ylides.<sup>14</sup> Despite these promising advances, exploration of straightforward methods that enable formation of multiple C-C bonds remains appealing.

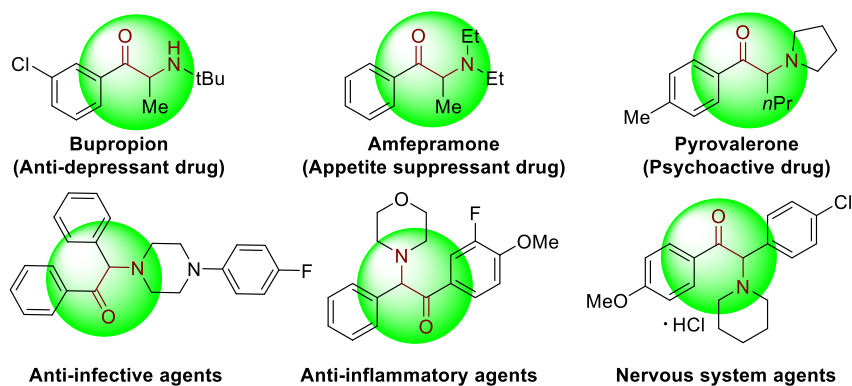
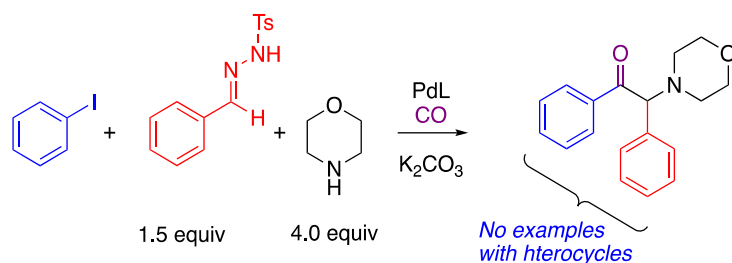


**Figure 2-1.** Selected pharmacologically active compounds containing  $\alpha$ -amino aryl ketones

Due to its low cost, high reactivity and abundance, CO has been extensively explored as a versatile C1 building block for the production of carbonyl-containing compounds and heterocycles.<sup>15</sup> Impressive achievements have been recorded in transition-metal catalyzed reactions of CO in multicomponent carbonylation reactions to construct carbonyl-containing molecules from simple starting materials.<sup>15d, 16</sup> Little attention, however, has been paid to the application of this strategy for the preparation of synthetically valuable  $\alpha$ -amino ketones. There is only one such report in the literature. In 2018, Wang, Zhang and co-workers described an elegant synthesis of  $\alpha$ -amino ketones via a Pd(0)-catalyzed four-component carbonylation reaction of aryl iodides, *N*-tosylhydrazones and amines under 1 atm of CO (Scheme 2-1).<sup>17</sup> Despite the synthetic potential of this four component coupling, this protocol is only applicable to aryl iodides and no examples with heteroaryl groups were reported.

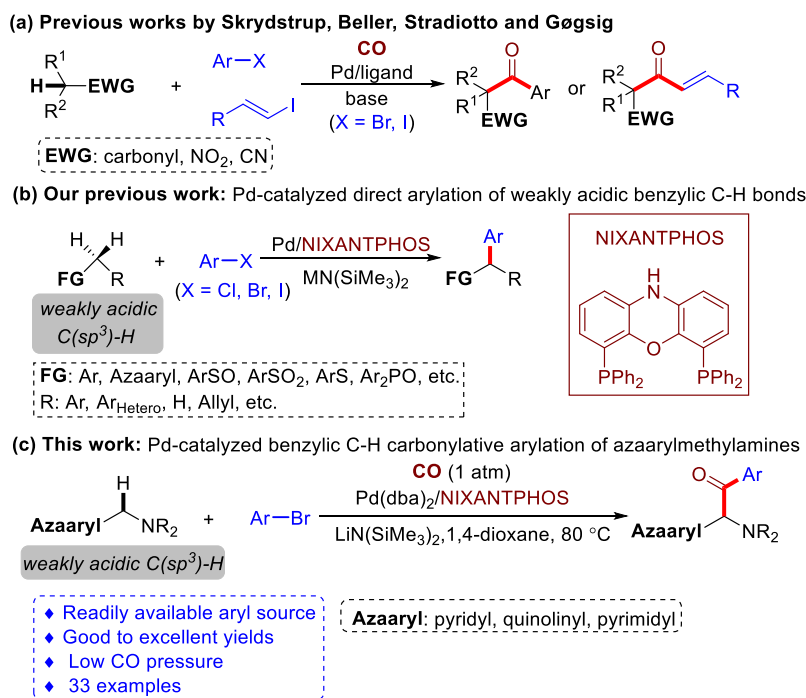


**Scheme 2-1.** Carbene-based approach of Wang and co-workers.

Recent progress has established the viability of palladium-catalyzed carbonylative cross-coupling reactions of acidic  $\text{C}(\text{sp}^3)\text{-H}$  bonds for the concurrent formation of two new  $\text{C-C}$  bonds with the introduction of a carbonyl group.<sup>18,19</sup> Early reports focused on the arylation of activated  $\text{C}(\text{sp}^3)\text{-H}$  bonds of malonate derivatives.<sup>18</sup> In 2012, Skrydstrup and co-workers first realized carbonylative  $\alpha$ -arylation of ketones with aryl iodides using CO in the presence of a catalytic amount of  $[\text{Pd}(\text{dba})_2]$  and a bidentate phosphine ligand to afford 1,3-diketones (Scheme 2-2, a).<sup>19a</sup> Subsequently, the same group accomplished carbonylative  $\alpha$ -arylation of monoester potassium malonate,<sup>19b</sup> acetylacetones,<sup>19d</sup> ketones,<sup>19e</sup> 2-oxindoles,<sup>19g</sup> nitromethanes,<sup>19h</sup> substituted 1,3-dioxin-4-ones,<sup>19i</sup> and cyanoacetates<sup>19j</sup> with aryl iodides and aryl bromides under palladium catalysis. Meanwhile, Beller and co-workers described the Pd-catalyzed carbonylative  $\alpha$ -arylation of ketones and nitriles with aryl iodides and pressurized CO gas (Scheme 2-2, a).<sup>19c,f</sup> These studies take advantage of strongly activated  $\text{C}(\text{sp}^3)\text{-H}$  bonds to facilitate deprotonation. The carbonylative  $\alpha$ -arylation of weakly acidic  $\text{C}(\text{sp}^3)\text{-H}$  bonds remains underdeveloped, despite the potential utility of such a method with a wide variety of pronucleophiles.

In recent years, our team has built a program around direct arylation of weakly acidic

C(sp<sup>3</sup>)-H bonds (pK<sub>a</sub> 25–43 in DMSO)<sup>20</sup> with aryl halides by employing palladium catalysts and suitable bases (Scheme 2-2, b). We called this approach deprotonative cross-coupling processes (DCCP).<sup>21</sup> Based on these studies from our lab, we envisioned that merging DCCP with carbonylation reactions would enable preparation of a host of new ketones. Herein we describe such a new and efficient process that allows highly selective carbonylative arylation of weakly acidic benzylic C(sp<sup>3</sup>)-H bonds of azaarylmethylamines with aryl bromides. These reactions are conveniently conducted with 1 atm of CO and a palladium catalyst to deliver α-amino aryl-azaarylmethyl-ketone products in good to excellent yields with broad substrate scope and good tolerance of functional groups (Scheme 2-2, c).



**Scheme 2-2.** Deprotonative carbonylative cross-coupling reactions.



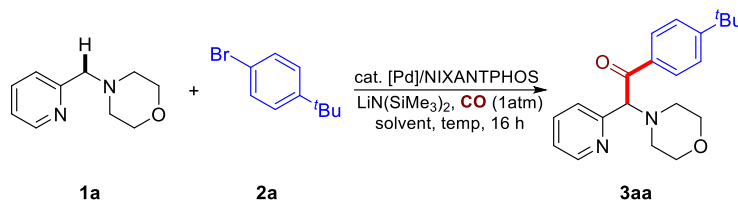
## 2.2 Results and Discussion

We started our studies by exploring the reaction conditions of benzylic C–H carbonylative arylation of 4-(pyridin-2-ylmethyl)morpholine (**1a**) with 1-bromo-4-(*tert*-butyl)benzene (**2a**) under 1 atm of CO gas. Considering that we have recently achieved the coupling of azaarylmethyl amines with aryl halides to generate aryl(azaaryl)methyl amines in 1,4-dioxane using a Pd(OAc)<sub>2</sub>/NIXANTPHOS-based catalyst together with LiN(SiMe<sub>3</sub>)<sub>2</sub> as the base,<sup>21c</sup> we first assessed the feasibility of the proposed reaction of **1a**, **2a** and CO (1 atm) at 65 °C for 16 h by employing the same catalytic system. After an HTE screening of solvents and bases, to our delight, the carbonylative arylation reaction indeed occurred, and the best combination was found to be LiN(SiMe<sub>3</sub>)<sub>2</sub> and 1,4-dioxane, which was very similar to the reported direct coupling reaction. Lab scale reaction using these conditions delivered the expected product **3aa** in 27% yield with the formation of the non-carbonylative coupling product (also called the direct coupling product) **3aa'** in 8% yield (Table 2-1, entry 1 and Supporting Information, Table 2-S2).

With an aim to improve the reaction efficiency, Dr. Haoqiang Zhao and I did further optimizations on lab scale. The performance of the coupling in other solvents, such as THF, CPME (cyclopentyl methyl ether) and DME were examined (Table 2-1, entries 2–4), but none outperform 1,4-dioxane. Replacement of LiN(SiMe<sub>3</sub>)<sub>2</sub> with NaN(SiMe<sub>3</sub>)<sub>2</sub> or KN(SiMe<sub>3</sub>)<sub>2</sub> failed to give better results, and the reaction was not promoted with LiO<sup>t</sup>Bu, NaO<sup>t</sup>Bu, or KO<sup>t</sup>Bu as the base (SI, Table 2-S2). The subsequent screening of palladium salts revealed the superiority of Pd(dba)<sub>2</sub> in this reaction, allowing the generation of product **3aa** in 43% yield (Table 2-1, entry 8). Unexpectedly, increasing the

loading of  $\text{LiN}(\text{SiMe}_3)_2$  to 3 equiv improved the yield of **3aa** to 89% with only a small amount of direct coupling byproduct **3aa'** (7%) (Table 2-1, entry 9 and SI, Table 2-S2). The yield of **3aa** could be further enhanced to 93% with an increase of reaction temperature to 80 °C (Table 2-1, entry 10), but a higher reaction temperature of 100 °C was found to be detrimental (Table 2-1, entry 11). Further examination of the stoichiometry indicated that increasing the amount of **2a** from 1.2 to 1.5 equiv resulted in almost exclusive formation of **3aa** in an excellent assay yield of 97% with 92% isolated yield (Table 2-1, entry 12). The phosphine ligand bound to palladium also proved to be critical. Variation of the bidentate phosphine ligand to dppe, dppb, dppp, dppf and Xantphos all led to substantial decreases in the reaction conversion (Supporting Information, Table 2-S2). Control experiments confirmed the dependency on both the phosphine ligand and the palladium source in this transformation (Table 2-1, entries 13 and 14). Increasing the CO pressure to 8.6 atm resulted in low yield (Table 2-1, entry 15), which suggested a higher CO pressure could potentially saturate the metal catalyst and deactivate it.

**Table 2-1.** Optimization of reaction conditions for benzylic C–H carbonylative arylation of **1a** with **2a**.



Entry	Pd source	Solvent	Temp (°C)	3aa yield (%) <sup>b</sup>
-------	-----------	---------	-----------	----------------------------

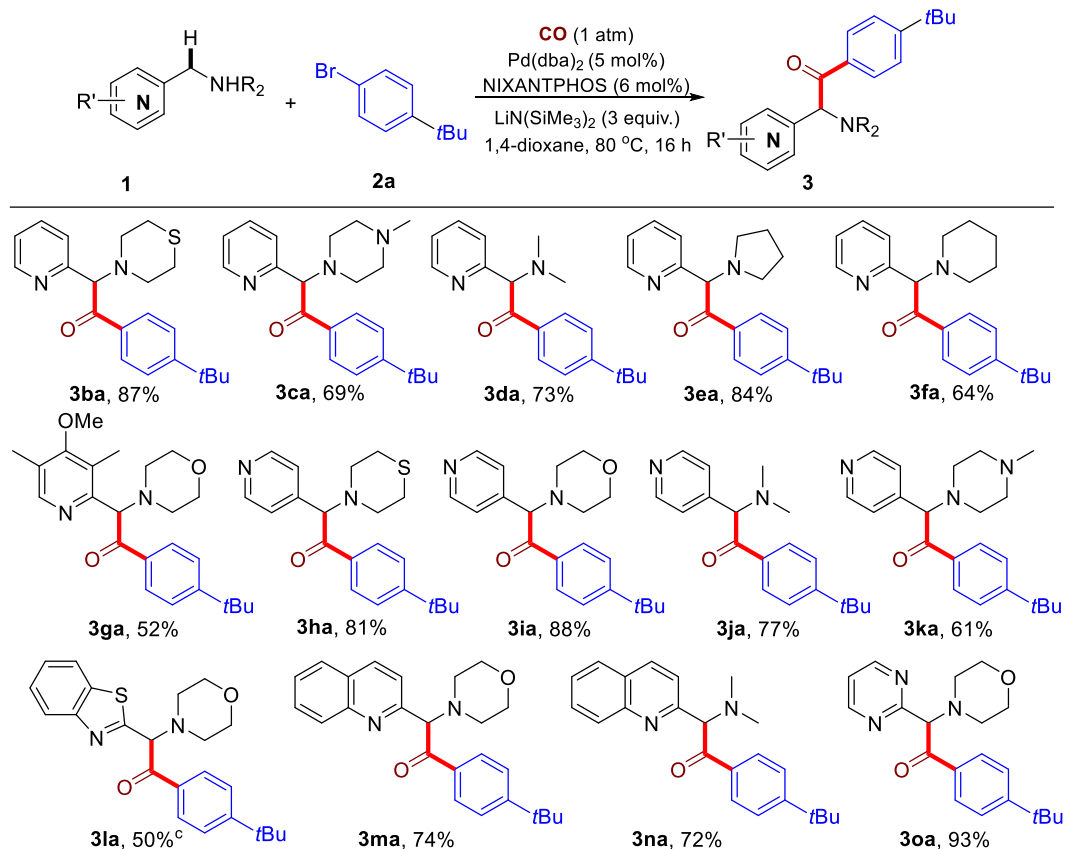
1	Pd(OAc) <sub>2</sub>	1,4-dioxane	65	27
2	Pd(OAc) <sub>2</sub>	THF	65	22
3	Pd(OAc) <sub>2</sub>	CPME	65	21
4	Pd(OAc) <sub>2</sub>	DME	65	10
5	Pd <sub>2</sub> (dba) <sub>3</sub>	1,4-dioxane	65	31
6	Pd G4 dimer	1,4-dioxane	65	37
7	[PdCl(allyl)] <sub>2</sub>	1,4-dioxane	65	7
8	Pd(dba) <sub>2</sub>	1,4-dioxane	65	43
9 <sup>c</sup>	Pd(dba) <sub>2</sub>	1,4-dioxane	65	89
10 <sup>c</sup>	Pd(dba) <sub>2</sub>	1,4-dioxane	80	93
11 <sup>c</sup>	Pd(dba) <sub>2</sub>	1,4-dioxane	100	89
<b>12<sup>c,d</sup></b>	<b>Pd(dba)<sub>2</sub></b>	1,4-dioxane	<b>80</b>	<b>97 (92)<sup>e</sup></b>
13 <sup>c,d,f</sup>	Pd(dba) <sub>2</sub>	1,4-dioxane	80	0
14 <sup>c,d</sup>	/	1,4-dioxane	80	0
<b>15<sup>c,d,g</sup></b>	<b>Pd(dba)<sub>2</sub></b>	<b>1,4-dioxane</b>	<b>80</b>	<b>4</b>

<sup>a</sup>Reaction conditions: **1a** (0.1 mmol), **2a** (0.12 mmol), LiN(SiMe<sub>3</sub>)<sub>2</sub> (2 equiv), [Pd] (5 mol%), NIXANTPHOS (6 mol%), solvent (1 mL). <sup>b</sup>Yields were determined by <sup>1</sup>H NMR analysis of unpurified reaction mixtures with internal standard CH<sub>2</sub>Br<sub>2</sub>. <sup>c</sup>LiN(SiMe<sub>3</sub>)<sub>2</sub> (2 equiv) was employed <sup>d</sup>**2a** (1.5 equiv) was employed. <sup>e</sup>Isolated yield. <sup>f</sup>In the absence of NIXANTPHOS. <sup>g</sup>CO (8.6 atm) was applied. Pd G4 dimer: Buchwald G4 Precatalysts; dba: dibenzylideneacetone.

With the optimized reaction conditions in hand, Dr. Haoqiang Zhao then evaluated the substrate scope of azaarylmethylamines and the results are summarized in Table 2. 2-Pyridylmethylamines (**1b–1f**) bearing thiomorpholine, methylpiperazine, dimethylamine, pyrrolidine and piperidine underwent smooth C–H carbonylative arylation to afford the expected  $\alpha$ -amino ketone products (**3ba–3fa**) in 64–87% yield. Substrate **1g** bearing a sterically hindered *ortho*-substituent on the pyridine ring was also reactive, delivering the

desired product **3ga** in 52% yield. The more acidic 4-pyridylmethylamines (**1h–1k**) containing different amino groups reacted efficiently to give the desired products (**3ah–3ak**) in 61–88% yield. In the case of 3-pyridylmethylamine, however, the reaction failed to yield any desired product, with recovery of most of the starting materials, even with the use of  $\text{KN}(\text{SiMe}_3)_2$  instead of  $\text{LiN}(\text{SiMe}_3)_2$  at 110 °C.<sup>21c</sup> It is likely that the higher  $\text{p}K_a$  of this pronucleophile (as least 3  $\text{p}K_a$  units difference) inhibits formation of sufficient quantities of the nucleophile and prevents the reaction from proceeding.<sup>20</sup> To further extend the scope of this carbonylative arylation, other azaarylmethylamines were tested. Notably, when 4-(benzo[d]thiazol-2-ylmethyl)morpholine **1l** was employed, the mixed products of ketone and enol structure (**3la**) were obtained in 50% yield, and the ratio was ketone: enol = 3:1. However, for other kinds of azaarylmethylamines like 2-(morpholinomethyl)benzo[d]oxazole, 4-((1-methyl-1H-imidazol-2-yl)methyl)morpholine, 4-benzylmorpholine or even 2-(ethoxymethyl)pyridine, the reaction failed to yield the desired products (See SI, Table S3). When 2-quinolinylmethyl amines **1m** and **1n** were employed, the corresponding products **3ma** and **3na** were obtained in 74% and 72% yields, respectively. Moreover, 2-pyrimidylmethylamine **1o** also reacted smoothly, affording product **3oa** in 93% yield.

**Table 2-2.** Pd-catalyzed benzylic C–H carbonylative arylation of azaarylmethylamines **1** with **2a**.<sup>a,b</sup>

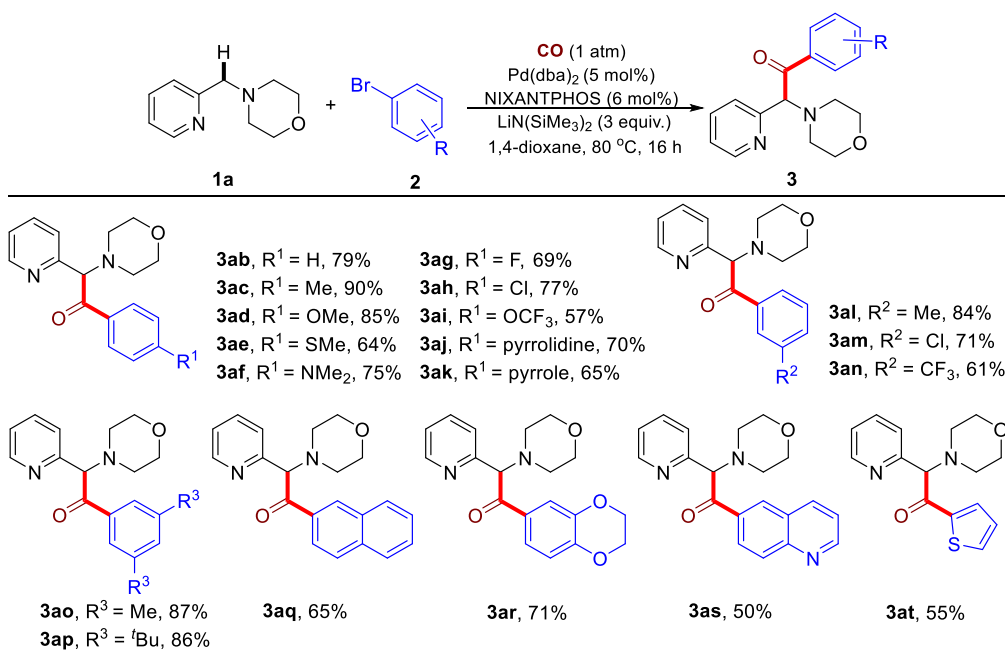


<sup>a</sup>Reaction conditions: **1** (0.2 mmol), **2a** (0.3 mmol), Pd(dba)<sub>2</sub> (5 mol%), NIXANTPHOS (6 mol%), LiN(SiMe<sub>3</sub>)<sub>2</sub> (3.0 equiv), 1,4-dioxane (2.0 mL), 80 °C, 16 h, under CO atmosphere (1 atm). <sup>b</sup>Isolated yields. <sup>c</sup>The mixture of ketone and enol forms have been obtained (ketone: enol = 3:1).

I continued to investigate the reaction of various aryl bromides with **1a** under 1 atm CO (Table 3). A variety of *para*-substituted aryl bromides bearing electron-donating groups (**2b–2f**, **2j** and **2k**) and electron-withdrawing groups (**2g–2i**) were all effective reaction partners, providing the corresponding products (**3ab–3ak**) in moderate to high yields (57–90%). Moreover, the reaction could be successfully extended to *meta*-substituted aryl bromides (**2l–2n**), delivering the desired products (**3al–3an**) in 61–84% yields. Lower yields were generally observed with electron-poor aryl bromides, possibly due to the partial decomposition of these aryl bromides in the presence of the base. Notably, 1-

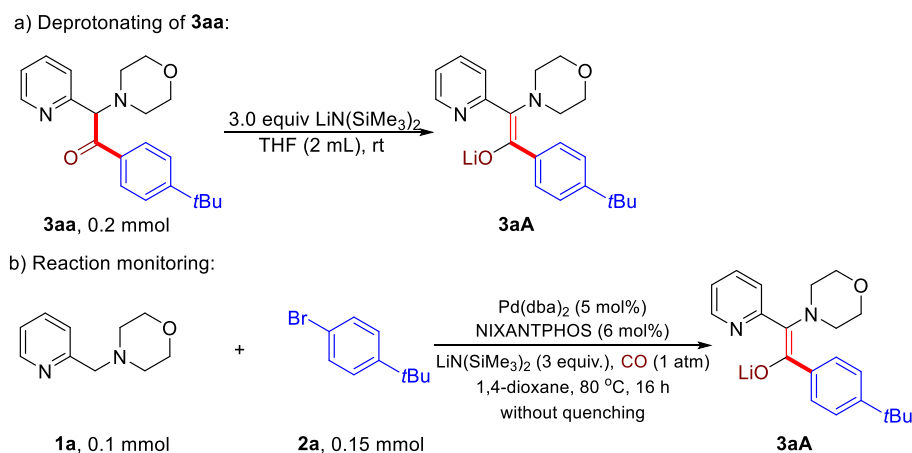
bromo-4-chlorobenzene (**2h**) and 1-bromo-3-chlorobenzene (**2m**) led to the formation of products **3ah** and **3am** in 77% and 71% yields, respectively, with the chloro group remaining intact during the reaction process. The Pd(NIXANTPHOS)-based catalysts is known to oxidatively add aryl chlorides at room temperature (see SI, Table 2-S2).<sup>21</sup> In the presence of CO, however, aryl chlorides were not reactive. These observations suggest to us that the palladium catalyst bears a CO ligand that tempers its ability to oxidatively add the stronger C–Cl bond of aryl chlorides. The multi-substituted aryl bromides (**3o–3r**) also readily engaged in the transformation to afford the corresponding products (**3ao–3ar**) in 65–87% yields. The generality of the current catalytic system was further demonstrated by the success of heteroaryl bromides **2s** and **2t** to generate **3as** and **3at** in 50% and 55% yields, respectively. It is noteworthy that the products of these reactions are rich in heterocycles.

**Table 2-3.** Pd-catalyzed benzylic C-H carbonylative arylation of **1a** with aryl bromides.<sup>a,b</sup>



<sup>a</sup>Reaction conditions: **1a** (0.2 mmol), **2** (0.3 mmol), Pd(dba)<sub>2</sub> (5 mol%), NIXANTPHOS (6 mol%), LiN(SiMe<sub>3</sub>)<sub>2</sub> (3.0 equiv), 1,4-dioxane (2.0 mL), 80 °C, 16 h, under CO atmosphere (1atm). <sup>b</sup>Isolated yields.

Preliminary studies were conducted to gain insight into the reaction pathway. We hypothesized that the product generated under the reaction conditions before workup was not the ketone, but the enolate that is protonated upon aqueous workup. Thus, we first prepared the enolate **3aA** by deprotonation of ketone **3aa** with LiN(SiMe<sub>3</sub>)<sub>2</sub> (Scheme 2-3, a). Next, the carbonylative  $\alpha$ -arylation reaction of **1a**, **2a** and CO was conducted, and the product characterized by NMR spectroscopy before quenching with water (Scheme 2-3, b). This product was found to be identical to the independently synthesized enolate **3aA**, confirming our hypothesis the enolate is the product of the reaction (Scheme 2-3).

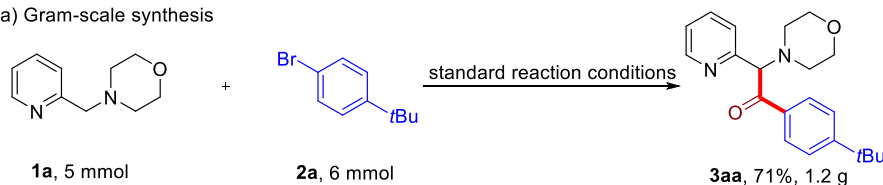


### Scheme 2-3. Detection of product precursor.

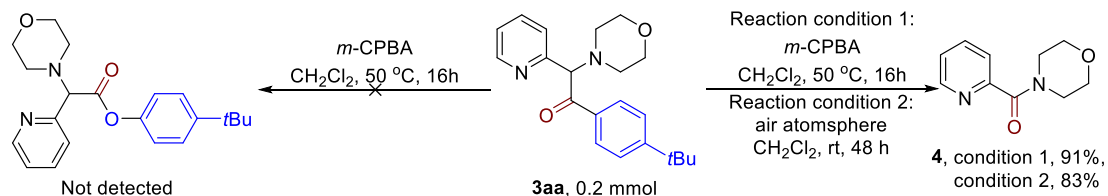
To showcase the synthetic utility of our method, we first conducted a gram-scale reaction of **1a**, **2a** and CO under the standard reaction conditions. The desired product **3aa** was obtained in 71% yield (1.2 g) (Scheme 2-4, a). Next, we attempted the transformation of the product ketones into other useful derivatives. Although Baeyer-Villiger oxidation of **3aa** with *m*-CPBA in CH<sub>2</sub>Cl<sub>2</sub> failed to give the desired ester, an unexpected oxidative

cleavage reaction occurred to give product **4** in 91% yield (Scheme 2-4, b). Notably, further study revealed that this oxidative cleavage reaction could take place under air oxidation to give a high yield of **4** (86%). Moreover, reduction of **3aa** with NaBH<sub>4</sub> in MeOH at room temperature for 16 h resulted in the formation of amino alcohol product **5** in 68% yield (Scheme 2-4, c). Finally, treatment of **3aa** with LiN(SiMe<sub>3</sub>)<sub>2</sub> and Me<sub>2</sub>NEt followed by addition of allyl chloroformate gave the allyl enol carbonate product **6** in 87% isolated yield as a single diastereomer (Scheme 2-4, d). As reported by the Stoltz group,<sup>22</sup> this enol carbonate product can undergo palladium-catalyzed enantioselective decarboxylative allylic alkylation to afford a chiral  $\alpha$ -quaternary ketone.

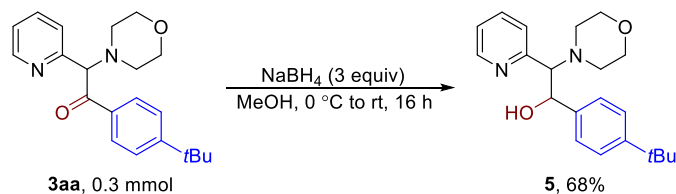
a) Gram-scale synthesis



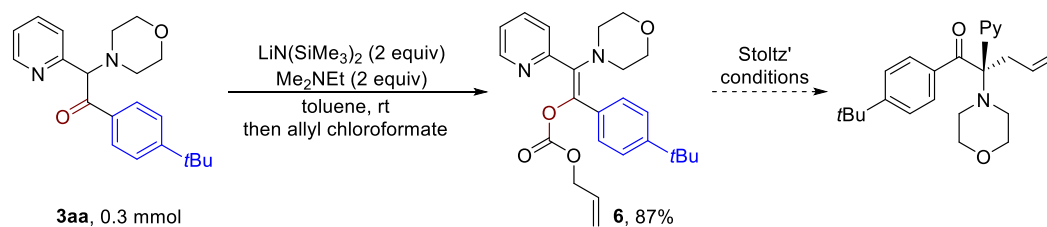
b) Oxidation of **3aa**



c) Reduction of **3aa**



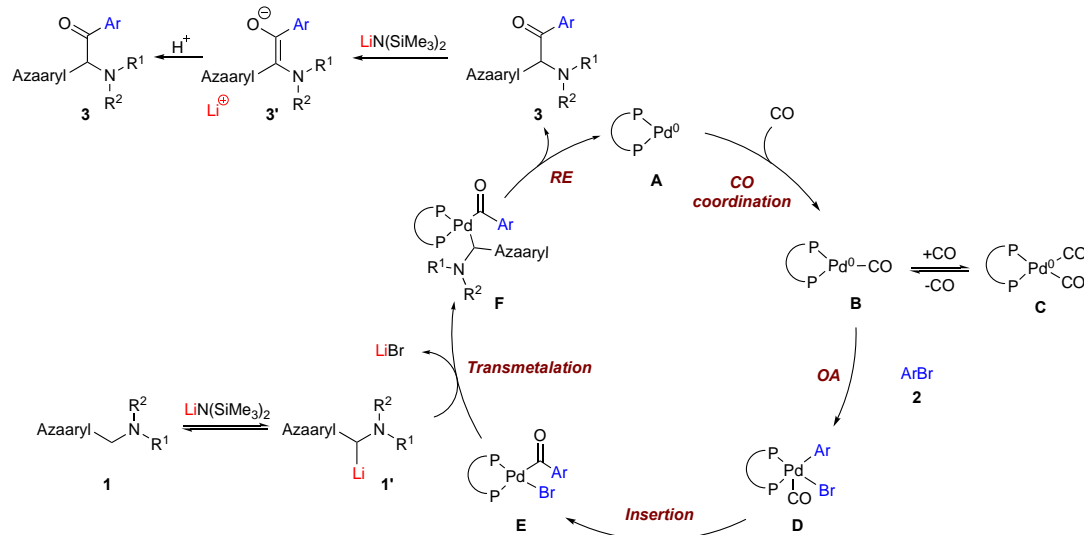
d) Synthesis of allyl enol carbonate product





#### Scheme 2-4. Synthetic Applications

Based on the aforementioned results in DCCP chemistry<sup>21</sup> and previous reports on carbonylative arylation,<sup>19,23</sup> a plausible mechanism is proposed in Scheme 2-5. The catalytic cycle starts with complexation of NIXANTPHOS and Pd(dba)<sub>2</sub> to yield the (NIXANTPHOS)Pd(0) species **A**.<sup>21a</sup> Under CO atmosphere, the Pd(0) species is proposed to undergo CO coordination to generate Pd(0) carbonyl (**B**) and dicarbonyl **C** complexes.<sup>23b</sup> Upon dissociation of CO from **C** to generate the 16 electron mono-carbonyl adduct **B**, oxidative addition of the aryl bromide **2** takes place to produce (NIXANTPHOS)Pd(CO)(Ar)Br-complex **D**. Intermediate **D** likely undergoes CO insertion into the Pd–Ar bond to furnish the acyl-Pd(II) complex **E**. Intermediate **E** reacts with the deprotonated pronucleophile **1'** in a transmetallation step to deliver the reductive elimination precursor **F**. Reductive elimination of **F** gives the ketone product **3** and Pd(0) species **A** to close the catalytic cycle. In the presence of excess LiN(SiMe<sub>3</sub>)<sub>2</sub> the ketone **3** is rapidly deprotonated, furnishing the enolate **3'**. Quenching the reaction with H<sub>2</sub>O results in the formation of the observed ketone product **3**. The direct coupling product likely forms when transmetallation takes place before CO insertion or if CO insertion is reversible. At this stage, we cannot rule out the possibility of an adduct between Pd(0) and the enolate, as described by Strydom and coworkers.<sup>19c</sup> Further investigations into the reaction mechanism will be presented in due course.



**Scheme 2-5.** Plausible Mechanism.

## 2.3 Conclusions

In conclusion, we have developed the carbonylative arylation of weakly acidic benzylic  $\text{C}(\text{sp}^3)\text{-H}$  bonds of azaarylmethylamines with aryl bromides and CO using a Pd catalyst. This work is unique in that it employs pronucleophiles with high  $\text{p}K_a$  values, suggesting a wide variety of previously overlooked substrates may be viable coupling partners in carbonylation reactions. The reaction is operative under 1 atm of CO and does not require high pressure equipment. This one-pot cascade process is applicable to the coupling of a wide range of azaarylmethylamines and aryl bromides, enabling facile access to useful  $\alpha$ -amino aryl-azaarylmethyl-ketones in moderate to high yields with good functional group tolerance. This work provides an attractive and complementary approach to prepare heteroatom-rich  $\alpha$ -amino ketones.

## 2.4 References

1. (a) Myers, M. C.; Wang, J.; Iera, J. A.; Bang, J.-k.; Hara, T.; Saito, S. i.; Zambetti, G. P.; Appella, D. H. *J. Am. Chem. Soc.* **2005**, *127*, 6152-6153. (b) Carroll, F. I.; Blough, B. E.; Abraham, P.; Mills, A. C.; Holleman, J. A.; Wolckenhauer, S. A.; Decker, A. M.; Landavazo, A.; McElroy, K. T.; Navarro, H. A. *J. Med. Chem.* **2009**, *52*, 6768-6781. (c) Meltzer, P. C.; Butler, D.; Deschamps, J. R.; Madras, B. K. *J. Med. Chem.* **2006**, *49*, 1420-1432. (d) Kolesnikova, T. O.; Khatsko, S. L.; Demin, K. A.; Shevyrin, V. A.; Kalueff, A. V. *ACS Chem. Neurosci.* **2018**, *10*, 168-174. (e) Nchinda, A. T.; Chibale, K.; Redelinghuys, P.; Sturrock, E. D. *Bioorg. Med. Chem. Lett.* **2006**, *16*, 4612-4615. (f) Váradi, A.; Palmer, T. C.; Haselton, N.; Afonin, D.; Subrath, J. J.; Le Rouzic, V.; Hunkele, A.; Pasternak, G. W.; Marrone, G. F.; Borics, A. *ACS Chem. Neurosci.* **2015**, *6*, 1570-1577. (g) Gevorgyan, G.; Gasparyan, N.; Papoyan, O.; Avakimyan, D.; Tatevosyan, A.; Panosyan, H. *Pharm. Chem. J.* **2017**, *51*, 107-110.
2. (a) Hill, R. K.; Nugara, P. N.; Holt, E. M.; Holland, K. P. *J. Org. Chem.* **1992**, *57*, 1045-1047. (b) Franzén, R. G. *J. Comb. Chem.* **2000**, *2*, 195-214. (c) Bouteiller, C.; Becerril-Ortega, J.; Marchand, P.; Nicole, O.; Barré, L.; Buisson, A.; Perrio, C. *Org. Biomol. Chem.* **2010**, *8*, 1111-1120. (d) Gediya, S. K.; Clarkson, G. J.; Wills, M. *J. Org. Chem.* **2020**, *85*, 11309-11330.
3. (a) Greck, C.; Drouillat, B.; Thomassigny, C. *Eur. J. Org. Chem.* **2004**, *2004*, 1377-1385. (b) Smith, A. M.; Hii, K. K. *Chem. Rev.* **2011**, *111*, 1637-1656. (c) Mailyan, A. K.; Eickhoff, J. A.; Minakova, A. S.; Gu, Z.; Lu, P.; Zakarian, A. *Chem. Rev.* **2016**, *116*, 4441-4557. (d) Zhou, F.; Liao, F.-M.; Yu, J.-S.; Zhou, J. *Synthesis.* **2014**, *46*, 2983-3003. (e) Vilaivan, T.; Bhanthumnavin, W. *Molecules.* **2010**, *15*, 917-958. (f) Marigo,

M.; Jørgensen, K. A. *Chem. Commun.* **2006**, 2001-2011. (g) Janey, J. M. *Angew. Chem. Int. Ed.* **2005**, *44*, 4292-4300. (h) de la Torre, A.; Tona, V.; Maulide, N. *Angew. Chem. Int. Ed.* **2017**, *56*, 12416-12423.

4. (a) Fisher, L. E.; Muchowski, J. M. *Org. Prep. Proced. Int.* **1990**, *22*, 399-484. (b) Cecere, G.; König, C. M.; Alleva, J. L.; MacMillan, D. W. *J. Am. Chem. Soc.* **2013**, *135*, 11521-11524. (c) Fisher, D. J.; Burnett, G. L.; Velasco, R.; Read de Alaniz, J. *J. Am. Chem. Soc.* **2015**, *137*, 11614-11617. (d) Ramakrishna, I.; Sahoo, H.; Baidya, M. *Chem. Commun.* **2016**, *52*, 3215-3218. (e) Huang, X.; Webster, R. D.; Harms, K.; Meggers, E. *J. Am. Chem. Soc.* **2016**, *138*, 12636-12642. (f) Ramakrishna, I.; Bhajammanavar, V.; Mallik, S.; Baidya, M. *Org. Lett.* **2017**, *19*, 516-519. (g) Zhou, Z.; Cheng, Q.-Q.; Kürti, L. *J. Am. Chem. Soc.* **2019**, *141*, 2242-2246.

5. (a) Erdik, E. *Tetrahedron.* **2004**, *40*, 8747-8782. (b) Wei, Y.; Lin, S.; Liang, F. *Org. Lett.* **2012**, *14*, 4202-4205. (c) Vander Wal, M. N.; Dilger, A. K.; MacMillan, D. W. *Chem. Sci.* **2013**, *4*, 3075-3079. (d) Xu, B.; Zhu, S. F.; Zuo, X. D.; Zhang, Z. C.; Zhou, Q. *Angew. Chem. Int. Ed.* **2014**, *53*, 3913-3916. (e) Miles, D. H.; Guasch, J.; Toste, F. D. *J. Am. Chem. Soc.* **2015**, *137*, 7632-7635. (f) Guha, S.; Rajeshkumar, V.; Kotha, S. S.; Sekar, G. *Org. Lett.* **2015**, *17*, 406-409.

6. (a) Lamani, M.; Prabhu, K. R. *Chem. Eur. J.* **2012**, *18*, 14638-14642. (b) Evans, R. W.; Zbieg, J. R.; Zhu, S.; Li, W.; MacMillan, D. W. *J. Am. Chem. Soc.* **2013**, *135*, 16074-16077. (c) Rajeshkumar, V.; Chandrasekar, S.; Sekar, G. *Org. Biomol. Chem.* **2014**, *12*, 8512-8518. (d) Lv, Y.; Li, Y.; Xiong, T.; Lu, Y.; Liu, Q.; Zhang, Q. *Chem. Commun.* **2014**, *50*, 2367-2369. (e) Xu, C.; Zhang, L.; Luo, S. *Angew. Chem.* **2014**, *126*, 4233-4237. (f) Jiang, Q.; Xu, B.; Zhao, A.; Jia, J.; Liu, T.; Guo, C. *J. Org. Chem.* **2014**,

- 79, 8750-8756. (g) Liang, S.; Zeng, C.-C.; Tian, H.-Y.; Sun, B.-G.; Luo, X.-G.; Ren, F.-z. *J. Org. Chem.* **2016**, *81*, 11565-11573. (h) Strehl, J.; Hilt, G. *Org. Lett.* **2020**, *22*, 5968-5972.
7. (a) Murry, J. A.; Frantz, D. E.; Soheili, A.; Tillyer, R.; Grabowski, E. J.; Reider, P. J. *J. Am. Chem. Soc.* **2001**, *123*, 9696-9697. (b) Mattson, A. E.; Scheidt, K. A. *Org. Lett.* **2004**, *6*, 4363-4366. (c) Mennen, S. M.; Gipson, J. D.; Kim, Y. R.; Miller, S. J. *J. Am. Chem. Soc.* **2005**, *127*, 1654-1655. (d) Li, G.-Q.; Dai, L.-X.; You, S.-L. *Chem. Commun.* **2007**, 852-854. (e) Garrett, M. R.; Tarr, J. C.; Johnson, J. S. *J. Am. Chem. Soc.* **2007**, *129*, 12944-12945. (f) Sun, L. H.; Liang, Z. Q.; Jia, W. Q.; Ye, S. *Angew. Chem.* **2013**, *125*, 5915-5918. (g) Zhang, H.-H.; Yu, S. *Org. Lett.* **2019**, *21*, 3711-3715. (h) Shu, X.; Huan, L.; Huang, Q.; Huo, H. *J. Am. Chem. Soc.* **2020**, *142*, 19058-19064.
8. Kells, K. W.; Chong, J. M. *J. Am. Chem. Soc.* **2004**, *126*, 15666-15667.
9. (a) Yang, H.; Li, H.; Wittenberg, R.; Egi, M.; Huang, W.; Liebeskind, L. S. *J. Am. Chem. Soc.* **2007**, *129*, 1132-1140. (b) Yang, H.; Liebeskind, L. S. *Org. Lett.* **2007**, *9*, 2993-2995. (c) Li, H.; Yang, H.; Liebeskind, L. S. *Org. Lett.* **2008**, *10*, 4375-4378. (d) Liebeskind, L. S.; Yang, H.; Li, H. *Angew. Chem.* **2009**, *121*, 1445-1449.
10. (a) Sun, T.; Hou, G.; Ma, M.; Zhang, X. *Adv. Synth. Catal.* **2011**, *353*, 253-256. (b) Wen, W.; Zeng, Y.; Peng, L.-Y.; Fu, L.-N.; Guo, Q.-X. *Org. Lett.* **2015**, *17*, 3922-3925.
11. (a) Ooi, T.; Takahashi, M.; Doda, K.; Maruoka, K. *J. Am. Chem. Soc.* **2002**, *124*, 7640-7641. (b) Frongia, A.; Secci, F.; Capitta, F.; Piras, P. P.; Sanna, M. L. *Chem. Commun.* **2013**, *49*, 8812-8814. (c) Zhang, X.; Staples, R. J.; Rheingold, A. L.; Wulff, W.

- D. *J. Am. Chem. Soc.* **2014**, *136*, 13971-13974. (d) Yadagiri, D.; Anbarasan, P. *Chem. Commun.* **2015**, *51*, 14203-14206.
12. (a) Villar, A.; Hövelmann, C. H.; Nieger, M.; Muñoz, K. *Chem. Commun.* **2005**, 3304-3306. (b) Prasad, P. K.; Reddi, R. N.; Sudalai, A. *Org. Lett.* **2016**, *18*, 500-503. (c) Shinde, M. H.; Kshirsagar, U. A. *Org. Biomol. Chem.* **2016**, *14*, 858-861. (d) Xu, S.; Wu, P.; Zhang, W. *Org. Biomol. Chem.* **2016**, *14*, 11389-11395.
13. (a) Tellitu, I.; Serna, S.; Herrero, M. T.; Moreno, I.; Domínguez, E.; SanMartin, R. *J. Org. Chem.* **2007**, *72*, 1526-1529. (b) Miura, T.; Biyajima, T.; Fujii, T.; Murakami, M. *J. Am. Chem. Soc.* **2012**, *134*, 194-196. (c) Cacchi, S.; Fabrizi, G.; Filisti, E.; Goggiamani, A.; Iazzetti, A.; Maurone, L. *Org. Biomol. Chem.* **2012**, *10*, 4699-4703. (d) Sueda, T.; Kawada, A.; Urashi, Y.; Teno, N. *Org. Lett.* **2013**, *15*, 1560-1563. (e) Chalotra, N.; Rizvi, M. A.; Shah, B. A. *Org. Lett.* **2019**, *21*, 4793-4797. (f) Zhang, Z.; Luo, Y.; Du, H.; Xu, J.; Li, P. *Chem. Sci.* **2019**, *10*, 5156-5161.
14. Guo, W.; Luo, Y.; Sung, H. H.-Y.; Williams, I. D.; Li, P.; Sun, J. *J. Am. Chem. Soc.* **2020**, *142*, 14384-14390.
15. (a) Ojima, I. *Chem. Rev.* **1988**, *88*, 1011-1030. (b) Brennführer, A.; Neumann, H.; Beller, M. *ChemCatChem.* **2009**, *1*, 28-41. (c) Franke, R.; Selent, D.; Börner, A. *Chem. Rev.* **2012**, *112*, 5675-5732. (d) Quesnel, J. S.; Arndtsen, B. A. *Pure Appl. Chem.* **2013**, *85*, 377-384. (e) Wu, X.-F.; Fang, X.; Wu, L.; Jackstell, R.; Neumann, H.; Beller, M. *Acc. Chem. Res.* **2014**, *47*, 1041-1053. (f) Wu, L.; Fang, X.; Liu, Q.; Jackstell, R.; Beller, M.; Wu, X.-F. *ACS Catal.* **2014**, *4*, 2977-2989. (g) Gautam, P.; Bhanage, B. M. *Catal. Sci. Technol.* **2015**, *5*, 4663-4702. (h) Bai, Y.; Davis, D. C.; Dai, M. *J. Org. Chem.* **2017**, *82*, 2319-2328. (i) Li, Y.; Hu, Y.; Wu, X.-F. *Chem. Soc. Rev.* **2018**, *47*, 172-194. (j)

- Peng, J.-B.; Geng, H.-Q.; Wu, X.-F. *Chem.* **2019**, *5*, 526-552. (k) Peng, J.-B.; Wu, F.-P.; Wu, X.-F. *Chem. Rev.* **2018**, *119*, 2090-2127.
16. (a) Zhu, J.; Bienaymé, H., *Multicomponent reactions*. John Wiley & Sons 2006. (b) Brennfürer, A.; Neumann, H.; Beller, M. *Angew. Chem. Int. Ed.* **2009**, *48*, 4114-4133.
17. Liu, Y.; Zhang, Z.; Zhang, S.; Zhang, Y.; Wang, J.; Zhang, Z. *Chem. Asian J.* **2018**, *13*, 3658-3663.
18. (a) Kobayashi, T.-a.; Tanaka, M. *Tetrahedron Lett.* **1986**, *27*, 4745-4748. (b) Negishi, E.-i.; Copéret, C.; Sugihara, T.; Shimoyama, I.; Zhang, Y.; Wu, G.; Tour, J. M. *Tetrahedron.* **1994**, *50*, 425-436. (c) Negishi, E.-i.; Makabe, H.; Shimoyama, I.; Wu, G.; Zhang, Y. *Tetrahedron.* **1998**, *54*, 1095-1106. (d) Zheng, Z.; Alper, H. *Org. Lett.* **2009**, *11*, 3278-3281.
19. (a) Gøgsig, T. M.; Taaning, R. H.; Lindhardt, A. T.; Skrydstrup, T. *Angew. Chem.* **2012**, *124*, 822-825. (b) Korsager, S.; Nielsen, D. U.; Taaning, R. H.; Skrydstrup, T. *Angew. Chem. Int. Ed.* **2013**, *52*, 9763-9766. (c) Schranck, J.; Tlili, A.; Alsabeh, P. G.; Neumann, H.; Stradiotto, M.; Beller, M. *Chem. Eur. J.* **2013**, *19*, 12624-12628. (d) Korsager, S.; Nielsen, D. U.; Taaning, R. H.; Lindhardt, A. T.; Skrydstrup, T. *Chem. Eur. J.* **2013**, *19*, 17687-17691. (e) Nielsen, D. U.; Lescot, C.; Gøgsig, T. M.; Lindhardt, A. T.; Skrydstrup, T. *Chem. Eur. J.* **2013**, *19*, 17926-17938. (f) Schranck, J.; Burhardt, M.; Bornschein, C.; Neumann, H.; Skrydstrup, T.; Beller, M. *Chem. Eur. J.* **2014**, *20*, 9534-9538. (g) Lian, Z.; Friis, S. D.; Skrydstrup, T. *Angew. Chem. Int. Ed.* **2014**, *53*, 9582-9586. (h) Lian, Z.; Friis, S. D.; Skrydstrup, T. *Chem. Commun.* **2015**, *51*, 3600-3603. (i)

- Makarov, I. S.; Kuwahara, T.; Jusseau, X.; Ryu, I.; Lindhardt, A. T.; Skrydstrup, T. *J. Am. Chem. Soc.* **2015**, *137*, 14043-14046. (j) Jensen, M. T.; Juhl, M.; Nielsen, D. U.; Jacobsen, M. F.; Lindhardt, A. T.; Skrydstrup, T. *J. Org. Chem.* **2016**, *81*, 1358-1366.
20. (a) Fraser, R. R.; Mansour, T. S.; Savard, S. *J. Org. Chem.* **1985**, *50*, 3232-3234. (b) Bordwell, F. G. *Acc. Chem. Res.* **1988**, *21*, 456-463.
21. (a) Zhang, J.; Bellomo, A.; Creamer, A. D.; Dreher, S. D.; Walsh, P. J. *J. Am. Chem. Soc.* **2012**, *134*, 13765-13772. (b) Bellomo, A.; Zhang, J.; Trongsirivat, N.; Walsh, P. J. *Chem. Sci.* **2013**, *4*, 849-857. (c) Kim, B.-S.; Jimenez, J.; Gao, F.; Walsh, P. J. *Org. Lett.* **2015**, *17*, 5788-5791. (d) Li, M.; González - Esguevillas, M.; Berritt, S.; Yang, X.; Bellomo, A.; Walsh, P. J. *Angew. Chem.* **2016**, *128*, 2875-2879. (e) Rivero, A. R.; Kim, B.-S.; Walsh, P. J. *Org. Lett.* **2016**, *18*, 1590-1593. (f) Yang, X.; Kim, B.-S.; Li, M.; Walsh, P. J. *Org. Lett.* **2016**, *18*, 2371-2374. (g) Jiménez, J.; Kim, B. S.; Walsh, P. J. *Adv. Synth. Catal.* **2016**, *358*, 2829-2837. (h) Zhang, J.; Sha, S.-C.; Bellomo, A.; Trongsirivat, N.; Gao, F.; Tomson, N. C.; Walsh, P. J. *J. Am. Chem. Soc.* **2016**, *138*, 4260-4266. (i) Li, M.; Yucel, B.; Jiménez, J.; Rotella, M.; Fu, Y.; Walsh, P. J. *Adv. Synth. Catal.* **2016**, *358*, 1910-1915. (j) Ablajan, K.; Panetti, G. B.; Yang, X.; Kim, B. S.; Walsh, P. J. *Adv. Synth. Catal.* **2017**, *359*, 1927-1932. (k) Gao, G.; Fu, Y.; Li, M.; Wang, B.; Zheng, B.; Hou, S.; Walsh, P. J. *Adv. Synth. Catal.* **2017**, *359*, 2890-2894. (l) Sha, S.-C.; Tcyrulnikov, S.; Li, M.; Hu, B.; Fu, Y.; Kozlowski, M. C.; Walsh, P. J. *J. Am. Chem. Soc.* **2018**, *140*, 12415-12423.
22. Lavernhe, R.; Alexy, E. J.; Zhang, H.; Stoltz, B. M. *Org. Lett.* **2020**.



23. (a) Miloserdov, F. M.; McMullin, C. L.; Belmonte, M. M. n.; Benet-Buchholz, J.; Bakhmutov, V. I.; Macgregor, S. A.; Grushin, V. V. *Organometallics*. **2014**, *33*, 736-752.
- (b) Wang, J. Y.; Strom, A. E.; Hartwig, J. F. *J. Am. Chem. Soc.* **2018**, *140*, 7979-7993.

## 2.5 Supporting Information

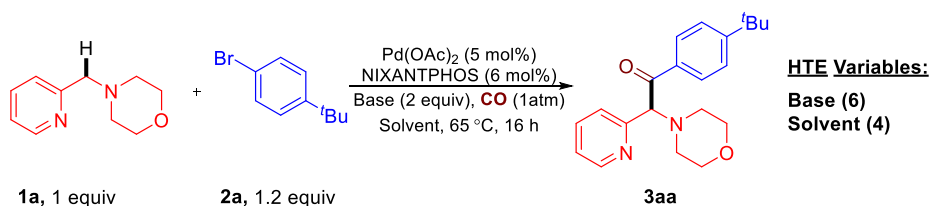
### 2.5.1 General information

Unless otherwise noted, all experiments were carried out in air and all commercially available chemicals, including organic solvents, were used as received from Aldrich, Acros or Strem without further purification.  $^1\text{H}$  NMR and  $^{13}\text{C}\{^1\text{H}\}$  NMR spectra were recorded on a Bruker Model Advance DMX 400 Spectrometer ( $^1\text{H}$  400 MHz and  $^{13}\text{C}$  101 MHz, respectively) or Bruker Model Advance DMX 500 Spectrometer ( $^1\text{H}$  500 MHz and  $^{13}\text{C}$  125 MHz, respectively). Chemical shifts ( $\delta$ ) are given in ppm and are referenced to residual solvent peaks.<sup>1, 1, 36, 36, 36</sup> Melting points were measured on X-4 melting point apparatus and are uncorrected. High resolution mass spectra (HRMS) were performed on a VG Autospec-3000 spectrometer. Column chromatography was performed with silica gel (200-300 mesh). Azaarylmethyl Amines were prepared according to the previous reports.<sup>1,2</sup>

### 2.5.2 Optimization of the reaction conditions

#### (a) HTE (High Throughput Experimentation) micro-scale (0.01 mmol) screen

**Table 2-S1.** Base and solvent screening.



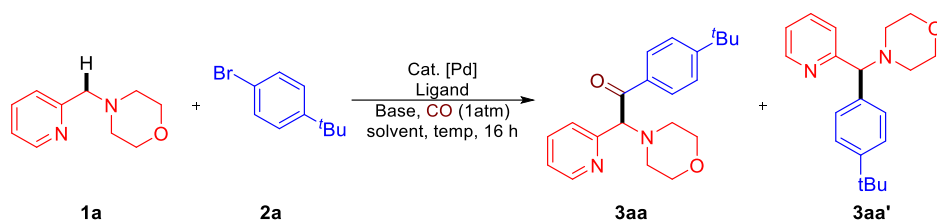
6 Base:  $\text{LiOtBu}$ ,  $\text{NaOtBu}$ ,  $\text{KOtBu}$ ,  $\text{LiN}(\text{SiMe}_3)_2$ ,  $\text{NaN}(\text{SiMe}_3)_2$ ,  $\text{KN}(\text{SiMe}_3)_2$ .

4 Solvent: Toluene, 1,4-dioxane, CMPE (cyclopentyl methyl ether), THF.

2:1 ratio relative to **1a** for base and 1.2:1 ratio for aryl bromide **2a**.

Entry	Base	Solvent	AY (%)
1	LiOtBu	Toluene	0
2	NaOtBu	Toluene	0
3	KotBu	Toluene	0
4	LiN(SiMe <sub>3</sub> ) <sub>2</sub>	Toluene	9
5	NaN(SiMe <sub>3</sub> ) <sub>2</sub>	Toluene	4
6	KN(SiMe <sub>3</sub> ) <sub>2</sub>	Toluene	2
7	LiOtBu	1,4-dioxane	0
8	NaOtBu	1,4-dioxane	0
9	KotBu	1,4-dioxane	0
10	LiN(SiMe <sub>3</sub> ) <sub>2</sub>	1,4-dioxane	22
11	NaN(SiMe <sub>3</sub> ) <sub>2</sub>	1,4-dioxane	6
12	KN(SiMe <sub>3</sub> ) <sub>2</sub>	1,4-dioxane	3
13	LiOtBu	CPME	0
14	NaOtBu	CPME	0
15	KotBu	CPME	0
16	LiN(SiMe <sub>3</sub> ) <sub>2</sub>	CPME	4
17	NaN(SiMe <sub>3</sub> ) <sub>2</sub>	CPME	0
18	KN(SiMe <sub>3</sub> ) <sub>2</sub>	CPME	0
19	LiOtBu	THF	0
20	NaOtBu	THF	0
21	KotBu	THF	0
22	LiN(SiMe <sub>3</sub> ) <sub>2</sub>	THF	7
23	NaN(SiMe <sub>3</sub> ) <sub>2</sub>	THF	0
24	KN(SiMe <sub>3</sub> ) <sub>2</sub>	THF	0

The lead hit from the screening was the combination of Pd(Oac)<sub>2</sub> (5 mol %), NIXANTPHOS (6 mol %), LiN(SiMe<sub>3</sub>)<sub>2</sub> (2 equiv), 1,4-dioxane as solvent under 1 atm CO at 65 °C for 16 h giving 22% assay yield of the desired carbonylation product **3aa**. A scale-up reaction on a 0.1 mmol scale using General Procedure for the Pd-Catalyzed Deprotonative Carbonylation of **1a** proved successful with 27% assay yield of **3aa** determined by <sup>1</sup>H NMR spectroscopy of the crude reaction mixture.

**(b) Lab scale (0.1 mmol) reaction conditions optimization****Table 2-S2.** Optimization of reaction conditions.a

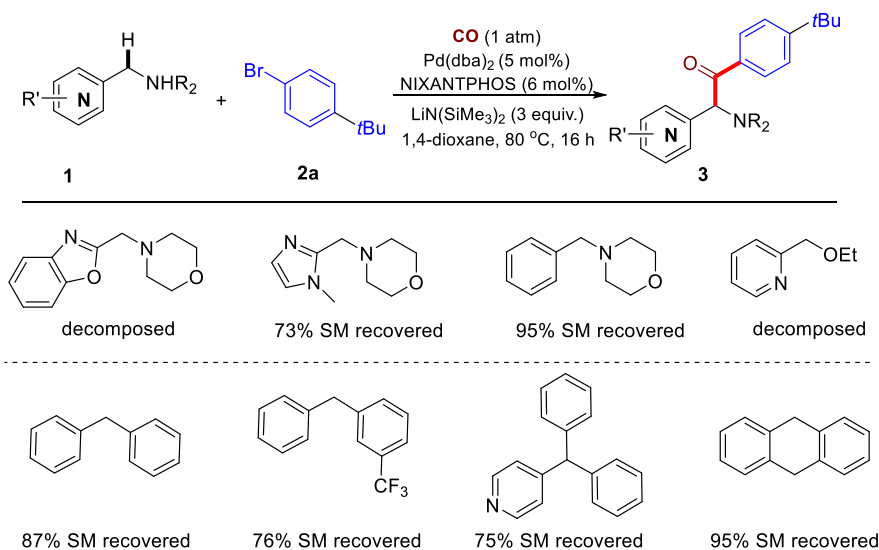
Entry	Pd source	Ligand	Solvent	Temp (°C)	1a:2a:base	Assay yield (%) <sup>b</sup>	
						3aa	3aa'
1	Pd(OAc) <sub>2</sub>	NIXANTPHOS	Toluene	65	1:1.2:2	18	5
2	Pd(OAc) <sub>2</sub>	NIXANTPHOS	DMSO	65	1:1.2:2	0	0
3	Pd(OAc) <sub>2</sub>	NIXANTPHOS	THF	65	1:1.2:2	22	4
4	Pd(OAc) <sub>2</sub>	NIXANTPHOS	CPME	65	1:1.2:2	21	9
5	Pd(OAc) <sub>2</sub>	NIXANTPHOS	DME	65	1:1.2:2	10	6
6	Pd(OAc) <sub>2</sub>	NIXANTPHOS	1,4-dioxane	65	1:1.2:2	27	8
7	Pd <sub>2</sub> (dba) <sub>3</sub>	NIXANTPHOS	1,4-dioxane	65	1:1.2:2	31	11
8	Pd(PPh <sub>3</sub> ) <sub>4</sub>	NIXANTPHOS	1,4-dioxane	65	1:1.2:2	22	trace
9	[PdCl(allyl)] <sub>2</sub>	NIXANTPHOS	1,4-dioxane	65	1:1.2:2	7	5
10	Pd G3 dimer	NIXANTPHOS	1,4-dioxane	65	1:1.2:2	32	trace
11	Pd(dba) <sub>2</sub>	NIXANTPHOS	1,4-dioxane	65	1:1.2:2	43	10
12	Pd G4 dimer	NIXANTPHOS	1,4-dioxane	65	1:1.2:2	37	14
13	Ni(acac) <sub>2</sub>	NIXANTPHOS	1,4-dioxane	65	1:1.2:2	0	0
14	Ni(COD) <sub>2</sub>	NIXANTPHOS	1,4-dioxane	65	1:1.2:2	0	0

15	NiBr <sub>2</sub>	NIXANTPHOS	1,4-dioxane	65	1:1.2:2	0	0
16 <sup>c</sup>	Pd(dba) <sub>2</sub>	NIXANTPHOS	1,4-dioxane	65	1:1.2:2	0	0
17 <sup>d</sup>	Pd(dba) <sub>2</sub>	NIXANTPHOS	1,4-dioxane	65	1:1.2:2	0	0
18 <sup>e</sup>	Pd(dba) <sub>2</sub>	NIXANTPHOS	1,4-dioxane	65	1:1.2:2	10	0
19 <sup>f</sup>	Pd(dba) <sub>2</sub>	NIXANTPHOS	1,4-dioxane	65	1:1.2:2	7	0
20 <sup>g</sup>	Pd(dba) <sub>2</sub>	NIXANTPHOS	1,4-dioxane	65	1:1.2:2	0	0
21	Pd(dba) <sub>2</sub>	NIXANTPHOS	1,4-dioxane	65	1:1.2:3	89	7
22	Pd(dba) <sub>2</sub>	dppf	1,4-dioxane	65	1:1.2:3	5	21
23	Pd(dba) <sub>2</sub>	dppp	1,4-dioxane	65	1:1.2:3	7	19
24	Pd(dba) <sub>2</sub>	dppb	1,4-dioxane	65	1:1.2:3	22	10
25	Pd(dba) <sub>2</sub>	dppe	1,4-dioxane	65	1:1.2:3	4	0
26	Pd(dba) <sub>2</sub>	Xantphos	1,4-dioxane	65	1:1.2:3	28	6
27 <sup>h</sup>	Pd(dba) <sub>2</sub>	NIXANTPHOS	1,4-dioxane	65	1:1.2:3	81	5
28 <sup>i</sup>	Pd(dba) <sub>2</sub>	NIXANTPHOS	1,4-dioxane	65	1:1.2:3	72	3
29	Pd(dba) <sub>2</sub>	NIXANTPHOS	1,4-dioxane	80	1:1.2:3	93	4
30	Pd(dba) <sub>2</sub>	NIXANTPHOS	1,4-dioxane	100	1:1.2:3	89	trace
31	Pd(dba) <sub>2</sub>	NIXANTPHOS	1,4-dioxane	rt	1:1.2:3	0	0
<b>32</b>	<b>Pd(dba)<sub>2</sub></b>	NIXANTPHOS	<b>1,4-dioxane</b>	<b>80</b>	<b>1:1.5:3</b>	<b>97 (92)<sup>j</sup></b>	<b>trace</b>

33 <sup>k</sup>	Pd(dba) <sub>2</sub>	NIXANTPHOS	1,4-dioxane	80	1:1.5:3	0	0
34 <sup>l</sup>	Pd(dba) <sub>2</sub>	NIXANTPHOS	1,4-dioxane	80	1:1.5:3	65	4
35 <sup>m</sup>	Pd(dba) <sub>2</sub>	NIXANTPHOS	1,4-dioxane	80	1:1.5:3	93	trace
36 <sup>n</sup>	Pd(dba) <sub>2</sub>	NIXANTPHOS	1,4-dioxane	80	1:1.5:3	4	0
37	Pd(dba) <sub>2</sub>	/	1,4-dioxane	80	1:1.5:3	0	0
38	/	NIXANTPHOS	1,4-dioxane	80	1:1.5:3	0	0

<sup>a</sup>**1a** (0.1 mmol, 1equiv), Pd source (5 mol%), ligand (6 mol%), solvent (0.1M). <sup>b</sup>Assay yields (AY) were determined by <sup>1</sup>H NMR analysis of unpurified reaction mixtures with internal standard CH<sub>2</sub>Br<sub>2</sub>. <sup>c</sup>12-crown-4 (2 equiv) was used. <sup>d</sup>TMEDA (2 equiv) was used. <sup>e</sup>NaN(SiMe<sub>3</sub>)<sub>2</sub> (3 equiv) was employed instead of LiN(SiMe<sub>3</sub>)<sub>2</sub>. <sup>f</sup>KN(SiMe<sub>3</sub>)<sub>2</sub> (3 equiv) was employed instead of LiN(SiMe<sub>3</sub>)<sub>2</sub>. <sup>g</sup>LDA (lithium diisopropylamide) (3 equiv) was employed instead of LiN(SiMe<sub>3</sub>)<sub>2</sub>. <sup>h</sup>1,4-Dioxane (0.2 mL) was employed. <sup>i</sup>1,4-Dioxane (0.05 mL) was employed. <sup>j</sup>Isolated yield. <sup>k</sup>1-Chloro-4-tertbutylbenzene was employed. <sup>l</sup>Pd(dba)<sub>2</sub> (2.5 mol%), NIXANTPHOS (3.0 mol%) was used. <sup>m</sup>Reaction time 8 h. <sup>n</sup>CO (8.6 atm) was employed. Pd G3 dimer: Buchwald G3 precatalysts; Pd G4 dimer: Buchwald G4 precatalysts; acac: acetylacetonate; COD: 1,5-cyclooctadiene; dba: dibenzylideneacetone.

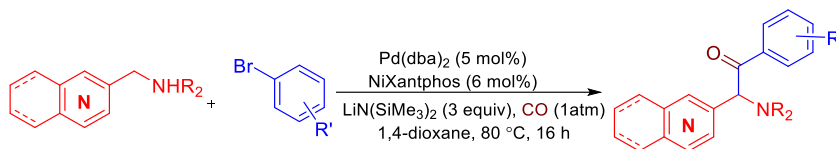
**Table 2-S3.** Non effective substrates in the reaction conditions.<sup>a</sup>



<sup>a</sup>Reaction conditions: **1** (0.2 mmol), **2a** (0.3 mmol), Pd(dba)<sub>2</sub> (5 mol%), NIXANTPHOS (6 mol%), LiN(SiMe<sub>3</sub>)<sub>2</sub> (3.0 equiv), 1,4-dioxane (2.0 mL), 80 °C, 16 h, under CO atmosphere (1 atm).

### 2.5.3. General Procedure for DCCC of Azaarylmethyl Amines

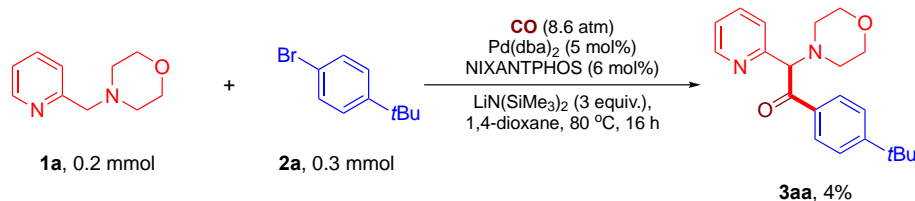
(a) General procedure under 1 atm CO.



An oven-dried 8 mL vial equipped with a stir bar was charged with Pd(dba)<sub>2</sub> (5 mol %) and NIXANTPHOS (6 mol %) under a nitrogen atmosphere in glove box. Next, 0.1M of 1,4-dioxane was taken up by syringe and added to the vial. The resulting solution stirred for 15 min at room temperature, during which time the mixture became red. This solution was used as the stock solution for this procedure. To an oven-dried 10 mL Schlenk tube with stir bar was added LiN(SiMe<sub>3</sub>)<sub>2</sub> (100.5 mg, 0.6 mmol, 3 equiv). A pipette was used to take 2 mL of the Pd/NIXANTPHOS stock solution and add it to the Schlenk tube. The resulting (dark green) solution was then stirred for 10 min at room temperature. Azaarylmethyl amine **1** (0.2 mmol, 1 equiv) and aryl bromide **2** (0.3 mmol, 1.5 equiv) were added to the reaction mixture, sequentially. The Schlenk tube was capped with rubber stopper and removed from the glove box. The reaction mixture was then degassed with CO by using Schlenk line, and connected with a CO balloon, placed in an 80 °C oil bath and stirred for 16 h. After this time, the flask was removed and stirred for 16 h at 80 °C. After this time, the tube was removed from the oil bath, allowed to cool to room temperature, uncapped carefully in a fume hood and the reaction quenched with two drops of H<sub>2</sub>O. After quench the color of the reaction mixture changed from brown to red. It was next diluted with 3.0 mL of ethyl acetate and filtered over a pad of MgSO<sub>4</sub> and Celite. The pad was rinsed with additional ethyl acetate (5.0 mL) and the resulting solution evaporated under vacuum to remove the volatile materials. The residue was

purified by column chromatography on silica gel using a mixture of ethyl acetate and hexanes to give the purified product.

(b) General procedure at high CO pressure.



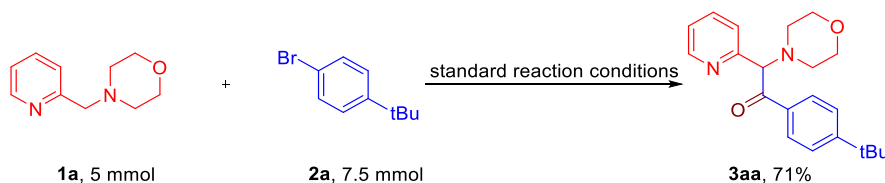
An oven-dried 8 mL vial equipped with a stir bar was sequentially added  $\text{Pd}(\text{dba})_2$  (5.8 mg, 0.01 mmol, 5 mol %) and NIXANTPHOS (6.6 mg, 0.012 mmol, 6 mol %) under a nitrogen atmosphere inside a glove box. Next, 2 mL of 1,4-dioxane was taken up by syringe and added to the flask at room temperature. The reaction mixture was stirred for 15 min at room temperature, until the mixture became red. Then  $\text{LiN}(\text{SiMe}_3)_2$  (100.5 mg, 0.6 mmol, 3 equiv) was added and the reaction mixture was stirred for 10 min at room temperature. Azaarylmethyl amine **1** (0.2 mmol, 1 equiv) and aryl bromide **2** (0.3 mmol, 1.5 equiv) were added to the reaction mixture, sequentially. The solution was then transferred to a 30 mL Parr Instruments 5000 Multiple Reactor system vessel. The reactor was then sealed, removed from the glovebox. The reaction vessel was then pressurized with CO at 8.6 atm. Reaction was run for 16 hours at 80 °C. After this time, reactor was cooled room temperature. The CO pressure was slowly released in a fume hood. Then the reactor was uncapped, and the reaction mixture was quenched with two drops of  $\text{H}_2\text{O}$ . The color of the reaction mixture changed from brown to red. It was next diluted with 3.0 mL of ethyl acetate and filtered over a pad of  $\text{MgSO}_4$  and Celite. The pad was rinsed with additional ethyl acetate (5.0 mL) and the resulting solution evaporated under vacuum to



remove the volatile materials. The assay yield was determined based on  $^1\text{H}$  NMR analysis by integration (< 4%).

## 2.5.4 The general procedure for synthetic applications

### (a) Gram-scale synthesis

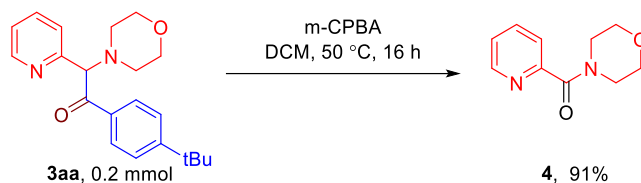


To an oven-dried 100 mL Schlenk flask with a stir bar were sequentially added  $\text{Pd}(\text{dba})_2$  (143.8 mg, 0.25 mmol, 5 mol %) and NIXANTPHOS (165.5 mg, 0.3 mmol, 6 mol %) under a nitrogen atmosphere inside a glove box. Next, 50 mL of 1,4-dioxane was taken up by syringe and added to the flask at room temperature. The reaction mixture was stirred for 30 min at room temperature, until the mixture became red. Then added  $\text{LiN}(\text{SiMe}_3)_2$  (2.5 g, 15 mmol, 3 equiv) and stirred for 20 min at room temperature. Pro-nucleophile **1a** (891.0 mg, 5 mmol, 1 equiv) and 4-*tert*-butyl-bromobenzene **2a** (1.6 g, 7.5 mmol, 1.5 equiv) were added to the reaction mixture sequentially. The Schlenk flask was capped, removed from the glove box, the reaction mixture was degassed with CO by using Schlenk line (the Schlenk flask was evacuated by Schlenk line and then refilled with CO gas), then connected with a CO balloon, and placed in an 80 °C oil bath and stirred for 16 h. After this time, the flask was removed from the oil bath, allowed to cool to room temperature, then the cap was carefully removed in the fume hood, exposing the solution to the atmosphere, and the reaction quenched with  $\text{H}_2\text{O}$  (1 mL). The color of the reaction mixture changed from dark brown to red. It was next diluted with 30 mL of ethyl acetate and filtered over a pad of  $\text{MgSO}_4$  and celite. The pad was rinsed with additional ethyl

acetate (50 mL) and evaporated under vacuum to remove the volatile materials. The residue was purified by column chromatography on silica gel using a mixture of ethyl acetate/hexanes (1/2, v/v) to give the pure product **3aa** (1.20 g, 71%) as yellow oil.

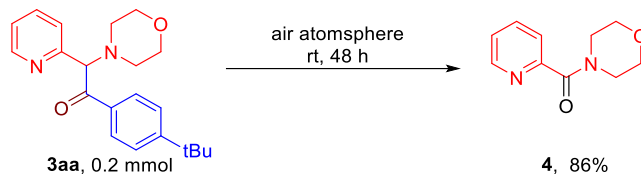
**(b) Oxidation of 3aa**

i) When *m*-CPBA was employed as an oxidant.<sup>3</sup>



A 20 mL reaction vial was charged with a stir bar and solution of 1-(4-(*tert*-butyl)phenyl)-2-morpholino-2-(pyridin-2-yl)ethan-1-one **3aa** (67.7 mg, 0.2 mmol) in 3 mL CHCl<sub>3</sub>. To the resulting clear solution was added *m*-CPBA as a solid (138.1 mg, 4 equiv) at room temperature with stirring, resulting in a brown suspension. The reaction mixture was heated to 50 °C in an oil bath and stirred for 16 h at this temperature. The reaction mixture was then allowed to cool to room temperature, quenched with 3 mL a solution of K<sub>2</sub>CO<sub>3</sub> (10%w/w) and extracted with CH<sub>2</sub>Cl<sub>2</sub> (3x5 mL). The combined organic layers were washed with brine, dried over Na<sub>2</sub>SO<sub>4</sub>, filtered and concentrated under reduced pressure to remove the volatile materials. The resulting brown crude oil was purified by flash chromatography on silica gel (eluted with hexanes/ethyl acetate = 1/1) to give the product **4** in 91% yield as a light-yellow oil. Characterization of **4** is given below.

ii) When placing **3aa** directly under air atmosphere.

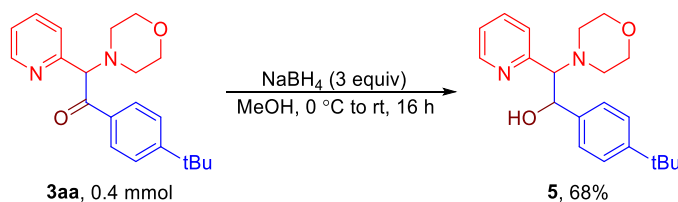


A 20 mL reaction vial was charged with a stir bar and a solution of 1-(4-(*tert*-butyl)phenyl)-2-morpholino-2-(pyridin-2-yl)ethan-1-one **3aa** (67.7 mg, 0.2 mmol) in 3 mL CHCl<sub>3</sub>. The open vial was stirred under air atmosphere for 48 h at room temperature. The reaction mixture was concentrated under reduced pressure. The brown crude oil was purified by flash chromatography on silica gel (eluted with hexanes/ethyl acetate = 1/1) to give the product **4** in 86% yield (33.1 mg) as a light-yellow oil.

#### morpholino(pyridin-2-yl)methanone (**4**)

Compound **4** was prepared following the general procedure, purified by column chromatography using EtOAc/hexanes (1:1, v/v), and isolated as a light yellow oil, 35.0 mg, 91%, <sup>1</sup>H NMR (400 MHz, CDCl<sub>3</sub>) δ 8.65 – 8.52 (m, 1H), 7.80 (td, *J* = 7.7, 1.8 Hz, 1H), 7.67 (d, *J* = 7.8 Hz, 1H), 7.42 – 7.30 (m, 1H), 3.80 (s, 4H), 3.67 (hept, *J* = 3.6, 2.7 Hz, 4H). <sup>13</sup>C{<sup>1</sup>H} NMR (101 MHz, CDCl<sub>3</sub>) δ 167.5, 153.6, 148.2, 137.2, 124.7, 124.2, 67.0, 66.8, 47.8, 42.8. HRMS (ESI) calcd. for C<sub>10</sub>H<sub>12</sub>N<sub>2</sub>O<sub>2</sub> [M+H]<sup>+</sup>: 193.0972, found:193.0979.

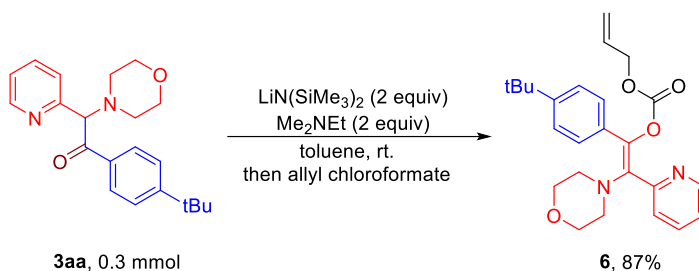
#### (c) Reduction of **3aa** to 1-(4-(*tert*-butyl)phenyl)-2-morpholino-2-(pyridin-2-yl)ethan-1-ol (**5**)



An 8 mL reaction vial was charged with a stir bar and a solution of 1-(4-(*tert*-butyl)phenyl)-2-morpholino-2-(pyridin-2-yl)ethan-1-one **3aa** (135.4 mg, 0.4 mmol) in 4

mL MeOH. The vial was placed in an ice water bath and stirred. To the clear solution cooled solution was added NaBH<sub>4</sub> as a solid (45.4 mg, 3 equiv) at 0 °C, which generated a brown suspension. After the addition (or in 15 min) at 0 °C, the reaction mixture was removed from the ice water bath, allowed to warm to room temperature and stirred for 16 h. The reaction mixture was then quenched with 1 mL of a solution of NH<sub>4</sub>Cl (10% w/w) and extracted with CH<sub>2</sub>Cl<sub>2</sub> (3x5 mL). The combined organic layers were dried over Na<sub>2</sub>SO<sub>4</sub>, filtered and concentrated under reduced pressure to remove the volatile materials. The crude brown oil was purified by flash chromatography on silica gel (eluted with hexanes/ethyl acetate = 1/1) to give the product **5** (68% yield, 92.6 mg) as a light-yellow oil. <sup>1</sup>H NMR (400 MHz, CDCl<sub>3</sub>) δ 8.54 (ddd, *J* = 5.0, 1.8, 0.9 Hz, 1H), 7.48 (td, *J* = 7.7, 1.9 Hz, 1H), 7.19 – 7.13 (m, 3H), 7.04 – 6.95 (m, 2H), 6.91 (dt, *J* = 7.8, 1.1 Hz, 1H), 5.79 (s, 1H), 5.38 (d, *J* = 3.9 Hz, 1H), 3.71 (ddd, *J* = 6.0, 3.6, 2.6 Hz, 4H), 3.53 (d, *J* = 4.0 Hz, 1H), 2.67 (dt, *J* = 10.1, 4.8 Hz, 2H), 2.56 (ddd, *J* = 11.4, 5.4, 3.6 Hz, 2H), 1.23 (s, 9H). <sup>13</sup>C{<sup>1</sup>H} NMR (101 MHz, CDCl<sub>3</sub>) δ 158.2, 149.6, 148.3, 139.7, 136.2, 125.7, 125.6, 124.7, 122.6, 74.8, 72.8, 67.1, 51.5, 34.3, 31.3. HRMS (ESI) calcd. for C<sub>21</sub>H<sub>28</sub>N<sub>2</sub>O<sub>2</sub> [M+H]<sup>+</sup>: 341.2224, found:341.2219.

**(d) Synthesis of (E)-allyl (1-(4-(tert-butyl)phenyl)-2-morpholino-2-(pyridin-2-yl)vinyl) carbonate (6)<sup>4</sup>**



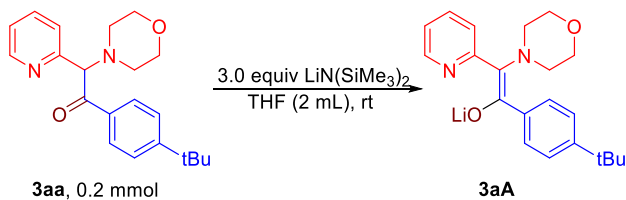
To an oven-dried Schlenk tube with a stir bar was added  $\text{LiN(SiMe}_3)_2$  (100.4 mg, 0.6 mmol) followed by toluene (1.0 mL) and *N,N*-dimethylethylamine (43  $\mu\text{L}$ ) in drybox. The resulting mixture stirred at 25 °C for 5 min. Next, a solution of ketone **3aa** (0.3 mmol) in toluene (1.0 mL) was then added and the reaction mixture stirred at 25 °C for an additional 30 min generating a yellow solution. The tube was then placed in a room temperature water bath and allyl chloroformate (63.8  $\mu\text{L}$ , 0.6 mmol) was added slowly over 5 min. The reaction was allowed to stir until no starting material remained by TLC (typically less than 1 h). The crude reaction mixture was diluted with  $\text{Et}_2\text{O}$  (5 mL) and then quenched with water. The color of the reaction mixture changed from red to light brown. The layers were separated, and the aqueous layer was extracted with  $\text{Et}_2\text{O}$  (5 mL) twice. The combined organic layers were dried over  $\text{Na}_2\text{SO}_4$ , filtered and concentrated. The crude product was purified by silica gel flash chromatography (eluted with hexanes/ethyl acetate = 2/1) to afford the desired enol carbonate **6** in 87% yield as a yellow oil, 110.3 mg, 87%.  $^1\text{H}$  NMR (400 MHz,  $\text{CDCl}_3$ )  $\delta$  8.67 – 8.58 (m, 1H), 7.68 (td,  $J = 7.7, 1.9$  Hz, 1H), 7.54 (dt,  $J = 7.7, 1.1$  Hz, 1H), 7.49 – 7.43 (m, 2H), 7.42 – 7.34 (m, 2H), 7.19 (ddd,  $J = 7.6, 4.8, 1.2$  Hz, 1H), 5.91 – 5.70 (m, 1H), 5.27 – 5.13 (m, 2H), 4.52 (dt,  $J = 5.7, 1.5$  Hz, 2H), 3.62 (t,  $J = 4.7$  Hz, 4H), 2.72 (t,  $J = 4.6$  Hz, 4H), 1.32 (s, 9H).  $^{13}\text{C}\{^1\text{H}\}$  NMR (101 MHz,  $\text{CDCl}_3$ )  $\delta$  155.5, 154.1, 151.1, 149.5, 139.8, 136.8, 136.2,

132.4, 131.5, 127.8, 125.0, 124.2, 122.7, 118.5, 68.5, 67.4, 50.9, 34.7, 31.3. HRMS (ESI) calcd. for  $C_{25}H_{30}N_2O_4$   $[M+H]^+$ : 423.2278, found: 423.2283.

## 2.5.5 Mechanistic studies

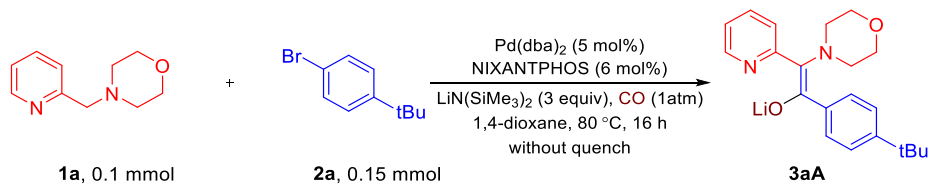
### (a) Detection of product precursor:

i) Deprotonation of **3aa**:



An oven-dried 20 mL vial equipped with a stir bar was charged with **3aa** (67.7 mg, 0.2 mmol) under a nitrogen atmosphere in the glove box. A solution of  $LiN(SiMe_3)_2$  (100.5 mg, 0.6 mmol) in 2.0 mL of dry THF was added with stirring at room temperature. After stirring for 3 h at room temperature, the color had changed from colorless to yellow. The resulting solution was evaporated under vacuum to remove the volatile materials. The resulting oil was taken up in 0.5 mL dry  $d^8$ -THF. The suspension formed was filtered through dry celite and the filtrate was carefully transferred to J-Young NMR tube that was then sealed. NMR data was then collected and the  $^1H$  NMR and  $^{13}C\{^1H\}$  NMR spectrum are shown below.

ii) Reaction monitoring:



An oven-dried 8 mL vial equipped with a stir bar under a nitrogen atmosphere in glove box was charged with Pd(dba)<sub>2</sub> (5 mol %), NIXANTPHOS (6 mol %) and 0.1 M of 1,4-dioxane was taken up by syringe and added to the vial. The resulting solution was stirred for 15 min at room temperature during which time the mixture became red. This solution was used as the stock solution. To an oven-dried 10 mL Schlenk tube in the glove box with stir bar was added LiN(SiMe<sub>3</sub>)<sub>2</sub> (50.3 mg, 0.3 mmol, 3 equiv). Next, 1 mL of the stock solution was added by pipette and the resulting solution stirred for 10 min at room temperature. 2-Pyridylmethylmorpholine **1a** (17.8 mg, 0.1 mmol, 1 equiv) and aryl bromide **2a** (32 mg, 0.15 mmol, 1.5 equiv) were sequentially added to the reaction mixture. The Schlenk tube was capped, removed from the glove box and the reaction mixture was degassed with CO by using Schlenk line, and connected with a CO balloon stirred for 16 h at 80 °C. After this time, the tube was removed from the oil bath, allowed to cool to room temperature, connected to a Schlenk line and evaporated under reduced pressure. While under vacuum, the tube was brought back into the glove box, the cap was carefully removed, and 0.5 mL dry *d*<sup>8</sup>-THF was added to the crude reaction mixture. The suspension was filtered through dry celite and the filtrate was carefully transferred to J-Young tube and NMR spectra acquired.

**Supplementary Figure S1:** <sup>1</sup>H NMR comparison of standard carbonylation product before aqueous workup, deprotonated **3aa**, and product **3aa** in *d*<sup>8</sup>-THF. These spectra support the contention that the product formed in the carbonylation reaction before workup is the enolate.

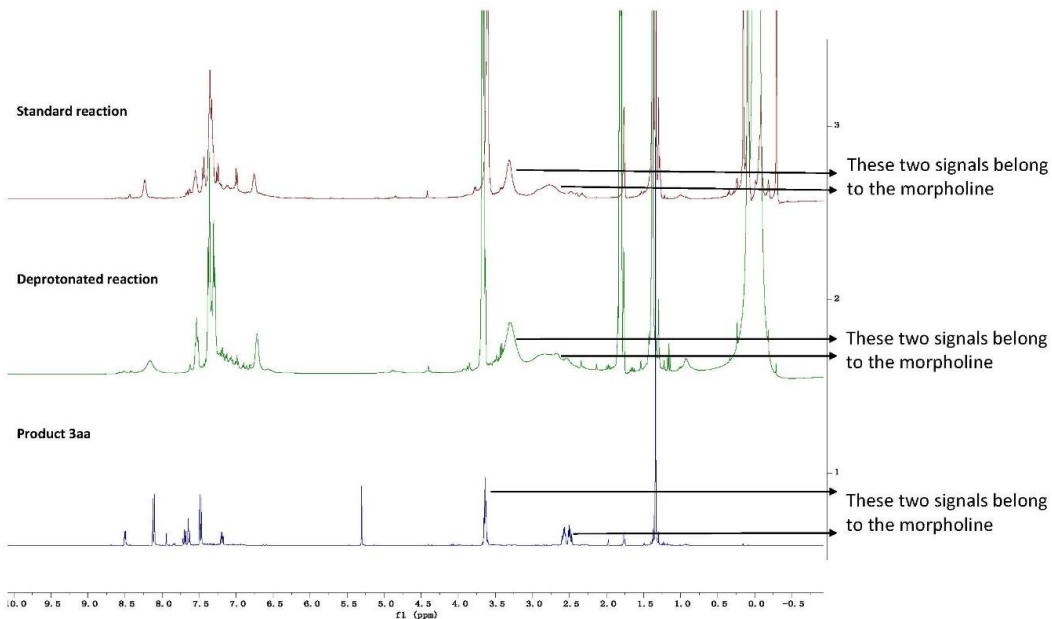


**Figure 2-S1:**  $^1\text{H}$  NMR comparison of standard carbonylation product before aqueous workup, deprotonated **3aa**, and product **3aa** in  $d_8$ -THF. These spectra support the contention that the product formed in the carbonylation reaction before workup is the enolate.

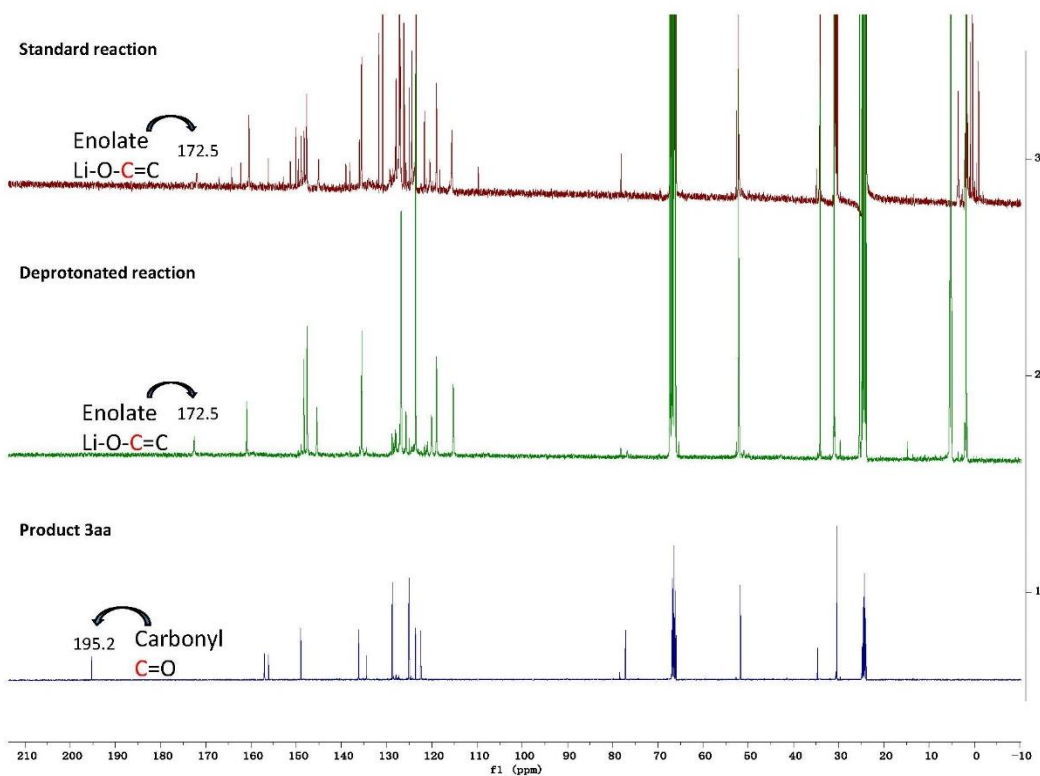
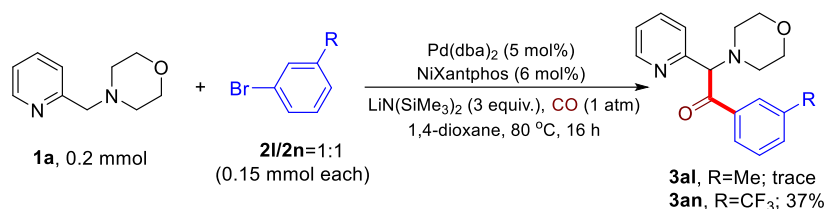




**Figure 2-S2:**  $^{13}\text{C}\{^1\text{H}\}$  NMR comparison of standard carbonylation product before aqueous workup, deprotonated **3aa**, and product **3aa** in  $d_8$ -THF. These spectra support the contention that the product formed in the carbonylation reaction before workup is the enolate.

**(b) Competition experiment**

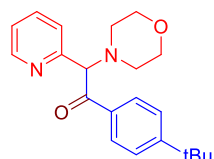


An oven-dried 8 mL vial equipped with a stir bar was charged with  $\text{Pd}(\text{dba})_2$  (5 mol %) and NIXANTPHOS (6 mol %) under a nitrogen atmosphere in glove box. 0.1 M of 1,4-dioxane was taken up by syringe and added to the vial at room temperature. The resulting mixture was stirred for 15 min at room temperature during which time the mixture became dark brown. This solution was used as a stock solution. In the dry box, to an oven-dried 10 mL Schlenk tube with stir bar was added  $\text{LiN}(\text{SiMe}_3)_2$  (100.4 mg, 0.6 mmol, 3 equiv). Using a pipette, 2 mL of the stock solution was added and the resulting solution stirred for 15 min at room temperature. During this time, the reaction mixture became red. The azaarylmethyl amine **1a** (35.6 mg, 0.2 mmol), *m*-bromotoluene **2l** (25.6 mg, 0.15 mmol) and 1-bromo-3-(trifluoromethyl)benzene **2n** (33.8 mg, 0.15 mmol) were sequentially added to the reaction mixture. The Schlenk tube was capped, removed from the glove box, degassed with CO by using Schlenk line, and connected with a CO balloon stirred for 16 h at 80 °C. After this time, the tube was removed from the oil bath, allowed to cool to room temperature, the cap was carefully removed in the fume hood, and the reaction mixture quenched with two drops of  $\text{H}_2\text{O}$ . After quench the color of the reaction

mixture changed from brown to red. The resulting solution was next diluted with 3.0 mL of ethyl acetate and filtered over a pad of MgSO<sub>4</sub> and celite. The pad was rinsed with additional ethyl acetate (5.0 mL) and evaporated under reduced pressure to give the crude brown mixture. The ratio of the two possible carbonylation products was determined based on <sup>1</sup>H NMR analysis by integration (**3an**, 37% and **3al**, trace < 2%).

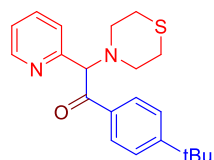
## 2.5.6 Characterization data for products

### 1-(4-(*tert*-butyl)phenyl)-2-morpholino-2-(pyridin-2-yl)ethan-1-one (**3aa**)



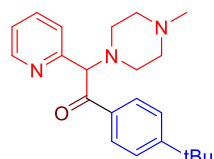
Compound **3aa** was prepared following the general procedure, purified by column chromatography using EtOAc/hexanes (1:2, v/v), and isolated as a yellow oil, 62.3 mg, 92%, <sup>1</sup>H NMR (400 MHz, CDCl<sub>3</sub>) δ 8.57 (ddd, *J* = 4.9, 1.8, 0.9 Hz, 1H), 8.10 – 8.02 (m, 2H), 7.65 (td, *J* = 7.7, 1.9 Hz, 1H), 7.58 (dt, *J* = 7.8, 1.1 Hz, 1H), 7.45 – 7.39 (m, 2H), 7.17 (ddd, *J* = 7.4, 4.9, 1.3 Hz, 1H), 5.25 (s, 1H), 3.81 – 3.68 (m, 4H), 2.62 (ddd, *J* = 9.9, 5.9, 3.4 Hz, 2H), 2.46 (tdd, *J* = 9.2, 4.5, 2.2 Hz, 2H), 1.30 (s, 9H). <sup>13</sup>C{<sup>1</sup>H} NMR (101 MHz, CDCl<sub>3</sub>) δ 196.2, 157.1, 156.0, 149.5, 136.9, 133.8, 129.0, 125.5, 123.9, 123.0, 77.7, 66.9, 52.1, 35.1, 31.0. HRMS (ESI) calcd. for C<sub>21</sub>H<sub>26</sub>N<sub>2</sub>O<sub>2</sub> [M+H]<sup>+</sup>: 339.2067, found: 339.2061.

### 1-(4-(*tert*-butyl)phenyl)-2-(pyridin-2-yl)-2-thiomorpholinoethan-1-one (**3ba**)



Compound **3ba** was prepared following the general procedure, purified by column chromatography using EtOAc/hexanes (1:2, v/v), and isolated as a brown oil, 61.6 mg, 87%, <sup>1</sup>H NMR (400 MHz, CDCl<sub>3</sub>) δ 8.55 (ddd, *J* = 4.9, 1.8, 0.9 Hz, 1H), 8.03 – 7.97 (m, 2H), 7.65 (td, *J* = 7.7, 1.8 Hz, 1H), 7.51 (dt, *J* = 7.9, 1.1 Hz, 1H), 7.43 – 7.37 (m, 2H), 7.17 (ddd, *J* = 7.5, 4.9, 1.2 Hz, 1H), 5.37 (s, 1H), 2.91 – 2.82 (m, 4H), 2.69 (t, *J* = 4.6 Hz, 4H), 1.29 (s, 9H). <sup>13</sup>C{<sup>1</sup>H} NMR (101 MHz, CDCl<sub>3</sub>) δ 197.0, 157.0, 156.2, 149.5, 136.7, 134.0, 128.9, 125.5, 124.0, 122.8, 77.0, 53.4, 35.1, 31.0, 28.0. HRMS (ESI) calcd. for C<sub>21</sub>H<sub>26</sub>N<sub>2</sub>OS [M+H]<sup>+</sup>: 355.1839, found: 355.1835.

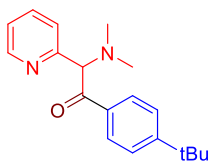
### 1-(4-(*tert*-butyl)phenyl)-2-(4-methylpiperazin-1-yl)-2-(pyridin-2-yl)ethan-1-one (**3ca**)



Compound **3ca** was prepared following the general procedure, purified by column chromatography using DCM/MeOH (10:1, v/v), and isolated as a brown oil, 48.5 mg, 69%, <sup>1</sup>H NMR (400 MHz, CDCl<sub>3</sub>) δ 8.53 (dd, *J* = 4.9, 1.6 Hz, 1H), 8.07 – 7.95 (m, 2H), 7.62 (td, *J* = 7.7, 1.8 Hz, 1H), 7.52 (d, *J* = 7.8 Hz, 1H), 7.38 (d, *J* = 8.4 Hz, 2H), 7.14 (ddd, *J* = 7.5, 4.8, 1.2 Hz, 1H), 5.27 (s, 1H), 2.70 (s, 5H), 2.61 (dd, *J* = 10.4, 5.0 Hz, 3H), 2.40 (s, 3H), 1.26 (s, 9H).

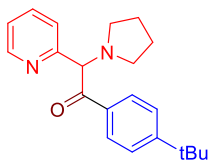
$^{13}\text{C}\{^1\text{H}\}$  NMR (101 MHz,  $\text{CDCl}_3$ )  $\delta$  196.1, 157.2, 155.8, 149.6, 136.9, 133.6, 129.0, 125.5, 123.9, 123.0, 76.8, 54.6, 50.3, 45.2, 35.1, 31.0. HRMS (ESI) calcd. for  $\text{C}_{22}\text{H}_{29}\text{N}_3\text{O}$   $[\text{M}+\text{H}]^+$ : 352.2383, found: 352.2377.

### 1-(4-(*tert*-butyl)phenyl)-2-(dimethylamino)-2-(pyridin-2-yl)ethan-1-one (3da)



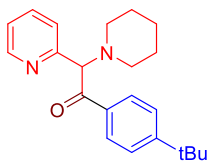
Compound **3da** was prepared following the general procedure, purified by column chromatography using EtOAc/hexanes (1:1, v/v), and isolated as a yellow oil, 43.3 mg, 73%,  $^1\text{H}$  NMR (400 MHz,  $\text{CDCl}_3$ )  $\delta$  8.56 (ddd,  $J = 4.9, 1.9, 1.0$  Hz, 1H), 8.12 – 8.01 (m, 2H), 7.65 (td,  $J = 7.7, 1.8$  Hz, 1H), 7.57 (dt,  $J = 8.0, 1.2$  Hz, 1H), 7.43 – 7.39 (m, 2H), 7.17 (ddd,  $J = 7.4, 4.9, 1.4$  Hz, 1H), 5.15 (s, 1H), 2.31 (s, 6H), 1.29 (s, 9H).  $^{13}\text{C}\{^1\text{H}\}$  NMR (101 MHz,  $\text{CDCl}_3$ )  $\delta$  196.8, 157.0, 156.9, 149.4, 136.9, 133.7, 129.0, 125.5, 123.7, 122.9, 78.4, 43.9, 35.1, 31.0. HRMS (ESI) calcd. for  $\text{C}_{19}\text{H}_{24}\text{N}_2\text{O}$   $[\text{M}+\text{H}]^+$ : 297.1961, found: 297.1965.

### 1-(4-(*tert*-butyl)phenyl)-2-(pyridin-2-yl)-2-(pyrrolidin-1-yl)ethan-1-one (3ea)



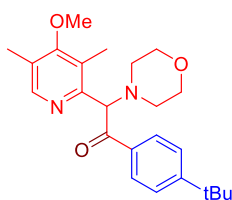
Compound **3ea** was prepared following the general procedure, purified by column chromatography using EtOAc/hexanes (1:2, v/v), and isolated as a yellow oil, 54.2 mg, 84%,  $^1\text{H}$  NMR (400 MHz,  $\text{CDCl}_3$ )  $\delta$  8.55 (dt,  $J = 4.9, 1.3$  Hz, 1H), 8.15 – 8.03 (m, 2H), 7.69 – 7.54 (m, 2H), 7.44 – 7.36 (m, 2H), 7.16 (ddd,  $J = 6.8, 4.9, 1.6$  Hz, 1H), 5.20 (s, 1H), 2.73 (dt,  $J = 8.4, 6.4$  Hz, 2H), 2.40 (dq,  $J = 8.4, 5.0, 4.0$  Hz, 2H), 1.87 – 1.76 (m, 4H), 1.29 (s, 9H).  $^{13}\text{C}\{^1\text{H}\}$  NMR (101 MHz,  $\text{CDCl}_3$ )  $\delta$  196.1, 157.4, 156.9, 149.2, 136.9, 133.4, 129.1, 125.4, 123.5, 122.8, 77.7, 52.6, 35.1, 31.0, 23.3. HRMS (ESI) calcd. for  $\text{C}_{21}\text{H}_{26}\text{N}_2\text{O}$   $[\text{M}+\text{H}]^+$ : 323.2118, found: 323.2112.

### 1-(4-(*tert*-butyl)phenyl)-2-(piperidin-1-yl)-2-(pyridin-2-yl)ethan-1-one (3fa)



Compound **3fa** was prepared following the general procedure, purified by column chromatography using EtOAc/hexanes (1:2, v/v), and isolated as a yellow oil, 43.1 mg, 64%,  $^1\text{H}$  NMR (400 MHz,  $\text{CDCl}_3$ )  $\delta$  8.54 (dt,  $J = 4.8, 1.4$  Hz, 1H), 8.13 – 8.03 (m, 2H), 7.67 – 7.59 (m, 2H), 7.43 – 7.39 (m, 2H), 7.15 (ddd,  $J = 6.8, 4.9, 1.9$  Hz, 1H), 5.23 (s, 1H), 2.52 (dt,  $J = 10.8, 5.3$  Hz, 2H), 2.42 (dq,  $J = 11.0, 5.5, 4.8$  Hz, 2H), 1.60 (q,  $J = 4.9$  Hz, 4H), 1.44 (q,  $J = 5.9$  Hz, 2H), 1.30 (s, 9H).  $^{13}\text{C}\{^1\text{H}\}$  NMR (101 MHz,  $\text{CDCl}_3$ )  $\delta$  197.4, 157.0, 156.8, 149.2, 136.6, 134.2, 129.0, 125.4, 123.9, 122.6, 78.2, 52.9, 35.1, 31.0, 26.0, 24.4. HRMS (ESI) calcd. for  $\text{C}_{22}\text{H}_{28}\text{N}_2\text{O}$   $[\text{M}+\text{H}]^+$ : 337.2274, found: 337.2269.

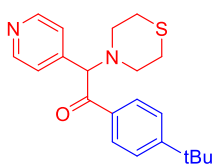
### 1-(4-(*tert*-butyl)phenyl)-2-(4-methoxy-3,5-dimethylpyridin-2-yl)-2-morpholinoethan-1-one (3ga)



Compound **3ga** was prepared following the general procedure, purified by column chromatography using EtOAc/hexanes (1:2, v/v), and isolated as a yellow oil, 41.2 mg, 52%,  $^1\text{H}$  NMR (400 MHz,  $\text{CDCl}_3$ )  $\delta$  8.15 (s, 1H), 7.90 – 7.82 (m, 2H), 7.37 – 7.31 (m, 2H), 5.34 (s, 1H), 3.75 (s, 3H), 3.68 (dt,  $J =$

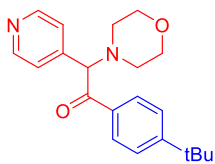
6.2, 3.4 Hz, 4H), 2.70 (q,  $J = 4.3$  Hz, 4H), 2.46 (s, 3H), 2.19 (s, 3H), 1.27 (s, 9H).  $^{13}\text{C}\{^1\text{H}\}$  NMR (101 MHz,  $\text{CDCl}_3$ )  $\delta$  196.5, 164.5, 156.2, 154.1, 149.3, 134.1, 128.5, 127.1, 125.6, 125.3, 74.8, 67.5, 59.9, 50.9, 35.0, 31.0, 13.3, 11.0. HRMS (ESI) calcd. for  $\text{C}_{24}\text{H}_{32}\text{N}_2\text{O}_3$   $[\text{M}+\text{H}]^+$ : 397.2486, found: 397.2480.

### 1-(4-(*tert*-butyl)phenyl)-2-(pyridin-4-yl)-2-thiomorpholinoethan-1-one (3ha)



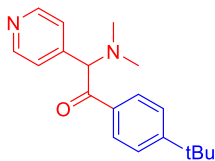
Compound **3ha** was prepared following the general procedure, purified by column chromatography using EtOAc/hexanes (1:2, v/v), and isolated as a brown oil, 57.4 mg, 81%,  $^1\text{H}$  NMR (400 MHz,  $\text{CDCl}_3$ )  $\delta$  8.59 – 8.50 (m, 2H), 7.99 – 7.90 (m, 2H), 7.46 – 7.40 (m, 2H), 7.36 – 7.30 (m, 2H), 5.07 (s, 1H), 2.86 (dt,  $J = 11.6, 5.1$  Hz, 2H), 2.78 (dt,  $J = 11.7, 4.8$  Hz, 2H), 2.67 (t,  $J = 5.0$  Hz, 4H), 1.30 (s, 9H).  $^{13}\text{C}\{^1\text{H}\}$  NMR (101 MHz,  $\text{CDCl}_3$ )  $\delta$  196.5, 157.6, 150.1, 144.6, 133.5, 128.7, 125.7, 124.4, 74.6, 53.3, 35.2, 31.0, 28.1. HRMS (ESI) calcd. for  $\text{C}_{21}\text{H}_{26}\text{N}_2\text{OS}$   $[\text{M}+\text{H}]^+$ : 355.1839, found: 355.1835.

### 1-(4-(*tert*-butyl)phenyl)-2-morpholino-2-(pyridin-4-yl)ethan-1-one (3ia)



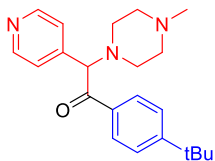
Compound **3ia** was prepared following the general procedure, purified by column chromatography using EtOAc/hexanes (1:2, v/v), and isolated as a yellow oil, 59.6 mg, 88%,  $^1\text{H}$  NMR (400 MHz,  $\text{CDCl}_3$ )  $\delta$  8.63 (s, 2H), 8.05 – 7.92 (m, 2H), 7.51 – 7.38 (m, 4H), 4.92 (s, 1H), 3.73 (ddd,  $J = 5.9, 3.8, 2.5$  Hz, 4H), 2.59 – 2.44 (m, 4H), 1.29 (s, 9H).  $^{13}\text{C}\{^1\text{H}\}$  NMR (101 MHz,  $\text{CDCl}_3$ )  $\delta$  195.8, 157.7, 150.1, 144.3, 133.4, 128.7, 128.3, 125.7, 75.2, 66.9, 52.0, 35.2, 31.0. HRMS (ESI) calcd. for  $\text{C}_{21}\text{H}_{26}\text{N}_2\text{OS}$   $[\text{M}+\text{H}]^+$ : 339.2067, found: 339.2061.

### 1-(4-(*tert*-butyl)phenyl)-2-(dimethylamino)-2-(pyridin-4-yl)ethan-1-one (3ja)



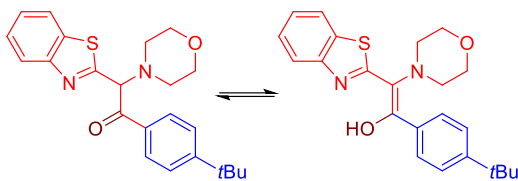
Compound **3ja** was prepared following the general procedure, purified by column chromatography using EtOAc/hexanes (1:1, v/v), and isolated as a yellow oil, 45.6 mg, 77%,  $^1\text{H}$  NMR (400 MHz,  $\text{CDCl}_3$ )  $\delta$  8.60 – 8.51 (m, 2H), 8.01 – 7.93 (m, 2H), 7.44 – 7.36 (m, 4H), 4.83 (s, 1H), 2.30 (s, 6H), 1.30 (s, 9H).  $^{13}\text{C}\{^1\text{H}\}$  NMR (101 MHz,  $\text{CDCl}_3$ )  $\delta$  196.4, 157.5, 150.1, 145.1, 133.3, 128.7, 125.7, 124.3, 75.7, 43.8, 35.2, 31.0. HRMS (ESI) calcd. for  $\text{C}_{19}\text{H}_{24}\text{N}_2\text{O}$   $[\text{M}+\text{H}]^+$ : 297.1961, found: 297.1965.

### 1-(4-(*tert*-butyl)phenyl)-2-(4-methylpiperazin-1-yl)-2-(pyridin-2-yl)ethan-1-one (3ka)



Compound **3ka** was prepared following the general procedure, purified by column chromatography using DCM/MeOH (10:1, v/v), and isolated as a brown oil, 42.9 mg, 61%,  $^1\text{H}$  NMR (400 MHz,  $\text{CDCl}_3$ )  $\delta$  8.57 – 8.47 (m, 2H), 8.01 – 7.89 (m, 2H), 7.46 – 7.33 (m, 4H), 4.94 (s, 1H), 2.81 – 2.43 (m, 8H), 2.37 (s, 3H), 1.28 (s, 9H).  $^{13}\text{C}\{^1\text{H}\}$  NMR (101 MHz,  $\text{CDCl}_3$ )  $\delta$  195.8, 157.7, 150.2, 144.5, 133.3, 128.7, 125.7, 124.3, 74.6, 54.7, 50.6, 45.3, 35.2, 31.0. HRMS (ESI) calcd. for  $\text{C}_{22}\text{H}_{29}\text{N}_3\text{O}$   $[\text{M}+\text{H}]^+$ : 352.2383, found: 352.2377.

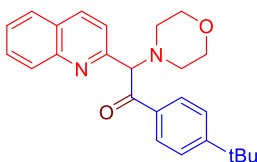
**2-(benzo[d]thiazol-2-yl)-1-(4-(tert-butyl)phenyl)-2-morpholinoethan-1-one : (*E*)-2-(benzo[d]thiazol-2-yl)-1-(4-(tert-butyl)phenyl)-2-morpholinoethen-1-ol = 3:1 (3la)**



Compound **3la** was prepared following the general procedure, purified by column chromatography using EtOAc/hexanes (1:4, v/v), and isolated as a white semi solid, 19 mg, 50%, <sup>1</sup>H NMR (400 MHz, C<sub>6</sub>D<sub>6</sub>) 8.19 (d, *J* = 8.0 Hz, 2H, keto-phenacylCH), 8.00 (d, *J* = 8.0 Hz, 1H, keto-benzothiazoleC(7)H),

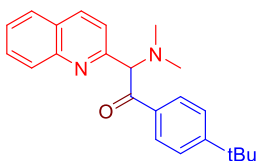
7.65 (d, *J* = 8.0 Hz, 2H, enol-phenacylCH), 7.64 (d, *J* = 8.0 Hz, 1H, enol-benzothiazoleC(7)H), 7.51 (d, *J* = 8.0 Hz, 1H, enol-benzothiazoleC(4)H), 7.40 (d, *J* = 8.0 Hz, 1H, keto-benzothiazoleC(4)H), 7.34 (d, *J* = 8.0 Hz, 2H, keto-phenacylCH), 7.16 (d, 2H, keto-phenacylCH), 7.13 (t, *J* = 8.0 Hz, 1H, enol-benzothiazoleC(5)H), 7.07 (t, *J* = 8.0 Hz, 1H, keto-benzothiazoleC(5)H), 7.00 (t, *J* = 8.0 Hz, 1H, enol-benzothiazoleC(6)H), 6.96 (t, *J* = 8.0 Hz, 1H, keto-benzothiazoleC(6)H), 5.68 (s, 1H, keto-CHCOAr), 3.61 – 3.48 (m, 4H, keto-morpholineCH, 4H, enol-morpholineCH), 2.79 – 2.52 (m, 4H, keto-morpholineCH, 4H, enol-morpholineCH), 1.21 (s, 9H, enol-tertbutylCH), 1.07 (s, 9H, keto-tertbutylCH). <sup>13</sup>C{<sup>1</sup>H} NMR (101 MHz, C<sub>6</sub>D<sub>6</sub>) δ 193.6, 176.1, 167.4, 162.5, 156.9, 153.0, 152.8, 152.4, 136.3, 134.0, 133.3, 133.0, 129.1, 128.3, 126.1, 125.7, 125.5, 125.1, 125.0, 124.0, 123.4, 121.6, 121.2, 120.9, 119.4, 72.4, 67.6, 66.8, 52.0, 51.5, 34.6, 31.0, 30.6, (several resonances is missing due to overlapping peaks). HRMS (ESI) calcd. For C<sub>23</sub>H<sub>26</sub>N<sub>2</sub>O<sub>2</sub>S [M+H]<sup>+</sup> : 395.1793, found: 395.1777.

**1-(4-(tert-butyl)phenyl)-2-morpholino-2-(quinolin-2-yl)ethan-1-one (3ma)**



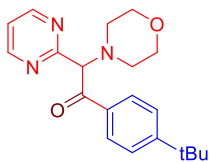
Compound **3ma** was prepared following the general procedure, purified by column chromatography using EtOAc/hexanes (1:1, v/v), and isolated as a brown oil, 57.5 mg, 74%, <sup>1</sup>H NMR (400 MHz, CDCl<sub>3</sub>) δ 8.19 – 8.14 (m, 2H), 8.14 – 8.09 (m, 2H), 7.78 – 7.73 (m, 2H), 7.68 (ddd, *J* = 8.5, 6.9, 1.5 Hz, 1H), 7.50 (ddd, *J* = 8.1, 6.9, 1.2 Hz, 1H), 7.43 – 7.38 (m, 2H), 5.46 (s, 1H), 3.83 – 3.71 (m, 4H), 2.70 (ddd, *J* = 10.0, 5.9, 3.4 Hz, 2H), 2.48 – 2.38 (m, 2H), 1.26 (s, 9H). <sup>13</sup>C{<sup>1</sup>H} NMR (101 MHz, CDCl<sub>3</sub>) δ 196.0, 157.2, 156.5, 147.9, 136.9, 133.9, 129.6, 129.4, 129.1, 127.6, 127.6, 126.9, 125.5, 120.9, 78.4, 66.9, 52.2, 35.1, 31.0. HRMS (ESI) calcd. for C<sub>25</sub>H<sub>28</sub>N<sub>2</sub>O<sub>2</sub> [M+H]<sup>+</sup>: 389.2224, found: 389.2230.

**1-(4-(tert-butyl)phenyl)-2-(dimethylamino)-2-(quinolin-2-yl)ethan-1-one (3na)**



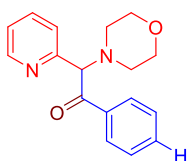
Compound **3na** was prepared following the general procedure, purified by column chromatography using EtOAc/hexanes (1:1, v/v), and isolated as a yellow oil, 49.9 mg, 72%, <sup>1</sup>H NMR (400 MHz, CDCl<sub>3</sub>) δ 8.21 – 8.14 (m, 2H), 8.14 – 8.07 (m, 2H), 7.77 – 7.65 (m, 3H), 7.49 (ddd, *J* = 8.1, 6.9, 1.3 Hz, 1H), 7.42 – 7.35 (m, 2H), 5.33 (s, 1H), 2.34 (s, 6H), 1.26 (s, 9H). <sup>13</sup>C{<sup>1</sup>H} NMR (101 MHz, CDCl<sub>3</sub>) δ 196.6, 157.4, 157.0, 147.8, 136.9, 133.8, 129.4, 129.4, 129.2, 127.6, 127.6, 126.7, 125.4, 120.8, 79.4, 44.1, 35.1, 31.0. HRMS (ESI) calcd. for C<sub>23</sub>H<sub>26</sub>N<sub>2</sub>O [M+H]<sup>+</sup>: 347.2118, found: 347.2113.

### 1-(4-(*tert*-butyl)phenyl)-2-morpholino-2-(pyrimidin-2-yl)ethan-1-one (30a)



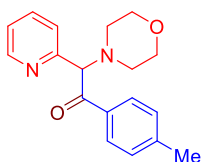
Compound **30a** was prepared following the general procedure, purified by column chromatography using EtOAc/hexanes (1:1, v/v), and isolated as a yellow oil, 63.1 mg, 93%,  $^1\text{H NMR}$  (400 MHz,  $\text{CDCl}_3$ )  $\delta$  8.71 (d,  $J = 4.9$  Hz, 2H), 7.97 (d,  $J = 8.6$  Hz, 2H), 7.42 – 7.34 (m, 2H), 7.16 (t,  $J = 4.9$  Hz, 1H), 5.42 (s, 1H), 3.75 (t,  $J = 4.6$  Hz, 4H), 2.68 (q,  $J = 4.0$  Hz, 4H), 1.27 (s, 9H).  $^{13}\text{C}\{^1\text{H}\}$  NMR (101 MHz,  $\text{CDCl}_3$ )  $\delta$  194.6, 165.6, 157.4, 156.9, 133.6, 128.8, 125.4, 119.7, 77.3, 67.1, 51.5, 35.1, 31.0. HRMS (ESI) calcd. for  $\text{C}_{20}\text{H}_{25}\text{N}_3\text{O}_2$   $[\text{M}+\text{H}]^+$ : 340.2020, found: 340.2016.

### 2-morpholino-1-phenyl-2-(pyridin-2-yl)ethan-1-one (3ab)



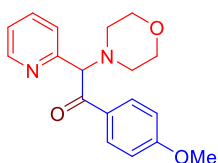
Compound **3ab** was prepared following the general procedure, purified by column chromatography using EtOAc/hexanes (1:2, v/v), and isolated as a yellow oil, 44.6 mg, 79%,  $^1\text{H NMR}$  (400 MHz,  $\text{CDCl}_3$ )  $\delta$  8.54 (dt,  $J = 4.9, 1.4$  Hz, 1H), 8.13 – 8.03 (m, 2H), 7.63 (td,  $J = 7.7, 1.8$  Hz, 1H), 7.55 (d,  $J = 7.9$  Hz, 1H), 7.51 – 7.44 (m, 1H), 7.38 (t,  $J = 7.8$  Hz, 2H), 7.15 (ddd,  $J = 7.4, 4.9, 1.3$  Hz, 1H), 5.26 (s, 1H), 3.81 – 3.68 (m, 4H), 2.61 (ddd,  $J = 10.1, 5.9, 3.4$  Hz, 2H), 2.48 (ddd,  $J = 10.7, 6.0, 3.3$  Hz, 2H).  $^{13}\text{C}\{^1\text{H}\}$  NMR (101 MHz,  $\text{CDCl}_3$ )  $\delta$  196.7, 155.7, 149.5, 136.9, 136.4, 133.3, 129.0, 128.5, 124.0, 123.0, 77.7, 66.9, 51.9. HRMS (ESI) calcd. for  $\text{C}_{17}\text{H}_{18}\text{N}_2\text{O}_2$   $[\text{M}+\text{H}]^+$ : 283.1441, found: 283.1437.

### 2-morpholino-2-(pyridin-2-yl)-1-(*p*-tolyl)ethan-1-one (3ac)



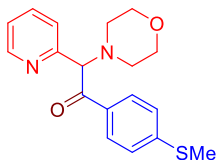
Compound **3ac** was prepared following the general procedure, purified by column chromatography using EtOAc/hexanes (1:2, v/v), and isolated as a yellow oil, 53.4 mg, 90%,  $^1\text{H NMR}$  (500 MHz,  $\text{CDCl}_3$ )  $\delta$  8.54 (dt,  $J = 4.9, 1.4$  Hz, 1H), 8.05 – 7.96 (m, 2H), 7.63 (td,  $J = 7.7, 1.8$  Hz, 1H), 7.57 (d,  $J = 7.8$  Hz, 1H), 7.22 – 7.12 (m, 3H), 5.24 (s, 1H), 3.79 – 3.69 (m, 4H), 2.67 – 2.58 (m, 2H), 2.48 (ddd,  $J = 10.8, 6.0, 3.4$  Hz, 2H), 2.34 (s, 3H).  $^{13}\text{C}\{^1\text{H}\}$  NMR (126 MHz,  $\text{CDCl}_3$ )  $\delta$  196.1, 155.8, 149.5, 144.2, 136.8, 133.9, 129.2, 129.1, 123.9, 123.0, 77.6, 66.9, 52.0, 21.6. HRMS (ESI) calcd. for  $\text{C}_{18}\text{H}_{20}\text{N}_2\text{O}_2$   $[\text{M}+\text{H}]^+$ : 297.1598, found: 297.1603.

### 1-(4-methoxyphenyl)-2-morpholino-2-(pyridin-2-yl)ethan-1-one (3ad)



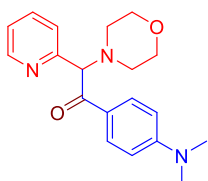
Compound **3ad** was prepared following the general procedure, purified by column chromatography using EtOAc/hexanes (1:1, v/v), and isolated as a yellow oil, 53.1 mg, 85%,  $^1\text{H NMR}$  (400 MHz,  $\text{CDCl}_3$ )  $\delta$  8.65 – 8.40 (m, 1H), 8.22 – 8.00 (m, 2H), 7.68 – 7.51 (m, 2H), 7.15 (ddd,  $J = 7.0, 5.0, 1.4$  Hz, 1H), 6.94 – 6.77 (m, 2H), 5.18 (s, 1H), 3.80 (s, 3H), 3.79 – 3.67 (m, 4H), 2.68 – 2.54 (m, 2H), 2.44 (ddd,  $J = 10.7, 6.0, 3.5$  Hz, 2H).  $^{13}\text{C}\{^1\text{H}\}$  NMR (101 MHz,  $\text{CDCl}_3$ )  $\delta$  195.0, 163.7, 156.1, 149.4, 136.8, 131.4, 129.4, 123.8, 122.9, 113.7, 77.7, 66.9, 55.4, 52.1. HRMS (ESI) calcd. for  $\text{C}_{18}\text{H}_{20}\text{N}_2\text{O}_3$   $[\text{M}+\text{H}]^+$ : 313.1547, found: 313.1552.

### 1-(4-(methylthio)phenyl)-2-morpholino-2-(pyridin-2-yl)ethan-1-one (3ae)



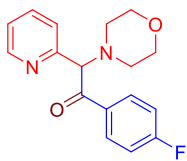
Compound **3ae** was prepared following the general procedure, purified by column chromatography using EtOAc/hexanes (1:1, v/v), and isolated as a brown oil, 42.0 mg, 64%,  $^1\text{H NMR}$  (400 MHz,  $\text{CDCl}_3$ )  $\delta$  8.54 (ddd,  $J = 5.0$ , 1.8, 0.9 Hz, 1H), 8.11 – 7.96 (m, 2H), 7.64 (td,  $J = 7.7$ , 1.8 Hz, 1H), 7.55 (dt,  $J = 7.9$ , 1.1 Hz, 1H), 7.23 – 7.09 (m, 3H), 5.18 (s, 1H), 3.81 – 3.67 (m, 4H), 2.65 – 2.55 (m, 2H), 2.50 – 2.40 (m, 5H).  $^{13}\text{C}\{^1\text{H}\}$  NMR (101 MHz,  $\text{CDCl}_3$ )  $\delta$  195.6, 155.8, 149.5, 146.4, 136.9, 132.5, 129.4, 124.8, 123.9, 123.0, 77.8, 66.9, 52.0, 14.6. HRMS (ESI) calcd. for  $\text{C}_{18}\text{H}_{20}\text{N}_2\text{O}_2\text{S}$   $[\text{M}+\text{H}]^+$ : 329.1318, found: 329.1316.

### 1-(4-(dimethylamino)phenyl)-2-morpholino-2-(pyridin-2-yl)ethan-1-one (3af)



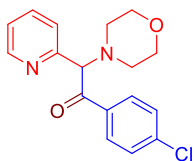
Compound **3af** was prepared following the general procedure, purified by column chromatography using EtOAc/hexanes (1:1, v/v), and isolated as a yellow oil, 48.8 mg, 75%,  $^1\text{H NMR}$  (400 MHz,  $\text{CDCl}_3$ )  $\delta$  8.52 (dt,  $J = 4.8$ , 1.4 Hz, 1H), 8.13 – 7.97 (m, 2H), 7.68 – 7.55 (m, 2H), 7.12 (td,  $J = 5.1$ , 3.2 Hz, 1H), 6.66 – 6.50 (m, 2H), 5.15 (s, 1H), 3.82 – 3.67 (m, 4H), 3.00 (s, 6H), 2.61 (ddd,  $J = 10.2$ , 5.9, 3.2 Hz, 2H), 2.41 (ddd,  $J = 11.1$ , 6.0, 3.2 Hz, 2H).  $^{13}\text{C}\{^1\text{H}\}$  NMR (101 MHz,  $\text{CDCl}_3$ )  $\delta$  194.1, 156.8, 153.5, 149.2, 136.7, 131.4, 124.4, 123.7, 122.7, 110.6, 77.3, 66.9, 52.2, 39.9. HRMS (ESI) calcd. for  $\text{C}_{19}\text{H}_{23}\text{N}_3\text{O}_2$   $[\text{M}+\text{H}]^+$ : 326.1863, found: 326.1869.

### 1-(4-fluorophenyl)-2-morpholino-2-(pyridin-2-yl)ethan-1-one (3ag)



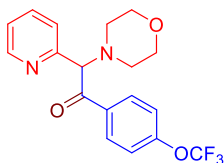
Compound **3ag** was prepared following the general procedure, purified by column chromatography using EtOAc/hexanes (1:2, v/v), and isolated as a yellow oil, 41.4 mg, 69%,  $^1\text{H NMR}$  (400 MHz,  $\text{CDCl}_3$ )  $\delta$  8.55 (ddd,  $J = 4.9$ , 1.9, 1.0 Hz, 1H), 8.27 – 8.05 (m, 2H), 7.65 (td,  $J = 7.7$ , 1.8 Hz, 1H), 7.54 (dt,  $J = 7.9$ , 1.1 Hz, 1H), 7.17 (ddd,  $J = 7.5$ , 4.9, 1.3 Hz, 1H), 7.12 – 7.02 (m, 2H), 5.18 (s, 1H), 3.83 – 3.67 (m, 4H), 2.67 – 2.53 (m, 2H), 2.46 (dddd,  $J = 11.1$ , 6.6, 3.7, 1.0 Hz, 2H).  $^{13}\text{C}\{^1\text{H}\}$  NMR (101 MHz,  $\text{CDCl}_3$ )  $\delta$  195.1, 167.1 (d,  $J^1_{\text{C-F}} = 256.5$  Hz), 155.6, 149.6, 136.9, 132.7 (d,  $J^4_{\text{C-F}} = 3.0$  Hz), 131.9 (d,  $J^3_{\text{C-F}} = 9.1$  Hz), 123.9, 123.1, 115.7 (d,  $J^2_{\text{C-F}} = 22.2$  Hz), 78.1, 66.9, 52.0.  $^{19}\text{F NMR}$  (376 MHz,  $\text{CDCl}_3$ )  $\delta$  -104.5. HRMS (ESI) calcd. for  $\text{C}_{17}\text{H}_{17}\text{FN}_2\text{O}_2$   $[\text{M}+\text{H}]^+$ : 301.1347, found: 301.1342.

### 1-(4-chlorophenyl)-2-morpholino-2-(pyridin-2-yl)ethan-1-one (3ah)



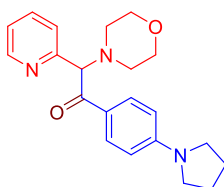
Compound **3ah** was prepared following the general procedure, purified by column chromatography using EtOAc/hexanes (1:2, v/v), and isolated as a yellow oil, 48.8 mg, 77%,  $^1\text{H NMR}$  (500 MHz,  $\text{CDCl}_3$ )  $\delta$  8.55 (dd,  $J = 4.8$ , 2.0 Hz, 1H), 8.15 – 7.98 (m, 2H), 7.65 (td,  $J = 7.7$ , 2.1 Hz, 1H), 7.53 (d,  $J = 7.9$  Hz, 1H), 7.36 (dd,  $J = 8.9$ , 2.1 Hz, 2H), 7.18 (ddd,  $J = 7.5$ , 4.9, 1.4 Hz, 1H), 5.18 (s, 1H), 3.82 – 3.71 (m, 4H), 2.68 – 2.55 (m, 2H), 2.48 (dt,  $J = 11.1$ , 4.3 Hz, 2H).  $^{13}\text{C}\{^1\text{H}\}$  NMR (126 MHz,  $\text{CDCl}_3$ )  $\delta$  195.5, 155.4, 149.6, 139.8, 136.9, 134.6, 130.5, 128.8, 124.0, 123.1, 78.1, 66.9, 51.9. HRMS (ESI) calcd. for  $\text{C}_{17}\text{H}_{17}\text{ClN}_2\text{O}_2$   $[\text{M}+\text{H}]^+$ : 317.1051, found: 317.1057.

### 2-morpholino-2-(pyridin-2-yl)-1-(4-(trifluoromethoxy)phenyl)ethan-1-one (3ai)



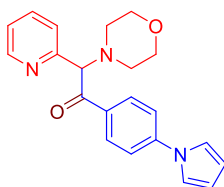
Compound **3ai** was prepared following the general procedure, purified by column chromatography using EtOAc/hexanes (1:2, v/v), and isolated as a brown oil, 41.8 mg, 57%,  $^1\text{H}$  NMR (400 MHz,  $\text{CDCl}_3$ )  $\delta$  8.56 (ddd,  $J = 4.9, 1.8, 0.9$  Hz, 1H), 8.21 – 8.17 (m, 2H), 7.67 (td,  $J = 7.7, 1.8$  Hz, 1H), 7.54 (dt,  $J = 7.9, 1.1$  Hz, 1H), 7.24 – 7.17 (m, 3H), 5.19 (s, 1H), 3.77 – 3.72 (m, 4H), 2.64 – 2.56 (m, 2H), 2.48 (dtd,  $J = 10.8, 4.0, 1.9$  Hz, 2H).  $^{13}\text{C}\{^1\text{H}\}$  NMR (101 MHz,  $\text{CDCl}_3$ )  $\delta$  195.2, 155.3, 149.6, 137.0, 134.4, 131.2, 129.6, 124.1 (q,  $J_{\text{C-F}} = 262.6$  Hz), 124.0, 123.2, 120.1, 78.2, 66.9, 51.9.  $^{19}\text{F}$  NMR (376 MHz,  $\text{CDCl}_3$ )  $\delta$  -57.58. HRMS (ESI) calcd. for  $\text{C}_{18}\text{H}_{17}\text{F}_3\text{N}_2\text{O}_3$   $[\text{M}+\text{H}]^+$ : 367.1264, found: 367.1260.

### 2-morpholino-2-(pyridin-2-yl)-1-(4-(pyrrolidin-1-yl)phenyl)ethan-1-one (3aj)



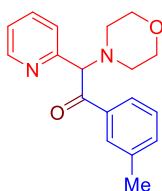
Compound **3aj** was prepared following the general procedure, purified by column chromatography using EtOAc/hexanes (1:1, v/v), and isolated as a yellow oil, 49.2 mg, 70%,  $^1\text{H}$  NMR (500 MHz,  $\text{CDCl}_3$ )  $\delta$  8.52 (d,  $J = 4.9$  Hz, 1H), 8.05 (d,  $J = 8.6$  Hz, 2H), 7.61 (d,  $J = 8.4$  Hz, 2H), 7.12 (s, 1H), 6.44 (d,  $J = 8.6$  Hz, 2H), 5.16 (s, 1H), 3.82 – 3.64 (m, 4H), 3.30 (d,  $J = 6.2$  Hz, 4H), 2.62 (t,  $J = 9.3$  Hz, 2H), 2.42 (t,  $J = 8.3$  Hz, 2H), 1.97 (q,  $J = 3.6$  Hz, 4H).  $^{13}\text{C}\{^1\text{H}\}$  NMR (126 MHz,  $\text{CDCl}_3$ )  $\delta$  193.9, 156.8, 151.1, 149.2, 136.8, 131.5, 123.9, 123.7, 122.7, 110.7, 77.2, 66.9, 52.2, 47.5, 25.4. HRMS (ESI) calcd. for  $\text{C}_{21}\text{H}_{25}\text{N}_3\text{O}_2$   $[\text{M}+\text{H}]^+$ : 352.2020, found: 352.2023.

### 1-(4-(1H-pyrrol-1-yl)phenyl)-2-morpholino-2-(pyridin-2-yl)ethan-1-one (3ak)



Compound **3ak** was prepared following the general procedure, purified by column chromatography using EtOAc/hexanes (1:2, v/v), and isolated as a brown oil, 45.2 mg, 65%,  $^1\text{H}$  NMR (400 MHz,  $\text{CDCl}_3$ )  $\delta$  8.57 (ddd,  $J = 4.9, 1.9, 0.9$  Hz, 1H), 8.27 – 8.16 (m, 2H), 7.67 (td,  $J = 7.7, 1.9$  Hz, 1H), 7.58 (dt,  $J = 7.9, 1.1$  Hz, 1H), 7.43 – 7.37 (m, 2H), 7.19 (ddd,  $J = 7.4, 4.9, 1.3$  Hz, 1H), 7.14 – 7.10 (m, 2H), 6.36 (t,  $J = 2.2$  Hz, 2H), 5.23 (s, 1H), 3.81 – 3.72 (m, 4H), 2.68 – 2.57 (m, 2H), 2.54 – 2.45 (m, 2H).  $^{13}\text{C}\{^1\text{H}\}$  NMR (101 MHz,  $\text{CDCl}_3$ )  $\delta$  195.3, 155.7, 149.6, 144.1, 137.0, 133.0, 131.0, 123.9, 123.1, 119.2, 118.9, 111.7, 78.0, 66.9, 52.0. HRMS (ESI) calcd. for  $\text{C}_{21}\text{H}_{21}\text{N}_3\text{O}_2$   $[\text{M}+\text{H}]^+$ : 348.1707, found: 348.1701.

### 2-morpholino-2-(pyridin-2-yl)-1-(m-tolyl)ethan-1-one (3al)

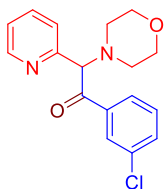


Compound **3al** was prepared following the general procedure, purified by column chromatography using EtOAc/hexanes (1:2, v/v), and isolated as a yellow oil, 49.8 mg, 84%,  $^1\text{H}$  NMR (400 MHz,  $\text{CDCl}_3$ )  $\delta$  8.56 (ddd,  $J = 4.9, 1.7, 0.9$  Hz, 1H), 8.04 – 7.78 (m, 2H), 7.65 (td,  $J = 7.7, 1.9$  Hz, 1H), 7.57 (dt,  $J = 7.9, 1.2$  Hz, 1H), 7.30 (td,  $J = 7.5, 3.6$  Hz, 2H), 7.17 (ddd,  $J = 7.5, 4.9, 1.3$  Hz, 1H), 5.27 (s, 1H), 3.84 – 3.68 (m, 4H), 2.62 (ddd,  $J = 10.0, 5.8, 3.5$  Hz, 2H), 2.55 – 2.44 (m, 2H),



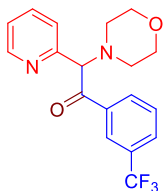
2.36 (s, 3H).  $^{13}\text{C}\{^1\text{H}\}$  NMR (101 MHz,  $\text{CDCl}_3$ )  $\delta$  196.9, 155.8, 149.5, 138.4, 136.9, 136.5, 134.1, 129.3, 128.4, 126.3, 123.9, 123.0, 77.6, 66.9, 52.0, 21.3. HRMS (ESI) calcd. for  $\text{C}_{18}\text{H}_{20}\text{N}_2\text{O}_2$   $[\text{M}+\text{H}]^+$ : 297.1598, found: 297.1603.

### 1-(3-chlorophenyl)-2-morpholino-2-(pyridin-2-yl)ethan-1-one (3am)



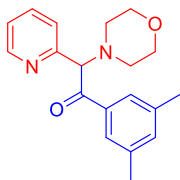
Compound **3am** was prepared following the general procedure, purified by column chromatography using EtOAc/hexanes (1:2, v/v), and isolated as a yellow oil, 48.8 mg, 77%,  $^1\text{H}$  NMR (400 MHz,  $\text{CDCl}_3$ )  $\delta$  8.54 (dt,  $J = 5.0, 1.3$  Hz, 1H), 8.14 – 7.87 (m, 2H), 7.65 (td,  $J = 7.7, 1.8$  Hz, 1H), 7.52 (dd,  $J = 7.9, 1.2$  Hz, 1H), 7.44 (ddd,  $J = 8.0, 2.2, 1.0$  Hz, 1H), 7.31 (t,  $J = 7.9$  Hz, 1H), 7.17 (ddd,  $J = 7.5, 4.9, 1.2$  Hz, 1H), 5.18 (s, 1H), 3.73 (dt,  $J = 6.0, 3.1$  Hz, 4H), 2.63 – 2.53 (m, 2H), 2.53 – 2.43 (m, 2H).  $^{13}\text{C}\{^1\text{H}\}$  NMR (101 MHz,  $\text{CDCl}_3$ )  $\delta$  195.6, 155.2, 149.7, 137.8, 137.0, 134.9, 133.2, 129.8, 129.0, 127.1, 124.0, 123.2, 77.9, 66.9, 51.8. HRMS (ESI) calcd. for  $\text{C}_{17}\text{H}_{17}\text{ClN}_2\text{O}_2$   $[\text{M}+\text{H}]^+$ : 317.1051, found: 317.1057.

### 2-morpholino-2-(pyridin-2-yl)-1-(3-(trifluoromethyl)phenyl)ethan-1-one (3an)



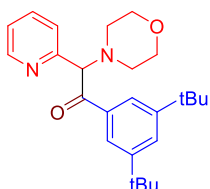
Compound **3an** was prepared following the general procedure, purified by column chromatography using EtOAc/hexanes (1:2, v/v), and isolated as a yellow oil, 42.7 mg, 61%,  $^1\text{H}$  NMR (400 MHz,  $\text{CDCl}_3$ )  $\delta$  8.56 (ddd,  $J = 4.9, 1.8, 0.9$  Hz, 1H), 8.40 (d,  $J = 1.9$  Hz, 1H), 8.33 (dt,  $J = 8.1, 1.5$  Hz, 1H), 7.77 – 7.72 (m, 1H), 7.67 (td,  $J = 7.7, 1.8$  Hz, 1H), 7.56 – 7.51 (m, 2H), 7.20 (ddd,  $J = 7.5, 4.9, 1.2$  Hz, 1H), 5.22 (s, 1H), 3.75 (ddd,  $J = 5.9, 3.6, 2.3$  Hz, 4H), 2.61 (ddd,  $J = 9.5, 7.2, 4.0$  Hz, 2H), 2.55 – 2.47 (m, 2H).  $^{13}\text{C}\{^1\text{H}\}$  NMR (101 MHz,  $\text{CDCl}_3$ )  $\delta$  195.5, 155.1, 149.7, 137.0, 136.7, 132.3, 131.6 (q,  $J_{\text{C-F}}^2 = 33.3$  Hz), 129.6 (q,  $J_{\text{C-F}}^3 = 4.0$  Hz), 129.1, 127.7 (q,  $J_{\text{C-F}}^1 = 273.7$  Hz), 126.0 (q,  $J_{\text{C-F}}^3 = 4.0$  Hz), 124.0, 123.2, 78.3, 66.9, 51.8.  $^{19}\text{F}$  NMR (376 MHz,  $\text{CDCl}_3$ )  $\delta$  -62.9. HRMS (ESI) calcd. for  $\text{C}_{18}\text{H}_{17}\text{F}_3\text{N}_2\text{O}_2$   $[\text{M}+\text{H}]^+$ : 351.1315, found: 351.1311.

### 1-(3,5-dimethylphenyl)-2-morpholino-2-(pyridin-2-yl)ethan-1-one (3ao)



Compound **3ao** was prepared following the general procedure, purified by column chromatography using EtOAc/hexanes (1:2, v/v), and isolated as a yellow oil, 54.0 mg, 87%,  $^1\text{H}$  NMR (500 MHz,  $\text{CDCl}_3$ )  $\delta$  8.57 – 8.52 (m, 1H), 7.69 (s, 2H), 7.64 (td,  $J = 7.7, 1.8$  Hz, 1H), 7.57 (d,  $J = 7.9$  Hz, 1H), 7.19 – 7.10 (m, 2H), 5.26 (s, 1H), 3.79 – 3.69 (m, 4H), 2.70 – 2.56 (m, 2H), 2.46 (ddt,  $J = 8.3, 5.8, 2.7$  Hz, 2H), 2.31 (s, 6H).  $^{13}\text{C}\{^1\text{H}\}$  NMR (126 MHz,  $\text{CDCl}_3$ )  $\delta$  197.1, 155.9, 149.5, 138.2, 136.9, 136.7, 135.1, 126.7, 123.9, 123.0, 77.5, 66.9, 52.0, 21.2. HRMS (ESI) calcd. for  $\text{C}_{19}\text{H}_{22}\text{N}_2\text{O}_2$   $[\text{M}+\text{H}]^+$ : 311.1754, found: 311.1743.

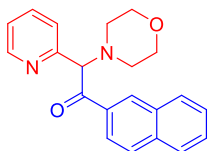
### 1-(3,5-di-tert-butylphenyl)-2-morpholino-2-(pyridin-2-yl)ethan-1-one (3ap)



Compound **3ap** was prepared following the general procedure, purified by column chromatography using EtOAc/hexanes (1:2, v/v), and isolated as a

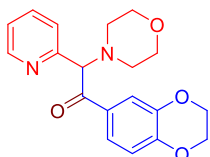
yellow oil, 67.9 mg, 86%,  $^1\text{H}$  NMR (400 MHz,  $\text{CDCl}_3$ )  $\delta$  8.57 (ddd,  $J = 4.9, 1.9, 1.0$  Hz, 1H), 8.00 (d,  $J = 1.9$  Hz, 2H), 7.63 (td,  $J = 7.7, 1.8$  Hz, 1H), 7.59 – 7.51 (m, 2H), 7.16 (ddd,  $J = 7.4, 4.9, 1.3$  Hz, 1H), 5.25 (s, 1H), 3.75 (dt,  $J = 5.8, 3.7$  Hz, 4H), 2.70 – 2.60 (m, 2H), 2.49 (dd,  $J = 6.6, 4.0$  Hz, 2H), 1.29 (s, 18H).  $^{13}\text{C}\{^1\text{H}\}$  NMR (101 MHz,  $\text{CDCl}_3$ )  $\delta$  196.7, 156.0, 150.9, 149.4, 136.7, 135.6, 127.3, 123.8, 123.4, 122.8, 78.3, 66.9, 51.9, 34.9, 31.2. HRMS (ESI) calcd. for  $\text{C}_{25}\text{H}_{34}\text{N}_2\text{O}_2$   $[\text{M}+\text{H}]^+$ : 395.2693, found: 395.2687.

### 2-morpholino-1-(naphthalen-2-yl)-2-(pyridin-2-yl)ethan-1-one (3aq)



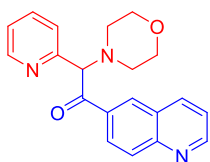
Compound **3aq** was prepared following the general procedure, purified by column chromatography using EtOAc/hexanes (1:2, v/v), and isolated as a brown oil, 42.5 mg, 64%,  $^1\text{H}$  NMR (400 MHz,  $\text{CDCl}_3$ )  $\delta$  8.72 (d,  $J = 1.7$  Hz, 1H), 8.56 (dt,  $J = 4.9, 1.4$  Hz, 1H), 8.10 (dd,  $J = 8.7, 1.8$  Hz, 1H), 7.95 (dd,  $J = 8.5, 1.6$  Hz, 1H), 7.86 – 7.75 (m, 2H), 7.69 – 7.59 (m, 2H), 7.59 – 7.49 (m, 2H), 7.16 (ddd,  $J = 6.8, 4.9, 1.8$  Hz, 1H), 5.43 (s, 1H), 3.85 – 3.71 (m, 4H), 2.67 (ddd,  $J = 9.9, 5.8, 3.4$  Hz, 2H), 2.52 (ddd,  $J = 10.7, 6.0, 3.3$  Hz, 2H).  $^{13}\text{C}\{^1\text{H}\}$  NMR (101 MHz,  $\text{CDCl}_3$ )  $\delta$  196.7, 155.8, 149.6, 136.9, 135.6, 133.7, 132.4, 131.1, 129.9, 128.7, 128.4, 127.7, 126.7, 124.4, 123.9, 123.0, 77.8, 67.0, 52.1. HRMS (ESI) calcd. for  $\text{C}_{21}\text{H}_{20}\text{N}_2\text{O}_2$   $[\text{M}+\text{H}]^+$ : 333.1598, found: 333.1603.

### 1-(2,3-dihydrobenzo[b][1,4]dioxin-6-yl)-2-morpholino-2-(pyridin-2-yl)ethan-1-one (3ar)



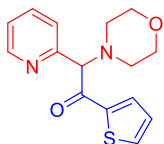
Compound **3ar** was prepared following the general procedure, purified by column chromatography using EtOAc/hexanes (1:2, v/v), and isolated as a yellow oil, 48.3 mg, 71%,  $^1\text{H}$  NMR (500 MHz,  $\text{CDCl}_3$ )  $\delta$  8.55 (dd,  $J = 5.0, 1.9$  Hz, 1H), 7.75 – 7.51 (m, 4H), 7.20 – 7.12 (m, 1H), 6.82 (dd,  $J = 9.1, 2.5$  Hz, 1H), 5.18 (s, 1H), 4.24 (ddd,  $J = 20.3, 6.0, 3.0$  Hz, 4H), 3.83 – 3.62 (m, 4H), 2.69 – 2.32 (m, 4H).  $^{13}\text{C}\{^1\text{H}\}$  NMR (126 MHz,  $\text{CDCl}_3$ )  $\delta$  194.9, 155.8, 149.5, 148.3, 143.3, 136.9, 130.1, 123.9, 123.3, 123.0, 118.5, 117.1, 77.4, 66.9, 64.7, 64.0, 52.0. HRMS (ESI) calcd. for  $\text{C}_{19}\text{H}_{20}\text{N}_2\text{O}_4$   $[\text{M}+\text{H}]^+$ : 341.1496, found: 341.1501

### 2-morpholino-2-(pyridin-2-yl)-1-(quinolin-6-yl)ethan-1-one (3as)



Compound **3as** was prepared following the general procedure, purified by column chromatography using EtOAc/hexanes (1:1, v/v), and isolated as a brown oil, 33.3 mg, 50%,  $^1\text{H}$  NMR (400 MHz,  $\text{CDCl}_3$ )  $\delta$  8.96 (dd,  $J = 4.2, 1.8$  Hz, 1H), 8.70 (d,  $J = 1.9$  Hz, 1H), 8.55 (dt,  $J = 5.0, 1.3$  Hz, 1H), 8.33 (dd,  $J = 8.9, 2.0$  Hz, 1H), 8.26 (dd,  $J = 8.3, 1.7$  Hz, 1H), 8.07 (d,  $J = 8.9$  Hz, 1H), 7.67 – 7.56 (m, 2H), 7.43 (dd,  $J = 8.4, 4.3$  Hz, 1H), 7.16 (ddd,  $J = 7.4, 4.9, 1.4$  Hz, 1H), 5.39 (s, 1H), 3.76 (dt,  $J = 5.7, 3.7$  Hz, 4H), 2.71 – 2.60 (m, 2H), 2.51 (ddd,  $J = 10.8, 5.9, 3.4$  Hz, 2H).  $^{13}\text{C}\{^1\text{H}\}$  NMR (101 MHz,  $\text{CDCl}_3$ )  $\delta$  196.2, 155.5, 152.8, 150.1, 149.6, 137.8, 137.0, 134.1, 130.9, 129.9, 128.2, 127.4, 124.0, 123.2, 121.9, 78.0, 66.9, 52.0. HRMS (ESI) calcd. for  $\text{C}_{20}\text{H}_{19}\text{N}_3\text{O}_2$   $[\text{M}+\text{H}]^+$ : 334.1550, found: 334.1556.

### 2-morpholino-2-(pyridin-2-yl)-1-(quinolin-6-yl)ethan-1-one (3at)



Compound **3at** was prepared following the general procedure, purified by column chromatography using EtOAc/hexanes (1:2, v/v), and isolated as a yellow oil, 31.7 mg, 55%,  $^1\text{H}$  NMR (400 MHz,  $\text{CDCl}_3$ )  $\delta$  8.56 (d,  $J = 4.9$  Hz, 1H), 8.03 (d,  $J = 3.8$  Hz, 1H), 7.73 – 7.58 (m, 3H), 7.23 – 7.16 (m, 1H), 7.10 (t,  $J = 4.5$  Hz, 1H), 5.01 (s, 1H), 3.76 (p,  $J = 3.0$  Hz, 4H), 2.63 (dt,  $J = 9.9, 4.5$  Hz, 2H), 2.48 (dt,  $J = 10.7, 4.6$  Hz, 2H).  $^{13}\text{C}\{^1\text{H}\}$  NMR (101 MHz,  $\text{CDCl}_3$ )  $\delta$  189.7, 155.6, 149.5, 143.0, 136.9, 134.7, 133.8, 128.2, 123.9, 123.1, 79.4, 66.8, 52.0. HRMS (ESI) calcd. for  $\text{C}_{15}\text{H}_{16}\text{N}_2\text{O}_2\text{S}$   $[\text{M}+\text{H}]^+$ : 289.1005, found: 289.1012.

- (a) Hahn, F. E.; Jahnke, M. C. *Angew. Chem., Int. Ed.* **2008**, *47*, 3122-3172. (b) Zhao, H.; Xu, J.; Chen, C.; Xu, X.; Pan, Y.; Zhang, Z.; Li, H.; Xu, L. *Advanced Synthesis & Catalysis*. **2018**. (c) Wang, Z.; Song, F.; Zhao, Y.; Huang, Y.; Yang, L.; Zhao, D.; Lan, J.; You, J. *Chemistry*. **2012**, *18*, 16616-20. (d) Odani, R.; Hirano, K.; Satoh, T.; Miura, M. *Angew Chem Int Ed Engl*. **2014**, *53*, 10784-8.

## Chapter 3 Palladium-catalyzed benzylic C(sp<sup>3</sup>)-H carbonylative arylation with aryl bromides

### 3.1 Introduction

Palladium mediated carbonylative cross-coupling reactions of aryl halides to make ketones has been one of the most popular research topics in transition metal-catalyzed carbonylation chemistry since its discovery in the 1930s.<sup>1</sup> Using a variety of organometallic reagents, aryl halides, and CO, these palladium-catalyzed coupling processes enable efficient construction of two C-C bonds to afford ketones in one step.<sup>2</sup> Since the first report in 2012,<sup>3</sup> the use of in situ generated carbanions from acidic C-H bonds (pro-nucleophiles) in carbonylation reactions has received much attention. Compared to conventional nucleophiles in carbonylative coupling reactions, pro-nucleophiles involving deprotonatable C-H bonds possess many advantages, such as being atom-economic and avoiding of prefunctionalized organometallics.

Great achievements have been made in carbonylative arylations of acidic C(sp<sup>3</sup>)-H bonds. Skrydstrup and co-workers reported palladium-catalyzed carbonylative  $\alpha$ -arylation of ketones with aryl iodides and aryl bromides, where bidentate phosphine ligands DPPP and Di-PrPF were used to synthesize 1,3-diketones (Scheme 1a, I).<sup>3a, 3b</sup> Meanwhile, Beller and co-workers described Pd-catalyzed carbonylative  $\alpha$ -arylation of acetone derivatives and  $\beta$ -ketonitriles with aryl iodides (Scheme 1a, II).<sup>3c, 3d</sup> Although these approaches provided useful carbonylation examples for both acidic (those with  $pK_a < 25$ ) and weakly acidic C-H bonds (those with  $pK_a > 25$ ), carbonylation of weakly

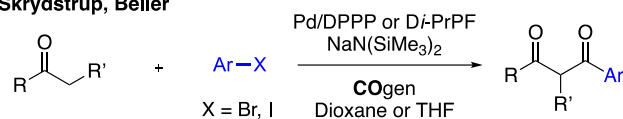
acidic C–H bonds remains underdeveloped. One possible work-around to this issue was reported by Skrydstrup and coworkers in 2014, who desired to prepare alkyl substituted  $\alpha$ -aryl ketones. Employing a three-step procedure, installation of an acyl group at the  $\alpha$ -position was first performed to increase the acidity of the remaining  $\alpha$ -protons. Next, the deprotonative carbonylation to give a 1,3-dicarbonyl intermediate was performed. Finally, the initial acyl group was removed under acidic conditions (Scheme 1a, III). Although this method provided access to products that were previously out of reach due to the elevated  $pK_a$ 's (higher than 30) of the pro-nucleophiles, the extra steps to add and remove the activating acyl group undermined the efficiency of the process.<sup>3e</sup>

To develop reactions at the weakly acidic C(sp<sup>3</sup>)–H bonds (those with  $pK_a > 25$ ), our group reported the first example of carbonylative arylation of azaarylmethylamines (Scheme 1b) with a NIXANTPHOS/Pd catalyst system.<sup>4</sup> This method exhibited good functional group tolerance in the synthesis of  $\alpha$ -amino ketones. Unfortunately, the method is limited to azaarylmethylamine pronucleophiles, and provided low yields when using electron-deficient aryl bromides. The most significant problem arose from the strong nucleophilicity of deprotonated pro-nucleophiles, where direct coupling with electrophiles was observed without the incorporation of CO into the product.<sup>5</sup> Thus, a general method for the carbonylation of weakly acid benzylic C–H bonds remains unknown.

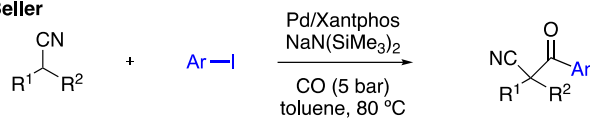
**Scheme 3-1.** Deprotonative carbonylative cross-coupling reactions

(a) **Previous works:** Pd-catalyzed acidic C-H carbonylative arylation

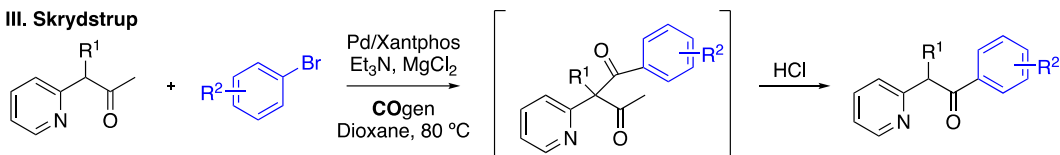
**I. Skrydstrup, Beller**



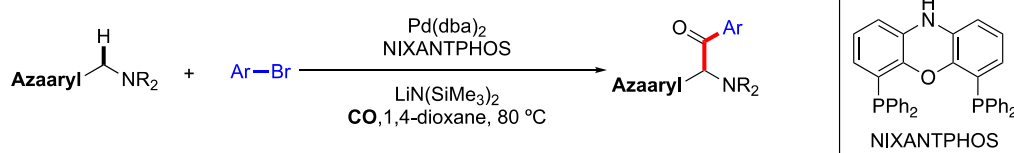
**II. Beller**



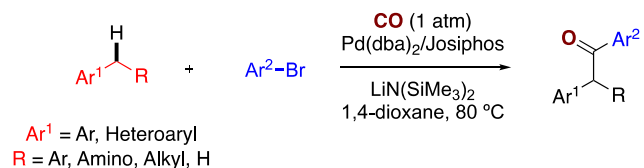
**III. Skrydstrup**



(b) **Our previous work:** Pd-catalyzed benzylic C-H carbonylative arylation of azaarylmethylamines



(c) **This work:** Pd-catalyzed benzylic C-H carbonylative arylation



$\alpha$ -Aryl ketones are key components of numerous biologically active compounds and display a wide range of medicinal and biological activities (Figure 1). For example  $\alpha$ -aryl ketone **A** exhibits very good inhibitory activity against phosphodiesterase 4 (PDE4). Upon PDE4 inhibition, the increase of intracellular cAMP promotes phosphorylation of specific proteins, leading to functional responses in the inflammatory cells.<sup>6</sup> In a second example, compound **B** inhibits heat shock protein 90 (HSP90). The inhibition of HSP90, a molecular chaperone, is widely used for treatment of cancers.<sup>7</sup> The  $\alpha$ -pyridyl ketones

motif **C** is an important precursor to both ML3403 and LN950, both of which are efficient p38 $\alpha$  MAP kinase inhibitors. The kinase p38 $\alpha$  MAP is a common target for treatment of pancreatic adenocarcinoma.<sup>8</sup> Compounds of the type **C** can be envisioned to result from the reaction of a 4-picoline derivative, aryl bromide, and CO under palladium catalysis. Unfortunately, current deprotonative carbonylative coupling methods are not applicable to this class of pro-nucleophiles.

Herein, we introduce a novel and highly efficient catalytic process that allows selective carbonylative cross coupling of weakly acidic benzylic C(sp<sup>3</sup>)-H bonds with aryl bromides. This method greatly expands the scope and increases the efficiency with weakly acidic pro-nucleophiles. While using very mild conditions with 1 atm of CO and a LiN(SiMe<sub>3</sub>)<sub>2</sub> base, the advantages of this method include low catalyst loading, low cost of the Pd source, high yields, and good functional group tolerance.

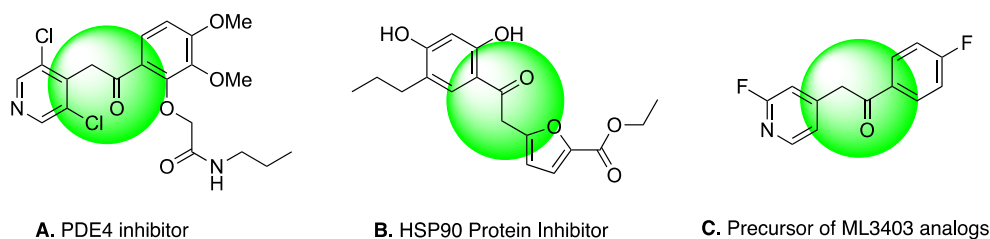


**Figure 3-1.** Selected pharmacologically active compounds containing  $\alpha$ -aryl ketones

### 3.2 Results and Discussion

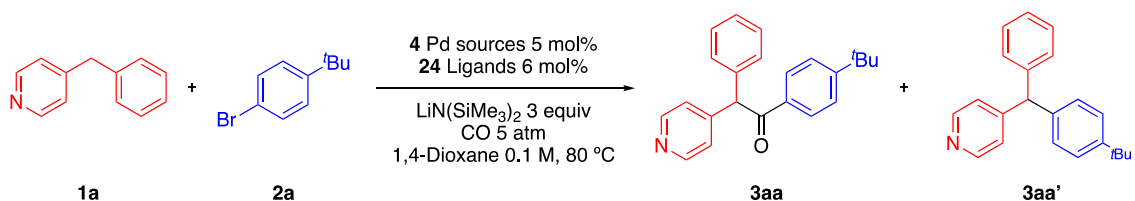
At the outset, our goals were to develop a catalytic system that not only has good reactivity with pro-nucleophiles of high pK<sub>a</sub> values but exhibits high selectivity toward formation of the carbonylative coupling product over the direct coupling byproduct (with no CO insertion). Rather than attempt to further optimize existing systems, we viewed the

best path forward to be to start anew by examining a collection of phosphine ligands in conjunction with palladium pre-catalysts. It is well known that ligand steric and electronic properties can have a dramatic impact on reactions with carbon monoxide.<sup>2</sup>

### 3.2.1 Optimization of DCCC with 4-benzylpyridine and Aryl Bromide 2a.

Pyridines are ubiquitous motifs in bioactive compounds,<sup>9</sup> including  $\alpha$ -aryl ketones. We, therefore, adopted the 4-pyridyl group in our optimization study. Using 4-benzylpyridine **1a** and 1-bromo-4-*tert*-butylbenzene **2a** as starting materials, we performed a 10  $\mu$ mol scale high throughput screen of 24 ligands and 4 palladium sources (Scheme 2). The ligands, including sterically and electronically diverse, mono- and bidentate phosphine ligands, were examined in combination with different Pd(0) and Pd(II) sources. The screen was conducted at 80 °C under 5 atm of CO (see the Supporting Information for details). The ligands were ranked by both yields of the corresponding ketone product and the selectivity against an internal standard (ketone product **3aa** versus direct coupling byproduct **3aa'**, Scheme 2).

#### Scheme 3-2. HTE Screen of Pd-Catalyzed Deprotonative Carbonylative Cross-coupling of 4-Benzylpyridine

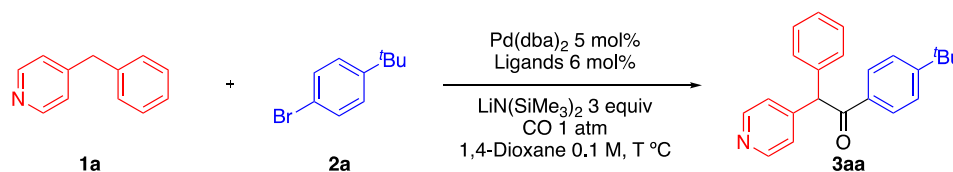


Of the ligands screened, Josiphos SL-J001-1 was the top hit, affording both the highest yield of product **3aa** and the best selectivity (**3aa** versus **3aa'**). Pd(0) sources outperformed Pd(II) sources. Repeating the best conditions on laboratory scale (0.2 mmol) using Pd(dba)<sub>2</sub> and Josiphos SL-J001-1 resulted in generation of **3aa** in 94% yield (Table1, entry 1). Since Josiphos SL-J001-1 was the only ligand used from the Josiphos family in the screening, we next tested



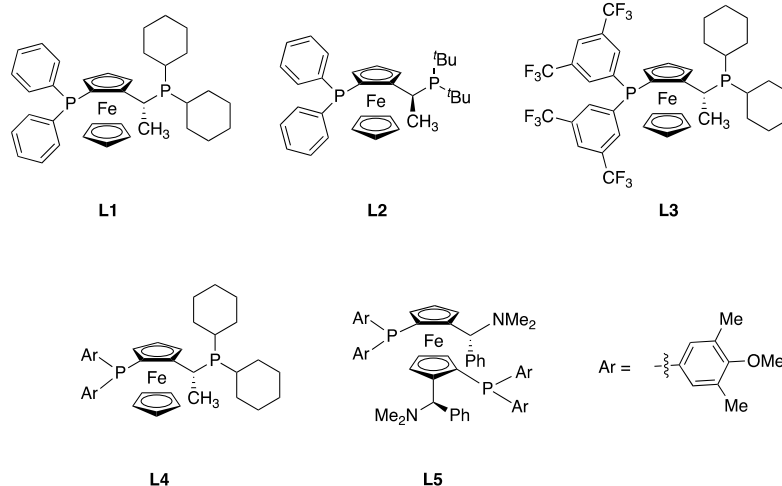
other representative Josiphos-type ligands **L2** – **L5**, including the sterically hindered **L2**, electron-poor **L3**, electron-rich **L4** and a MandyPhos ligand **L5**. These ligands afforded lower yields (Table 1, entry 2–5). It is interesting to note that there were no direct coupling byproducts (**3aa'**) formed with these ligands. Conducting the reaction at a lower temperature (65 °C) caused a 30% decrease in yield (Table 1, entry 6). Using Pd(OAc)<sub>2</sub> resulted in a drop in yield from 94% to 70%. Reactions conducted without the palladium catalyst did not give any product (Table 1, entry 7 and 8).

**Table 3-1. Examination of different members of the Josiphos family of ligands.<sup>a</sup>**



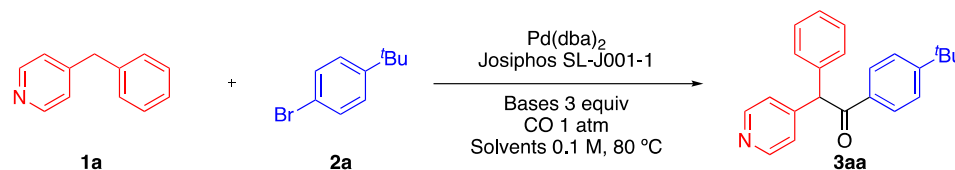
Entry	Pd Source	Ligand	Temp (°C)	Yields (%)
1	Pd(dba) <sub>2</sub>	<b>L1</b>	80	94%
2	Pd(dba) <sub>2</sub>	<b>L2</b>	80	62%
3	Pd(dba) <sub>2</sub>	<b>L3</b>	80	2%
4	Pd(dba) <sub>2</sub>	<b>L4</b>	80	55%
5	Pd(dba) <sub>2</sub>	<b>L5</b>	80	8%
6	Pd(dba) <sub>2</sub>	<b>L1</b>	65	64%
7	Pd(OAc) <sub>2</sub>	<b>L1</b>	80	70%

8	None	None	80	0
---	------	------	----	---



Further optimization on lab scale was performed to examine the impact of different bases and solvents. Replacement of  $\text{LiN}(\text{SiMe}_3)_2$  with  $\text{NaN}(\text{SiMe}_3)_2$ , or  $\text{KN}(\text{SiMe}_3)_2$  resulted in only 15–23% yields (Table 2, entries 2 and 3). The reaction did not perform as well in THF (86%) or cyclopentyl methyl ether (CPME, 76%) (Table 2, entries 4 and 5). Decreasing the catalyst loading to 1.0 mol % resulted in no change in the yield (Table 2, entries 6 and 7), while further reduction of the catalyst loading to 0.5 mol% failed to afford the desired products.

**Table 3-2. Optimization of DCCC with 4-benzylpyridine and Aryl Bromide 2a**



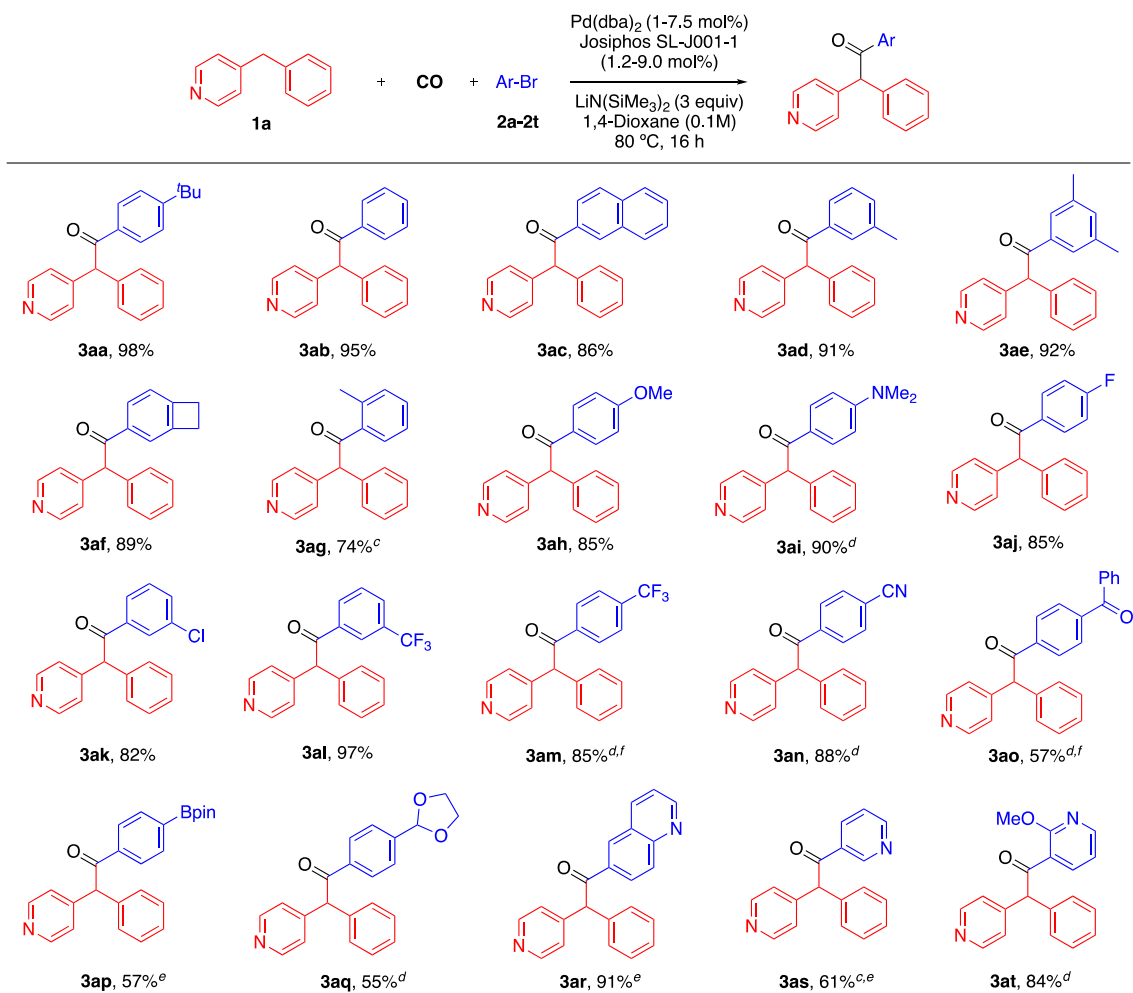
Entry	Catalyst loading	Solvent	Base	Yields (%)
1	5.0%	Dioxane	LiN(SiMe <sub>3</sub> ) <sub>2</sub>	99%
2	5.0%	Dioxane	NaN(SiMe <sub>3</sub> ) <sub>2</sub>	23%
3	5.0%	Dioxane	KN(SiMe <sub>3</sub> ) <sub>2</sub>	15%
4	5.0%	CPME	LiN(SiMe <sub>3</sub> ) <sub>2</sub>	76%
5	5.0%	THF	LiN(SiMe <sub>3</sub> ) <sub>2</sub>	86%
6	2.5%	Dioxane	LiN(SiMe <sub>3</sub> ) <sub>2</sub>	98%
7	1.0%	Dioxane	LiN(SiMe <sub>3</sub> ) <sub>2</sub>	97%
8	0.5%	Dioxane	LiN(SiMe <sub>3</sub> ) <sub>2</sub>	0

### 3.2.2 Scope of the carbonylative arylation reaction

With the optimized reaction conditions in hand (Table 2, entry 7), we explored the scope of aryl bromides with 4-benzylpyridine (Table 3, **1a**). Aryl bromides bearing a variety of electron donating and electron withdrawing substituents exhibited good to excellent yields. As expected, aryl bromides bearing electron-neutral alkyl groups or extended pi-systems (**2a–2f**, 86–98% yields) and electron-rich aryl bromides containing 4-OMe and 4-NMe<sub>2</sub> (**2h–2i**, 85–90% yields) smoothly afforded the corresponding ketone products. Among these, the benzocyclobutane-derived aryl bromide is noteworthy. This method also successfully converted sterically hindered 2-bromotoluene **2g** to ketone product in 74% yield.

It is noteworthy that our previously reported method<sup>4</sup> gave poor yields with electron-deficient aryl bromides. In contrast, the current method exhibited excellent reactivity with aryl bromides bearing electronegative (4-F) and electron withdrawing (3-Cl, 3-CF<sub>3</sub>, 4-CF<sub>3</sub> and 4-CN) substituents (**2j–2n**) (82– 97%). 4-Bromobenzophenone **2o** was also tolerated upon carbonylation at a lower reaction temperature of 40 °C with higher catalyst loading (5 mol% Pd). Acetal substituted and 4-Bpin substituted bromobenzenes **2p** and **2q** were carbonylated at higher catalyst loading to afford the desired products in 55–57% yield. The finding that the B(pin)-containing product was formed is remarkable, given that aryl bromides are well known to undergo cross-coupling reactions with aryl boronic acid derivatives under basic conditions in the Suzuki reaction. Of course, this product could be further elaborated in palladium catalyzed coupling processes.<sup>10</sup> In addition to bromobenzene derivatives, heteroaryl bromides were also well-tolerated with the current catalytic system. While 6-bromoquinoline **2r** reacted efficiently to give the desired product **3ar** in 91% yield, 3-bromopyridine **2s** afforded the desired product in 61% yield. When a methoxy group was present at 2-position of 3-bromopyridine, reducing the binding ability of the pyridyl nitrogen, the ketone product **3at** was generated in 84% yield.

**Table 3-3.** Scope of Aryl Bromides in Pd-Catalyzed Carbonylative Arylation<sup>a,b</sup>



<sup>a</sup>Reactions conducted on a 0.1 mmol scale using 1% Pd(dba)<sub>2</sub>, 1.2% Josiphos SL-J001-1, 1 equiv 4-benzylpyridine, 3 equiv LiN(SiMe<sub>3</sub>)<sub>2</sub>, and 1.5 equiv aryl bromide at 0.1 M. <sup>b</sup>Isolated yield after chromatographic purification. <sup>c</sup>100 °C.

<sup>d</sup>5.0 mol% Pd(dba)<sub>2</sub> and 6.0 mol% Josiphos SL-J001-1. <sup>e</sup>7.5 mol% Pd(dba)<sub>2</sub> and 9.0 mol% Josiphos SL-J001-1. <sup>f</sup>40 °C, 20 h.

The scope of the carbonylative arylation with various arylmethane or heteroarylmethane pro-nucleophiles and 1-bromo-4-*tert*-butylbenzene (**2a**) is presented in Table 4. 4-Benzylpyridine derivatives bearing electron donating (4-*tert*-Bu, **1b**), electronegative (4-F, **1c**) and electron withdrawing (3-CF<sub>3</sub>, **1d**) groups provided the corresponding products

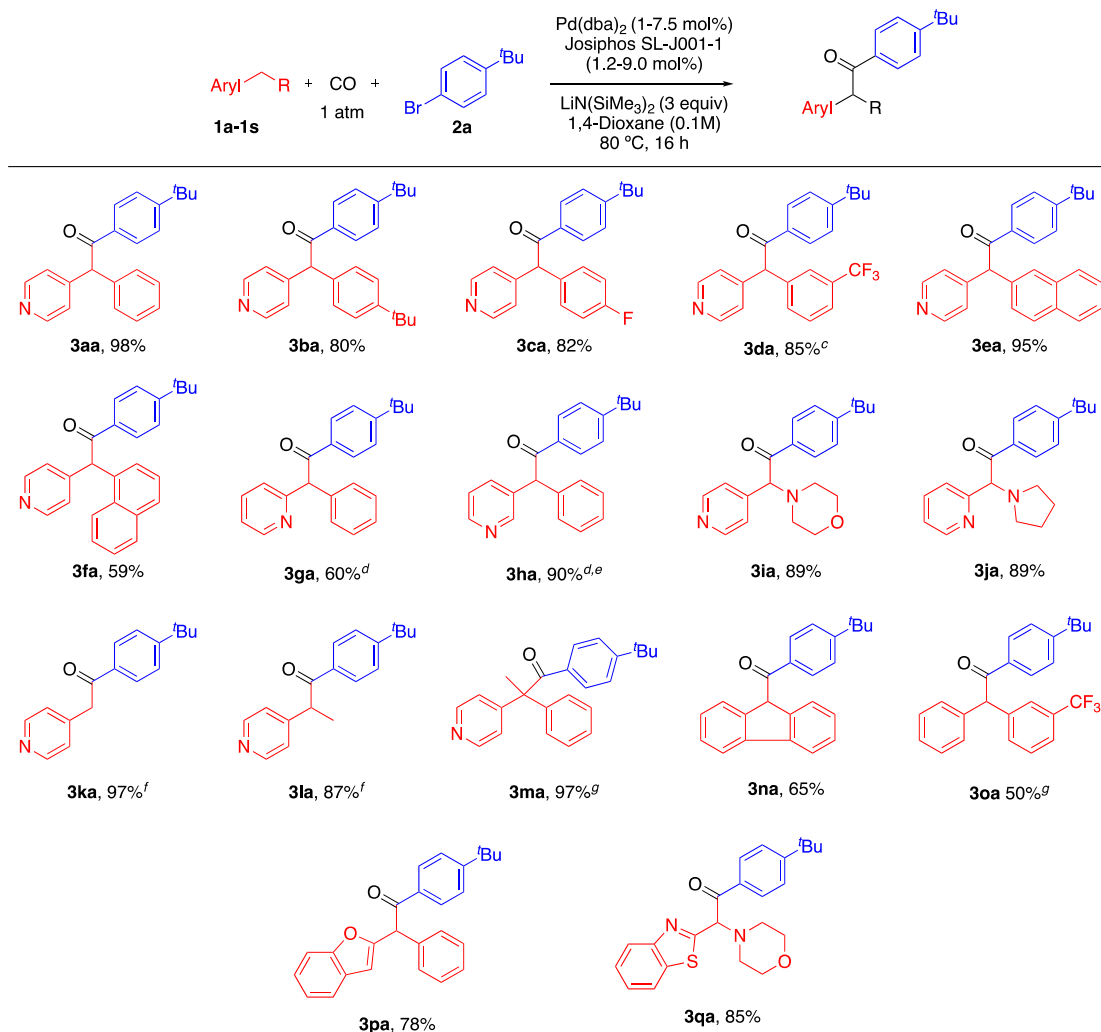
in 80–85% yields. When switching from 4-phenyl pyridine (**1a**) to the more hindered 1-naphthyl analog (**1f**), a decrease in yield to 59% was observed. On the other hand, the 2-naphthyl derivative (**1e**) gave the expected ketone in 95% yield.

We were next interested in exploring the scope of the heterocyclic group. When 4-benzylpyridine ( $pK_a = 26.7$  in DMSO)<sup>11</sup> was substituted with the less acidic 3-benzyl pyridine **1h** ( $pK_a = 30.15$  in DMSO)<sup>11</sup>, and 2 extra equivalents of  $\text{LiN}(\text{SiMe}_3)_2$  were added, a 90% yield was observed. However, 2-benzylpyridine **1g** ( $pK_a = 28.2$ ),<sup>11</sup> with an acidity between 3- and 4- benzylpyridines, only afforded 60% yield under conditions with a higher catalyst loading (7.5 mol%). Higher base loadings did not increase the yield. In addition to benzyl pyridines, this catalytic system was also compatible with azaarylmethylamines. Thus, 4-pyridylmethyl morpholine **1i** and 2-pyridylmethyl pyrrolidine **1j** both delivered ketone products in 89% yield, which is comparable to the reported yields in the Pd/NIXANTPHOS system.<sup>4</sup>

To further expand the scope of this method, different classes of pro-nucleophiles were examined. 4-Picoline **1k** and 4-ethylpyridine **1l** both afforded 89% yield of the ketone products. It is surprising that, although the products of these reactions are significantly more acidic than the starting pro-nucleophiles, no products derived from overcarbonylation were observed. We next examined the behavior of tertiary benzylic pro-nucleophiles. For example, when 4-(1-phenylethyl)pyridine (**1m**) was employed in the carbonylation, the product containing a quaternary  $\alpha$ -carbonyl compound was obtained in 97% yield. Unfortunately, the product was nearly racemic in all attempts.

To test the limits of our carbonylation catalyst, less acidic substrates were examined. We previously employed diphenylmethane ( $pK_a$  value of 32.2 in DMSO)<sup>11</sup> and its derivatives in the direct coupling with aryl bromides and chlorides to afford triphenylmethanes.<sup>12</sup> Under the direct coupling conditions,  $\text{KN}(\text{SiMe}_3)_2$  was necessary whereas  $\text{LiN}(\text{SiMe}_3)_2$  was ineffective unless additives (diamines or crown ethers) were employed.<sup>13</sup> Unfortunately, diphenylmethane did not afford any ketone products under the carbonylation conditions with either  $\text{LiN}(\text{SiMe}_3)_2$ ,  $\text{NaN}(\text{SiMe}_3)_2$  or  $\text{KN}(\text{SiMe}_3)_2$ . Following to our previous study on additive effects on deprotonative cross-coupling of diphenylmethanes,<sup>13</sup> crown ether additives were tested, but no did not positively impact the reaction yields (see Experimental section). Addition of an electron withdrawing 3- $\text{CF}_3$  substituent on the diphenylmethane (**1o**) was sufficient to increase the reactivity, resulting in the product **3oa** in 50% yield. By comparison, the more acidic fluorene **1n**, with a  $pK_a$  of 22.6 in DMSO,<sup>11</sup> afforded the product in 65% yield. Finally, we wished to examine the use of other heterocyclic derivatives in the carbonylative coupling process. Two representative heterocycles, benzofuran and benzothiazole were successfully carbonylated to generate products **3pa** and **3qa** in 78% and 85% yields, respectively.

**Table 3-4.** Scope of pro-nucleophiles in Pd-Catalyzed Carbonylative Arylation<sup>a,b</sup>



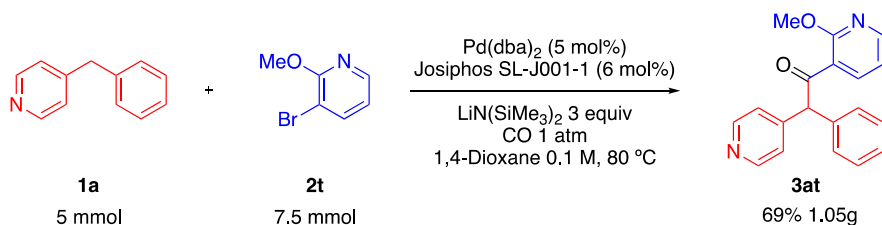
<sup>a</sup>Reactions conducted on a 0.1 mmol scale using 1% Pd(dba)<sub>2</sub>, 1.2% Josiphos SL-J001-1, 1 equiv of pronucleophile **1a-1s**, 3 equiv of LiN(SiMe<sub>3</sub>)<sub>2</sub>, and 1.5 equiv of **2a** at 0.1 M. <sup>b</sup>Isolated yield after chromatographic purification. <sup>c</sup>5.0 mol% Pd(dba)<sub>2</sub> and 6.0 mol% Josiphos SL-J001-1. <sup>d</sup>7.5 mol% Pd(dba)<sub>2</sub> and 9.0 mol% Josiphos SL-J001-1. <sup>e</sup>5 equiv of LiN(SiMe<sub>3</sub>)<sub>2</sub> and 3 equiv of **2a**. <sup>f</sup>1 equiv of **2a**, and 1.2 equiv of arylmethane. <sup>g</sup>THF used as solvent.

To showcase the synthetic utility of our method, we conducted a gram-scale reaction of **1a**, **2t** and CO under the standard reaction conditions (Scheme 3). Use of 5 mmol of 4-benzylpyridine led to the successful synthesis of 1.05 g (3.45 mmol) ketone product **3at** under the carbonylation conditions. The yield of the gram-scale synthesis was 69%, which was 15% lower than the small-



scale synthesis. The difference in yield is probably due to poor mixing efficiency, which is an essential factor in gas reactions.

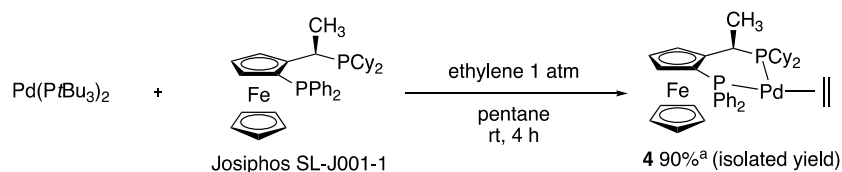
### Scheme 3-3. Gram-scale synthesis examples



### 3.2.3 Mechanistic Studies

To gain insight into the mechanism of the carbonylation reaction, we first wanted to identify the resting state of the catalyst. It is noteworthy that although  $\text{Pd(dba)}_2$  was an effective precatalyst for the carbonylation process, it created complexity when studying the mechanism due to the liberated dibenzylideneacetone. Dibenzylideneacetone can bind to palladium even while a bidentate ligand is on the metal center.<sup>14</sup> Based on previously published work by Hartwig and co-workers, a bidentate phosphine bonded Pd ethylene complex would easily react with CO to form  $\text{L}_2\text{Pd(CO)}_2$ .<sup>15</sup> Thus, (Josiphos)Pd(ethylene) (**4**) was synthesized by purging ethylene gas through a solution of  $\text{Pd[P}(t\text{Bu})_3]_2$  and Josiphos in pentane (Scheme 4). The ethylene complex was generated as after 4 h as white solid in 90% isolated yield.

### Scheme 3-4. Synthesis of (Josiphos)Pd( $\text{C}_2\text{H}_4$ ) complex **4**<sup>a</sup>



The ethylene complex **4** was characterized by NMR spectroscopy, and its structure was determined by X-ray crystallography (Figure 2). Complex **4** was stable to loss of ethylene under vacuum and could be stored at  $-13\text{ }^{\circ}\text{C}$  for more than a year. Complex **4** was then applied to the carbonylative reaction conditions and found to be an effective catalyst that maintain similar yields to the  $\text{Pd}(\text{dba})_2$ -based catalyst (see the Experimental for details). The solid-state structure of  $\text{Pd}(0)$  complex **4** was determined by X-ray crystallography (Figure 2). In the solid state, this complex displays a distorted tetrahedral geometry, where the bite angle of Josiphos is  $97.52(4)^{\circ}$ . The C1–C2 bond distance is  $1.396(10)\text{ \AA}$ , which is lengthened relative to the carbon-carbon double bond in ethylene ( $1.3305\text{ \AA}$ ),<sup>16</sup> indicating a donation of electron density into ethylene  $\pi^*$  orbital, which is similar to previously reported  $(\text{DCPP})\text{Pd}(\text{C}_2\text{H}_4)$  complex ( $1.402\text{ \AA}$ ).<sup>15a</sup>

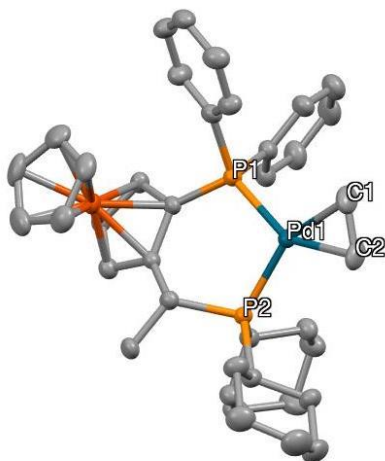
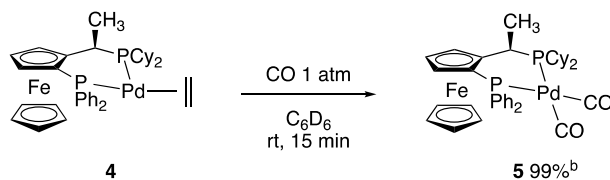


**Figure 3-2.** Crystal structure of **4** with selected bond lengths ( $\text{\AA}$ ): P1–Pd1 =  $2.2828(12)$ , P2–Pd1 =  $2.3110(12)$ , Pd1–C1 =  $2.132(6)$ , Pd1–C2 =  $2.133(5)$ , C1–C2 =  $1.396(10)$ . Selected bond angles ( $\text{deg } ^{\circ}$ ): P1–Pd1–P2 =  $97.52(4)$ , C1–Pd1–P1 =  $111.6(2)$ , C2–Pd1–P2 =  $112.79(18)$ , C1–Pd1–C2 =  $38.2(3)$ .

We assumed that Pd-carbonyl complexes would be key intermediates in the carbonylative coupling reactions and, therefore, set out to synthesize and characterize these complexes. The bis-carbonyl compound (Josiphos)Pd(CO)<sub>2</sub> **5** was synthesized by application of 1.0 atm of CO to the ethylene complex **4** in a solution in C<sub>6</sub>D<sub>6</sub> in a J-Young NMR tube. After a process of cooling the J-Young tube in liquid nitrogen, evacuating the headspace under vacuum, warming the system to room temperature and pressurizing with 1 atm of CO, the substitution of ethylene in **4** by CO finished in 15 min in 99% yield (Scheme 5) The bis-carbonyl compound **5** was not stable in the absence of CO. After exposure to N<sub>2</sub>, the complex decomposed in 30 min. Similar stability was observed by Hartwig for (DCPP)Pd(CO)<sub>2</sub> complex.<sup>15a</sup> The <sup>31</sup>P{<sup>1</sup>H} NMR spectrum of **5** consisted of two doublets at 5.2 ppm and 42.8 ppm with a coupling constant of 13.0 Hz. The <sup>13</sup>C{<sup>1</sup>H} NMR spectrum had a broad resonance at 195.7 ppm for the carbonyl ligands.

**Scheme 3-5.** Synthesis of (Josiphos)Pd(CO)<sub>2</sub> complex **5**<sup>a</sup>



<sup>a</sup>Yield of bis-carbonyl complex determined by <sup>31</sup>P NMR spectroscopy with PMes<sub>3</sub> as an internal standard.

To determine the number and bonding mode of the CO ligands bound to Pd under conditions relevant to the catalytic process, we first conducted the reaction in Scheme 5 with <sup>13</sup>C labeled CO. It was hoped that we could see the <sup>13</sup>C–Pd–P coupling pattern in the resultant complex. However, only one broad resonance at 187.5 ppm was observed in

the  $^{13}\text{C}$  NMR in  $\text{C}_6\text{D}_6$  at room temperature, which is between the  $^{13}\text{C}$  NMR chemical shifts of **5** (195.7 ppm) and free CO (184 ppm). This observation is consistent with rapid exchange between bound and free  $^{13}\text{CO}$ .<sup>15b</sup> A similar observation was made by Hartwig and coworkers in their examination of CO binding to DCPD-Pd(0).<sup>15a</sup> To complement the NMR spectral data, we next measured solution-phase IR spectra of the Pd(0) carbonyl complex generated from **4** under 1.0 atm of CO in 1,4-dioxane- $d_8$ . Two C–O stretches were observed at 2010 and 1964  $\text{cm}^{-1}$  (see Appendix A3), which is consistent with the formulation of the Pd(0) species as a tetrahedral complex with two terminal carbonyl ligands. There are several reported (bisphosphine)Pd(CO)<sub>2</sub> complexes that possess similar IR patterns and frequencies, i.e. (DCPD)Pd(CO)<sub>2</sub> with two stretches at 1993 and 1949  $\text{cm}^{-1}$  by Hartwig<sup>15a</sup>, (dtbpe)Pd(CO)<sub>2</sub> with two stretches at 2012 and 1969  $\text{cm}^{-1}$  by Pörschke,<sup>15b</sup> (DIPPP)Pd(CO)<sub>2</sub> with two stretches at 2002 and 1961  $\text{cm}^{-1}$  by Bunel,<sup>15c</sup> and (Xantphos)Pd(CO)<sub>2</sub> with two stretches at 2014 and 1974  $\text{cm}^{-1}$  by Grushin and Macgregor.<sup>17</sup>

Our complex **5** was then crystallized by cooling the  $\text{C}_6\text{D}_6$  solution to 10 °C under 1 atm of CO atmosphere. The X-ray crystallography indicated a pseudo-tetrahedral dicarbonyl structure with a molecule of  $\text{C}_6\text{D}_6$  co-crystallized (Figure 3). The relevant bond distances and angles are provided in the caption to Figure 2. The structure of **5** possesses a tight bite angle, with P1–Pd1–P2 angle of 93.29(6)° while the C1–Pd1–C2 angle was 117.4(3)°. The C1–O1 and C2–O2 bond distances are 1.124 (9) and 1.134(9) respectively. These C–O bond lengths are very similar to the C–O bond lengths in other reported terminal CO bonded Pd(0) complexes.<sup>15a, 15b, 17</sup>

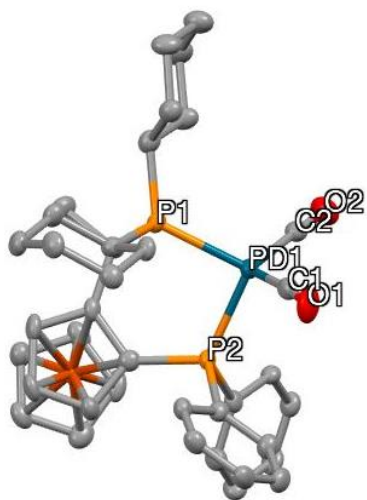


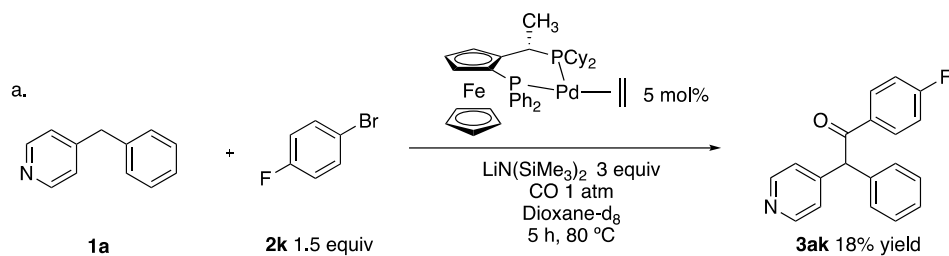
**Figure 3-3.** Crystal structure of **5** with selected bond lengths (Å): P1–Pd1 = 2.3931(17), P2–Pd1 = 2.3735(18), Pd1–C1 = 1.982(8), Pd1–C2 = 1.957(7), C1–O1 = 1.124 (9), C2–O2 = 1.134(9). Selected bond angles (deg °): P1–Pd1–P2 = 93.29(6), C1–Pd1–P1 = 112.3(2), C2–Pd1–P2 = 115.3(2), C1–Pd1–C2 = 117.4(3).

### 3.2.4 Identification of the Catalyst Resting State.

We next set out to identify the catalyst resting state. Thus, the carbonylation of 4-benzylpyridine with 4-fluoro-1-bromobenzene was conducted at 80 °C in 1,4-dioxane- $d_8$  with (Josiphos)Pd(ethylene) **4** as the pre-catalyst (Scheme 6). After 5 h at 80 °C, the NMR tube was removed from the heating bath and  $^1\text{H}$  and  $^{31}\text{P}$  NMR spectra were acquired at room temperature. By  $^1\text{H}$  NMR it was found that 18% of the product had been generated. The  $^{31}\text{P}$  NMR spectrum consisted of two doublets at 18.9 ppm and 80.5 ppm with a coupling constant of 13.0 Hz (Figure 4a), which correspond to the two doublets in dicarbonyl complex **5** (Figure 4b). Based on the similarity of the  $^{31}\text{P}\{^1\text{H}\}$  NMR chemical shifts and splitting pattern, the resting state of the catalyst appears to be (Josiphos)Pd(CO) $_2$ . We note that a similar resting-state species was observed by Hartwig

in a similar type of carbonylation reaction with a bidentate phosphine ligand and palladium catalyst.<sup>15a</sup>

**Scheme 3-6.** Identification of catalyst resting state.<sup>a</sup>



<sup>a</sup>Conversion was determined with <sup>1</sup>H NMR spectroscopy with 1,3,5-trimethoxybenzene as an internal standard.

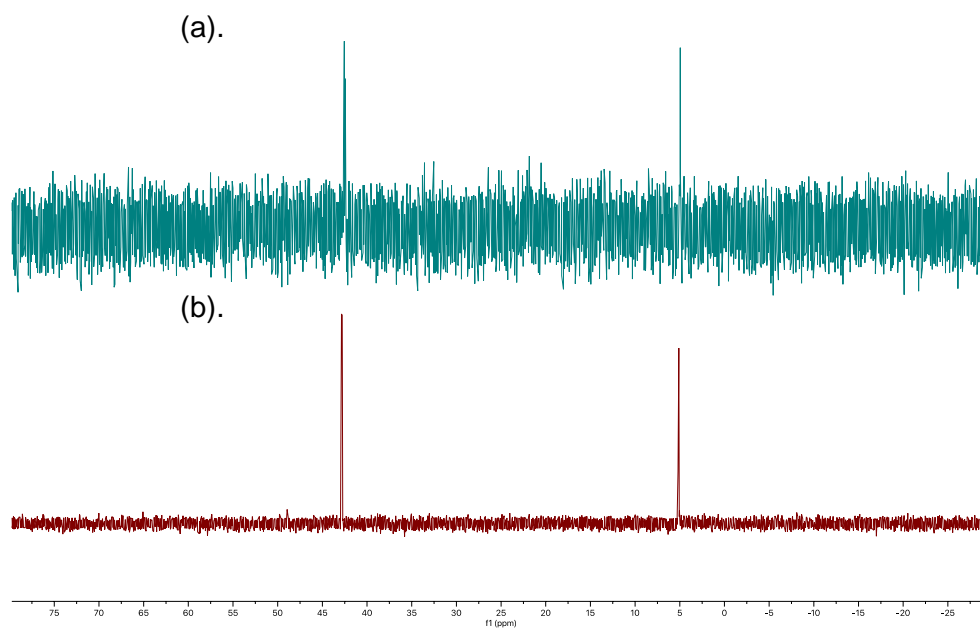
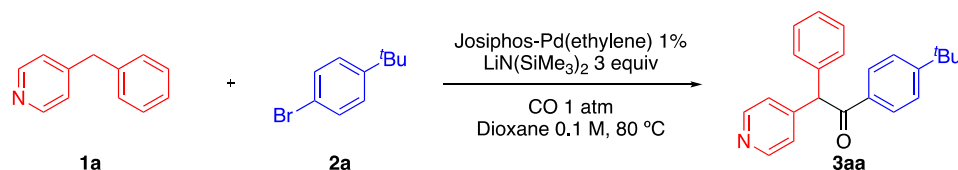


**Figure 3-4.** (a). Room-temperature <sup>31</sup>P{<sup>1</sup>H} NMR spectra of a catalytic reaction at partial conversion conducted at 80 °C. (b) <sup>31</sup>P{<sup>1</sup>H} NMR spectra of **5**.

### 3.2.5 Study of the turnover-limiting step

We next desired to study the turnover limiting step of the catalytic reaction through kinetic studies. An initial rate study of the reaction with 4-benzylpyridine and different equivalents of 1-bromo-4-*tert*-butylbenzene **2a** were conducted under pseudo-first-order conditions of excess **2a** at 80 °C in 1,4-dioxane (Scheme 7). The loading of ethylene complex **4** was kept at 1 mol% in this study to ensure the accurate measurement of the rates. First, reaction rate at each concentration of **2a** was measured by time course study of the reaction over 2 hours (conversion < 10%, SI, S24). The generation of ketone product **3aa** was measured by monitoring the <sup>1</sup>H NMR of four parallel reactions being quenched at four time points (30 min, 60 min, 90 min, 120 min). Then the observed rate constant  $k_{\text{obs}}$  was calculated based on the reaction rates and concentration of **2a**. The initial reaction rate  $k_{\text{obs}}$  of the reaction exhibited a linear relationship with respect to the concentration of the aryl bromide. The dependence of the rate on the concentration of 1-bromo-4-*tert*-butylbenzene was determined to be first order based on the linear relationship between  $k_{\text{obs}}$  and [ArBr] (Figure 5a). Further time course study of the carbonylative arylation reaction at different CO pressures (1, 2, and 4 atm) suggested that higher CO pressures reduced the reaction rate (Figure 5b).

**Scheme 3-7.** Determination of the rate Constants  $k_{\text{obs}}$  from the initial rate study.



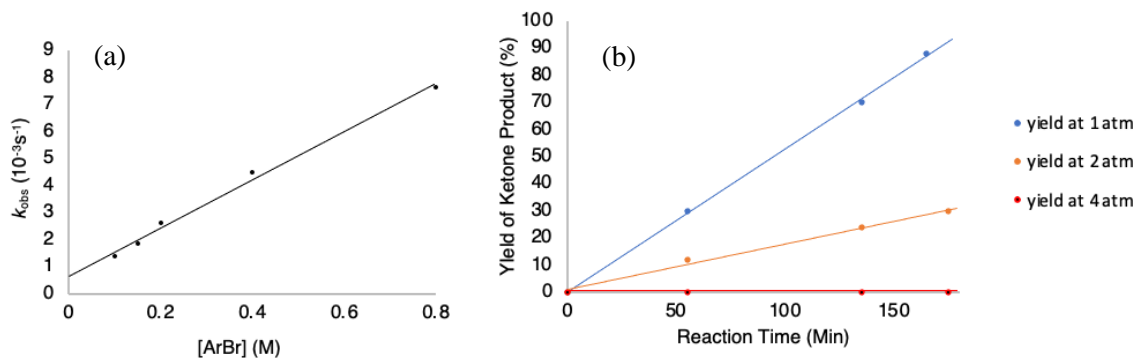


**Figure 3-5.** (a) Dependence of the observed rate constant ( $k_{\text{obs}}$ ) on the concentration of ArBr (0.1–0.8 M) with **4** as the pre-catalyst, pCO = 1 atm and **1a** = 0.1 M at 80 °C within 2.5 h, and (b) Time course study of the reaction with **4** as the pre-catalyst at various pressures of CO (1–4 atm) with **2a** = 0.15 M, **1a** = 0.1 M.

### 3.2.6 Study of key intermediates

We next wanted to explore other likely intermediates in the carbonylation reaction, such as (Josiphos)Pd(Ar)Br and (Josiphos)Pd(COAr)Br. Using Pd(*Pt*Bu<sub>3</sub>)<sub>2</sub>, we synthesized (Josiphos)Pd(II) aryl halide complexes by first adding aryl bromides to Pd(*Pt*Bu<sub>3</sub>)<sub>2</sub> and stirring in toluene at room temperature for 12 h. Next, Josiphos was added to the mixture to substitute *Pt*Bu<sub>3</sub>. As might be expected, the inequivalent phosphorus centers of the Josiphos ligand gave rise to two isomeric oxidative addition products (Scheme 8a). In the case of 4-fluoro-1-bromobenzene, the ratio of **6** : **6'** was 1 : 2. Presumably the minor isomer has the aryl group positioned next to the bulkier PCy<sub>2</sub> moiety. Subsequent experiments demonstrated that the ratio of the two isomers was influenced by the steric and electronic parameters of the aryl substituent. Compared to Ar = 4-C<sub>6</sub>H<sub>4</sub>-F, a more sterically hindered 1-bromonaphthalene gave a higher ratio between the isomers (1 : 8). Meanwhile, 2-bromotoluene afforded a 1 : 10 ratio of two isomers. Surprisingly, when using 4-bromobenzotrifluoride **2m** to conduct the oxidative addition reaction in Scheme 8,





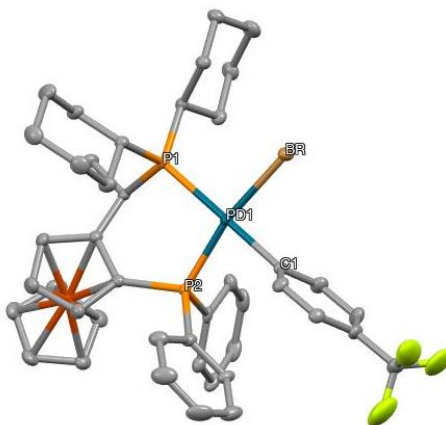
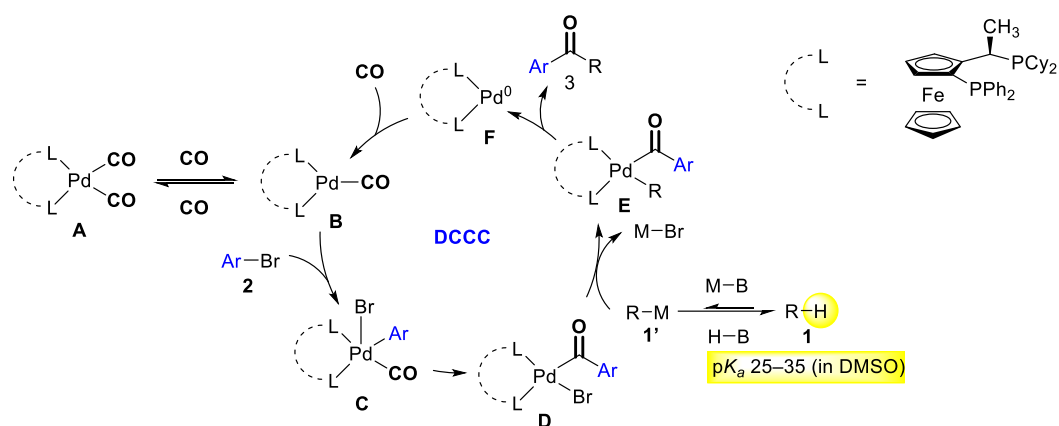


**Figure 3-6.** Crystal structure of **6m'** with selected bond lengths (Å): P1–Pd1 = 2.3792(10), P2–Pd1 = 2.2508(10), Pd1–C1 = 2.045(4), Pd1–Br = 2.4792(5). Selected bond angles (deg °): P1–Pd1–P2 = 95.38(3), P1–Pd1–Br = 85.76(3), P2–Pd1–C1 = 84.60(11), C1–Pd1–Br = 84.28(11).

Based on the previous reports in deprotonative cross-coupling processes<sup>12-13, 18</sup> and carbonylative cross-coupling processes,<sup>3e, 4, 19</sup> a plausible mechanism is proposed in Scheme 9. The catalytic cycle starts with complexation of Josiphos and Pd(dba)<sub>2</sub> under CO to yield the resting state species (Josiphos)Pd(CO)<sub>2</sub> **A**. The (Josiphos)Pd(CO)<sub>2</sub> species is proposed to undergo reversible dissociation of CO from **A** to generate the 16-electron (Josiphos)Pd(CO) mono-carbonyl complex **B**. Turnover-limiting oxidative addition of the aryl bromide **5** takes place to produce (Josiphos)Pd(CO)(Ar)Br complex **C**. Intermediate **C** likely undergoes CO insertion into the Pd–Ar bond to furnish the acyl-Pd(II) complex **D**. Acyl intermediate **D** is expected to react with the deprotonated pronucleophile **4'** in a transmetalation step to deliver the reductive elimination precursor **E**. Reductive elimination of **E** gives the ketone product **3**, which will be deprotonated to give the enolate and Pd(0) species **F**. Intermediate **F** will bind CO to regenerate (Josiphos)Pd(CO) **B** and close the catalytic cycle.

According to previous studies of deprotonative cross-coupling reactions,  $\text{KN}(\text{SiMe}_3)_2$  was nearly always the base that gave the highest yields.<sup>13, 18c</sup> In contrast, in the carbonylative coupling process  $\text{KN}(\text{SiMe}_3)_2$  results in a significant decrease in yield (85% less compared to Li). Although we propose a transmetalation step with  $(\text{Josiphos})\text{Pd}(\text{Ar})\text{Br}$ , we cannot rule out the possibility of direct attack of the nucleophile on the acyl group of  $(\text{Josiphos})\text{Pd}(\text{COAr})\text{Br}$ .



**Scheme 3-9.** Proposed mechanism for palladium-catalyzed carbonylative arylation of weakly acid C–H bonds.

### 3.3 CONCLUSIONS

In conclusion, we have developed a general method for the palladium-catalyzed carbonylative arylation of weakly acidic benzylic  $\text{C}(\text{sp}^3)\text{-H}$  bonds with aryl bromides. This new catalyst system enables coupling of pro-nucleophiles with high  $\text{p}K_{\text{a}}$  values (approaching a  $\text{p}K_{\text{a}}$  value of 32 in DMSO). Pro-nucleophiles suitable for these coupling reactions include heteroarylmethane derivatives that contain functional groups commonly observed in medications. The low catalyst loading of 1% and low pressure of CO (1 atm) are attractive features of this chemistry, increasing its potential for industrial applications.

It is worth noting that the ligand used in this method is enantioenriched, but due to the formation of enolate products, only racemic materials are obtained. Future efforts will focus on tertiary pro-nucleophiles containing tertiary C–H bonds, with the goal to construct chiral quaternary carbon centers.

### 3.4 REFERENCES

1. (a) Wu, X.-F. *RSC Advances*. **2016**, *6*, 83831-83837. (b) Barnard, C. F. J. *Organometallics*. **2008**, *27*, 5402-5422. (c) Tu, T.; Fang, W.; Zhu, H.; Deng, Q.; Liu, S.; Liu, X.; Shen, Y. *Synthesis*. **2014**, *46*, 1689-1708. (d) Peng, J.-B.; Geng, H.-Q.; Wu, X.-F. *Chem*. **2019**, *5*, 526-552.
2. Brennfuhrer, A.; Neumann, H.; Beller, M. *Angew. Chem. Int. Ed. Engl.* **2009**, *48*, 4114-33.

3. (a) Gøgsig, T. M.; Taaning, R. H.; Lindhardt, A. T.; Skrydstrup, T. *Angewandte Chemie*. **2012**, *124*, 822-825. (b) Nielsen, D. U.; Lescot, C.; Gøgsig, T. M.; Lindhardt, A. T.; Skrydstrup, T. *Chemistry—A European Journal*. **2013**, *19*, 17926-17938. (c) Schranck, J.; Tlili, A.; Alsabeh, P. G.; Neumann, H.; Stradiotto, M.; Beller, M. *Chemistry*. **2013**, *19*, 12624-8. (d) Schranck, J.; Burhardt, M.; Bornschein, C.; Neumann, H.; Skrydstrup, T.; Beller, M. *Chemistry*. **2014**, *20*, 9534-8. (e) Jusseau, X.; Yin, H.; Lindhardt, A. T.; Skrydstrup, T. *Chemistry*. **2014**, *20*, 15785-9.
4. Zhao, H.; Hu, B.; Xu, L.; Walsh, P. J. *Chem Sci*. **2021**, *12*, 10862-10870.
5. Zhang, J.; Bellomo, A.; Creamer, A. D.; Dreher, S. D.; Walsh, P. J. *J. Am. Chem. Soc*. **2012**, *134*, 13765-72.
6. Felding, J.; Sorensen, M. D.; Poulsen, T. D.; Larsen, J.; Andersson, C.; Refer, P.; Engell, K.; Ladefoged, L. G.; Thormann, T.; Vinggaard, A. M.; Hegardt, P.; Sohoel, A.; Nielsen, S. F. *J. Med. Chem*. **2014**, *57*, 5893-903.
7. Huang, R.; Ayine-Tora, D. M.; Muhammad Rosdi, M. N.; Li, Y.; Reynisson, J.; Leung, I. K. H. *Bioorg Med Chem Lett*. **2017**, *27*, 277-281.
8. Heider, F.; Haun, U.; Doring, E.; Kudolo, M.; Sessler, C.; Albrecht, W.; Laufer, S.; Koch, P. *Molecules*. **2017**, *22*.
9. (a) Vitaku, E.; Smith, D. T.; Njardarson, J. T. *J. Med. Chem*. **2014**, *57*, 10257-74. (b) Taylor, R. D.; MacCoss, M.; Lawson, A. D. *J. Med. Chem*. **2014**, *57*, 5845-59.

10. (a) Hooshmand, S. E.; Heidari, B.; Sedghi, R.; Varma, R. S. *Green Chemistry*. **2019**, *21*, 381-405. (b) Martin, R.; Buchwald, S. L. *Acc. Chem. Res.* **2008**, *41*, 1461-73.
11. Bordwell, F. G. *Acc. Chem. Res.* **1988**, *21*, 456-463.
12. Zhang, J.; Bellomo, A.; Trongsirawat, N.; Jia, T.; Carroll, P. J.; Dreher, S. D.; Tudge, M. T.; Yin, H.; Robinson, J. R.; Schelter, E. J.; Walsh, P. J. *J. Am. Chem. Soc.* **2014**, *136*, 6276-87.
13. Bellomo, A.; Zhang, J.; Trongsirawat, N.; Walsh, P. J. *Chem. Sci.* **2013**, *4*, 849-857.
14. (a) Amatore, C.; Broeker, G.; Jutand, A.; Khalil, F. *Journal of the American Chemical Society*. **1997**, *119*, 5176-5185. (b) Amatore, C.; Jutand, A. *Coord. Chem. Rev.* **1998**, *178-180*, 511-528.
15. (a) Wang, J. Y.; Strom, A. E.; Hartwig, J. F. *J. Am. Chem. Soc.* **2018**, *140*, 7979-7993. (b) Trebbe, R.; Goddard, R.; Ruffinowska, A.; Seevogel, K.; Pörschke, K.-R. *Organometallics*. **1999**, *18*, 2466-2472. (c) Perez, P. J.; Calabrese, J. C.; Bunel, E. E. *Organometallics*. **2000**, *20*, 337-345.
16. Craig, N. C.; Groner, P.; McKean, D. C. *J. Phys. Chem. A*. **2006**, *110*, 7461-9.
17. Miloserdov, F. M.; McMullin, C. L.; Belmonte, M. M. n.; Benet-Buchholz, J.; Bakhmutov, V. I.; Macgregor, S. A.; Grushin, V. V. *Organometallics*. **2014**, *33*, 736-752.
18. (a) Zhang, J.; Bellomo, A.; Creamer, A. D.; Dreher, S. D.; Walsh, P. J. *Journal of the American Chemical Society*. **2012**, *134*, 13765-13772. (b) Zhang, J.; Sha, S. C.;

Bellomo, A.; Trongsirawat, N.; Gao, F.; Tomson, N. C.; Walsh, P. J. *J. Am. Chem. Soc.* **2016**, *138*, 4260-6. (c) Sha, S. C.; Tcyrulnikov, S.; Li, M.; Hu, B.; Fu, Y.; Kozlowski, M. C.; Walsh, P. J. *J. Am. Chem. Soc.* **2018**, *140*, 12415-12423.

19. Nielsen, D. U.; Lescot, C.; Gogsig, T. M.; Lindhardt, A. T.; Skrydstrup, T. *Chemistry*. **2013**, *19*, 17926-38.

## 3.5 Experimental

### 3.5.1 General Methods

Unless otherwise noted, all reactions were performed under nitrogen using oven-dried glassware and standard Schlenk or vacuum line techniques. Air- and moisture-sensitive solutions were handled under nitrogen and transferred via syringe. Anhydrous solvents were purchased from Acros and used as solvent without further purification. Unless otherwise stated, reagents were commercially available and used as purchased without further purification. Chemicals were purchased from Strem, Sigma-Aldrich, Acros, TCI America or Alfa Aesar. Other solvents were purchased from Fisher Scientific. The progress of the reactions was monitored by thin-layer chromatography using Silica Gel HL 250  $\mu\text{m}$  TLC plates and visualized by short-wave ultraviolet light. Silica gel (230–400 mesh, Silicycle) was used for flash chromatography. The  $^1\text{H}$  NMR and  $^{13}\text{C}\{^1\text{H}\}$  NMR spectra were obtained using a Bruker Model Advance DMX 400 Spectrometer ( $^1\text{H}$  400 MHz and  $^{13}\text{C}\{^1\text{H}\}$  101 MHz, respectively) or Bruker Model Advance DMX 500 Spectrometer ( $^1\text{H}$  500 MHz and  $^{13}\text{C}\{^1\text{H}\}$  125 MHz, respectively). Chemical shifts are reported in units of parts per million (ppm) downfield from tetramethylsilane (TMS), and all coupling constants are reported in hertz. High resolution mass spectrometry (HRMS) data were obtained on a Waters LC-TOF mass spectrometer (model LCT-XE Premier) using electrospray ionization (ESI) in positive or negative mode, depending on the analyte.

### 3.5.2 Representative Microscale High-throughput Experimentation

#### General Experimental.

The experimental procedures in this work were similar to the reported processes.<sup>1</sup> Screening reactions were carried out in 1 mL vials (30 mm height  $\times$  8 mm diameter) in a 96-well plate



aluminum reactor block. Liquid chemicals were dosed using multi-channel or single-channel pipettors. Solid chemicals were dosed manually as solutions or slurries in appropriate solvents. Undesired additional solvent was removed using a GeneVac system located inside the glovebox. The reactions were heated and shaken on a heating block with a rotary shaker using glass beads to assist mixing. The reactions were partially sealed in the 96-well plate during reaction. Below each reactor vial in the aluminum 96-well plate was a 0.062 mm thick silicon-rubber gasket. Directly above the glass vial reactor tops was a pierced 0.062 mm thick silicon-rubber gaskets. The entire assembly was compressed between a porous aluminum top and the reactor base with 9 evenly placed screws.

*Set up:*

Experiments were set up inside a glovebox under a nitrogen atmosphere. A 96-well aluminum block containing 1 mL glass vials was predosed with Pd sources (0.5  $\mu\text{mol}$ ) and ligand (ligand was used in a 2.4:1 ratio relative to Pd for monodentate ligands and 1.2:1 ratio for bidentate ligands) in THF. The solvent was evacuated to dryness using a Genevac vacuum centrifuge, and  $\text{LiN}(\text{SiMe}_3)_2$  (30  $\mu\text{mol}$ ) in THF was added to the ligand/catalyst mixture. The solvent was removed on the Genevac, and a glass bead was then added to each reaction vial. 1-Bromo-4-*tert*-butylbenzene (15  $\mu\text{mol}$ /reaction), 4-benzylpyridine (10  $\mu\text{mol}$ /reaction) were then dosed together into each reaction vial as a solution in 1,4-dioxane (100  $\mu\text{L}$ , 0.1 M). The 96-well plate was then placed and sealed in a gas block. The gas block was transferred out of the glovebox and charged with CO gas with a pressure of 5 atmosphere. Then the gas block was sealed again and shaken on a rotary shaker and heated at 80  $^\circ\text{C}$  for 24 h.

*Work up:*

After 24 h, The gas block was removed from the rotary shaker and cooled in a fume hood for 1 h. Then the gas block was connected to a gas release system to release the pressure. The gas block was then opened to air in the fume hood. After 10 min, 0.001 mmol of 4,4'-di-*tert*-butylbiphenyl in 500  $\mu$ L of acetonitrile was pipetted into each vial. The plate was then covered again with a Teflon perfluoroalkoxy copolymer resin sealing gasket and above that, two more 0.062 mm thick silicon-rubber gaskets. The entire assembly was compressed between an aluminum top and the reactor base with 9 evenly placed screws. The vials stirred for 20 min to extract the product and to ensure good homogenization. The vials were then centrifuged for 2 min to separate undissolved solids. Into a separate 96-well LC block was added 700  $\mu$ L of acetonitrile, followed by 25  $\mu$ L of the centrifuged reaction solution. The LC block was then sealed with a silicon-rubber storage mat and mounted on an HPLC instrument for analysis.

**Scheme 1-S3.** Ligand screening for carbonylative arylation of **1a** with **2a**.

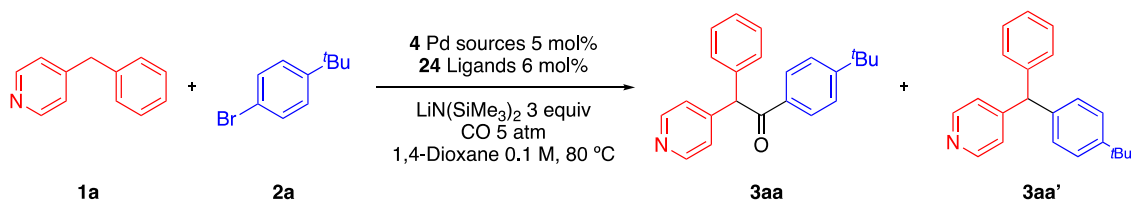


**Table 1-S3.** Ligands examined: used in a 4:1 ratio relative to Pd for monodentate ligands and 2:1 ratio for bidentate ligands.

	I	II	III	IV	V	VI
A	DCPE	DPPE	DPPH	BiPhep	PyBOX	AdBrettPhos
B	NiXantphos	DPPP	BiNAP	P(Et) <sub>3</sub> ·HBF <sub>4</sub>	4,4'-Di- <i>tert</i> -butyl-2,2'-dipyridyl	cBRIDP
C	Josiphos SL-J001-1	DPPB	(S)-Ph-GarPhos	dtbpf	ditbuXphos	CataCXium A
D	DPPM	DPPPE	DPPF	P(tBu)Cy <sub>2</sub>	Cphos	CataCXium Pcy

**Table 2-S3.** Pd sources examined: Pd(dba)<sub>2</sub>, Pd(OAc)<sub>2</sub>, Pd<sub>2</sub>(dba)<sub>3</sub> and Pd G4 dimer (5 mol % of Pd) were screened with 24 sterically and electronically diverse, mono- and bidentate phosphine (from the Table above).

	I-VI	VII-XII
A-D	Pd(OAc) <sub>2</sub>	Pd <sub>2</sub> (dba) <sub>3</sub>
E-H	Pd(dba) <sub>2</sub>	Pd G4 dimer

**Data analysis:** Performance of ligands and Palladium sources were determined by both yields of the ketone product **3aa** (indicted by the LC area ratio of product **3aa** over internal standard 4,4'-di-*tert*-butylbiphenyl), and selectivity (indicated by LC area ratio of product over byproduct **3aa'**).

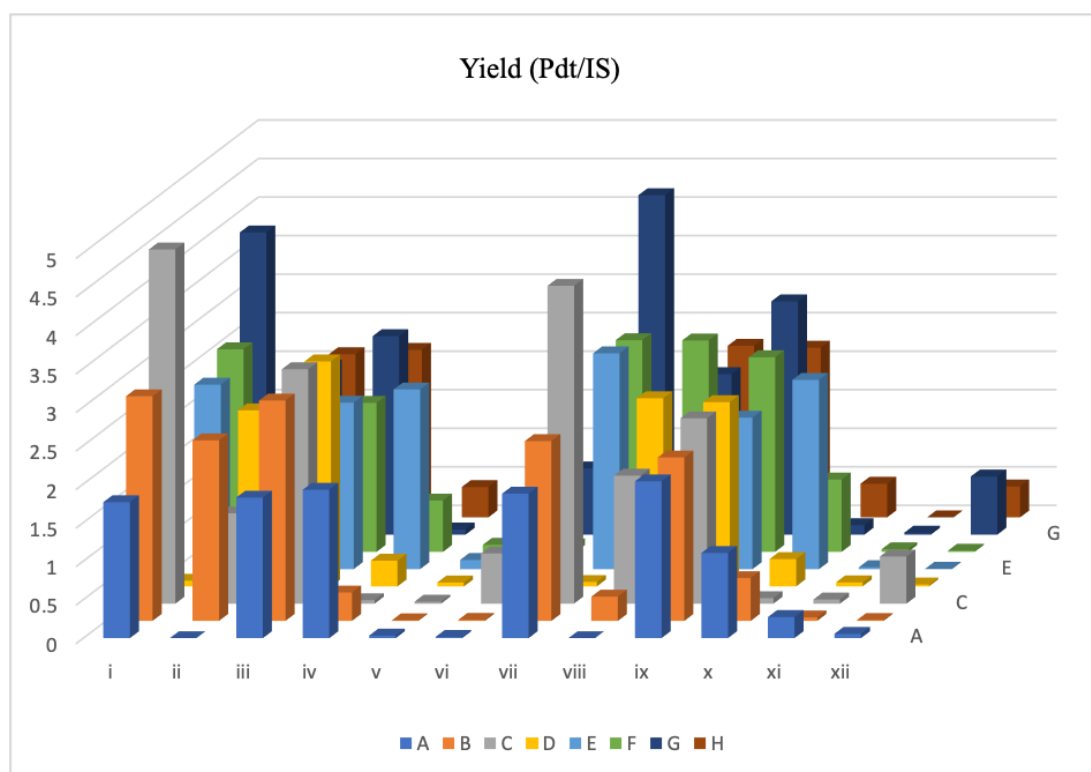


**Chart 1-S3.** Reactivity of different ligands and Pd sources

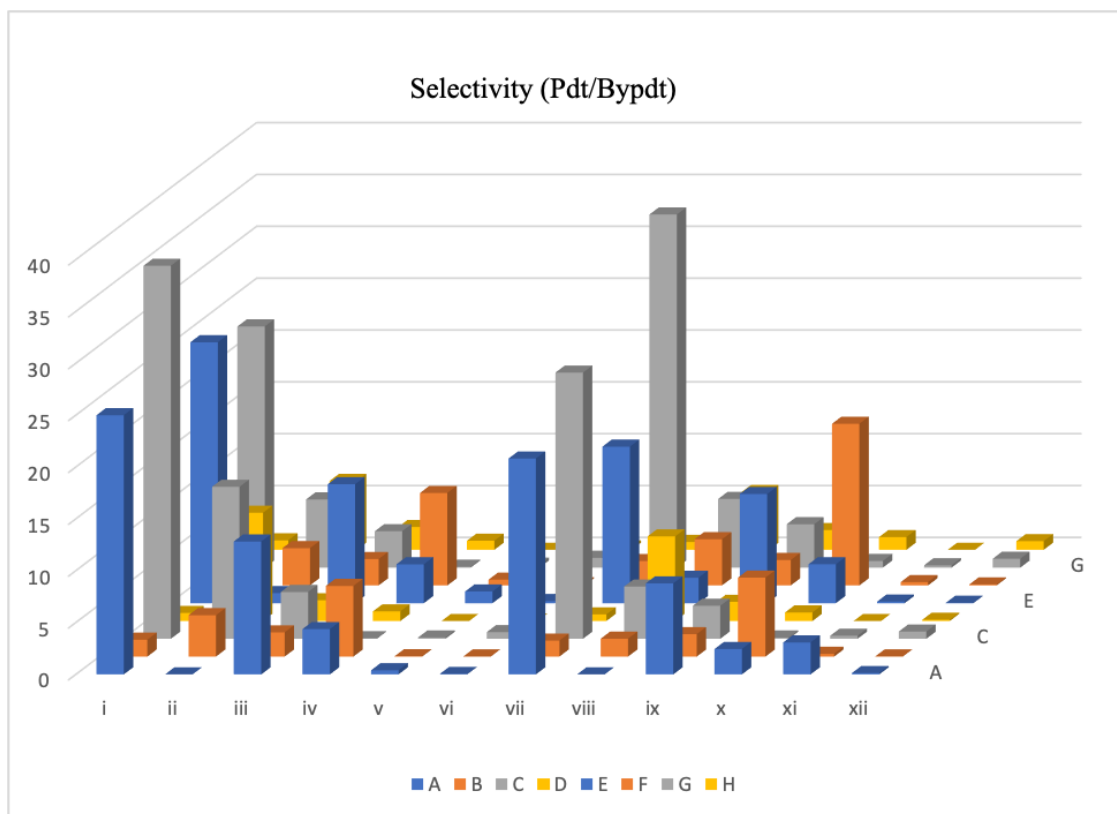


**Chart 2-S3.** Selectivity of different ligands and Pd sources

The lead hit from the screening was the combination of Pd(dba)<sub>2</sub> (5 mol %) and Josiphos SL-J001-1 (6 mol %). A scale-up reaction on a 0.1 mmol scale using the same catalytic system under 1 atm of CO as HTE proved successful with isolation of **3aa** in 94% yield.

### 3.5.3 Optimization of the Reaction Conditions

#### General procedure for reaction optimization

An oven-dried 8 mL vial with septum cap equipped with a stir bar was charged with LiN(SiMe<sub>3</sub>)<sub>2</sub> (50.5 mg, 0.30 mmol, 3.0 equiv) under a nitrogen atmosphere. A solution of [Pd] 0.005 mmol and bisphosphine (0.006 mmol) in 1 mL of dry 1,4-dioxane was added to the reaction vial. Then 4-benzylpyridine **1a** (16.9 mg, 16 μL, 0.1 mmol, 1 equiv) and 1-bromo-4-*tert*-butylbenzene (26 μL,

0.15 mmol, 1.5 equiv) were added to the reaction mixture, sequentially. The reaction vial was capped and removed from the glove box. Then the vial was purged with CO on a Schlenk line, by bubbling CO gas through a long needle under the solvent while another short needle was used as the outlet of gas. Bubbling was maintained for 5 min at rt before the short needle and then the long needle were removed. Then the vial was taped with electrical tape, stirred, and heated at 80 °C for 16 h. After the reaction period, the vial was cooled in ice bath and opened in a fume hood. After a minute for releasing leftover CO, the reaction was quenched with two drops of H<sub>2</sub>O, diluted with 3 mL of ethyl acetate, and filtered over a pad of MgSO<sub>4</sub> and silica. The pad was rinsed with additional 5 mL of ethyl acetate, and the solution was concentrated in vacuo. The crude material was loaded onto a silica gel column and purified by flash chromatography.

### **3.5.4 General Procedure for Benzylic Carbonylative Arylation**

#### **a) General procedure under 1 atm CO.**

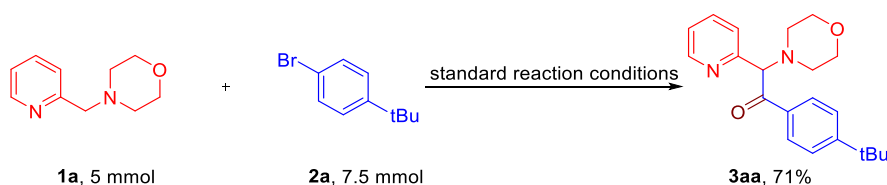
##### **Stock solution of Josiphos and Pd (0.005 M)**

An oven-dried 20 mL vial equipped with a stir bar was charged with Pd(dba)<sub>2</sub> (29 mg, 0.05 mmol) and Josiphos SL-J001-1·C<sub>2</sub>H<sub>5</sub>OH (38.4 mg, 0.06 mmol) under a nitrogen atmosphere in glove box. Next, 10 mL of 1,4-dioxane was taken up by syringe and added to the vial. The resulting solution stirred for 30 min at room temperature. After the solution changed from dark brown to red, the solution was used as the stock solution for this procedure.

##### **Reactions using the stock solution**

An oven-dried 8 mL vial with a septum cap equipped with a stir bar was charged with  $\text{LiN}(\text{SiMe}_3)_2$  (50.5 mg, 0.30 mmol, 3.0 equiv) under a nitrogen atmosphere. A solution (from a stock solution) of  $\text{Pd}(\text{dba})_2$  (0.58 mg, 0.001 mmol) and Josiphos SL-J001-1· $\text{C}_2\text{H}_5\text{OH}$  (0.77 mg, 0.0012 mmol) in 200  $\mu\text{L}$  of dry 1,4-dioxane was taken up by an Eppendorf pipetter and added to the reaction vial. Then 4-benzylpyridine **1a** (16.9 mg, 16  $\mu\text{L}$ , 0.1 mmol, 1 equiv) and 1-bromo-4-tert-butylbenzene (26  $\mu\text{L}$ , 0.15 mmol, 1.5 equiv) were added to the reaction mixture, sequentially. The reaction vial was capped and removed from the glove box. Then the vial was purged with CO using a Schlenk line, by bubbling CO gas through a long needle under the solvent surface for 5 min. Another short needle was used as the outlet of gas. Then the vial was taped with electrical tape, stirred, and heated at 80 °C for 16 h. Then the vial was cooled in ice bath and opened in a fume hood. After a minute for releasing leftover CO, the reaction was quenched with two drops of  $\text{H}_2\text{O}$ , diluted with 3 mL of ethyl acetate, and filtered over a pad of  $\text{MgSO}_4$  and silica. The pad was rinsed with additional 5 mL of ethyl acetate, and the solution was concentrated in vacuo. The crude material was loaded onto a silica gel column and purified by flash chromatography.

**(b) Scheme 2-S3. Gram-scale synthesis**

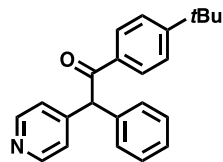


To an oven-dried 500 mL Schlenk flask with a stir bar were sequentially added  $\text{Pd}(\text{dba})_2$  (143.8 mg, 0.13 mmol, 2.5 mol %) and Josiphos SL-J001-1· $\text{C}_2\text{H}_5\text{OH}$  (96.1 mg, 0.15 mmol, 3 mol %) under a nitrogen atmosphere inside a glove box. Next, 50 mL of 1,4-dioxane was taken up by syringe and added to the flask at room temperature. The reaction mixture was stirred for 30 min at room temperature, until the mixture became red. Then  $\text{LiN}(\text{SiMe}_3)_2$  (2.5 g, 15 mmol, 3 equiv), 4-

benzylpyridine **1a** (846.1 mg, 797.5  $\mu$ L, 5 mmol, 1 equiv) and 3-bromo-2-methoxypyridine **2t** (1.4 g, 889.3  $\mu$ L, 7.5 mmol, 1.5 equiv) were added to the reaction mixture sequentially. The Schlenk flask was capped, removed from the glove box, the reaction mixture was degassed with CO by using Schlenk line (the Schlenk flask was evacuated on the Schlenk line and then refilled with CO gas), then connected with a CO balloon, and placed in an 80 °C oil bath and stirred for 16 h. Then the flask was removed from the oil bath, allowed to cool to room temperature, then the cap was carefully removed in a fume hood, exposing the solution to the atmosphere, and the reaction quenched with H<sub>2</sub>O (40 mL). The color of the reaction mixture changed from dark brown to red. It was next extracted with 3  $\times$  30 mL of ethyl acetate and dried over MgSO<sub>4</sub>. The combined organic solution was evaporated under vacuum to remove the volatile materials. The residue was purified by column chromatography on Biotage KP-Amino column using a mixture of ethyl acetate/hexanes (1/4, v/v) to give the pure product **3at** (1.05 g, 69%) as white solid.

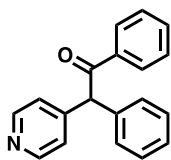
### 3.5.5 Characterization data for $\alpha$ -Aryl ketones

#### 1-(4-(*tert*-butyl)phenyl)-2-phenyl-2-(pyridin-4-yl)ethan-1-one (**3aa**)



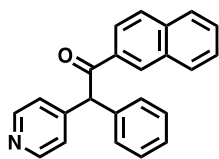
Compound **3aa** was prepared following the general procedure, purified by column chromatography using EtOAc/hexanes (1:4, v/v), and isolated as a white solid, 32.2 mg, 98%, <sup>1</sup>H NMR (400 MHz, CDCl<sub>3</sub>)  $\delta$  8.59 – 8.54 (m, 2H), 7.96 (d, *J* = 8.6 Hz, 2H), 7.47 (d, *J* = 8.6 Hz, 2H), 7.41 – 7.31 (m, 5H), 7.22 – 7.18 (m, 2H), 6.02 (s, 1H), 1.34 (s, 9H). <sup>13</sup>C NMR (101 MHz, CDCl<sub>3</sub>)  $\delta$  196.37, 157.39, 149.94, 148.29, 137.46, 133.71, 129.15, 129.05, 128.98, 127.74, 125.79, 124.39, 58.56, 35.18, 31.02. HRMS (ESI) calcd. for C<sub>23</sub>H<sub>23</sub>NO [M+H]<sup>+</sup>: 330.1858, found: 330.1864.

### 1,2-diphenyl-2-(pyridin-4-yl)ethan-1-one (3ab)



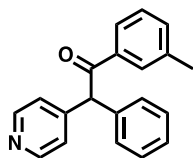
Compound **3ab** was prepared following the general procedure, purified by column chromatography using EtOAc/hexanes (1:4, v/v), and isolated as a white solid, 27.8 mg, 86%,  $^1\text{H}$  NMR (400 MHz,  $\text{CDCl}_3$ )  $\delta$  8.57 (d,  $J = 5.2$  Hz, 2H), 8.04 – 7.97 (m, 2H), 7.60 – 7.54 (m, 1H), 7.45 (dd,  $J = 8.5, 7.1$  Hz, 2H), 7.41 – 7.35 (m, 2H), 7.34 – 7.29 (m, 3H), 7.22 – 7.18 (m, 2H), 6.03 (s, 1H).  $^{13}\text{C}$  NMR (101 MHz,  $\text{CDCl}_3$ )  $\delta$  196.80, 149.94, 148.13, 137.26, 136.30, 133.51, 129.21, 129.03, 128.98, 128.80, 127.82, 124.39, 58.69. HRMS (ESI) calcd. for  $\text{C}_{21}\text{H}_{26}\text{N}_2\text{O}_2$   $[\text{M}+\text{H}]^+$ : 274.1232, found: 274.1218. HRMS (ESI) calcd. for  $\text{C}_{19}\text{H}_{15}\text{NO}$   $[\text{M}+\text{H}]^+$ : 274.1232, found: 274.1218.

### 1-(naphthalen-2-yl)-2-phenyl-2-(pyridin-4-yl)ethan-1-one (3ac)



Compound **3ac** was prepared following the general procedure, purified by column chromatography using EtOAc/hexanes (1:4, v/v), and isolated as a white solid, 25.9 mg, 95%,  $^1\text{H}$  NMR (500 MHz,  $\text{CDCl}_3$ )  $\delta$  8.59 (d,  $J = 5.9$  Hz, 2H), 8.55 (d,  $J = 1.8$  Hz, 1H), 8.07 (dd,  $J = 8.7, 1.8$  Hz, 1H), 7.94 (d,  $J = 8.2$  Hz, 1H), 7.88 (t,  $J = 8.7$  Hz, 2H), 7.62 (ddd,  $J = 8.2, 6.8, 1.3$  Hz, 1H), 7.56 (ddd,  $J = 8.2, 6.8, 1.3$  Hz, 1H), 7.40 – 7.36 (m, 4H), 7.35 – 7.29 (m, 1H), 7.28 – 7.24 (m, 2H), 6.20 (s, 1H).  $^{13}\text{C}$  NMR (126 MHz,  $\text{CDCl}_3$ )  $\delta$  196.78, 149.84, 148.41, 137.37, 135.67, 133.63, 132.43, 130.89, 129.73, 129.25, 129.07, 128.90, 128.74, 127.85, 127.78, 126.98, 124.49, 124.40, 58.71. HRMS (ESI) calcd. for  $\text{C}_{23}\text{H}_{17}\text{NO}$   $[\text{M}+\text{H}]^+$ : 324.1388, found: 324.1382.

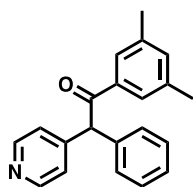
### 2-phenyl-2-(pyridin-4-yl)-1-(*m*-tolyl)ethan-1-one (3ad)



Compound **3ad** was prepared following the general procedure, purified by column chromatography using EtOAc/hexanes (1:4, v/v), and isolated as a white solid, 26.1 mg, 91%,  $^1\text{H}$  NMR (400 MHz,  $\text{CDCl}_3$ )  $\delta$  8.58 (s, 2H), 7.83 (s, 1H), 7.79 (d,  $J = 7.4$  Hz, 1H), 7.41 – 7.35 (m, 3H), 7.34 – 7.29 (m, 4H), 7.26 (d,  $J = 5.0$  Hz, 2H), 6.05 (s, 1H), 2.39 (s, 3H).  $^{13}\text{C}$  NMR (101 MHz,  $\text{CDCl}_3$ )  $\delta$  196.80, 149.48, 148.86, 138.73, 137.09, 136.26, 134.41, 129.44, 129.26, 129.00, 128.67, 127.89, 126.23, 124.80, 58.66, 21.39. HRMS (ESI) calcd. for  $\text{C}_{20}\text{H}_{17}\text{NO}$   $[\text{M}+\text{H}]^+$ : 288.1388, found: 288.1391.

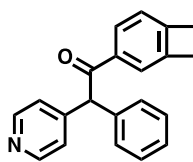
### 1-(3,5-dimethylphenyl)-2-phenyl-2-(pyridin-4-yl)ethan-1-one (3ae)





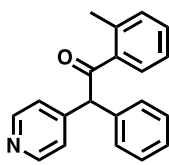
Compound **3ae** was prepared following the general procedure, purified by column chromatography using EtOAc/hexanes (1:4, v/v), and isolated as a white solid, 27.7 mg, 92%,  $^1\text{H}$  NMR (400 MHz,  $\text{CDCl}_3$ )  $\delta$  8.61 (s, 2H), 7.62 (s, 2H), 7.40 – 7.35 (m, 2H), 7.32 (d,  $J = 7.0$  Hz, 3H), 7.30 – 7.23 (m, 2H), 7.20 (s, 1H), 6.05 (s, 1H), 2.35 (s, 6H).  $^{13}\text{C}$  NMR (101 MHz,  $\text{CDCl}_3$ )  $\delta$  197.05, 149.39, 149.01, 138.51, 137.23, 136.44, 135.32, 129.21, 129.02, 127.82, 126.75, 124.82, 58.55, 21.29. HRMS (ESI) calcd. for  $\text{C}_{21}\text{H}_{19}\text{NO}$   $[\text{M}+\text{H}]^+$ : 302.1545, found: 302.1546.

### 1-(bicyclo[4.2.0]octa-1(6),2,4-trien-3-yl)-2-phenyl-2-(pyridin-4-yl)ethan-1-one (3af)



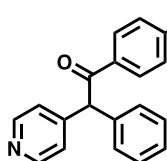
Compound **3af** was prepared following the general procedure, purified by column chromatography using EtOAc/hexanes (1:4, v/v), and isolated as a white solid, 26.6 mg, 89%,  $^1\text{H}$  NMR (400 MHz,  $\text{CDCl}_3$ )  $\delta$  8.56 (d,  $J = 5.1$  Hz, 2H), 7.92 (dd,  $J = 7.7, 1.5$  Hz, 1H), 7.69 (d,  $J = 1.6$  Hz, 1H), 7.40 – 7.34 (m, 2H), 7.31 (dd,  $J = 6.8, 1.1$  Hz, 3H), 7.21 – 7.17 (m, 2H), 7.12 (dd,  $J = 7.7, 0.9$  Hz, 1H), 6.01 (s, 1H), 3.21 (s, 4H).  $^{13}\text{C}$  NMR (101 MHz,  $\text{CDCl}_3$ )  $\delta$  197.02, 152.66, 149.94, 148.41, 146.30, 137.59, 135.46, 129.13, 129.03, 128.49, 127.69, 124.39, 122.99, 122.82, 58.63, 29.97, 29.47. HRMS (ESI) calcd. for  $\text{C}_{21}\text{H}_{17}\text{NO}$   $[\text{M}+\text{H}]^+$ : 300.1388, found: 300.1383.

### 2-phenyl-2-(pyridin-4-yl)-1-(*o*-tolyl)ethan-1-one (3ag)



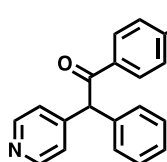
Compound **3ag** was prepared following the general procedure at a temperature of 100 °C, purified by column chromatography using EtOAc/hexanes (1:4, v/v), and isolated as a yellow oil, 21.2 mg, 74%.  $^1\text{H}$  NMR (400 MHz,  $\text{CDCl}_3$ )  $\delta$  8.62 – 8.54 (m, 2H), 7.69 (dd,  $J = 7.8, 1.4$  Hz, 1H), 7.41 – 7.35 (m, 3H), 7.35 – 7.31 (m, 3H), 7.28 – 7.22 (m, 4H), 5.90 (s, 1H), 2.48 (s, 3H).  $^{13}\text{C}$  NMR (101 MHz,  $\text{CDCl}_3$ )  $\delta$  200.22, 149.93, 148.18, 139.19, 137.43, 137.18, 132.21, 131.79, 129.12, 129.02, 128.72, 127.79, 125.78, 124.28, 61.05, 21.42. HRMS (ESI) calcd. for  $\text{C}_{20}\text{H}_{17}\text{NO}$   $[\text{M}+\text{H}]^+$ : 288.1388, found: 288.1402.

### 1-(4-methoxyphenyl)-2-phenyl-2-(pyridin-4-yl)ethan-1-one (3ah)



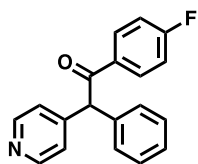
Compound **3ah** was prepared following the general procedure, purified by column chromatography using EtOAc/hexanes (1:4, v/v), and isolated as a white solid, 25.8 mg, 85%. <sup>1</sup>H NMR (400 MHz, CDCl<sub>3</sub>) δ 8.57 – 8.52 (m, 2H), 8.00 (d, *J* = 8.9 Hz, 2H), 7.39 – 7.29 (m, 5H), 7.21 – 7.17 (m, 2H), 6.92 (d, *J* = 8.9 Hz, 2H), 5.98 (s, 1H), 3.86 (s, 3H). <sup>13</sup>C NMR (101 MHz, CDCl<sub>3</sub>) δ 195.26, 163.78, 149.89, 148.43, 137.63, 131.36, 129.23, 129.13, 129.02, 127.70, 124.42, 113.99, 58.35, 55.53. HRMS (ESI) calcd. for C<sub>20</sub>H<sub>17</sub>NO<sub>2</sub> [M+H]<sup>+</sup>: 304.1338, found: 304.1329.

### 1-(4-(dimethylamino)phenyl)-2-phenyl-2-(pyridin-4-yl)ethan-1-one (3ai)



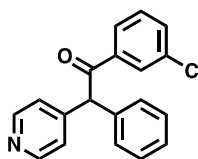
Compound **3ai** was prepared following the general procedure with 5 mol% Pd(dba)<sub>2</sub> and 6 mol% Josiphos, purified by column chromatography using EtOAc/hexanes (1:1, v/v), and isolated as a white solid, 28.5mg, 90%. <sup>1</sup>H NMR (400 MHz, CDCl<sub>3</sub>) δ 8.53 – 8.49 (m, 2H), 7.91 (d, *J* = 9.1 Hz, 2H), 7.36 – 7.26 (m, 5H), 7.21 – 7.17 (m, 2H), 6.64 – 6.58 (m, 2H), 5.94 (s, 1H), 3.04 (s, 6H). <sup>13</sup>C NMR (101 MHz, CDCl<sub>3</sub>) δ 194.48, 153.54, 149.73, 149.15, 138.30, 131.28, 129.07, 128.94, 127.41, 124.52, 124.02, 110.76, 57.79, 39.99. HRMS (ESI) calcd. for C<sub>21</sub>H<sub>20</sub>N<sub>2</sub>O [M+H]<sup>+</sup>: 317.1654, found: 317.1654.

### 1-(4-fluorophenyl)-2-phenyl-2-(pyridin-4-yl)ethan-1-one (3aj)



Compound **3aj** was prepared following the general procedure, purified by column chromatography using EtOAc/hexanes (1:4, v/v), and isolated as a white solid, 24.7 mg, 85%. <sup>1</sup>H NMR (400 MHz, CDCl<sub>3</sub>) δ 8.60 – 8.53 (m, 2H), 8.07 – 7.99 (m, 2H), 7.40 – 7.35 (m, 2H), 7.34 – 7.28 (m, 3H), 7.19 – 7.16 (m, 2H), 7.10 (t, *J* = 8.6 Hz, 2H), 5.96 (s, 1H). <sup>13</sup>C NMR (101 MHz, CDCl<sub>3</sub>) δ 195.22, 167.12, 164.57, 149.96, 147.91, 137.07, 132.63 (d, *J*<sub>c-f</sub> = 3.0 Hz), 131.71 (d, *J*<sub>c-f</sub> = 9.1 Hz), 129.13 (d, *J*<sub>c-f</sub> = 32.3 Hz), 127.94, 124.36, 115.97 (d, *J*<sub>c-f</sub> = 22.2 Hz), 58.72. <sup>19</sup>F NMR (376 MHz, CDCl<sub>3</sub>) δ -104.00. HRMS (ESI) calcd. for C<sub>19</sub>H<sub>14</sub>FNO [M+H]<sup>+</sup>: 292.1138, found: 292.1106.

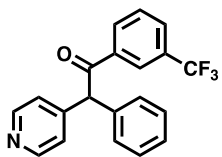
### 1-(3-chlorophenyl)-2-phenyl-2-(pyridin-4-yl)ethan-1-one (3ak)



Compound **3ak** was prepared following the general procedure, purified by column chromatography using EtOAc/hexanes (1:4, v/v), and isolated as a white solid, 25.3 mg, 82%. <sup>1</sup>H NMR (500 MHz, CDCl<sub>3</sub>) δ 8.61 – 8.55 (m, 2H),

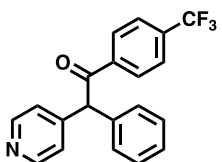
7.98 (t,  $J = 1.9$  Hz, 1H), 7.86 (dt,  $J = 7.8, 1.4$  Hz, 1H), 7.56 – 7.51 (m, 1H), 7.39 (m, 3H), 7.36 – 7.29 (m, 3H), 7.22 – 7.17 (m, 2H), 5.96 (s, 1H).  $^{13}\text{C}$  NMR (126 MHz,  $\text{CDCl}_3$ )  $\delta$  195.54, 149.75, 147.94, 137.79, 136.66, 135.19, 133.46, 130.11, 129.37, 128.99, 128.96, 128.06, 127.04, 124.39, 58.83. HRMS (ESI) calcd. for  $\text{C}_{19}\text{H}_{14}\text{ClNO}$   $[\text{M}+\text{H}]^+$ : 308.0842, found: 308.0835.

### 2-phenyl-2-(pyridin-4-yl)-1-(3-(trifluoromethyl)phenyl)ethan-1-one (3al)



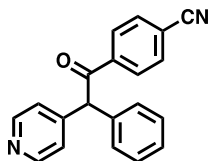
Compound **3al** was prepared following the general procedure, purified by column chromatography using EtOAc/hexanes (1:3, v/v), and isolated as a white solid, 35.1 mg, 97%,  $^1\text{H}$  NMR (400 MHz,  $\text{CDCl}_3$ )  $\delta$  8.63 – 8.53 (m, 2H), 8.27 (d,  $J = 1.9$  Hz, 1H), 8.16 (dt,  $J = 7.9, 1.4$  Hz, 1H), 7.82 (ddt,  $J = 7.7, 1.8, 0.9$  Hz, 1H), 7.59 (t,  $J = 7.8$  Hz, 1H), 7.40 (tt,  $J = 6.7, 1.2$  Hz, 2H), 7.36 – 7.30 (m, 3H), 7.22 – 7.17 (m, 2H), 5.99 (s, 1H).  $^{13}\text{C}$  NMR (101 MHz,  $\text{CDCl}_3$ )  $\delta$  195.48, 150.03, 147.45, 136.74, 136.52, 132.04, 131.50 (q,  $J_{\text{c-f}} = 32.3$  Hz), 129.87 (q,  $J_{\text{c-f}} = 4.0$  Hz), 129.49, 129.43, 128.95, 128.14, 125.77 (q,  $J_{\text{c-f}} = 4.0$  Hz), 124.29, 123.50 (q,  $J_{\text{c-f}} = 273.7$  Hz), 58.92.  $^{19}\text{F}$  NMR (376 MHz,  $\text{CDCl}_3$ )  $\delta$  -62.94. HRMS (ESI) calcd. for  $\text{C}_{19}\text{H}_{14}\text{F}_3\text{NO}$   $[\text{M}+\text{H}]^+$ : 342.1106, found: 342.1108.

### 2-phenyl-2-(pyridin-4-yl)-1-(4-(trifluoromethyl)phenyl)ethan-1-one (3am)



Compound **3am** was prepared following the general procedure with 5 mol%  $\text{Pd}(\text{dba})_2$  and 6 mol% Josiphos at 40 °C, purified by column chromatography using EtOAc/hexanes (1:3, v/v), and isolated as a white solid, 29.1 mg, 85%.  $^1\text{H}$  NMR (500 MHz,  $\text{CDCl}_3$ )  $\delta$  8.59 (d,  $J = 4.8$  Hz, 2H), 8.10 (d,  $J = 8.1$  Hz, 2H), 7.71 (d,  $J = 8.2$  Hz, 2H), 7.40 (m, 2H), 7.37 – 7.29 (m, 3H), 7.20 (d,  $J = 4.9$  Hz, 2H), 5.99 (s, 1H).  $^{13}\text{C}$  NMR (126 MHz,  $\text{CDCl}_3$ )  $\delta$  195.81, 149.85, 147.55, 138.87, 136.51, 134.69 (q,  $J_{\text{c-f}} = 32.8$  Hz), 129.44, 129.30, 128.95, 128.15, 125.87 (q,  $J_{\text{c-f}} = 3.8$  Hz), 124.66, 123.42 (q,  $J_{\text{c-f}} = 274.7$  Hz), 59.17.  $^{19}\text{F}$  NMR (376 MHz,  $\text{CDCl}_3$ )  $\delta$  -63.26. HRMS (ESI) calcd. for  $\text{C}_{20}\text{H}_{14}\text{F}_3\text{NO}$   $[\text{M}+\text{H}]^+$ : 342.1106, found: 342.1111.

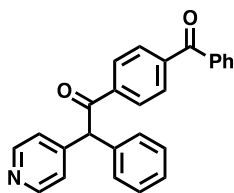
### 4-(2-phenyl-2-(pyridin-4-yl)acetyl)benzotrile (3an)



Compound **3an** was prepared following the general procedure with 5 mol%  $\text{Pd}(\text{dba})_2$  and 6 mol% Josiphos, purified by column chromatography using EtOAc/hexanes (1:2, v/v), and isolated as a yellow solid, 26.3 mg, 88%.  $^1\text{H}$

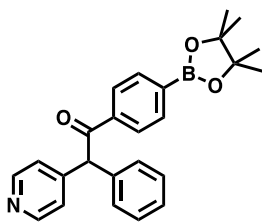
NMR (400 MHz, CDCl<sub>3</sub>) δ 8.56 (d, *J* = 5.3 Hz, 2H), 8.09 – 8.03 (m, 2H), 7.74 – 7.69 (m, 2H), 7.41 – 7.30 (m, 4H), 7.29 – 7.26 (m, 1H), 7.18 – 7.15 (m, 2H), 5.96 (s, 1H). <sup>13</sup>C NMR (101 MHz, CDCl<sub>3</sub>) δ 195.56, 150.06, 147.18, 139.16, 136.30, 132.62, 129.51, 129.35, 128.93, 128.24, 124.28, 117.73, 116.65, 59.14. HRMS (ESI) calcd. for C<sub>20</sub>H<sub>14</sub>N<sub>2</sub>O [M+H]<sup>+</sup>: 299.1184, found: 299.1176.

### 1-(4-benzoylphenyl)-2-phenyl-2-(pyridin-4-yl)ethan-1-one (3ao)



Compound **3ao** was prepared following the general procedure with 5 mol% Pd(dba)<sub>2</sub> and 6 mol% Josiphos at 40 °C, purified by column chromatography using EtOAc/hexanes (1:3, v/v), and isolated as a white solid, 21.5 mg, 57%. <sup>1</sup>H NMR (500 MHz, CDCl<sub>3</sub>) δ 8.60 (s, 2H), 8.10 (d, *J* = 8.1 Hz, 2H), 7.84 (d, *J* = 7.9 Hz, 2H), 7.81 – 7.77 (m, 2H), 7.63 (t, *J* = 7.4 Hz, 1H), 7.50 (t, *J* = 7.7 Hz, 2H), 7.40 (t, *J* = 7.3 Hz, 2H), 7.37 – 7.31 (m, 3H), 7.25 (d, *J* = 4.0 Hz, 2H), 6.05 (s, 1H). <sup>13</sup>C NMR (126 MHz, CDCl<sub>3</sub>) δ 196.19, 195.68, 149.42, 148.37, 141.65, 138.67, 136.71, 136.61, 133.10, 130.15, 130.09, 129.44, 129.02, 128.87, 128.52, 128.13, 124.61, 59.17. HRMS (ESI) calcd. for C<sub>26</sub>H<sub>19</sub>NO<sub>2</sub> [M+H]<sup>+</sup>: 378.1494, found: 378.1494.

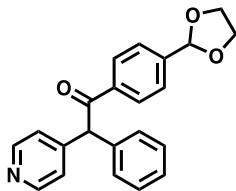
### 2-phenyl-2-(pyridin-4-yl)-1-(4-(4,4,5,5-tetramethyl-1,3,2-dioxaborolan-2-yl)phenyl)ethan-1-one (3ap)



Compound **3ap** was prepared following the general procedure with 7.5 mol% Pd(dba)<sub>2</sub> and 9 mol% Josiphos, purified by column chromatography using EtOAc/hexanes (1:4, v/v), and isolated as a white solid, 22.7 mg, 57%. <sup>1</sup>H NMR (500 MHz, CDCl<sub>3</sub>) δ 8.58 (d, *J* = 5.1 Hz, 2H), 7.99 – 7.95 (m, 2H), 7.87 (d, *J* = 8.0 Hz, 2H), 7.37 (m, 2H), 7.34 – 7.29 (m, 5H), 6.06 (s, 1H), 1.35 (s, 12H). <sup>13</sup>C NMR (126 MHz, CDCl<sub>3</sub>) δ 196.65, 150.27, 148.06, 137.88, 136.70, 135.10, 129.38, 129.01, 128.05, 127.95, 125.06, 84.31, 58.91, 24.88, 24.85. HRMS (ESI) calcd. for C<sub>25</sub>H<sub>26</sub>BNO<sub>3</sub> [M+H]<sup>+</sup>: 400.2084, found: 400.2092.

### 1-(4-(1,3-dioxolan-2-yl)phenyl)-2-phenyl-2-(pyridin-4-yl)ethan-1-one (3aq)

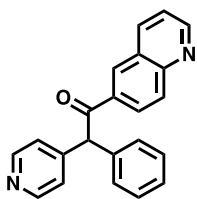
Compound **3ap** was prepared following the general procedure with 5 mol% Pd(dba)<sub>2</sub> and 6 mol% Josiphos, purified by column chromatography using EtOAc/hexanes (1:3, v/v), and isolated as a



346.1438.

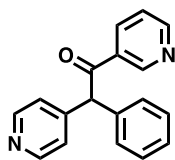
yellow oil, 19.0 mg, 55%.  $^1\text{H}$  NMR (400 MHz,  $\text{CDCl}_3$ )  $\delta$  8.58 – 8.54 (m, 2H), 8.04 – 8.00 (m, 2H), 7.58 – 7.54 (m, 2H), 7.40 – 7.34 (m, 2H), 7.33 – 7.29 (m, 3H), 7.20 – 7.17 (m, 2H), 6.00 (s, 1H), 5.85 (s, 1H), 4.12 – 4.04 (m, 4H).  $^{13}\text{C}$  NMR (101 MHz,  $\text{CDCl}_3$ )  $\delta$  196.42, 149.95, 147.98, 143.39, 137.10, 136.78, 129.23, 129.12, 129.02, 127.85, 126.84, 124.38, 102.78, 65.43, 58.83. HRMS (ESI) calcd. for  $\text{C}_{22}\text{H}_{19}\text{NO}_3$   $[\text{M}+\text{H}]^+$ : 346.1443, found:

### 2-phenyl-2-(pyridin-4-yl)-1-(quinolin-6-yl)ethan-1-one (3ar)



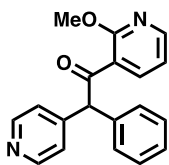
Compound **3ar** was prepared following the general procedure with 7.5 mol%  $\text{Pd}(\text{dba})_2$  and 9 mol% Josiphos, purified by column chromatography using EtOAc/hexanes (1:2, v/v), and isolated as a yellow solid, 29.5 mg, 91%.  $^1\text{H}$  NMR (500 MHz,  $\text{CDCl}_3$ )  $\delta$  9.02 (dd,  $J = 4.2, 1.7$  Hz, 1H), 8.59 (d,  $J = 5.1$  Hz, 2H), 8.52 (d,  $J = 2.0$  Hz, 1H), 8.28 (dd,  $J = 8.9, 2.0$  Hz, 1H), 8.25 (dd,  $J = 8.2, 1.8$  Hz, 1H), 8.15 (d,  $J = 8.8$  Hz, 1H), 7.49 (dd,  $J = 8.3, 4.2$  Hz, 1H), 7.42 – 7.31 (m, 5H), 7.26 (d,  $J = 5.8$  Hz, 2H), 6.17 (s, 1H).  $^{13}\text{C}$  NMR (126 MHz,  $\text{CDCl}_3$ )  $\delta$  196.17, 153.00, 150.11, 149.65, 148.32, 137.68, 136.94, 134.04, 130.66, 130.39, 129.39, 129.02, 128.12, 128.05, 127.46, 124.52, 122.13, 58.97. HRMS (ESI) calcd. for  $\text{C}_{22}\text{H}_{16}\text{N}_2\text{O}$   $[\text{M}+\text{H}]^+$ : 325.1341, found: 325.1338.

### 2-phenyl-1-(pyridin-3-yl)-2-(pyridin-4-yl)ethan-1-one (3as)



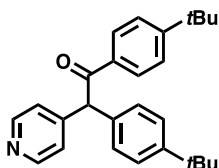
Compound **3as** was prepared following the general procedure with 7.5 mol%  $\text{Pd}(\text{dba})_2$  and 9 mol% Josiphos at 100 °C, purified by column chromatography using EtOAc/hexanes (1:1, v/v), and isolated as a yellow oil, 16.7 mg, 61%.  $^1\text{H}$  NMR (500 MHz,  $\text{CDCl}_3$ )  $\delta$  9.21 (d,  $J = 2.3$  Hz, 1H), 8.76 (dd,  $J = 4.8, 1.7$  Hz, 1H), 8.59 (d,  $J = 5.1$  Hz, 2H), 8.27 (d,  $J = 8.0$  Hz, 1H), 7.43 – 7.37 (m, 3H), 7.36 – 7.29 (m, 3H), 7.22 (d,  $J = 5.1$  Hz, 2H), 5.96 (s, 1H).  $^{13}\text{C}$  NMR (126 MHz,  $\text{CDCl}_3$ )  $\delta$  195.58, 153.75, 150.36, 149.63, 147.69, 136.27, 136.22, 131.52, 129.50, 128.99, 128.23, 124.46, 123.78, 59.23. HRMS (ESI) calcd. for  $\text{C}_{18}\text{H}_{14}\text{N}_2\text{O}$   $[\text{M}+\text{H}]^+$ : 275.1184, found: 275.1185.

### 1-(2-methoxy-3-pyridin-3-yl)-2-phenyl-2-(pyridin-4-yl)ethan-1-one (3at)



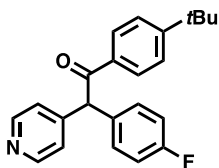
Compound **3at** was prepared following the general procedure with 5 mol% Pd(dba)<sub>2</sub> and 6 mol% Josiphos, purified by column chromatography using EtOAc/hexanes (1:1, v/v), and isolated as a yellow solid, 25.4 mg, 84%. <sup>1</sup>H NMR (400 MHz, CDCl<sub>3</sub>) δ 8.55 (d, *J* = 5.2 Hz, 2H), 8.30 (dd, *J* = 4.9, 2.0 Hz, 1H), 8.08 (dd, *J* = 7.6, 2.0 Hz, 1H), 7.37 – 7.32 (m, 2H), 7.31 – 7.25 (m, 3H), 7.23 – 7.18 (m, 2H), 6.98 (dd, *J* = 7.5, 4.9 Hz, 1H), 6.21 (s, 1H), 4.00 (s, 3H). <sup>13</sup>C NMR (101 MHz, CDCl<sub>3</sub>) δ 197.84, 161.24, 151.19, 149.82, 148.14, 140.75, 137.06, 129.31, 128.81, 127.59, 124.41, 121.54, 117.36, 61.87, 53.70. HRMS (ESI) calcd. for C<sub>19</sub>H<sub>16</sub>N<sub>2</sub>O<sub>2</sub> [M+H]<sup>+</sup>: 305.1290, found: 305.1294.

### 1,2-bis(4-(*tert*-butyl)phenyl)-2-(pyridin-4-yl)ethan-1-one (**3ba**)



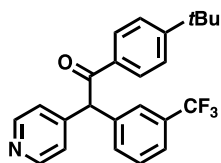
Compound **3ba** was prepared following the general procedure, purified by column chromatography using EtOAc/hexanes (1:10, v/v), and isolated as a white solid, 30.8 mg, 80%. <sup>1</sup>H NMR (400 MHz, CDCl<sub>3</sub>) δ 8.55 (d, *J* = 5.1 Hz, 2H), 7.96 (d, *J* = 8.2 Hz, 2H), 7.47 (d, *J* = 8.3 Hz, 2H), 7.37 (d, *J* = 8.0 Hz, 2H), 7.26 – 7.20 (m, 4H), 5.98 (s, 1H), 1.34 (s, 9H), 1.31 (s, 9H). <sup>13</sup>C NMR (101 MHz, CDCl<sub>3</sub>) δ 196.55, 157.29, 150.60, 149.89, 148.52, 134.30, 133.84, 128.98, 128.60, 126.05, 125.76, 124.38, 58.07, 35.17, 34.51, 31.29, 31.03. HRMS (ESI) calcd. for C<sub>27</sub>H<sub>31</sub>NO [M+H]<sup>+</sup>: 386.2484, found: 386.2481.

### 1-(4-(*tert*-butyl)phenyl)-2-(4-fluorophenyl)-2-(pyridin-4-yl)ethan-1-one (**3ca**)



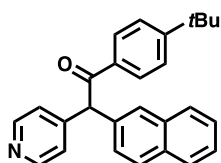
Compound **3ca** was prepared following the general procedure, purified by column chromatography using EtOAc/hexanes (1:10, v/v), and isolated as a white solid, 28.5 mg, 82%. <sup>1</sup>H NMR (400 MHz, CDCl<sub>3</sub>) δ 8.59 – 8.54 (m, 2H), 7.97 – 7.92 (m, 2H), 7.50 – 7.45 (m, 2H), 7.31 – 7.29 (m, 1H), 7.28 – 7.26 (m, 1H), 7.20 – 7.16 (m, 2H), 7.10 – 7.03 (m, 2H), 6.00 (s, 1H), 1.34 (s, 9H). <sup>13</sup>C NMR (101 MHz, CDCl<sub>3</sub>) δ 196.28, 162.24 (d, *J*<sub>C-F</sub> = 248.5 Hz), 157.61, 150.06, 148.12, 133.51, 133.25 (d, *J*<sub>C-F</sub> = 3.0 Hz), 130.7 (d, *J*<sub>C-F</sub> = 8.1 Hz), 128.95, 125.86, 124.20, 116.05 (d, *J*<sub>C-F</sub> = 21.2 Hz), 57.56, 35.20, 31.01. <sup>19</sup>F NMR (376 MHz, CDCl<sub>3</sub>) δ -114.36. HRMS (ESI) calcd. for C<sub>23</sub>H<sub>22</sub>FNO [M+H]<sup>+</sup>: 348.1764, found: 348.1766.

### 1-(4-(*tert*-butyl)phenyl)-2-(pyridin-4-yl)-2-(3-(trifluoromethyl)phenyl)ethan-1-one (**3da**)



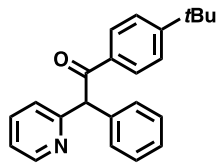
Compound **3da** was prepared following the general procedure with 5 mol% Pd(dba)<sub>2</sub> and 6 mol% Josiphos, purified by column chromatography using EtOAc/hexanes (1:4, v/v), and isolated as a white solid, 33.7 mg, 85%. <sup>1</sup>H NMR (400 MHz, CDCl<sub>3</sub>) δ 8.67 – 8.53 (m, 2H), 7.98 – 7.92 (m, 2H), 7.59 (q, *J* = 2.6 Hz, 2H), 7.50 (dq, *J* = 9.1, 2.5, 1.8 Hz, 4H), 7.26 – 7.20 (m, 2H), 6.09 (s, 1H), 1.34 (s, 9H). <sup>13</sup>C NMR (101 MHz, CDCl<sub>3</sub>) δ 195.70, 157.89, 150.17, 147.49, 138.49, 133.33, 132.50, 131.36 (q, *J*<sub>C-F</sub> = 32.3 Hz), 129.48, 128.96, 125.97, 125.86 (q, *J*<sub>C-F</sub> = 4.0 Hz), 124.66 (q, *J*<sub>C-F</sub> = 4.0 Hz), 123.87 (q, *J*<sub>C-F</sub> = 273.7 Hz), 124.15, 57.94, 35.24, 30.99. <sup>19</sup>F NMR (376 MHz, CDCl<sub>3</sub>) δ -62.55. HRMS (ESI) calcd. for C<sub>24</sub>H<sub>22</sub>F<sub>3</sub>NO [M+H]<sup>+</sup>: 398.1732, found: 398.1731.

### 1-(4-(*tert*-butyl)phenyl)-2-(naphthalen-2-yl)-2-(pyridin-4-yl)ethan-1-one (**3ea**)



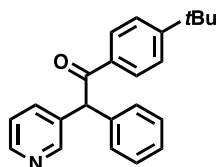
Compound **3ea** was prepared following the general procedure, purified by column chromatography using EtOAc/hexanes (1:5, v/v), and isolated as a white solid, 36.2 mg, 95%. <sup>1</sup>H NMR (400 MHz, CDCl<sub>3</sub>) δ 8.58 – 8.54 (m, 2H), 8.04 (ddt, *J* = 7.9, 5.3, 2.7 Hz, 1H), 7.96 – 7.92 (m, 1H), 7.92 – 7.88 (m, 2H), 7.86 (d, *J* = 8.1 Hz, 1H), 7.58 – 7.53 (m, 2H), 7.47 – 7.39 (m, 3H), 7.33 (dd, *J* = 7.2, 1.2 Hz, 1H), 7.22 – 7.18 (m, 2H), 6.73 (s, 1H), 1.31 (s, 9H). <sup>13</sup>C NMR (101 MHz, CDCl<sub>3</sub>) δ 196.65, 157.35, 149.91, 147.61, 134.42, 133.51, 133.29, 131.06, 129.33, 128.89, 128.74, 127.11, 127.07, 126.14, 125.82, 125.57, 124.81, 122.78, 55.10, 35.16, 31.00. HRMS (ESI) calcd. for C<sub>27</sub>H<sub>25</sub>NO [M+H]<sup>+</sup>: 380.2014, found: 380.2022.

### 1-(4-(*tert*-butyl)phenyl)-2-phenyl-2-(pyridin-2-yl)ethan-1-one (**3ga**)



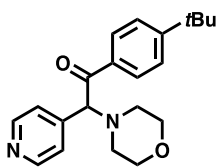
Compound **3ga** was prepared following the general procedure with 7.5 mol% Pd(dba)<sub>2</sub> and 9 mol% Josiphos, purified by column chromatography using EtOAc/hexanes (1:4, v/v), and isolated as a white solid, 19.7 mg, 60%. <sup>1</sup>H NMR (500 MHz, CDCl<sub>3</sub>) δ 8.58 (ddd, *J* = 4.9, 1.8, 0.9 Hz, 1H), 8.04 – 7.98 (m, 2H), 7.67 (td, *J* = 7.7, 1.9 Hz, 1H), 7.47 – 7.40 (m, 4H), 7.39 – 7.34 (m, 3H), 7.32 – 7.29 (m, 1H), 7.20 (ddd, *J* = 7.5, 4.9, 1.2 Hz, 1H), 6.38 (s, 1H), 1.32 (s, 9H). <sup>13</sup>C NMR (126 MHz, CDCl<sub>3</sub>) δ 196.96, 159.29, 156.94, 148.88, 137.78, 136.96, 134.01, 129.20, 129.10, 128.97, 127.48, 125.62, 124.15, 122.10, 61.69, 35.11, 31.04. HRMS (ESI) calcd. for C<sub>23</sub>H<sub>23</sub>NO [M+H]<sup>+</sup>: 330.1858, found: 330.1885.

### 1-(4-(*tert*-butyl)phenyl)-2-phenyl-2-(pyridin-3-yl)ethan-1-one (**3ha**)



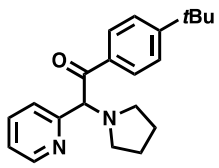
Compound **3ha** was prepared following the general procedure with 7.5 mol% Pd(dba)<sub>2</sub> and 9 mol% Josiphos and 5 equiv of LiN(SiMe<sub>3</sub>)<sub>2</sub>, purified by column chromatography using EtOAc/hexanes (1:4, v/v), and isolated as a yellow solid, 29.6 mg, 90%. <sup>1</sup>H NMR (500 MHz, CDCl<sub>3</sub>) δ 8.56 (d, *J* = 2.2 Hz, 1H), 8.52 (dd, *J* = 4.9, 1.6 Hz, 1H), 8.01 – 7.94 (m, 2H), 7.67 (dt, *J* = 8.0, 1.9 Hz, 1H), 7.51 – 7.44 (m, 2H), 7.39 – 7.32 (m, 4H), 7.31 – 7.26 (m, 2H), 6.06 (s, 1H), 1.33 (s, 9H). <sup>13</sup>C NMR (126 MHz, CDCl<sub>3</sub>) δ 196.72, 157.30, 150.02, 148.20, 138.21, 137.11, 135.34, 133.66, 129.18, 129.02, 128.85, 127.58, 125.78, 123.50, 56.68, 35.17, 31.03. HRMS (ESI) calcd. for C<sub>23</sub>H<sub>23</sub>NO [M+H]<sup>+</sup>: 330.1858, found: 330.1857.

### 1-(4-(*tert*-butyl)phenyl)-2-morpholino-2-(pyridin-4-yl)ethan-1-one (**3ia**)



Compound **3ia** was prepared following the general procedure, purified by column chromatography using EtOAc/hexanes (1:2, v/v), and isolated as a yellow oil, 30.1 mg, 89%. <sup>1</sup>H NMR (400 MHz, CDCl<sub>3</sub>) δ 8.63 – 8.51 (m, 2H), 8.05 – 7.96 (m, 2H), 7.49 – 7.44 (m, 2H), 7.44 – 7.40 (m, 2H), 4.95 (s, 1H), 3.82 – 3.71 (m, 4H), 2.61 – 2.48 (m, 4H), 1.33 (s, 9H). <sup>13</sup>C NMR (101 MHz, CDCl<sub>3</sub>) δ 195.84, 157.69, 150.26, 144.35, 133.38, 128.74, 125.75, 124.37, 75.23, 66.88, 52.00, 35.19, 30.99. HRMS (ESI) calcd. for C<sub>21</sub>H<sub>26</sub>N<sub>2</sub>O<sub>2</sub> [M+H]<sup>+</sup>: 339.2073, found: 339.2073.

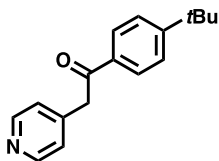
### 1-(4-(*tert*-butyl)phenyl)-2-(pyridin-2-yl)-2-(pyrrolidin-1-yl)ethan-1-one (**3ja**)



Compound **3ja** was prepared following the general procedure, purified by column chromatography using EtOAc/hexanes (1:2, v/v), and isolated as a yellow oil, 28.6 mg, 89%. <sup>1</sup>H NMR (400 MHz, CDCl<sub>3</sub>) δ 8.58 (ddd, *J* = 4.9, 1.8, 1.0 Hz, 1H), 8.16 – 8.10 (m, 2H), 7.69 – 7.60 (m, 2H), 7.45 – 7.40 (m, 2H), 7.18 (ddd, *J* = 6.8, 4.9, 1.6 Hz, 1H), 5.23 (s, 1H), 2.76 (dt, *J* = 8.2, 6.4 Hz, 2H), 2.48 – 2.40 (m, 2H), 1.83 (dpd, *J* = 10.0, 6.8, 6.4, 3.6 Hz, 4H), 1.31 (s, 9H). <sup>13</sup>C NMR (101 MHz, CDCl<sub>3</sub>) δ 196.12, 157.43, 156.89, 149.26, 136.96, 133.45, 129.16, 125.43, 123.51, 122.86, 77.71, 52.57, 35.09, 31.02, 23.32. HRMS (ESI) calcd. for C<sub>21</sub>H<sub>26</sub>N<sub>2</sub>O [M+H]<sup>+</sup>: 323.2123, found: 323.2130.

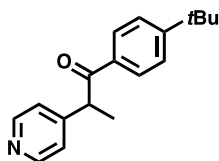
### 1-(4-(*tert*-butyl)phenyl)-2-(pyridin-4-yl)ethan-1-one (**3ka**)





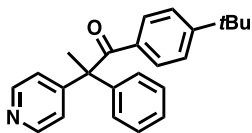
Compound **3ka** was prepared following the general procedure, and 1 equiv of **2a** and 1.2 equiv of **1k** was used. The product was purified by column chromatography using EtOAc/hexanes (1:10, v/v), and isolated as a yellow oil, 24.5 mg, 97%, <sup>1</sup>H NMR (500 MHz, CDCl<sub>3</sub>) δ 8.62 – 8.54 (m, 2H), 7.98 – 7.93 (m, 2H), 7.54 – 7.50 (m, 2H), 7.27 – 7.23 (m, 2H), 4.29 (s, 2H), 1.36 (s, 9H). <sup>13</sup>C NMR (126 MHz, CDCl<sub>3</sub>) δ 195.43, 157.60, 149.54, 144.19, 133.61, 128.51, 125.82, 125.06, 44.56, 35.21, 31.05. HRMS (ESI) calcd. for C<sub>17</sub>H<sub>19</sub>NO [M+H]<sup>+</sup>: 254.1545, found: 254.1525.

### 1-(4-(*tert*-butyl)phenyl)-2-(pyridin-4-yl)propan-1-one (**3la**)



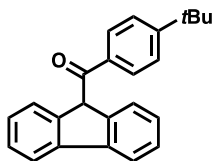
Compound **3la** was prepared following the general procedure, and 1 equiv of **2a** and 1.2 equiv of **1l** was used. The product was purified by column chromatography using EtOAc/hexanes (1:10, v/v), and isolated as a yellow oil, 23.2 mg, 87%. <sup>1</sup>H NMR (500 MHz, CDCl<sub>3</sub>) δ 8.57 – 8.52 (m, 2H), 7.92 – 7.87 (m, 2H), 7.47 – 7.43 (m, 2H), 7.28 – 7.26 (m, 2H), 4.71 (q, *J* = 6.9 Hz, 1H), 1.56 (d, *J* = 6.9 Hz, 3H), 1.33 (s, 9H). <sup>13</sup>C NMR (126 MHz, CDCl<sub>3</sub>) δ 198.55, 157.24, 150.77, 149.91, 133.28, 128.69, 125.72, 123.21, 46.89, 35.14, 31.01, 18.98. HRMS (ESI) calcd. for C<sub>18</sub>H<sub>21</sub>NO [M+H]<sup>+</sup>: 268.1701, found: 268.1695.

### 1-(4-(*tert*-butyl)phenyl)-2-phenyl-2-(pyridin-4-yl)propan-1-one (**3ma**)



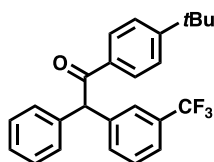
Compound **3ma** was prepared following the general procedure in THF, purified by column chromatography using EtOAc/hexanes (1:4, v/v), and isolated as a white solid, 32.6 mg, 95%, <sup>1</sup>H NMR (500 MHz, CDCl<sub>3</sub>) δ 8.57 – 8.52 (m, 2H), 7.53 – 7.49 (m, 2H), 7.43 (m, 2H), 7.41 – 7.36 (m, 1H), 7.36 – 7.32 (m, 2H), 7.31 – 7.28 (m, 2H), 7.09 – 7.05 (m, 2H), 2.08 (s, 3H), 1.29 (s, 9H). <sup>13</sup>C NMR (126 MHz, CDCl<sub>3</sub>) δ 200.91, 155.80, 154.30, 149.41, 141.61, 133.63, 129.94, 128.95, 128.10, 127.67, 125.06, 123.69, 60.31, 34.98, 31.01, 27.61. HRMS (ESI) calcd. for C<sub>24</sub>H<sub>25</sub>NO [M+H]<sup>+</sup>: 344.2014, found: 344.2013.

### (4-(*tert*-butyl)phenyl)(9*H*-fluoren-9-yl)methanone (**3na**)



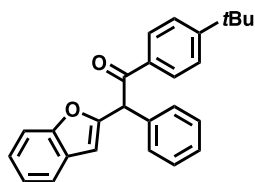
Compound **3na** was prepared following the general procedure, purified by column chromatography using EtOAc/hexanes (1:4, v/v), and isolated as a white solid, 21.2 mg, 65%,  $^1\text{H NMR}$  (500 MHz,  $\text{CDCl}_3$ )  $\delta$  7.87 (d,  $J = 7.6$  Hz, 2H), 7.75 – 7.70 (m, 2H), 7.46 (t,  $J = 7.5$  Hz, 2H), 7.44 – 7.38 (m, 4H), 7.31 (dd,  $J = 7.5, 1.2$  Hz, 2H), 5.63 (s, 1H), 1.32 (s, 9H).  $^{13}\text{C NMR}$  (126 MHz,  $\text{CDCl}_3$ )  $\delta$  197.44, 157.01, 142.61, 141.57, 133.73, 129.15, 127.97, 127.52, 125.59, 125.17, 120.47, 58.91, 35.12, 31.03. HRMS (ESI) calcd. for  $\text{C}_{24}\text{H}_{22}\text{O}$   $[\text{M}+\text{H}]^+$ : 327.1749, found: 327.1751.

### 1-(4-(*tert*-butyl)phenyl)-2-phenyl-2-(3-(trifluoromethyl)phenyl)ethan-1-one (3oa)



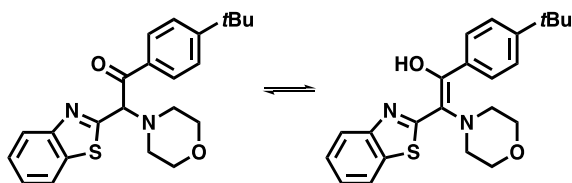
Compound **3oa** was prepared following the general procedure in THF, purified by column chromatography using EtOAc/hexanes (1:4, v/v), and isolated as a pale yellow oil, 19.8 mg, 50%,  $^1\text{H NMR}$  (400 MHz,  $\text{C}_6\text{D}_6$ )  $\delta$  7.92 (d,  $J = 8.5$  Hz, 2H), 7.65 (s, 1H), 7.33 (d,  $J = 7.9$  Hz, 1H), 7.22 (d,  $J = 7.7$  Hz, 1H), 7.17 (d,  $J = 7.5$  Hz, 2H), 7.11 – 7.07 (m, 2H), 7.02 (t,  $J = 7.4$  Hz, 2H), 6.95 (d,  $J = 7.4$  Hz, 1H), 6.88 (t,  $J = 7.9$  Hz, 1H), 5.81 (s, 1H), 1.06 (s, 9H).  $^{13}\text{C NMR}$  (126 MHz,  $\text{CDCl}_3$ )  $\delta$  197.02, 157.22, 140.35, 138.36, 133.85, 132.70, 130.83 (q,  $J_{\text{C-F}} = 32.8$  Hz), 129.09, 128.98, 128.59, 128.53, 128.41, 128.37, 127.53, 125.95 (q,  $J_{\text{C-F}} = 3.8$  Hz), 125.75, 124.00 (q,  $J_{\text{C-F}} = 3.8$  Hz), 124.08 (q,  $J_{\text{C-F}} = 273.4$  Hz), 58.92, 35.16, 31.03.  $^{19}\text{F NMR}$  (376 MHz,  $\text{CDCl}_3$ )  $\delta$  -62.00. HRMS (ESI) calcd. for  $\text{C}_{25}\text{H}_{23}\text{F}_3\text{O}$   $[\text{M}+\text{H}]^+$ : 397.1779, found: 397.1783.

### 2-(benzofuran-2-yl)-1-(4-(*tert*-butyl)phenyl)-2-phenylethan-1-one (3pa)



Compound **3pa** was prepared following the general procedure, purified by column chromatography using EtOAc/hexanes (1:5, v/v), and isolated as a white solid, 28.7 mg, 78%,  $^1\text{H NMR}$  (500 MHz,  $\text{CDCl}_3$ )  $\delta$  8.03 (d,  $J = 8.2$  Hz, 2H), 7.53 – 7.46 (m, 5H), 7.46 – 7.43 (m, 1H), 7.40 (t,  $J = 7.7$  Hz, 2H), 7.37 – 7.32 (m, 1H), 7.28 – 7.23 (m, 1H), 7.21 (td,  $J = 7.5, 1.2$  Hz, 1H), 6.55 – 6.52 (m, 1H), 6.19 (s, 1H), 1.35 (s, 9H).  $^{13}\text{C NMR}$  (126 MHz,  $\text{CDCl}_3$ )  $\delta$  194.73, 157.27, 155.94, 155.04, 135.94, 133.52, 129.16, 129.00, 128.45, 127.87, 125.75, 123.95, 122.68, 120.88, 111.14, 105.95, 53.60, 35.17, 31.05. HRMS (ESI) calcd. for  $\text{C}_{25}\text{H}_{23}\text{F}_3\text{O}$   $[\text{M}+\text{H}]^+$ : 369.1855, found: 369.1852.

**2-(benzo[d]thiazol-2-yl)-1-(4-(tert-butyl)phenyl)-2-morpholinoethan-1-one : (*E*)-2-(benzo[d]thiazol-2-yl)-1-(4-(tert-butyl)phenyl)-2-morpholinoethen-1-ol = 3:1 (3qa)**



Compound **3ra** was prepared following the general procedure, purified by column chromatography using EtOAc/hexanes (1:3, v/v), and isolated as a white semi solid, 33.5 mg, 85%. NMR and HRMS spectra matches published data.<sup>1a</sup>

### 3.5.6 Mechanistic Study

#### Synthesis of Palladium Complexes

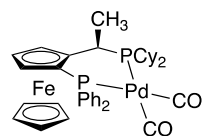
##### (*Josiphos*)Pd(*C*<sub>2</sub>H<sub>4</sub>) (**4**)

An 8 mL oven-dried vial equipped with a Teflon-coated stir bar was charged with Pd[P(*t*Bu)<sub>3</sub>]<sub>2</sub> (27.2 mg, 0.053 mmol), *Josiphos* SL-J001-1•C<sub>2</sub>H<sub>5</sub>OH (40 mg, 0.62 mmol) in 3 mL of pentane. This orange solution was capped with a septum and stirred for 5 min in a glovebox. Then the vial was transferred out of the glovebox, a long needle with an ethylene gas flow was pierced through the septum and reached the bottom of the vial. Then a vent needle was pierced through the septum allowing ethylene flush through the reaction mixture. The reaction was stirred vigorously under a continuous flow of ethylene for 4 h at rt to obtain a white precipitate. The resulting suspension was imported into a glovebox, and the precipitate was isolated on a fritted glass funnel, washed with pentane (3 x 1 mL), and dried under vacuum to obtain ethylene complex **4** (67 mg, 90%) as white powder. Single crystals of ethylene complex **4** were obtained by cooling a saturated solution of **4** in at -13 °C under 760 Torr of ethylene. <sup>1</sup>H NMR (500 MHz, C<sub>6</sub>D<sub>6</sub>) δ 8.13 – 8.04 (m, 2H), 7.43 – 7.36 (m, 2H), 7.20 – 7.16 (m, 2H), 7.12 (td, *J* = 7.1, 6.7, 2.2 Hz, 1H), 7.01 (td, *J* = 7.7, 2.0 Hz, 2H), 6.96 – 6.91 (m, 1H), 4.27 – 4.22 (m, 2H), 4.08 (d, *J* = 2.7 Hz, 1H), 3.58 (d, *J* = 0.9 Hz, 5H), 3.50 (qd, *J* = 7.4, 2.9 Hz, 1H), 3.34 (td, *J* = 13.8, 5.6 Hz, 1H), 3.28 – 3.11 (m, 2H), 2.78 (ddt, *J* = 13.0, 9.9,

6.5 Hz, 1H), 2.09 (d,  $J = 16.9$  Hz, 1H), 1.94 – 1.60 (m, 11H), 1.49 (q,  $J = 8.7, 7.4$  Hz, 6H), 1.40 – 1.30 (m, 3H), 1.23 – 0.97 (m, 4H).  $^{13}\text{C}$  NMR (126 MHz,  $\text{C}_6\text{D}_6$ )  $\delta$  141.93, 141.80, 141.75, 135.52, 135.36, 131.81, 131.70, 129.25, 128.96, 128.19, 127.41, 127.35, 126.93, 95.68, 95.64, 95.47, 95.44, 77.25, 77.08, 74.42, 69.97, 69.26, 69.20, 68.24, 68.22, 44.58, 44.40, 44.15, 43.92, 34.33, 34.30, 34.07, 33.33, 33.23, 32.51, 32.48, 32.45, 32.41, 32.19, 32.15, 32.11, 30.63, 29.44, 29.36, 29.02, 28.94, 28.11, 28.00, 27.76, 27.70, 26.74, 26.64, 26.58, 26.53, 26.24, 22.36, 14.90, 14.86, 13.91.  $^{31}\text{P}$  NMR (162 MHz,  $\text{C}_6\text{D}_6$ )  $\delta$  47.46 (d,  $J = 32.4$  Hz), 11.26 (d,  $J = 32.4$  Hz).

### (Josiphos)Pd(CO)<sub>2</sub> (**5**)

In a glove box, a J-Young NMR tube was charged with ethylene complex **4** (7.4 mg, 0.01 mmol) and 0.45 mL of  $\text{C}_6\text{D}_6$ . The J-Young tube was transferred out of the glovebox, and connected to a Schlenk line. The resulting yellow solution was cooled in liquid nitrogen, and the headspace was evacuated under vacuum. The NMR tube was warmed to room temperature and pressurized with 1 atm of CO. The solution was shaken for 1 min and re-pressurized with 1 atm CO, and this process was repeated three times. The solution changed from yellow to light orange. NMR spectra was obtained in the J-Young NMR tube.  $^1\text{H}$  NMR (500 MHz,  $\text{C}_6\text{D}_6$ )  $\delta$  8.18 – 8.10 (m, 2H), 7.46 – 7.38 (m, 2H), 7.21 – 7.17 (m, 2H), 7.11 (dd,  $J = 7.4, 1.7$  Hz, 1H), 7.06 (td,  $J = 7.6, 2.0$  Hz, 2H), 6.99 – 6.95 (m, 1H), 4.17 – 4.12 (m, 2H), 4.00 (t,  $J = 2.5$  Hz, 1H), 3.57 (s, 5H), 3.35 – 3.28 (m, 1H), 1.96 (d,  $J = 11.3$  Hz, 1H), 1.84 (s, 3H), 1.76 – 1.61 (m, 8H), 1.53 (t,  $J = 10.1$  Hz, 2H), 1.42 (t,  $J = 7.4$  Hz, 3H), 1.34 (d,  $J = 6.6$  Hz, 3H), 1.19 – 1.05 (m, 3H), 0.98 (t,  $J = 6.0$  Hz, 2H).  $^{13}\text{C}$  NMR (126 MHz,  $\text{C}_6\text{D}_6$ )  $\delta$  195.61, 143.97, 143.94, 143.76, 140.50, 140.36, 134.82, 134.66, 131.61, 131.49, 129.27, 127.48, 127.29, 94.64, 94.59, 94.44, 94.39, 77.46, 77.36, 74.45, 69.43, 69.37, 68.10, 68.07, 34.07, 33.72, 33.69, 33.60, 32.73, 32.64, 32.29, 32.23, 32.22, 30.40, 30.26, 30.17, 30.15, 28.28, 28.22, 28.01, 27.91, 27.77, 27.71, 26.77, 26.68, 26.66, 26.56, 26.41, 26.26, 22.35, 14.91, 14.87, 13.91.  $^{31}\text{P}$  NMR (162 MHz,  $\text{C}_6\text{D}_6$ )  $\delta$  42.82 (d,  $J = 13.0$  Hz), 5.16 (d,  $J = 13.0$  Hz). IR (1,4-dioxane- $d_8$ ):  $\nu_{\text{CO}} = 2012, 1969$   $\text{cm}^{-1}$ .



### Determination of Yield

In a glove box, a J-Young NMR tube was charged with ethylene complex **4** (7.4 mg, 0.01 mmol), trimesitylphosphine (7.5 mg, 0.019 mmol) and 0.45 mL of  $\text{C}_6\text{D}_6$ . The J-Young tube was transferred out of the glovebox and connected to a Schlenk line. The resulting solution was cooled in liquid nitrogen, and the headspace was evacuated under vacuum. The NMR tube was warmed to room temperature and pressurized with 1 atm of CO. The solution was shaken for 1 min and re-pressurized with 1 atm CO, and this process was repeated three times. The solution changed from yellow to light orange. By  $^{31}\text{P}$  NMR spectroscopy, the yield of **5** was determined to be 99% relative to trimesitylphosphine.

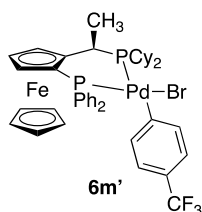
### Single Crystals of **5**

In a glove box, a J-Young NMR tube was charged with ethylene complex **4** (14.7 mg, 0.02 mmol) and 0.30 mL of  $\text{C}_6\text{D}_6$ . The J-Young tube was transferred out of the glovebox and connected to a Schlenk line. The resulting yellow solution was cooled in liquid nitrogen, and the headspace was

evacuated under vacuum. The NMR tube was warmed to room temperature and pressurized with 1 atm of CO. The solution was shaken for 1 min and re-pressurized with 1 atm CO, and this process was repeated three times. The solution changed from yellow to orange. The J-Young NMR tube was transferred to a freezer at 10 °C for 2 days to obtain yellow crystals of **5** on the wall of the J-Young tube.

#### General Procedure for the Syntheses of Pd(II) Aryl Bromide Complexes (**6j**, **6u**, **6g** and **6m**)

In a glove box, a 20 mL vial equipped with a Teflon stir bar was charged with Pd[P(<sup>t</sup>Bu)<sub>3</sub>]<sub>2</sub> (102.0 mg, 0.2 mmol), and 0.08 mmol (4 equiv) of aryl bromides in 5 mL toluene. This light-yellow solution was capped and stirred for 12 h at room temperature in a glovebox. Then Josiphos SL-J001-1•C<sub>2</sub>H<sub>5</sub>OH (140.0 mg, 0.219 mmol) was added to the reaction mixture. The resulting yellow solution was stirred for 4 h at room temperature. Pentane (10 mL) was added to the reaction, and the resulting suspension was cooled to -13 °C for 12 h to obtain a light-yellow precipitate. The precipitate was isolated on a fritted glass funnel and washed with pentane (3 x 1 mL).



The reaction to obtain complex **6m'** was performed following the general procedure with a 112.0 μL (0.8 mmol) of 4-fluorobenzotrifluoride. The reaction mixture first turned light green after addition of aryl bromide, and then turned orange after addition of Josiphos. Compound **6m** was obtained as white powder by direct filtration of the reaction mixture without adding pentane (111.1 mg, 60%). <sup>1</sup>H NMR (500 MHz, CD<sub>2</sub>Cl<sub>2</sub>) δ 8.38 – 8.24 (m, 2H), 7.78 – 7.62 (m, 3H), 7.28 – 7.22 (m, 1H), 7.08 (td, *J* = 7.8, 2.7 Hz, 2H), 6.98 – 6.46 (m, 6H), 4.65 – 4.57 (m, 1H), 4.43 – 4.31 (m, 2H), 3.60 (s, 5H), 3.15 (m, 2H), 2.37 (s, 1H), 2.09 (m, 7H), 1.92 – 1.77 (m, 5H), 1.68 (dd, *J* = 23.5, 13.9 Hz, 3H), 1.59 – 1.13 (m, 9H). <sup>31</sup>P NMR (162 MHz, CD<sub>2</sub>Cl<sub>2</sub>) δ 45.12 (d, *J* = 37.3 Hz), 21.55 (d, *J* = 37.3 Hz). <sup>19</sup>F NMR (376 MHz, CD<sub>2</sub>Cl<sub>2</sub>) δ -61.95.

#### Determination of Catalyst Resting State

In a glove box, an oven-dried 8 mL vial with septum cap equipped with a stir bar was charged with (Josiphos)Pd(C<sub>2</sub>H<sub>4</sub>) (3.7 mg, 0.005 mmol), LiN(SiMe<sub>3</sub>)<sub>2</sub> (50.5 mg, 0.30 mmol, 3.0 equiv) and 1,3,5-trimethoxybenzene (5.6 mg, 0.033 mmol) internal standard under a nitrogen atmosphere. Then 1 mL of 1,4-dioxane-d<sub>8</sub>, 4-benzylpyridine (16 μL, 0.1 mmol) and 4-fluorobromobenzene (16.5 μL, 0.15 mmol) were added to the solution. The reaction vial was capped and stirred for 5 min. Then 0.5 mL of the reaction solution was transferred into a J-Young NMR tube. The J-Young tube was transferred out of the glovebox and cooled in liquid nitrogen, the headspace of the J-Young tube was evacuated. Then the J-Young NMR tube was then warmed to room temperature and pressurized with 1 atm of CO. The J-Young tube was then placed into an oil bath preheated to 80 °C. The

J-Young tube was removed from the oil bath cooled to room temperature and monitored by  $^1\text{H}$ ,  $^{31}\text{P}$  and  $^{19}\text{F}$  NMR every 1 hour. After 6 hours, the J-Young tube was removed from the oil bath and opened in a well-ventilated fume hood. The resulting mixture was quenched with  $\text{H}_2\text{O}$  (40 mL). The color of the reaction mixture changed from dark brown to red. It was next extracted with  $3 \times 30$  mL of ethyl acetate and dried over  $\text{MgSO}_4$ . The combined organic solution was evaporated under vacuum to remove the volatile materials. The  $^1\text{H}$  NMR was recorded to show a crude yield of 24% with respect to 0.1 mmol of  $\text{CH}_2\text{Br}_2$  as the internal standard.

### Time Course Study

**Scheme S3.** Preliminary reactions were performed to determine the reaction time of initial rate study.

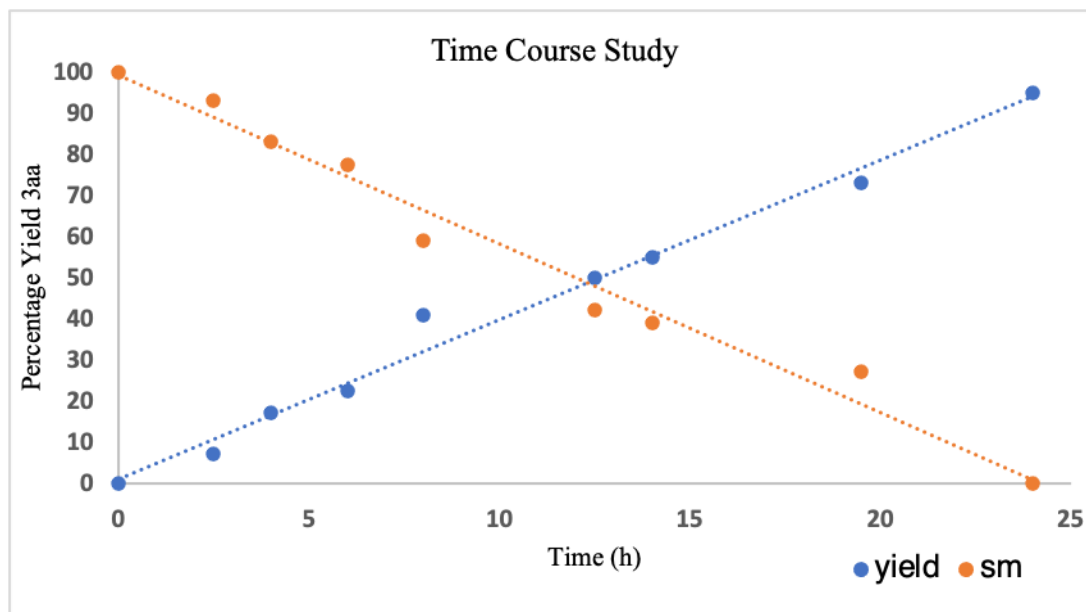
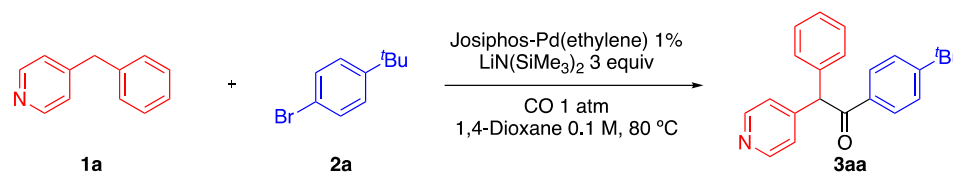
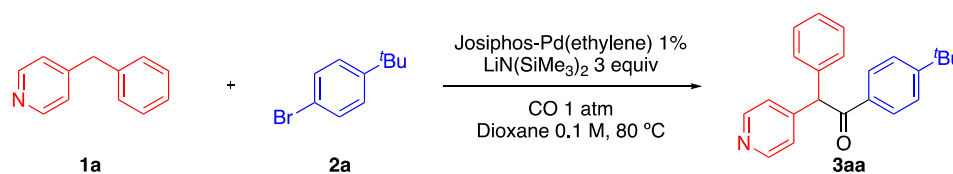


**Chart 3-S3.** Reaction time course study results

Based on the time course study of the reaction, we chose first 3 hours of the reaction to keep the reaction system simple to study, when the conversion of the reaction was less than 10%.

**9 Parallel reactions were set up.** An oven-dried 8 mL vial with septum cap equipped with a stir bar was charged with  $\text{LiN}(\text{SiMe}_3)_2$  (50.5 mg, 0.30 mmol, 3.0 equiv) under a nitrogen atmosphere. A solution (from a stock solution) of ethylene complex **4** (0.74 mg, 0.001 mmol) in 1 mL of dry 1,4-dioxane was added to each reaction vial. Then 4-benzylpyridine **1a** (16.9 mg, 16  $\mu\text{L}$ , 0.1 mmol, 1 equiv) and 1-bromo-4-*tert*-butylbenzene **2a** (26  $\mu\text{L}$ , 0.15 mmol, 1.5 equiv) were added to the reaction mixture, sequentially. The reaction vial was capped and removed from the glove box. Then the vial was purged with CO using a Schlenk line by bubbling CO gas through a long needle under the solvent surface for 5 min. Another short needle was used as the outlet of gas. Then the vial was taped with electrical tape, stirred, and heated at 80 °C for 16 h. Then the vial was cooled in ice bath and opened in a fume hood. After a minute for releasing leftover CO, the reaction was quenched with two drops of  $\text{H}_2\text{O}$ , diluted with 3 mL of ethyl acetate, and filtered over a pad of  $\text{MgSO}_4$  and silica. The pad was rinsed with additional 4 mL of ethyl acetate, and the solution was concentrated in vacuo. The crude material was loaded onto a silica gel column and purified by flash chromatography. Percentage yields of **3aa** and remaining starting material **1a** were determined by  $^1\text{H}$  NMR ( $\text{CDCl}_3$ ) spectra of the crude material using an internal standard ( $\text{CH}_2\text{Br}_2$ , one vial added with 7.0  $\mu\text{L}$ , 0.1 mmol).

### Initial Rate Study



**Scheme 4-S3.** Dependence of the observed rate constant ( $k_{\text{obs}}$ ) on the concentration ArBr (0.1–0.8 M) with **4** as the pre-catalyst,  $p\text{CO} = 1$  atm and **1a** = 0.1 M at 80 °C within 2.5 h.

### General Procedure

A series of separate parallel reactions were carried out to monitor the conversion rate of the reaction for each concentration of **2a**. Four parallel oven-dried 8 mL reaction vials equipped with stir bars were charged with compound **1a** (16.9 mg, 0.1 mmol, 1.0 equiv) and 1-bromo-4-*tert*-butylbenzene **2a** (1.0, 1.5, 2.0, 4.0, 8.0 equiv) in a glove box under a nitrogen atmosphere at room temperature. (Josiphos)Pd(C<sub>2</sub>H<sub>4</sub>) **4** (1.0 mol %) and 1 mL of dry 1,4-dioxane were added to every reaction vial under nitrogen. Next, LiN(SiMe<sub>3</sub>)<sub>2</sub> (3.0 equiv) was added to each vial. The vials were capped and removed from the glove box. Then each vial was purged with CO using a Schlenk line, by bubbling CO gas through a long needle under the solvent surface for 5 min. Another short needle was used as the outlet of gas. Then the vial was taped with electrical tape, stirred, and heated at 80 °C. Each of the four vials of the same concentration of **2a** was cooled in ice bath and opened in a fume hood sequentially after every 30 min. After a minute for releasing leftover CO, each reaction was quenched with two drops of H<sub>2</sub>O, diluted with 3 mL of ethyl acetate, and filtered over a pad of MgSO<sub>4</sub> and silica. The solution was concentrated in vacuo. <sup>1</sup>H NMR (CDCl<sub>3</sub>) spectra of the crude material was acquired to determine the yield of **3aa** based on integration against an internal standard (CH<sub>2</sub>Br<sub>2</sub> to each vial was added 7.0 μL, 0.1 mmol).

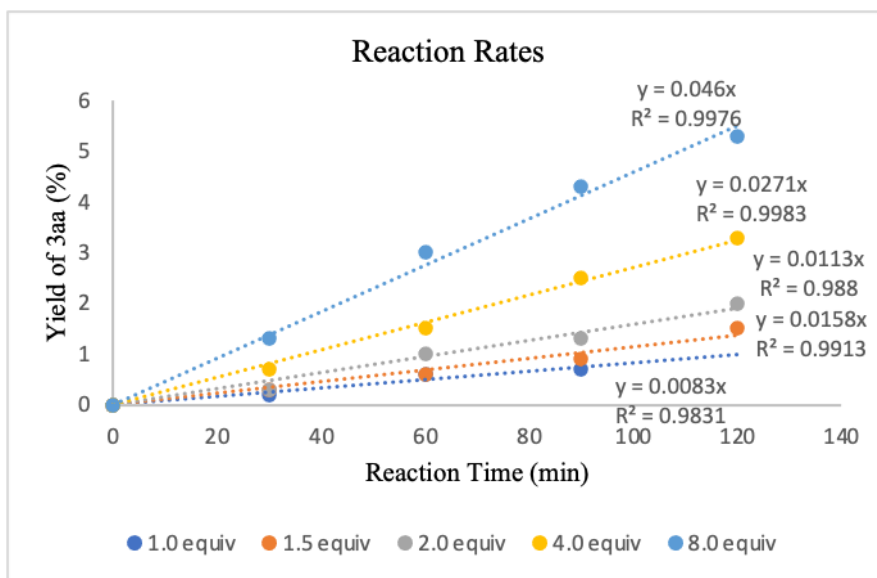


**Chart 4-S3.** Reaction rates at different **2a** concentrations

Observed reaction rate constants were determined by plotting the yields obtained with 120 min for each equivalence of **2a**. The linear fit that pass through (0, 0) results in rate of each reaction. Then the observed rate constant was calculated by dividing each rate by the initial concentration of **2a**. Then  $-\ln(k)$  versus  $-\ln[2a]$  was also plotted.



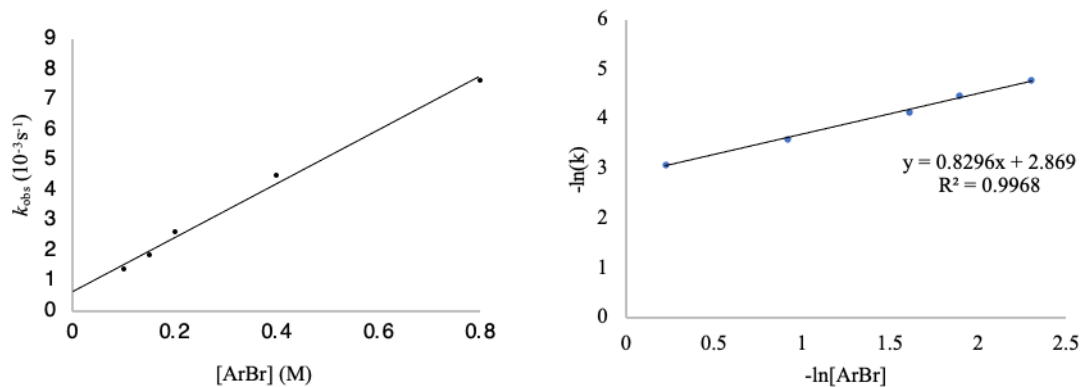


**Chart 5-S3.** Dependence of the observed rate constant ( $k_{\text{obs}}$ ) on the concentration ArBr

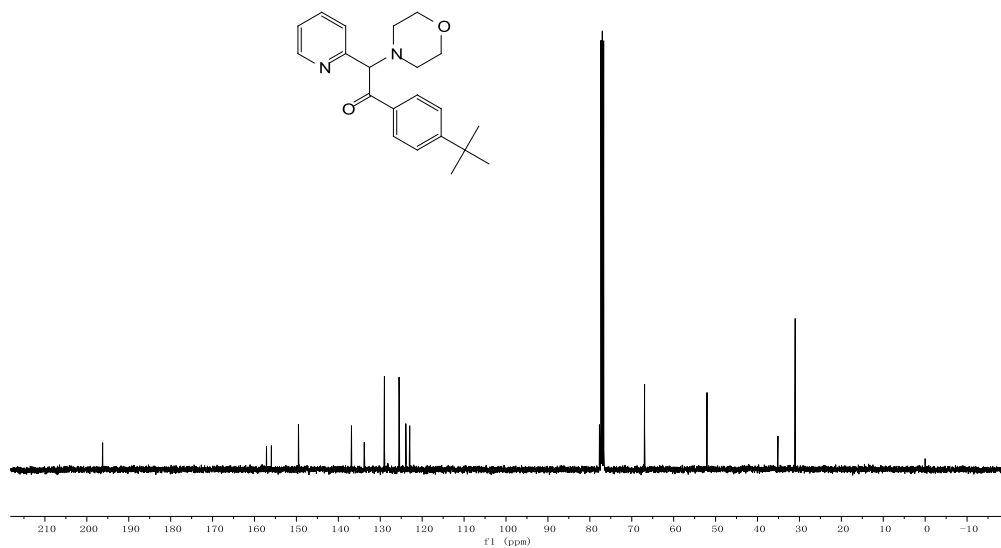
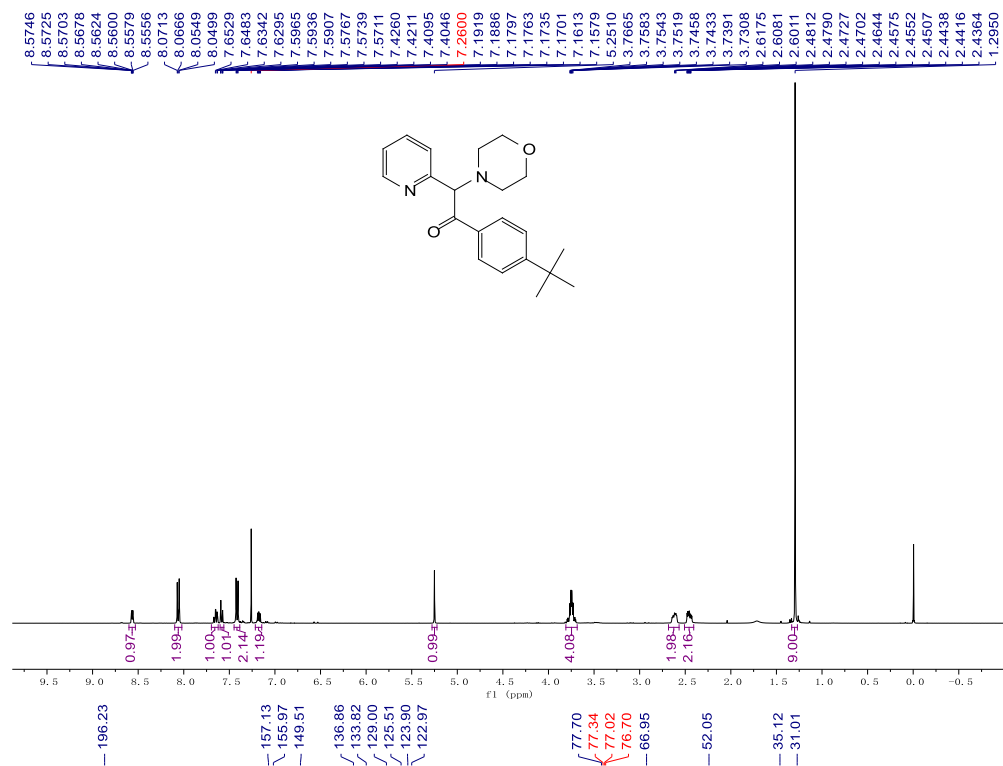
1. (a) Zhao, H.; Hu, B.; Xu, L.; Walsh, P. J. *Chem Sci.* **2021**, *12*, 10862-10870. (b)

Zhang, J.; Bellomo, A.; Creamer, A. D.; Dreher, S. D.; Walsh, P. J. *J. Am. Chem. Soc.*

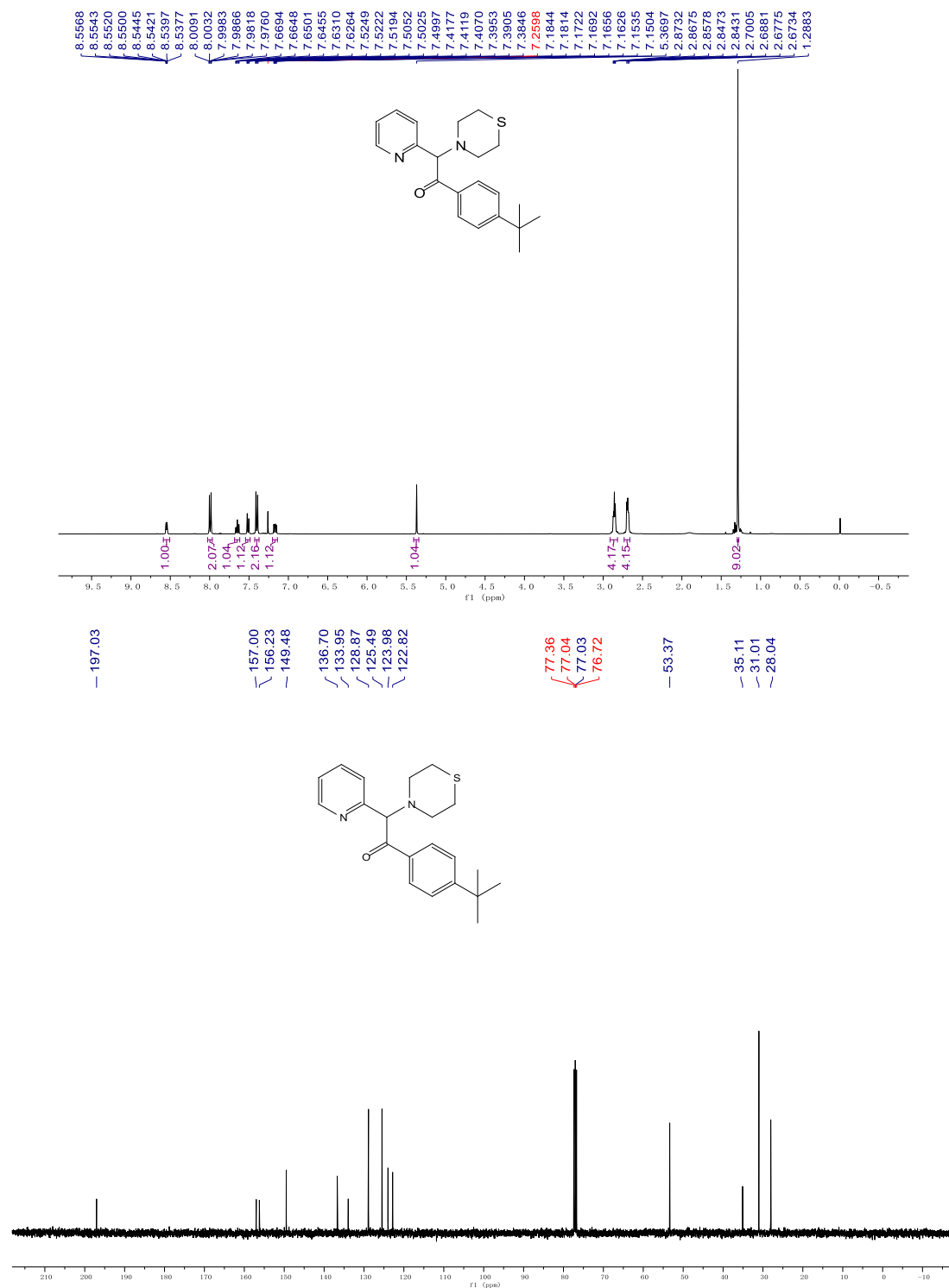
**2012**, *134*, 13765-72.

## Appendix A. NMR Spectra for Chapter 2

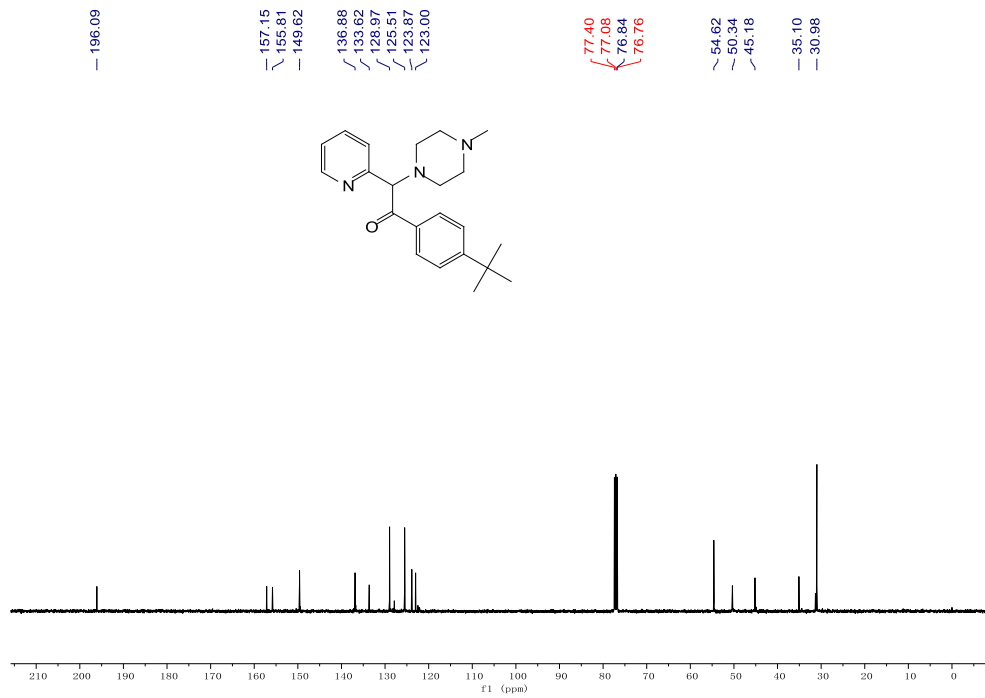
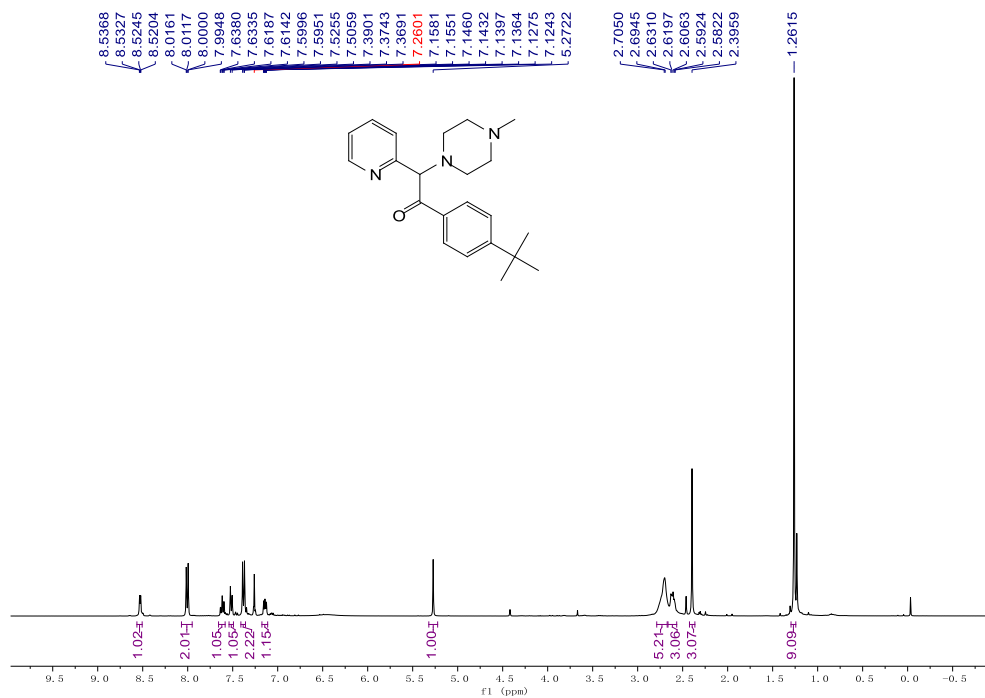
$^1\text{H}$  and  $^{13}\text{C}\{^1\text{H}\}$  NMR spectra of compound **3aa** in  $\text{CDCl}_3$



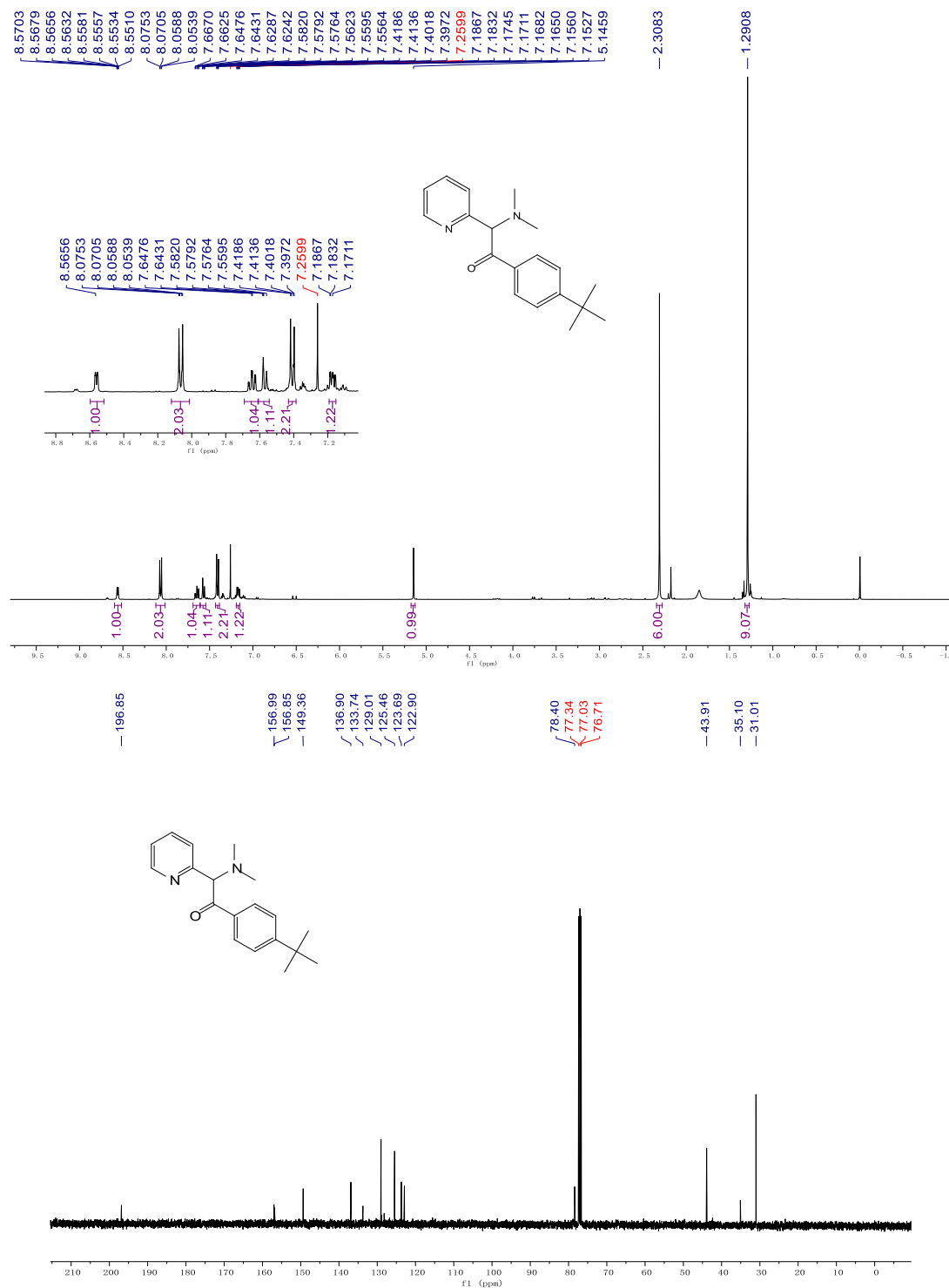
$^1\text{H}$  and  $^{13}\text{C}\{^1\text{H}\}$  NMR spectra of compound **3ba** in  $\text{CDCl}_3$



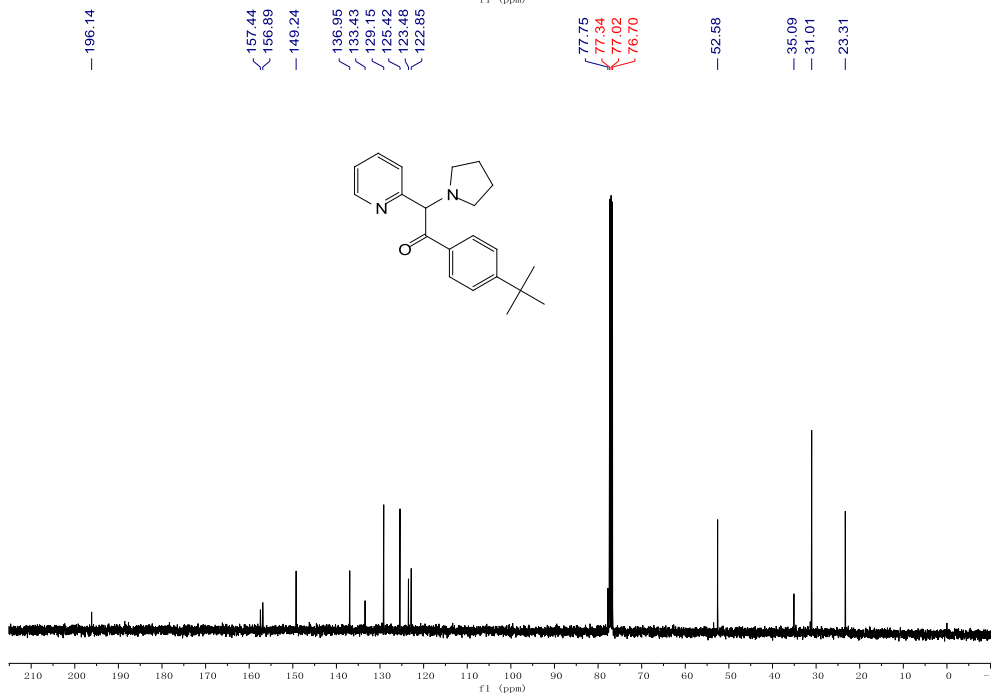
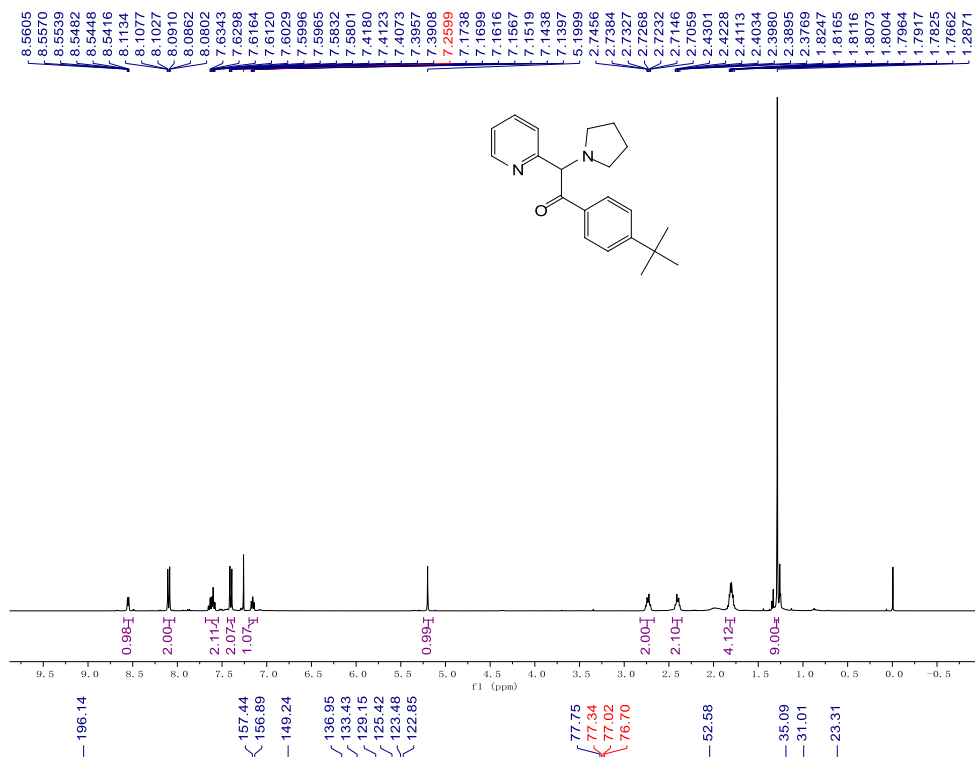
$^1\text{H}$  and  $^{13}\text{C}\{^1\text{H}\}$  NMR spectra of compound **3a** in  $\text{CDCl}_3$



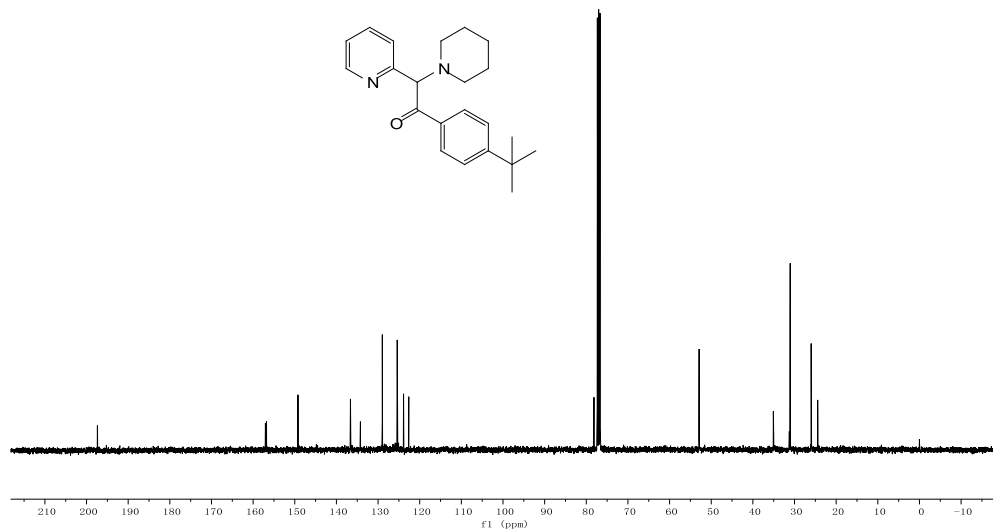
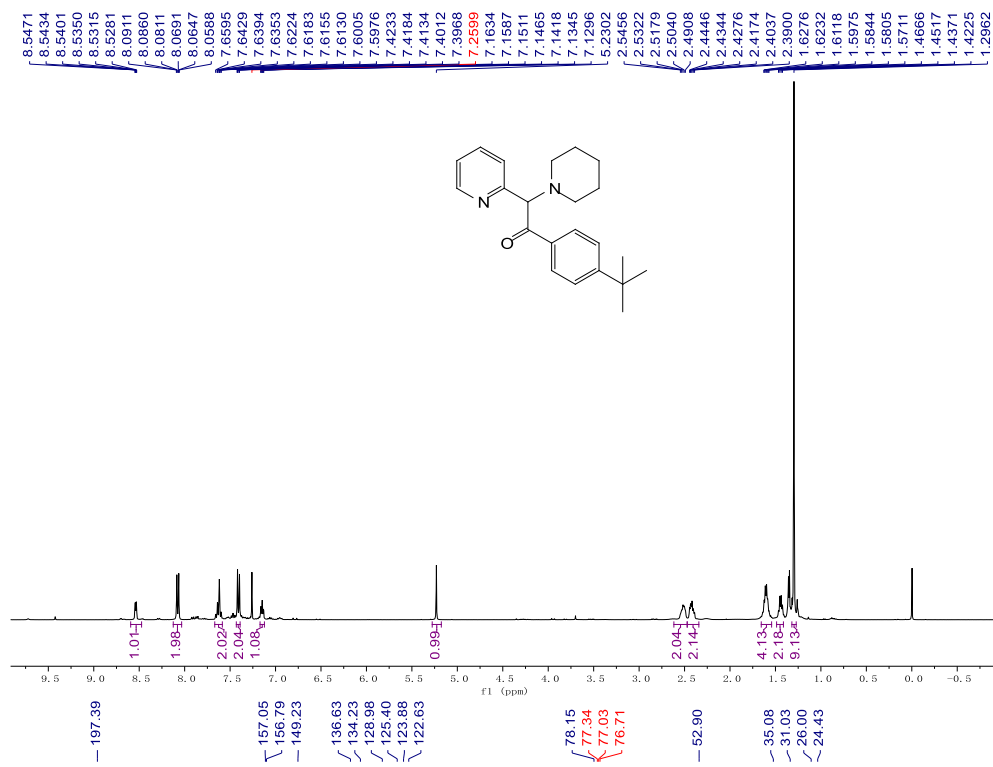
$^1\text{H}$  and  $^{13}\text{C}\{^1\text{H}\}$  NMR spectra of compound **3da** in  $\text{CDCl}_3$



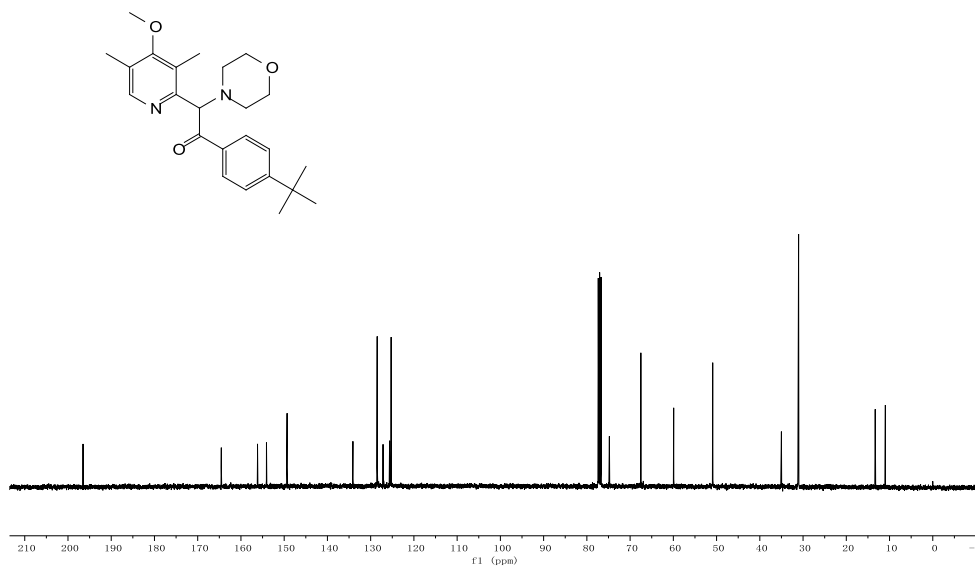
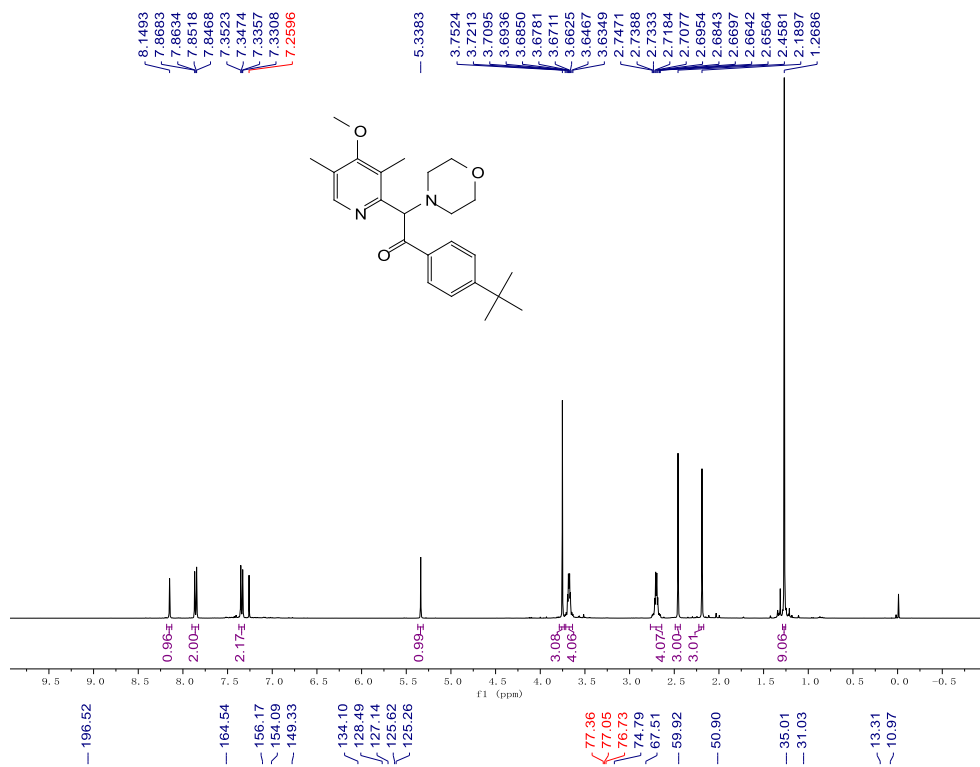
$^1\text{H}$  and  $^{13}\text{C}\{^1\text{H}\}$  NMR spectra of compound **3ea** in  $\text{CDCl}_3$



$^1\text{H}$  and  $^{13}\text{C}\{^1\text{H}\}$  NMR spectra of compound **3fa** in  $\text{CDCl}_3$

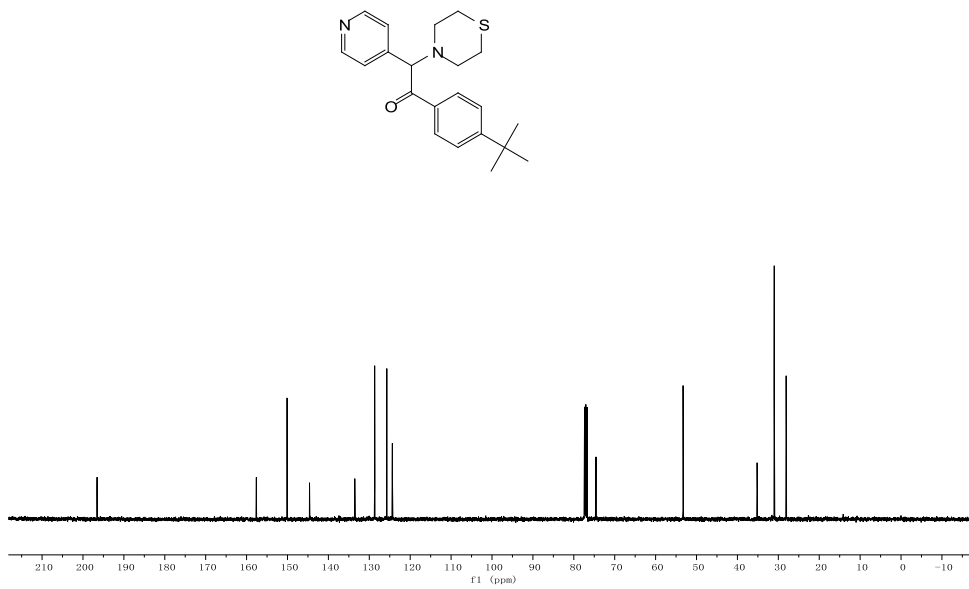
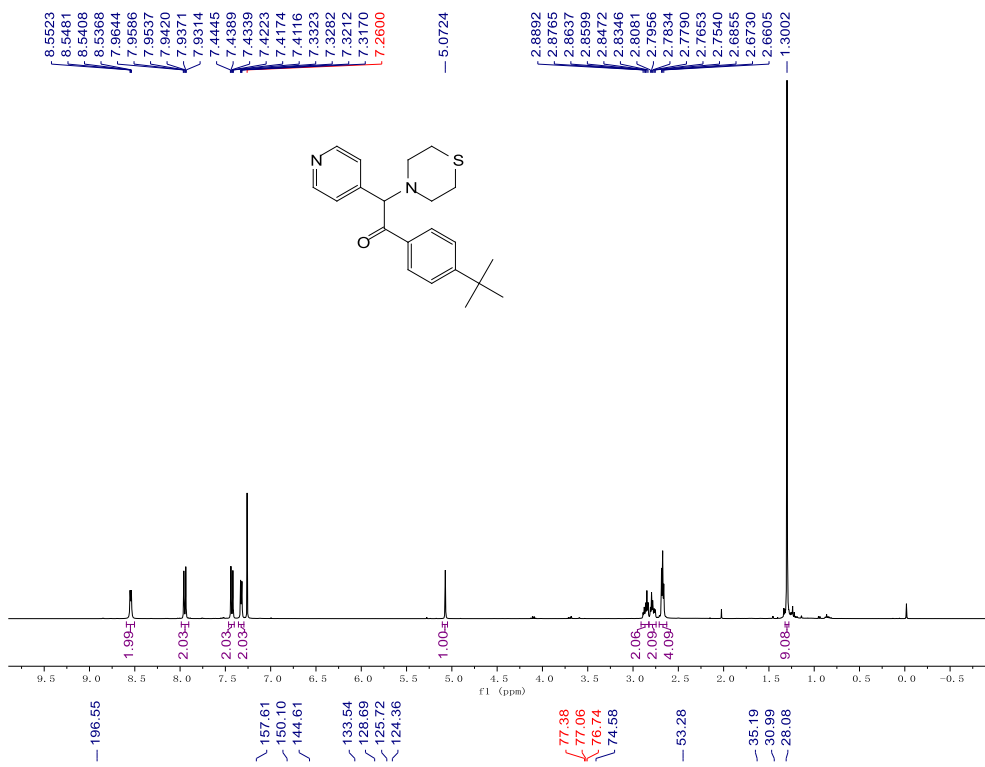


$^1\text{H}$  and  $^{13}\text{C}\{^1\text{H}\}$  NMR spectra of compound **3ga** in  $\text{CDCl}_3$

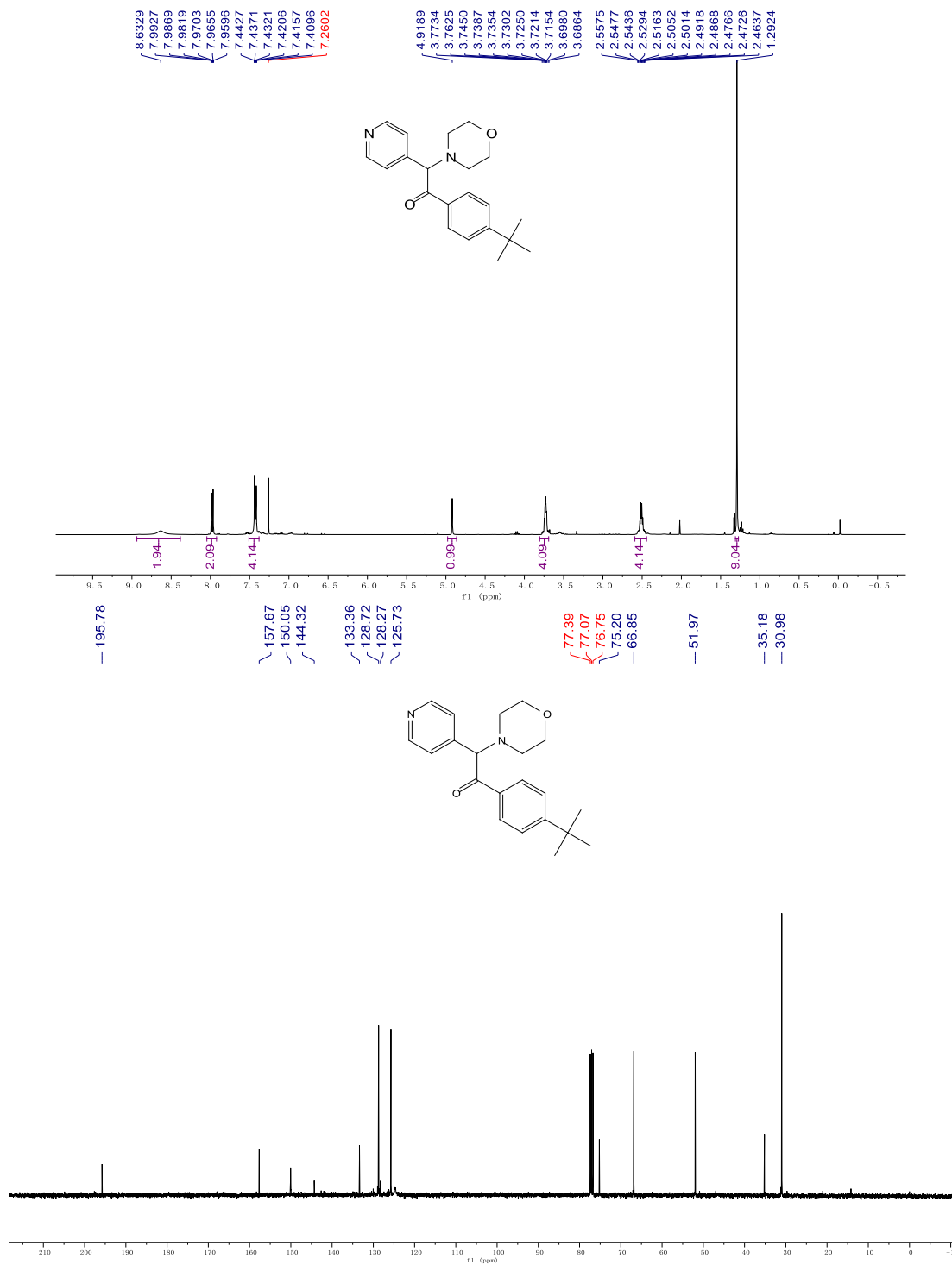




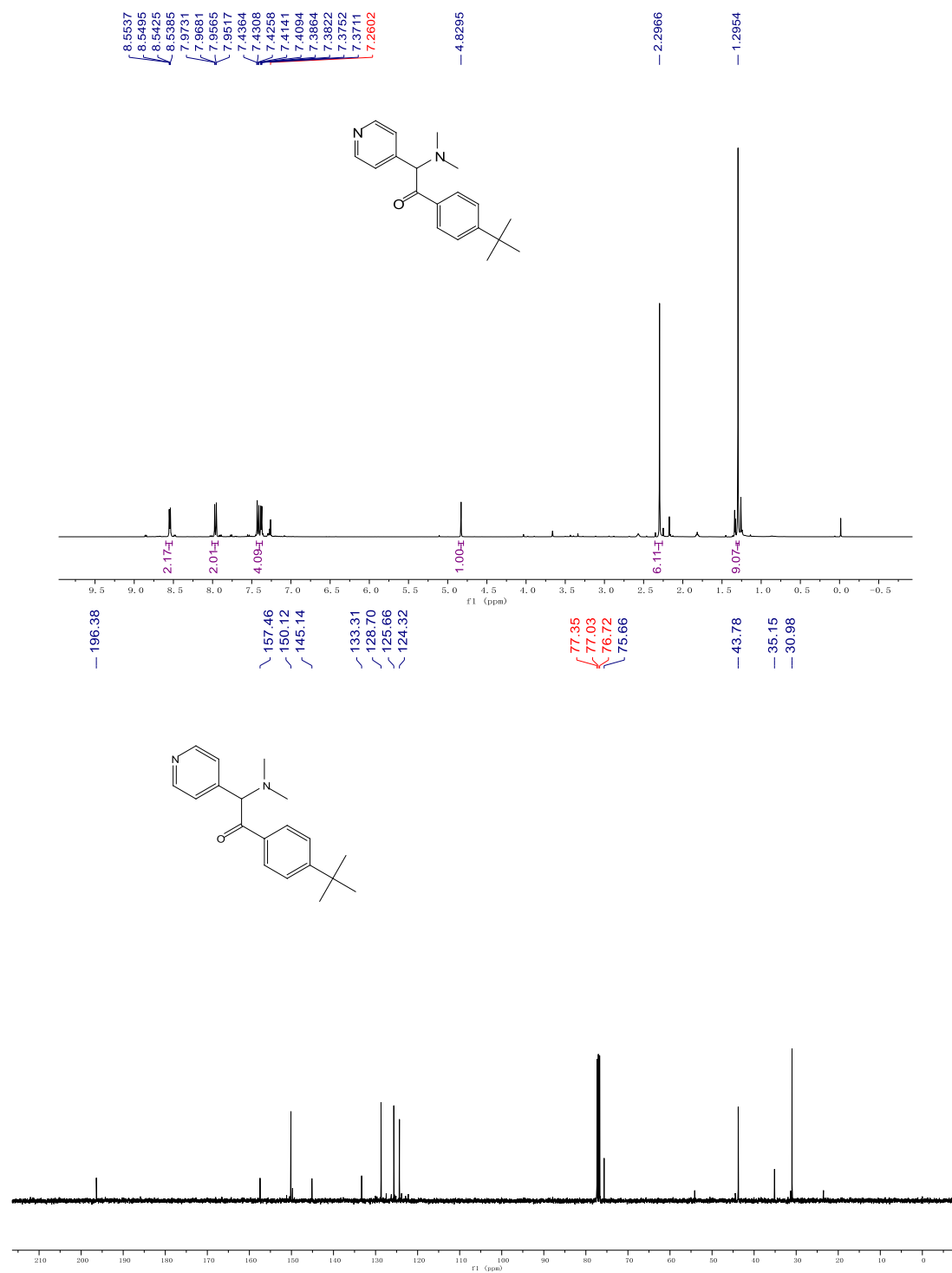
$^1\text{H}$  and  $^{13}\text{C}\{^1\text{H}\}$  NMR spectra of compound **3ha** in  $\text{CDCl}_3$



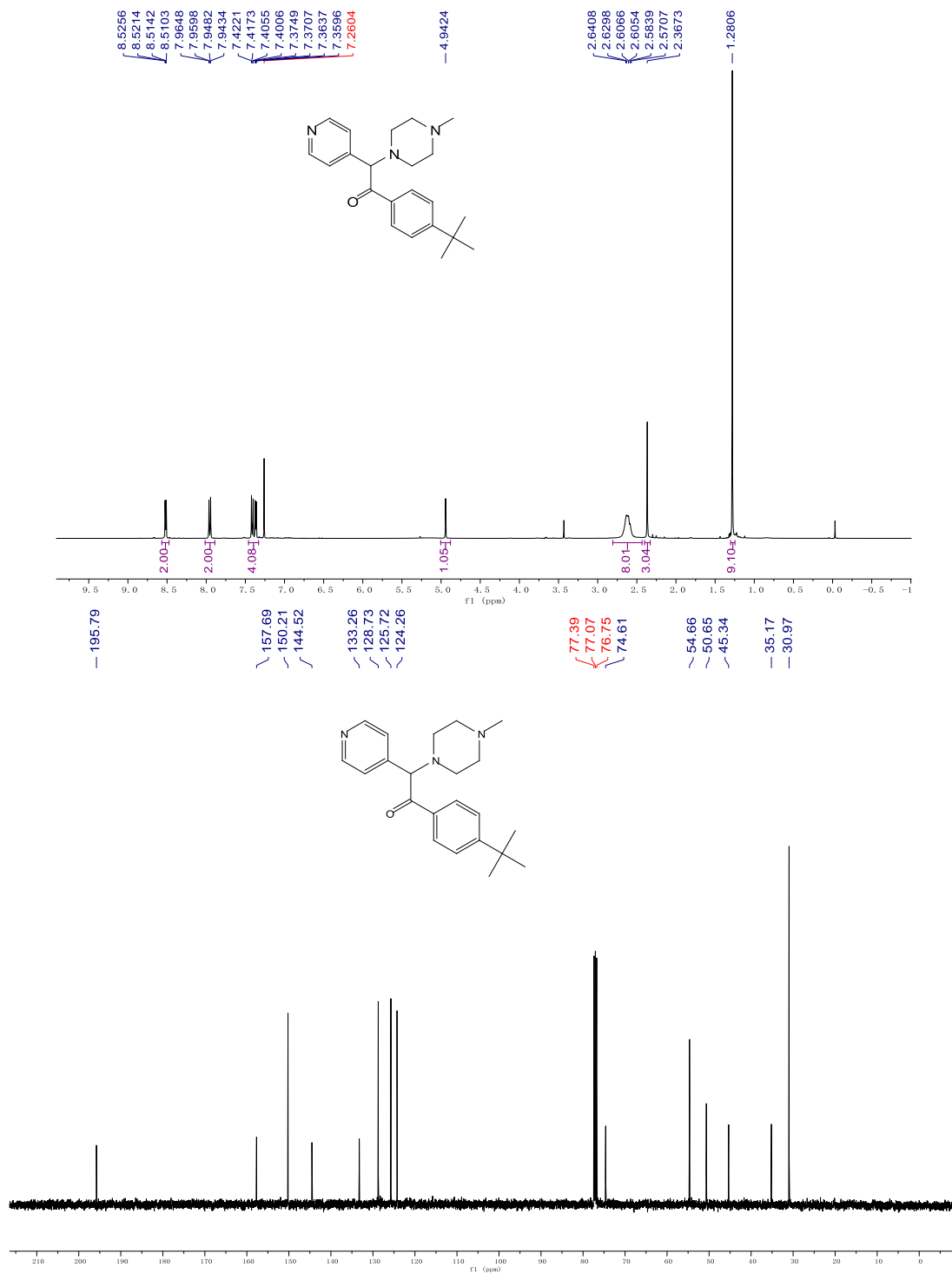
$^1\text{H}$  and  $^{13}\text{C}\{^1\text{H}\}$  NMR spectra of compound **3ia** in  $\text{CDCl}_3$



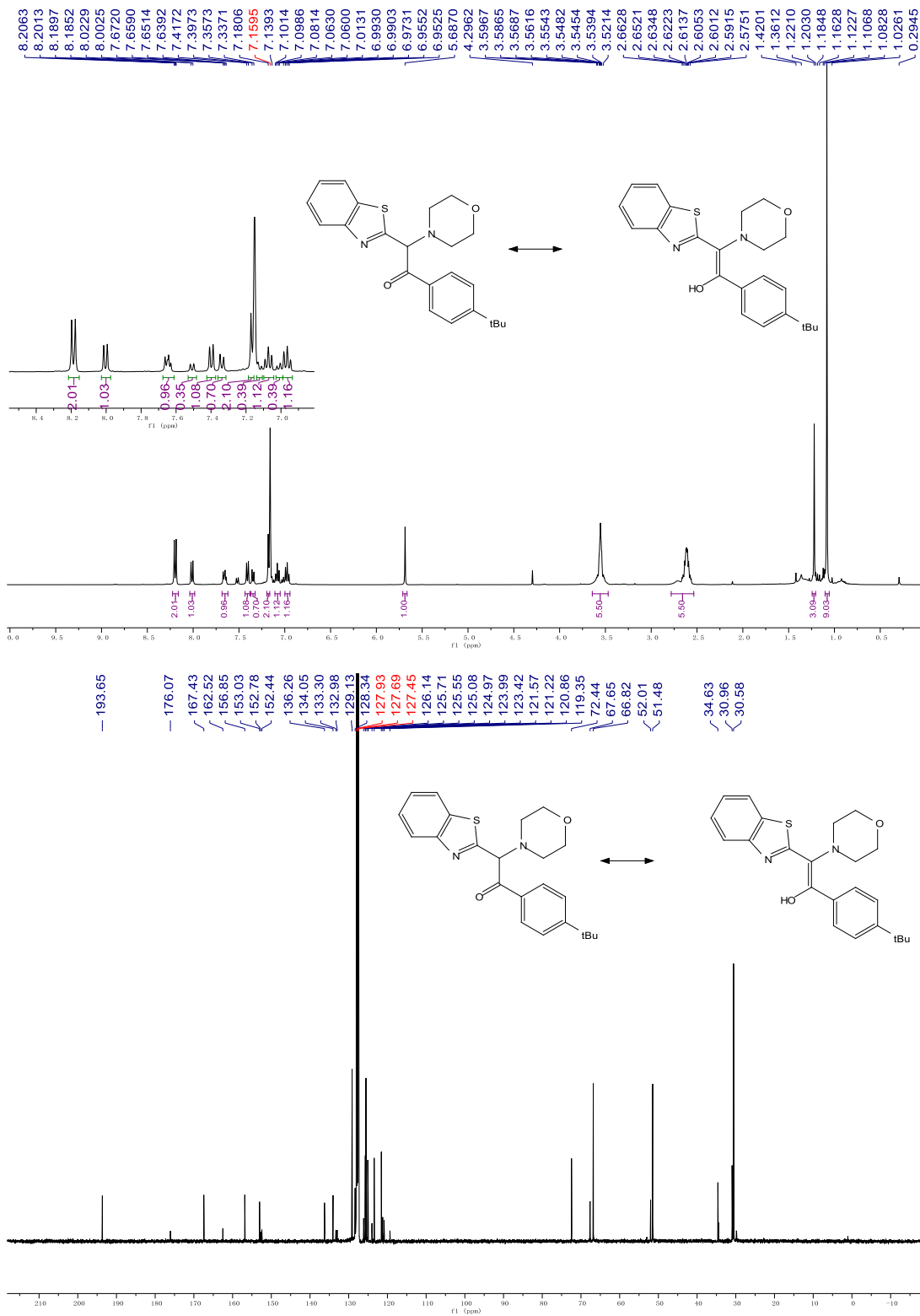
$^1\text{H}$  and  $^{13}\text{C}\{^1\text{H}\}$  NMR spectra of compound **3ja** in  $\text{CDCl}_3$



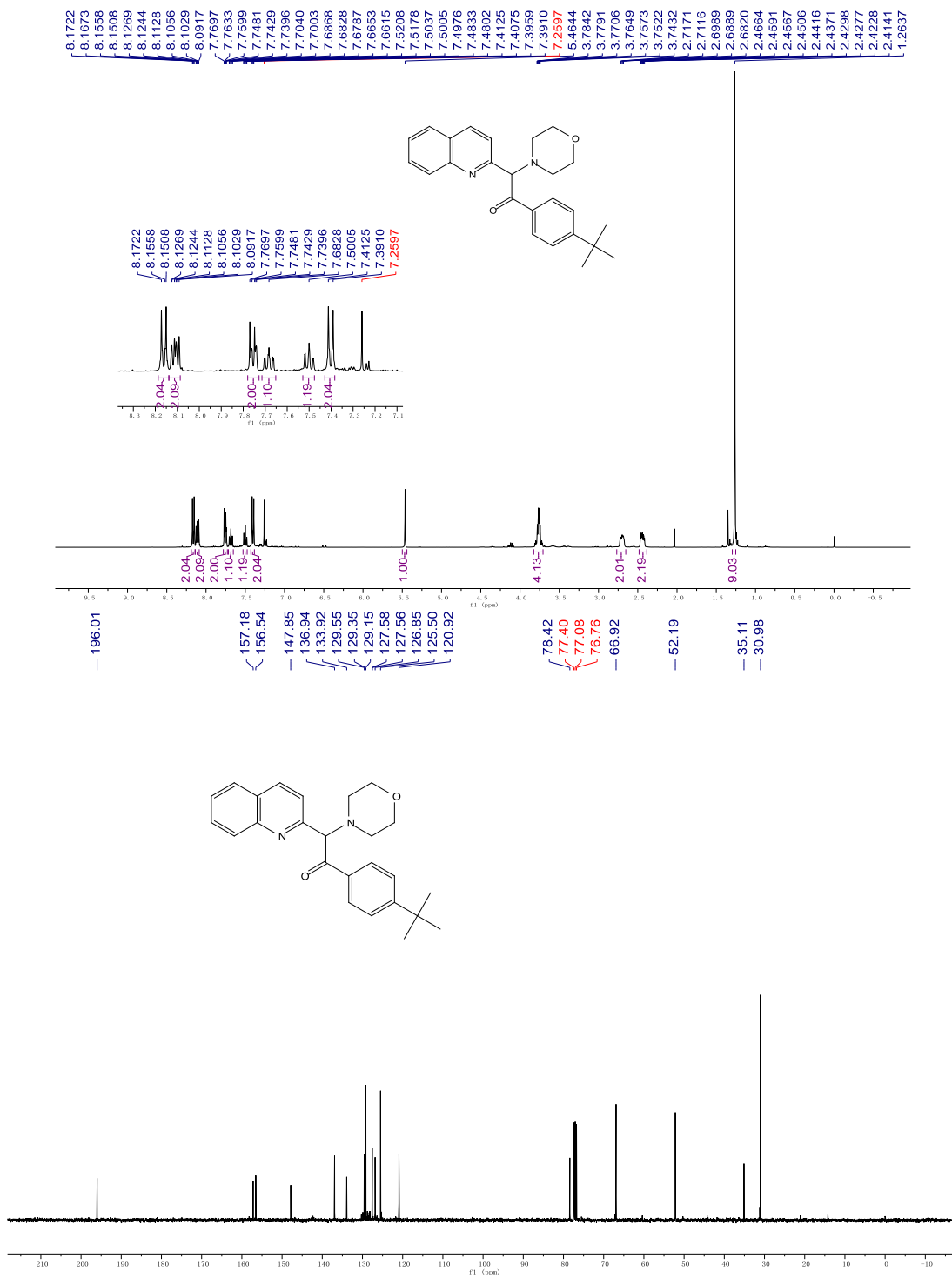
$^1\text{H}$  and  $^{13}\text{C}\{^1\text{H}\}$  NMR spectra of compound **3ka** in  $\text{CDCl}_3$



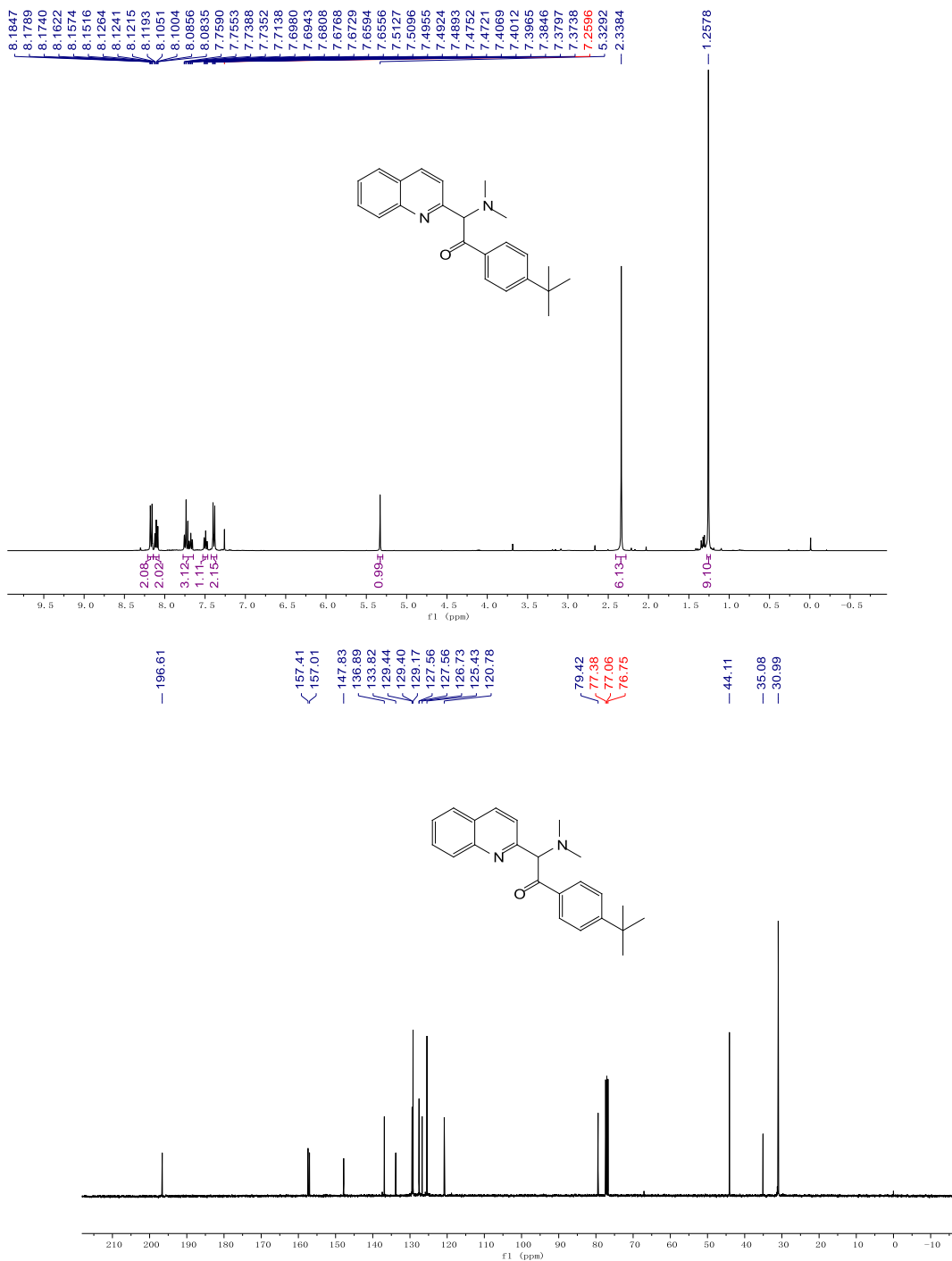
$^1\text{H}$  and  $^{13}\text{C}\{^1\text{H}\}$  NMR spectra of compound **3la** in  $\text{C}_6\text{D}_6$



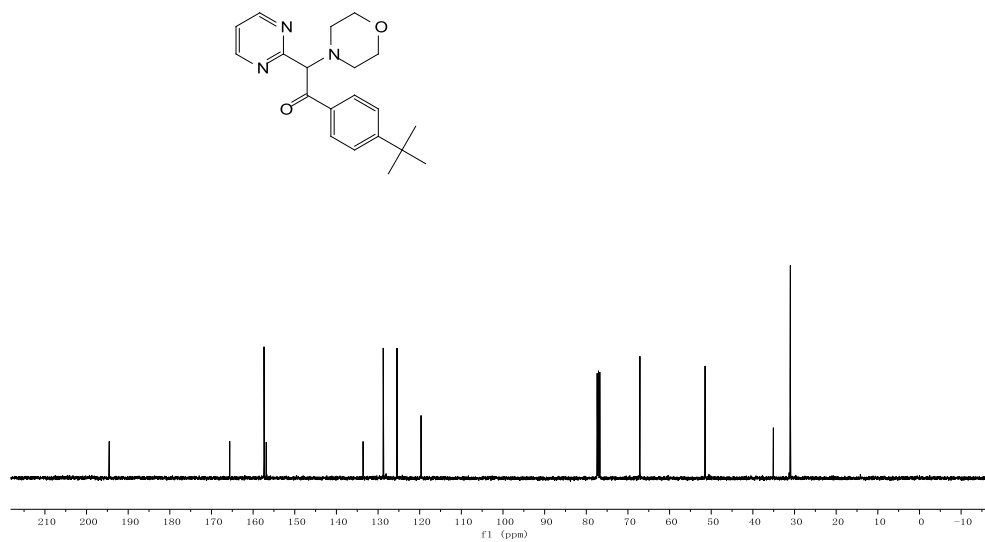
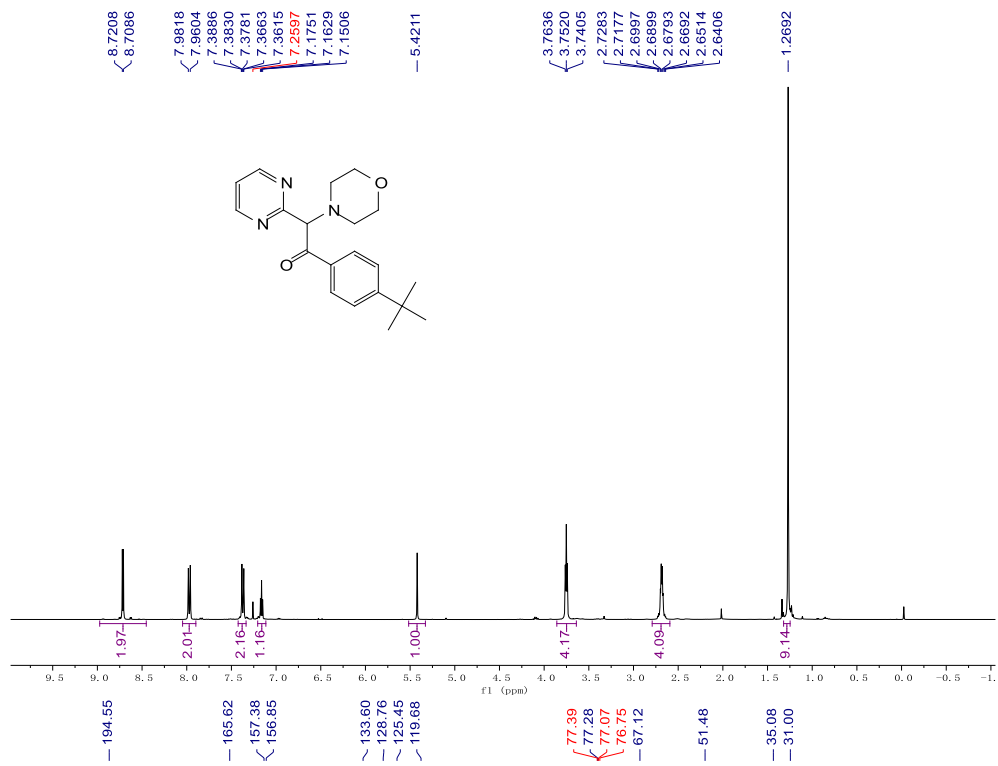
$^1\text{H}$  and  $^{13}\text{C}\{^1\text{H}\}$  NMR spectra of compound **3ma** in  $\text{CDCl}_3$



$^1\text{H}$  and  $^{13}\text{C}\{^1\text{H}\}$  NMR spectra of compound **3na** in  $\text{CDCl}_3$

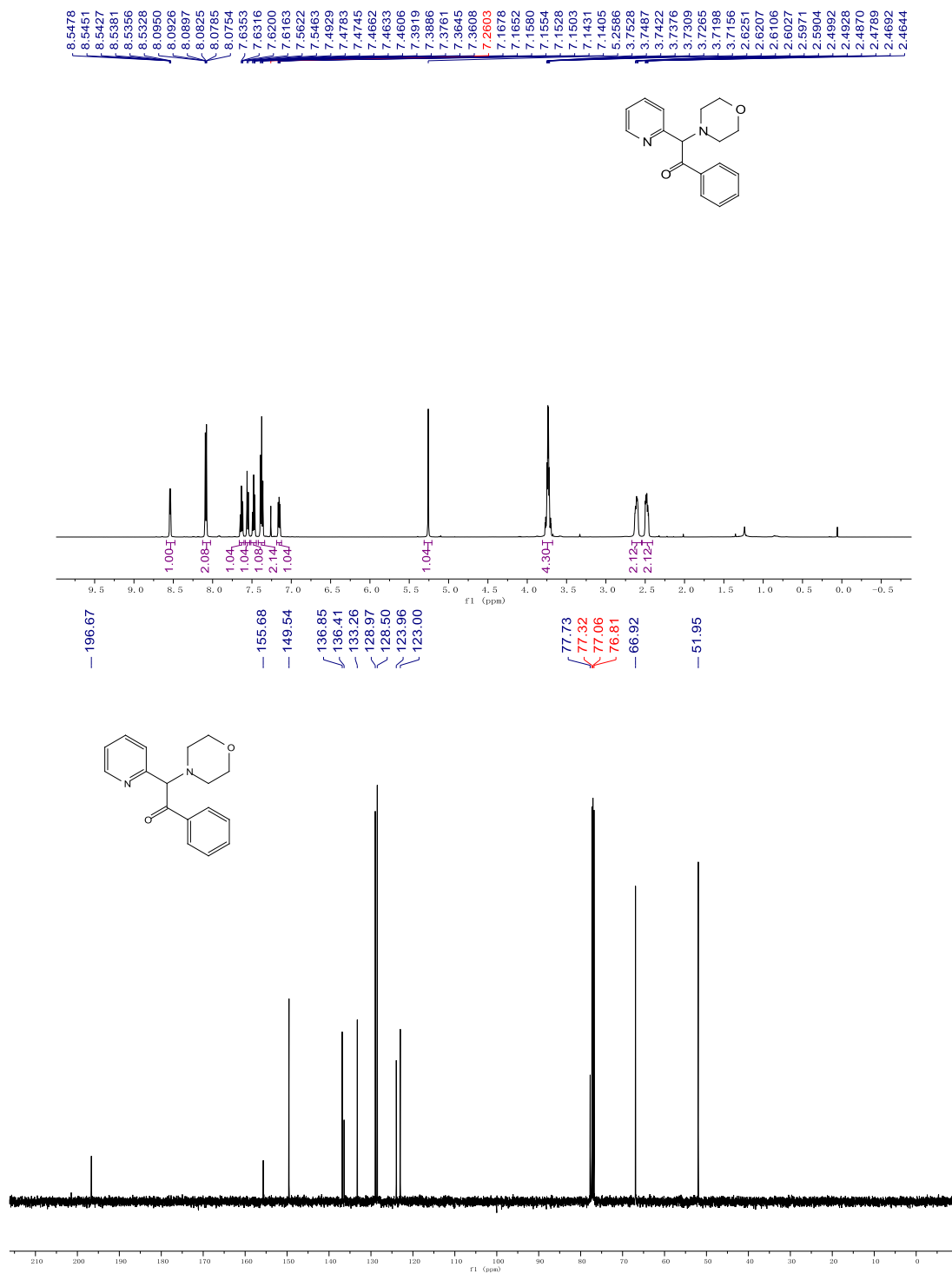


$^1\text{H}$  and  $^{13}\text{C}\{^1\text{H}\}$  NMR spectra of compound **30a** in  $\text{CDCl}_3$

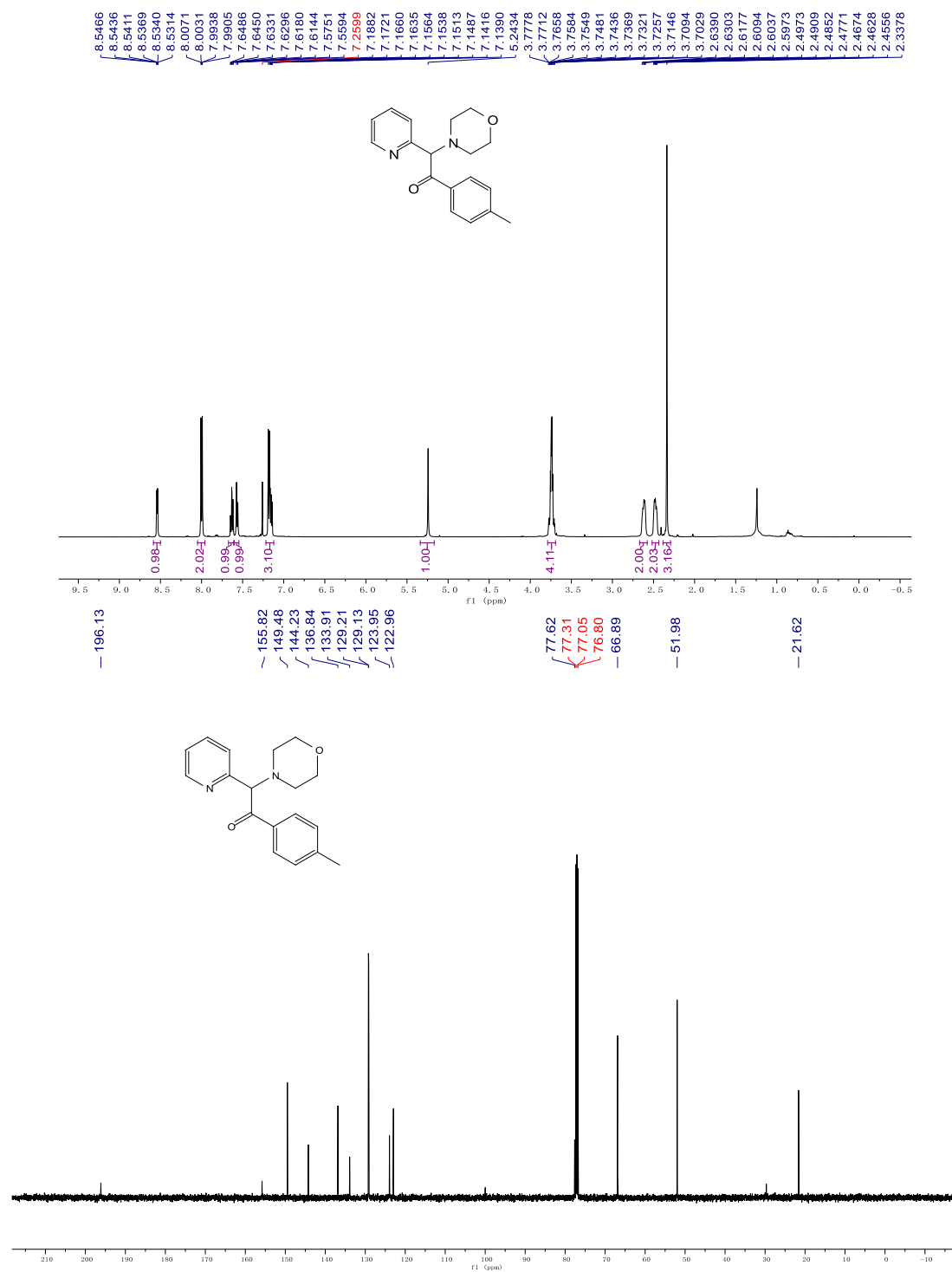




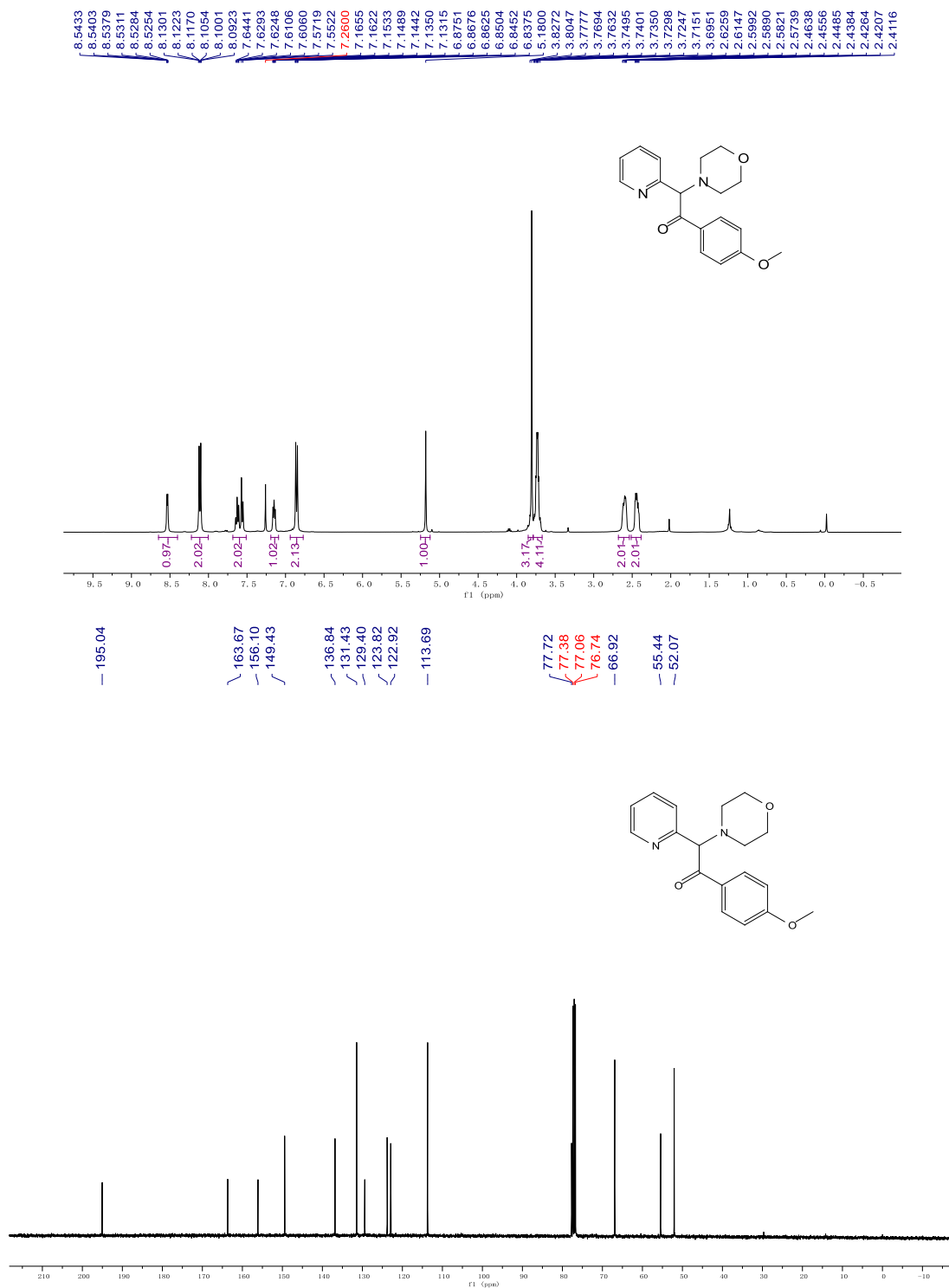
$^1\text{H}$  and  $^{13}\text{C}\{^1\text{H}\}$  NMR spectra of compound **3ab** in  $\text{CDCl}_3$



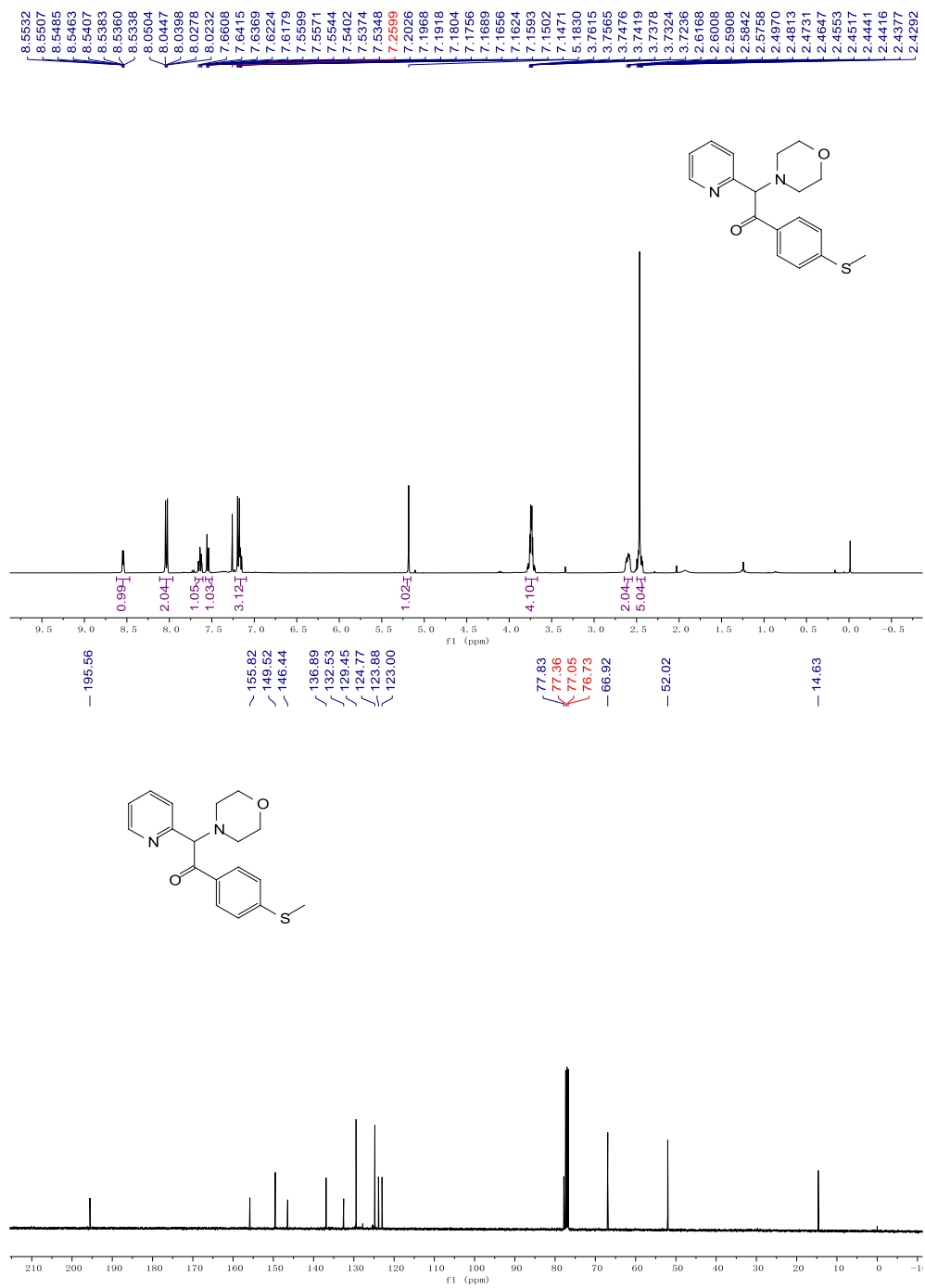
$^1\text{H}$  and  $^{13}\text{C}\{^1\text{H}\}$  NMR spectra of compound **3ac** in  $\text{CDCl}_3$



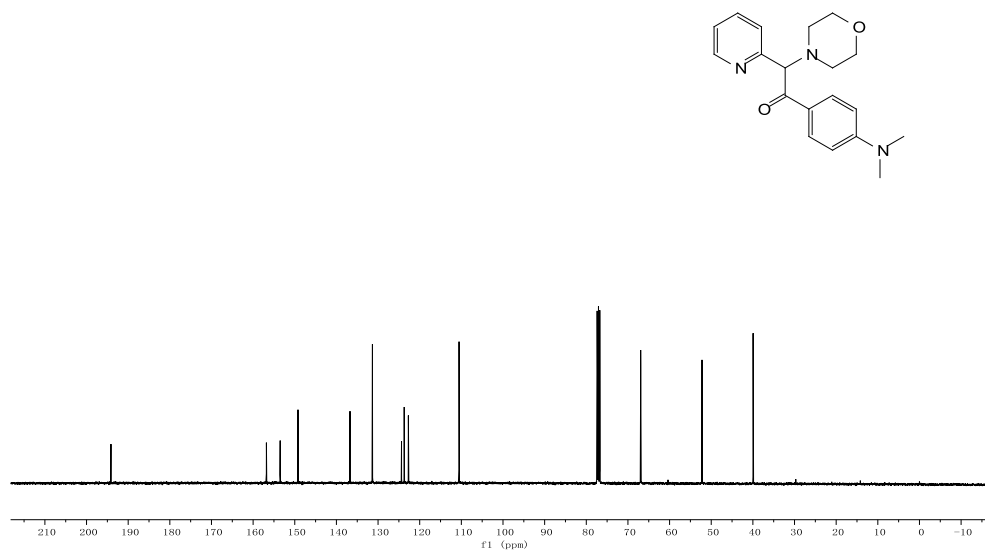
$^1\text{H}$  and  $^{13}\text{C}\{^1\text{H}\}$  NMR spectra of compound **3ad** in  $\text{CDCl}_3$



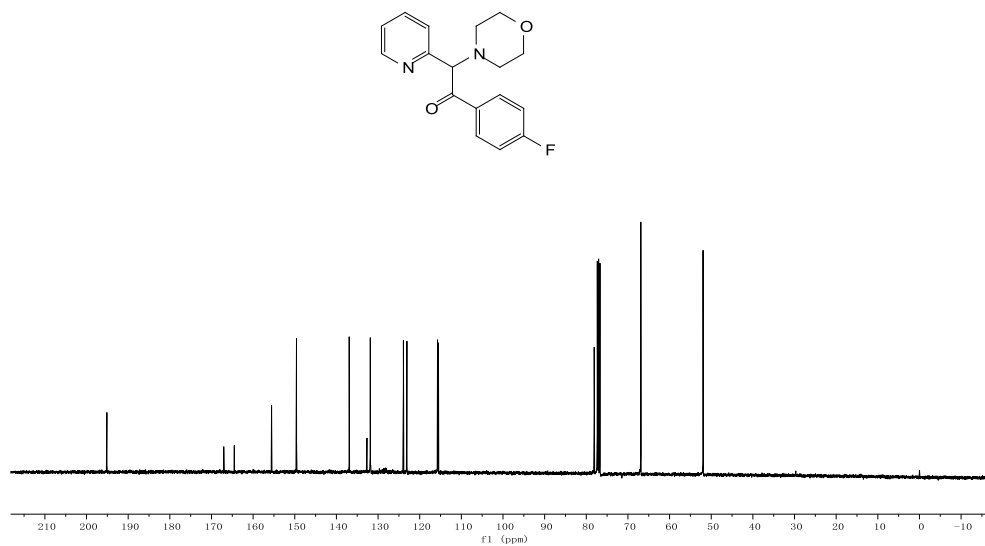
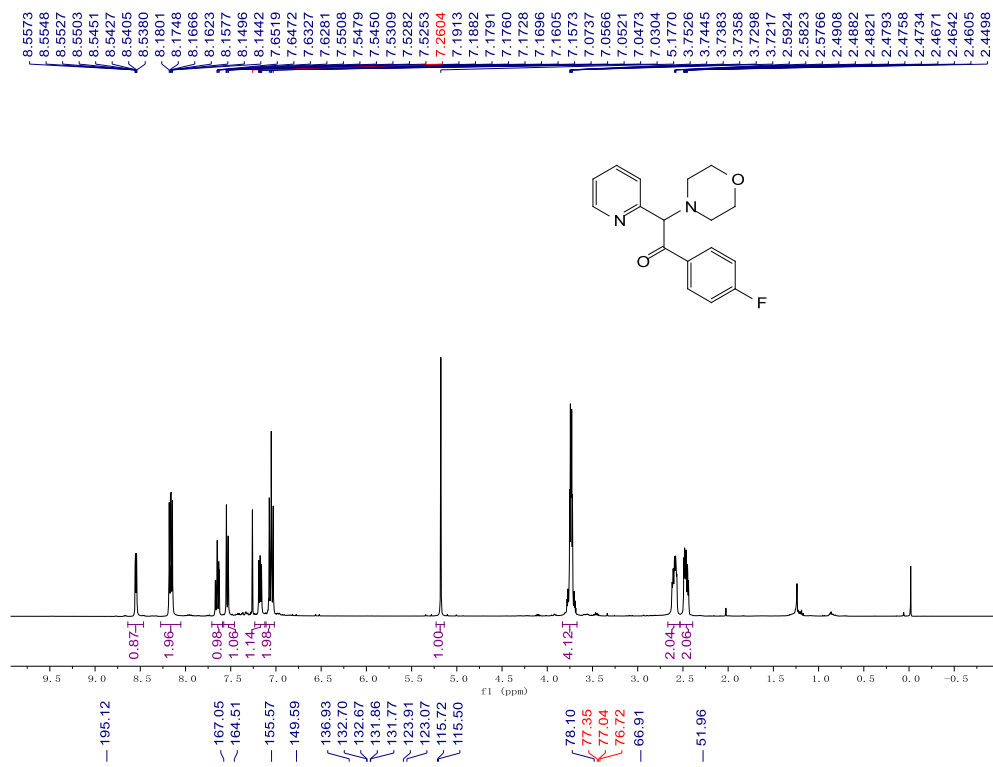
$^1\text{H}$  and  $^{13}\text{C}\{^1\text{H}\}$  NMR spectra of compound **3ae** in  $\text{CDCl}_3$

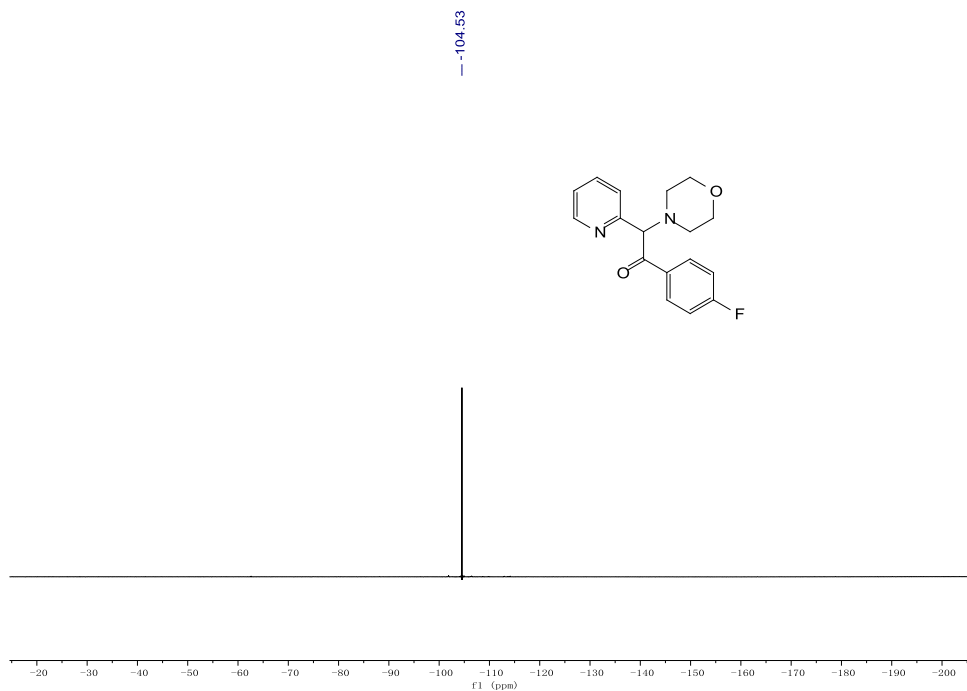


$^1\text{H}$  and  $^{13}\text{C}\{^1\text{H}\}$  NMR spectra of compound **3af** in  $\text{CDCl}_3$

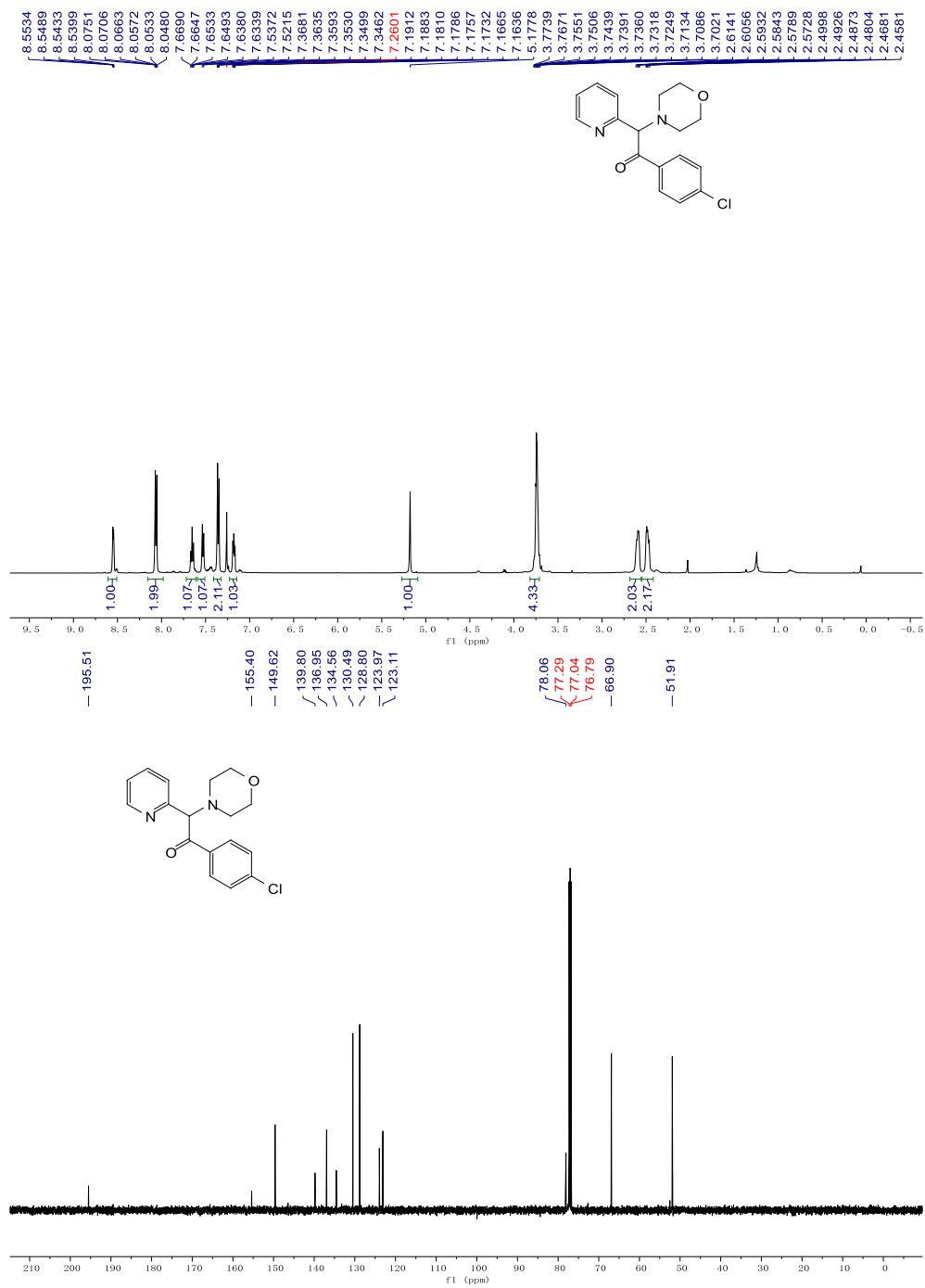


$^1\text{H}$ ,  $^{13}\text{C}\{^1\text{H}\}$  and  $^{19}\text{F}$  NMR spectra of compound **3ag** in  $\text{CDCl}_3$



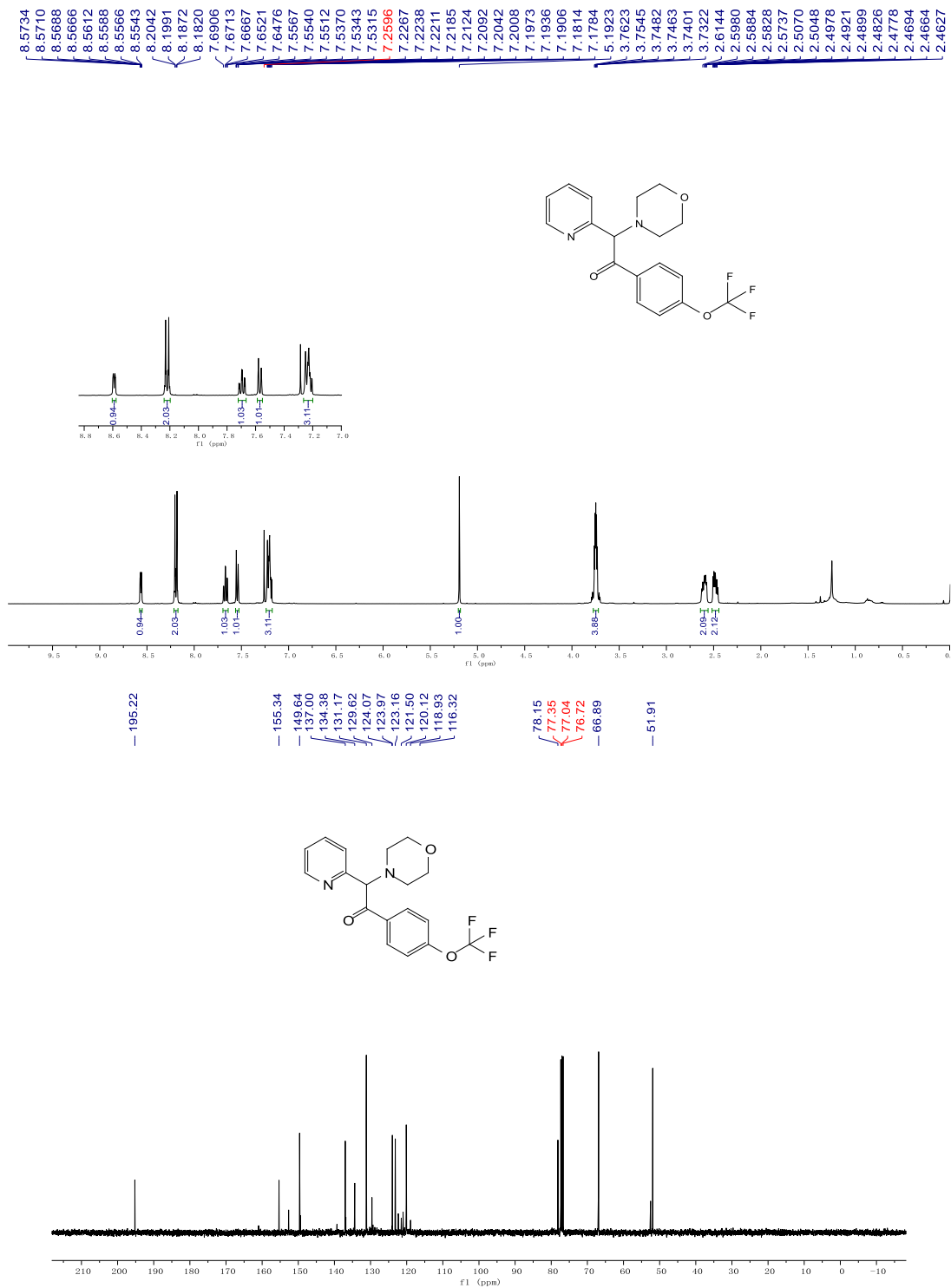


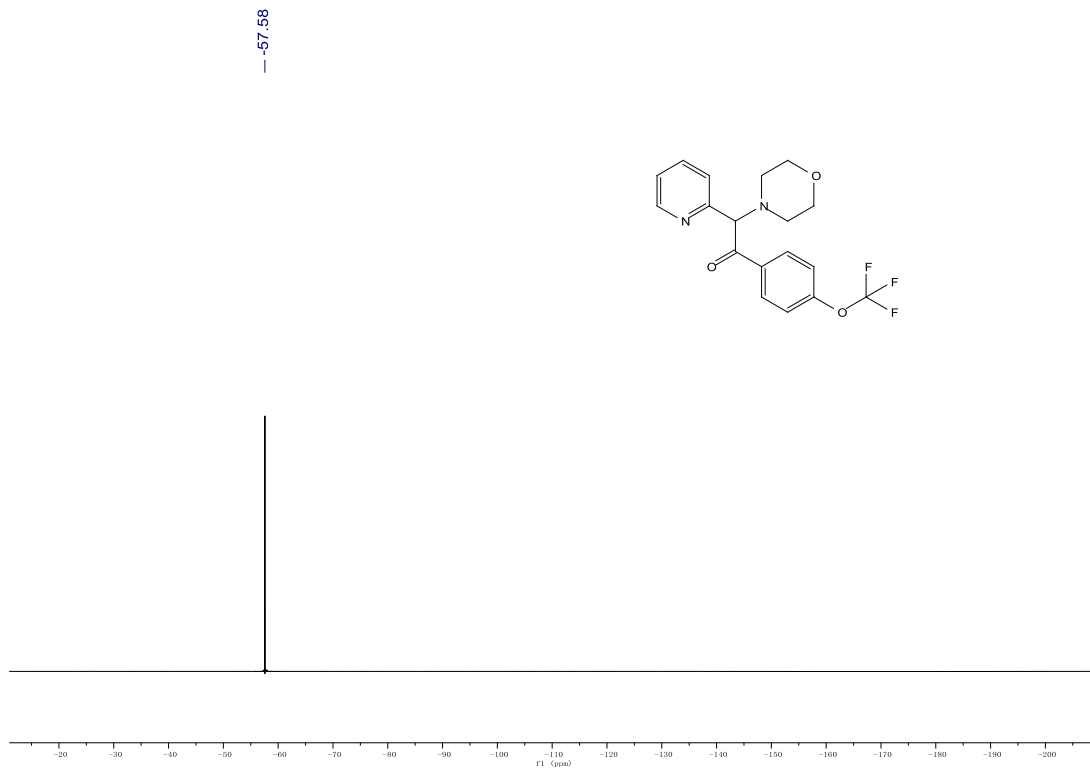
$^1\text{H}$  and  $^{13}\text{C}\{^1\text{H}\}$  NMR spectra of compound **3ah** in  $\text{CDCl}_3$



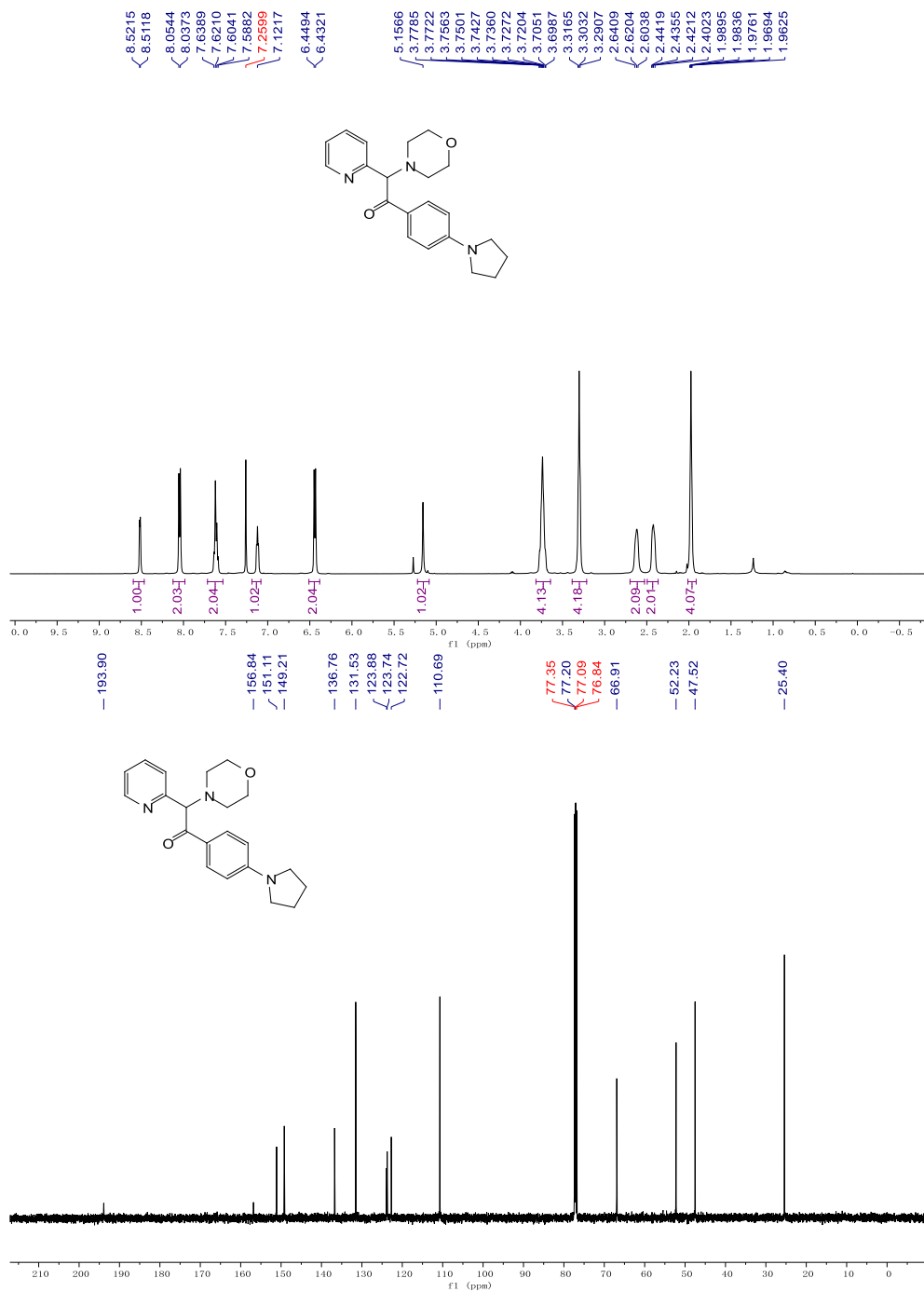


$^1\text{H}$ ,  $^{13}\text{C}\{^1\text{H}\}$  and  $^{19}\text{F}$  NMR spectra of compound **3ai** in  $\text{CDCl}_3$

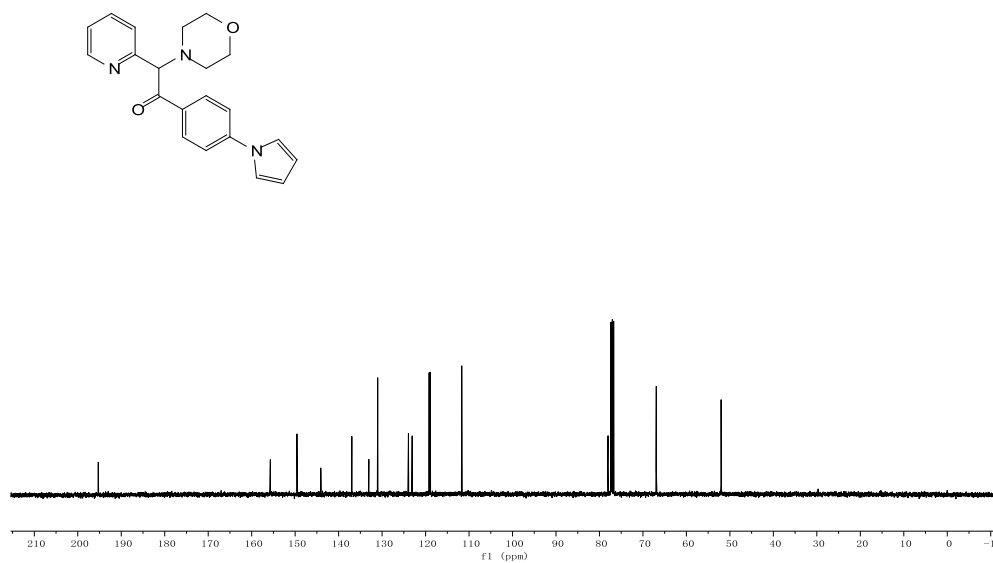
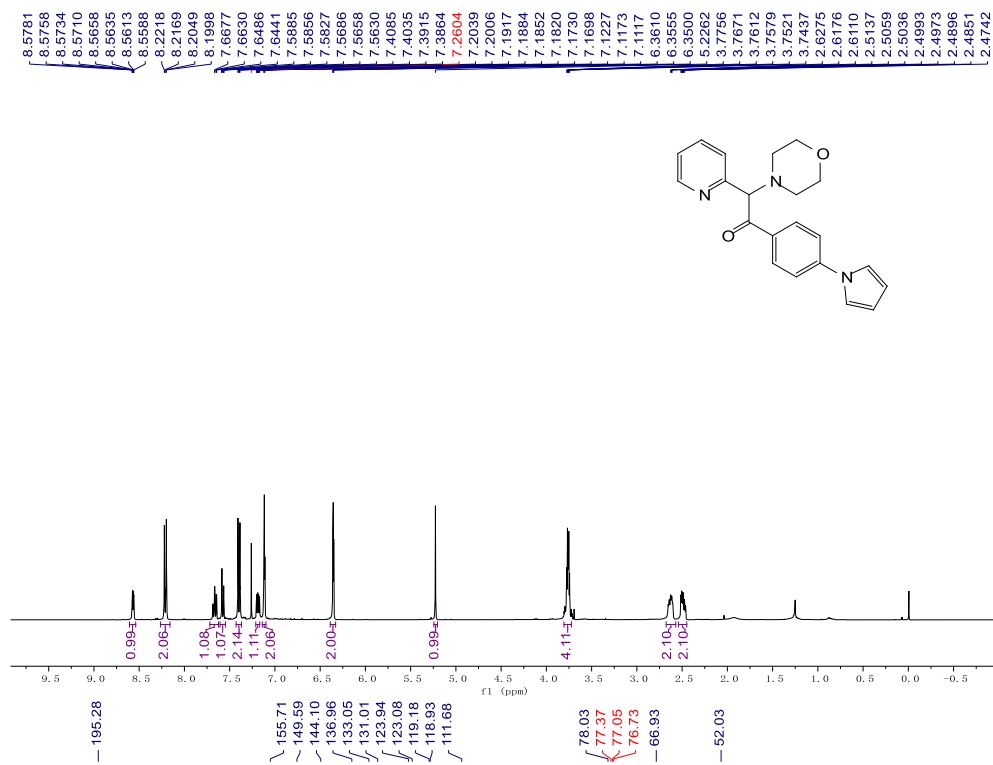




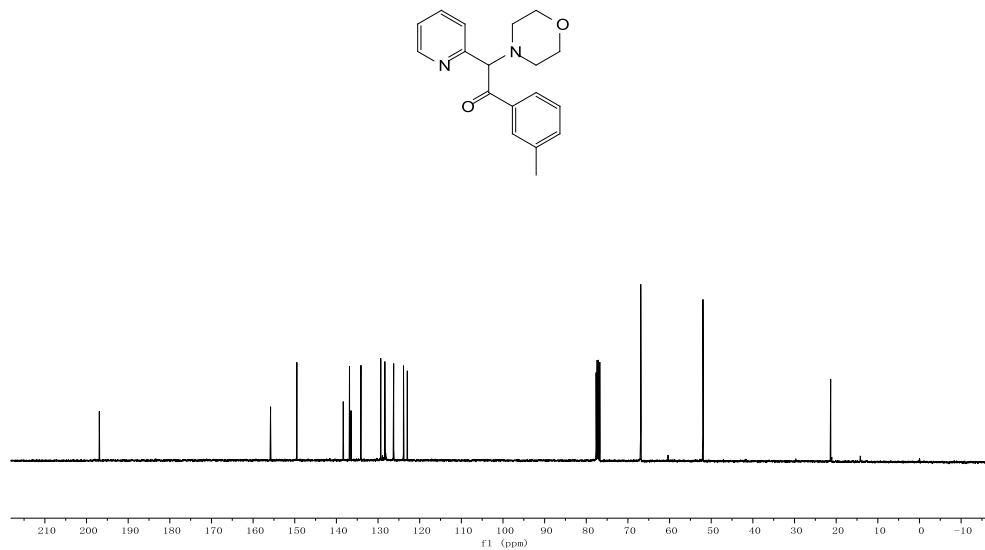
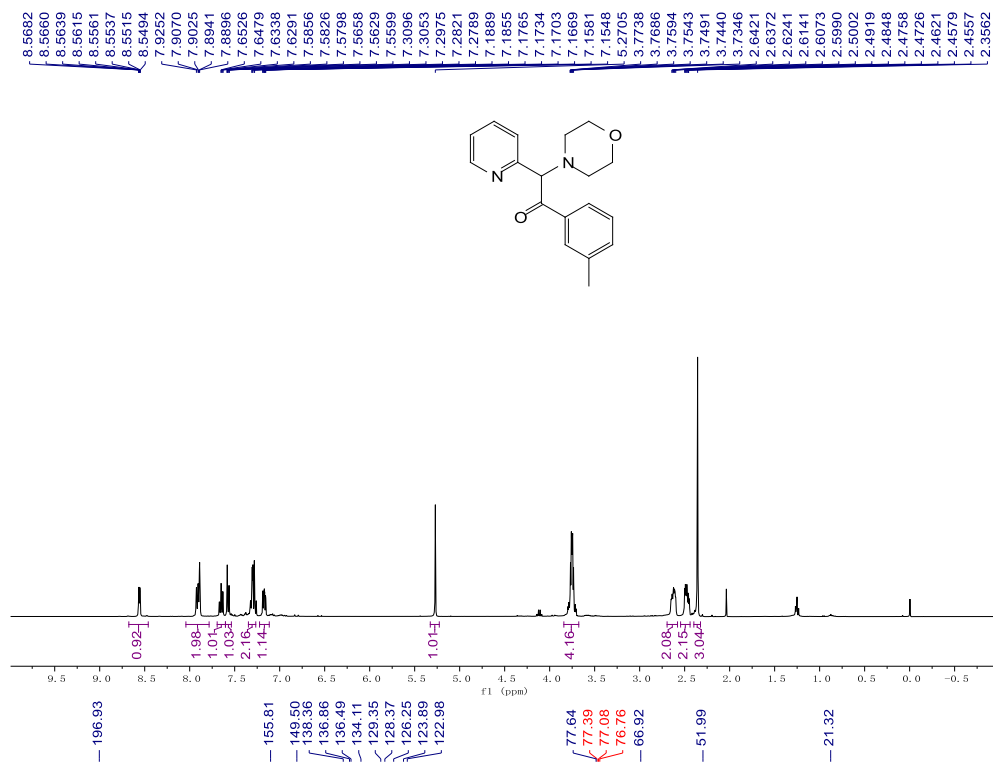
$^1\text{H}$  and  $^{13}\text{C}\{^1\text{H}\}$  NMR spectra of compound **3aj** in  $\text{CDCl}_3$



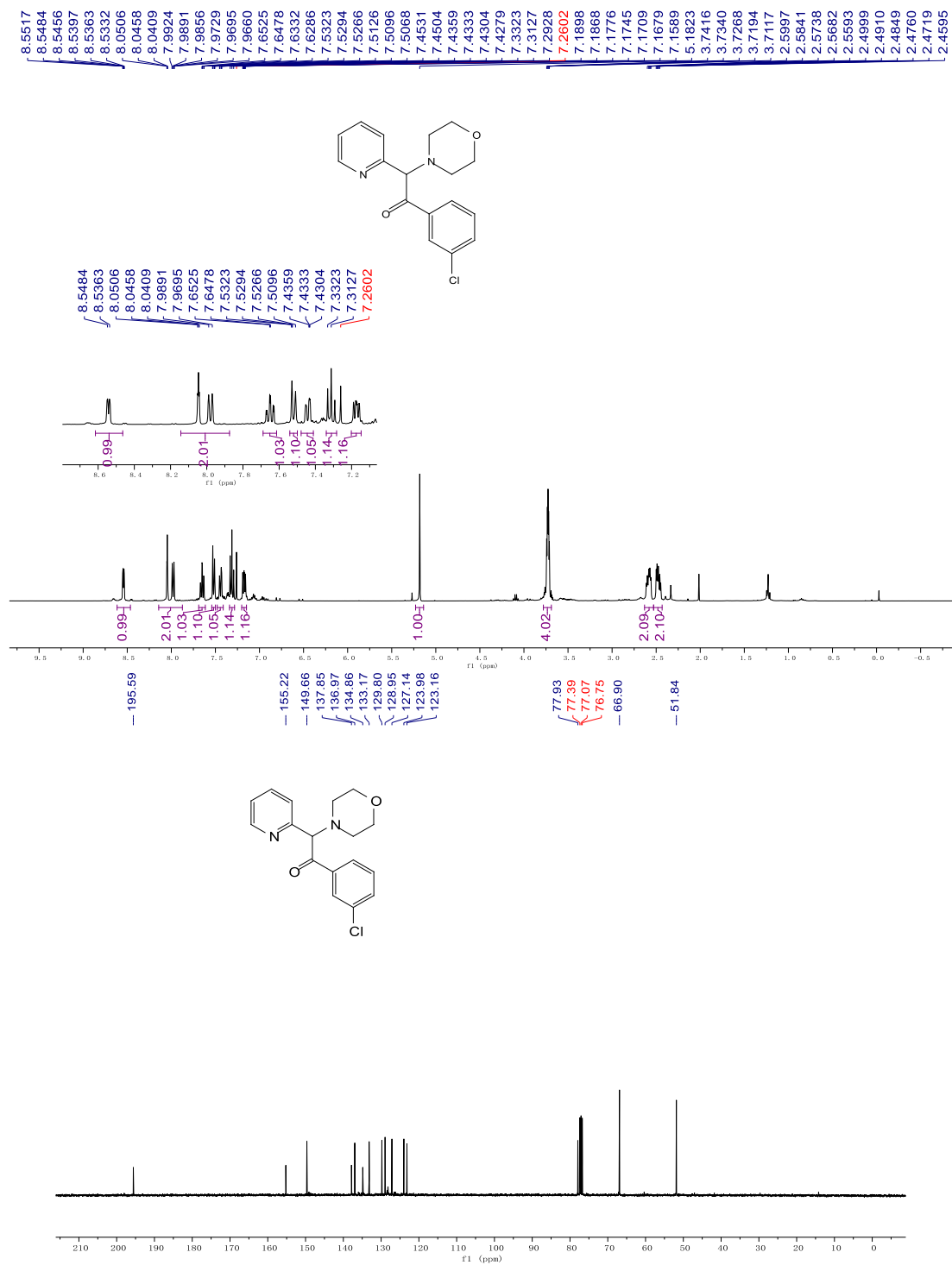
$^1\text{H}$  and  $^{13}\text{C}\{^1\text{H}\}$  NMR spectra of compound **3ak** in  $\text{CDCl}_3$



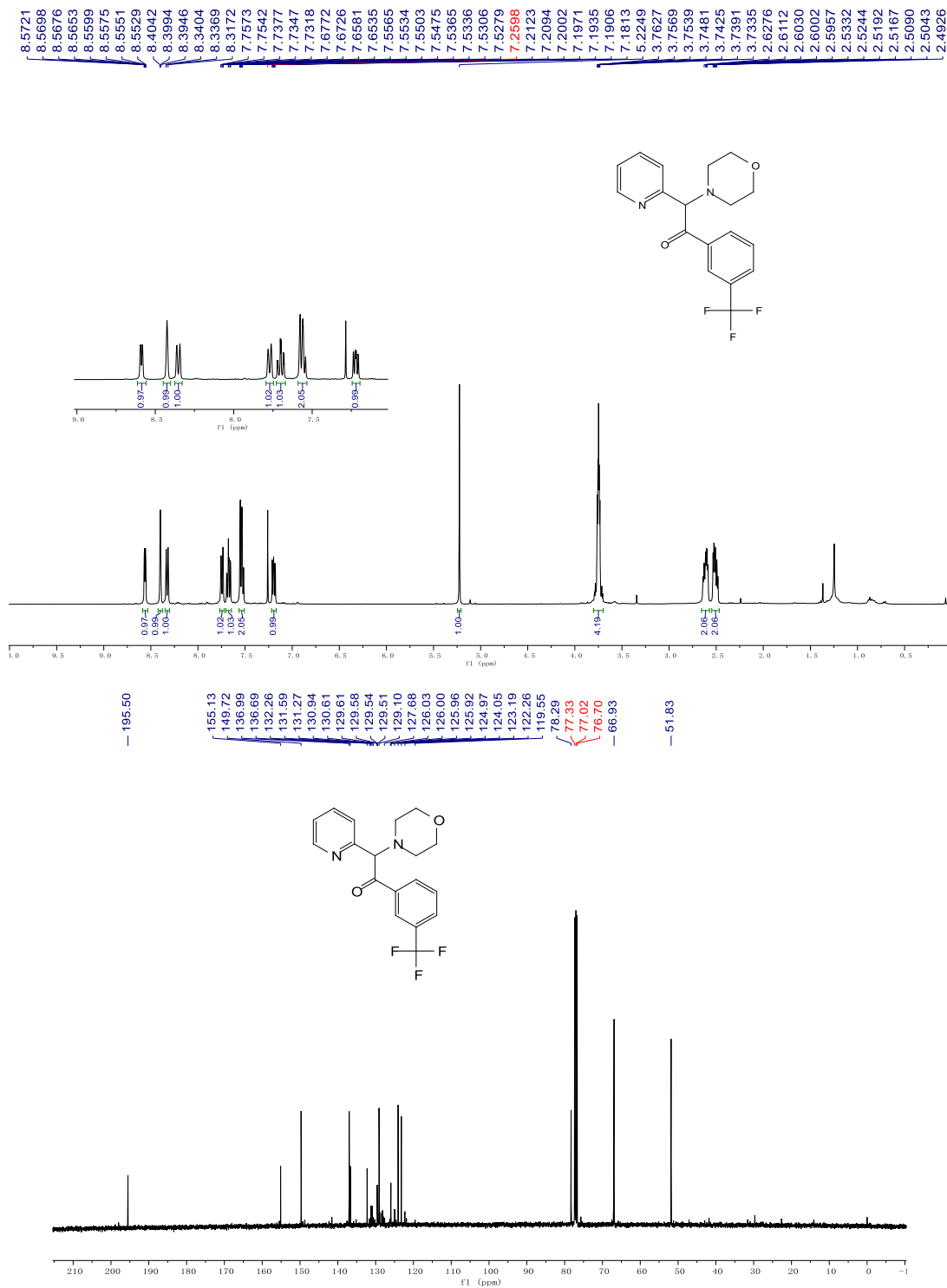
$^1\text{H}$  and  $^{13}\text{C}\{^1\text{H}\}$  NMR spectra of compound **3al** in  $\text{CDCl}_3$



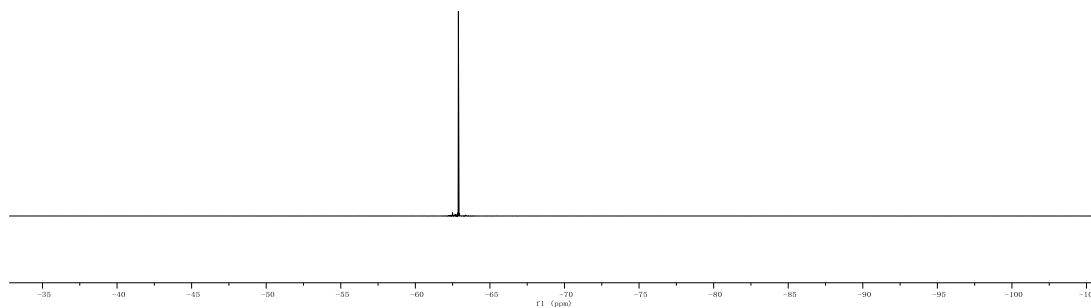
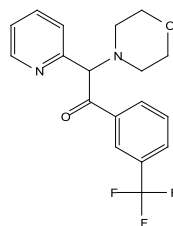
$^1\text{H}$  and  $^{13}\text{C}\{^1\text{H}\}$  NMR spectra of compound **3am** in  $\text{CDCl}_3$



$^1\text{H}$ ,  $^{13}\text{C}\{^1\text{H}\}$  and  $^{19}\text{F}$  NMR spectra of compound **3an** in  $\text{CDCl}_3$

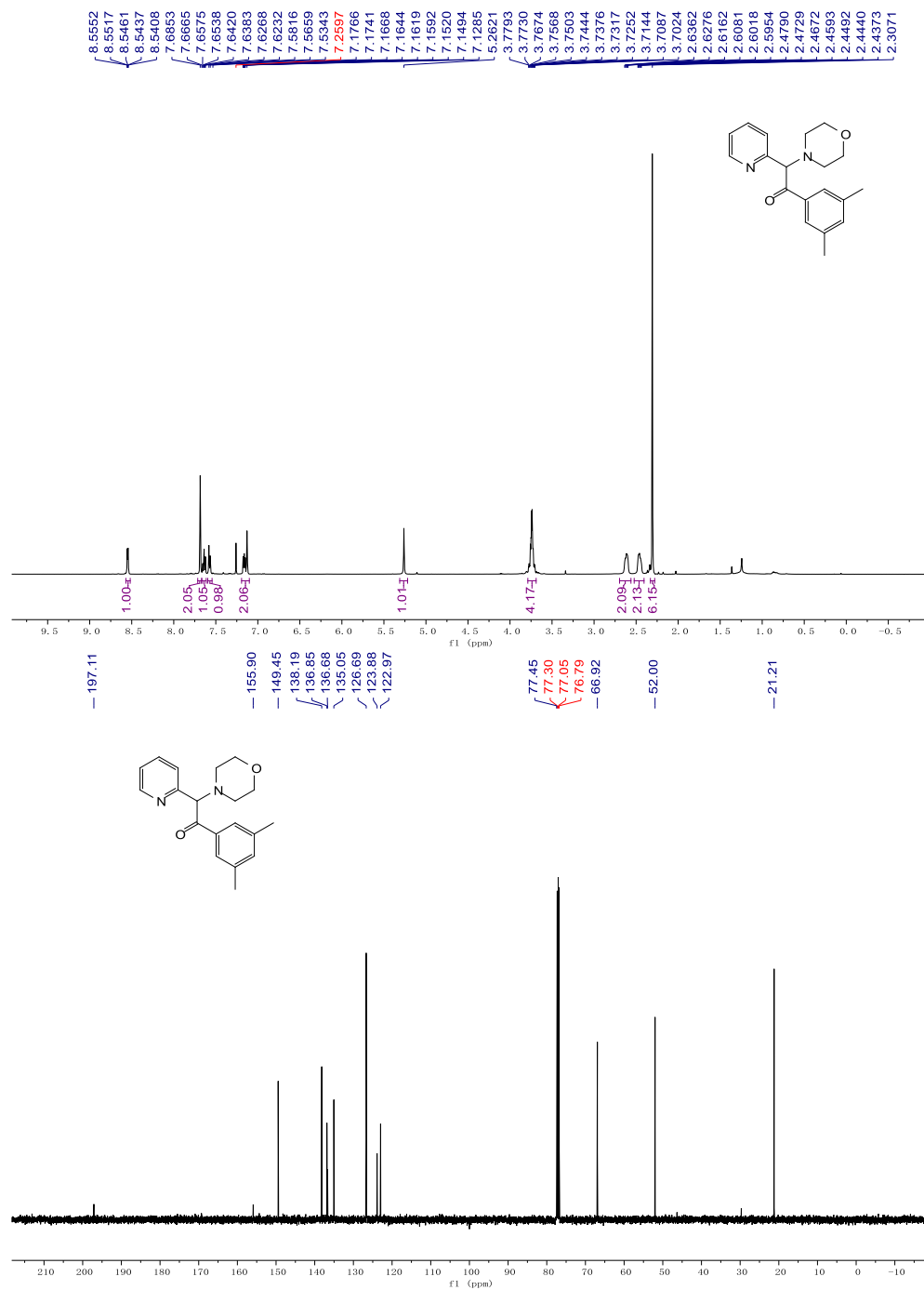


-62.89

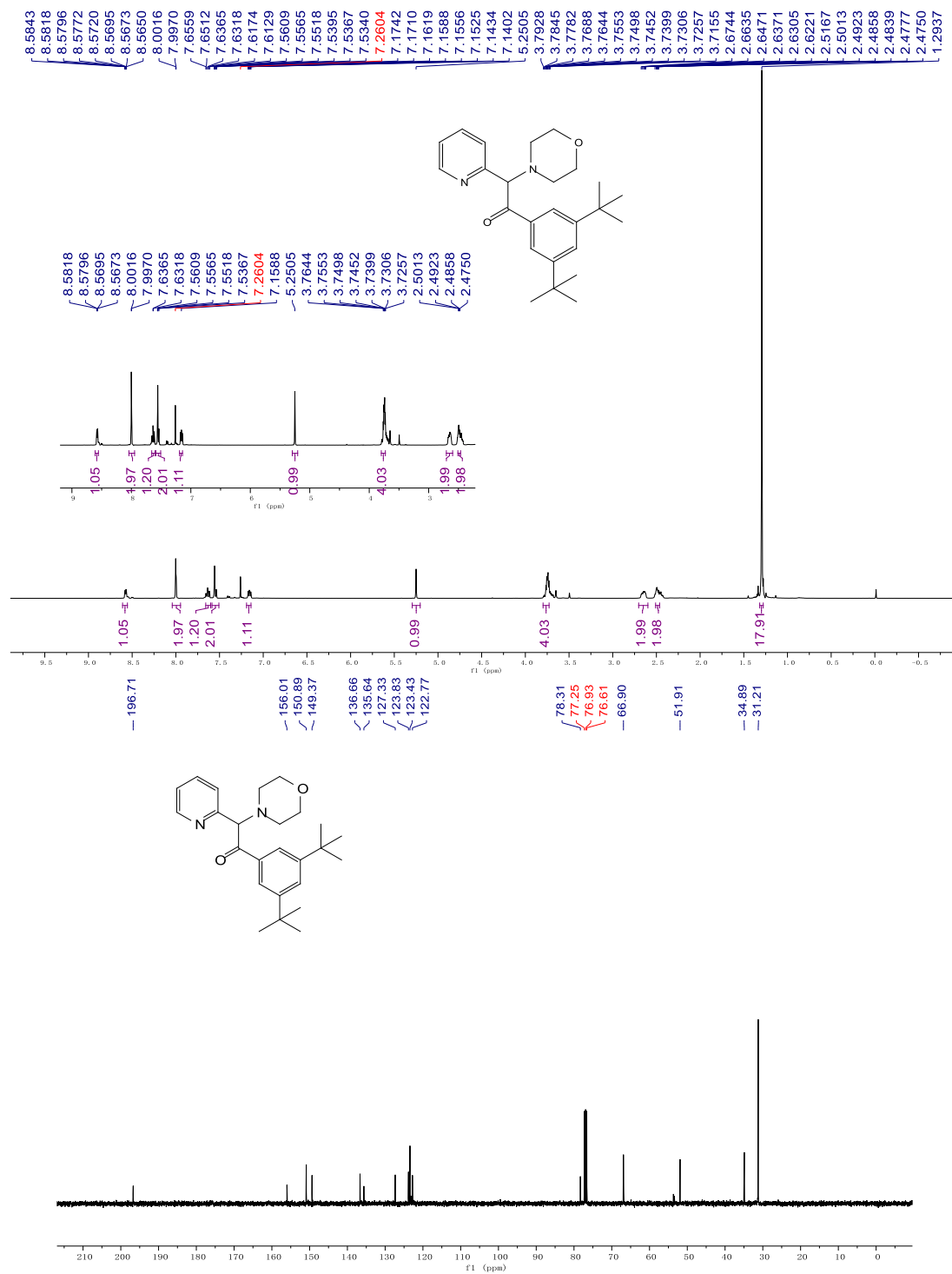




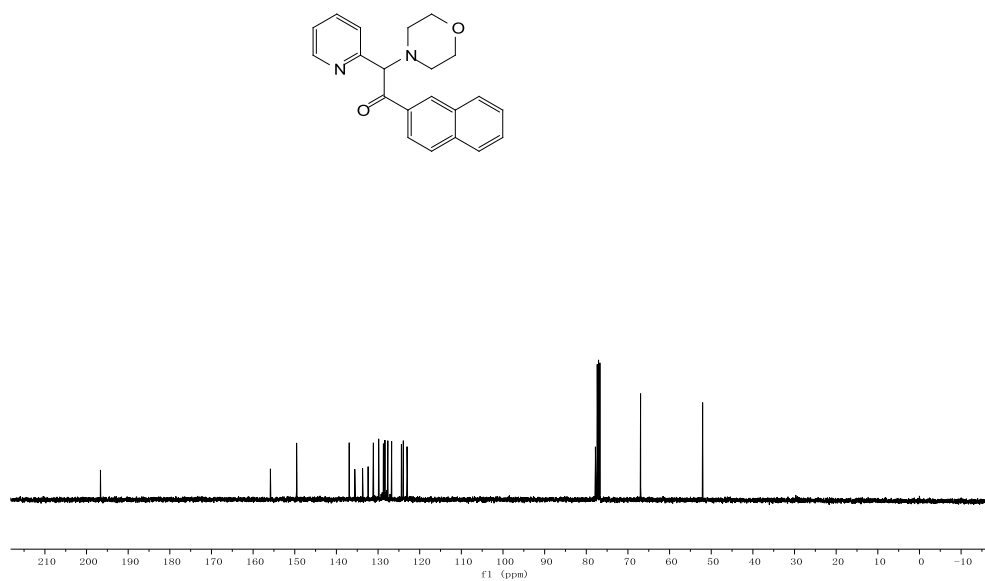
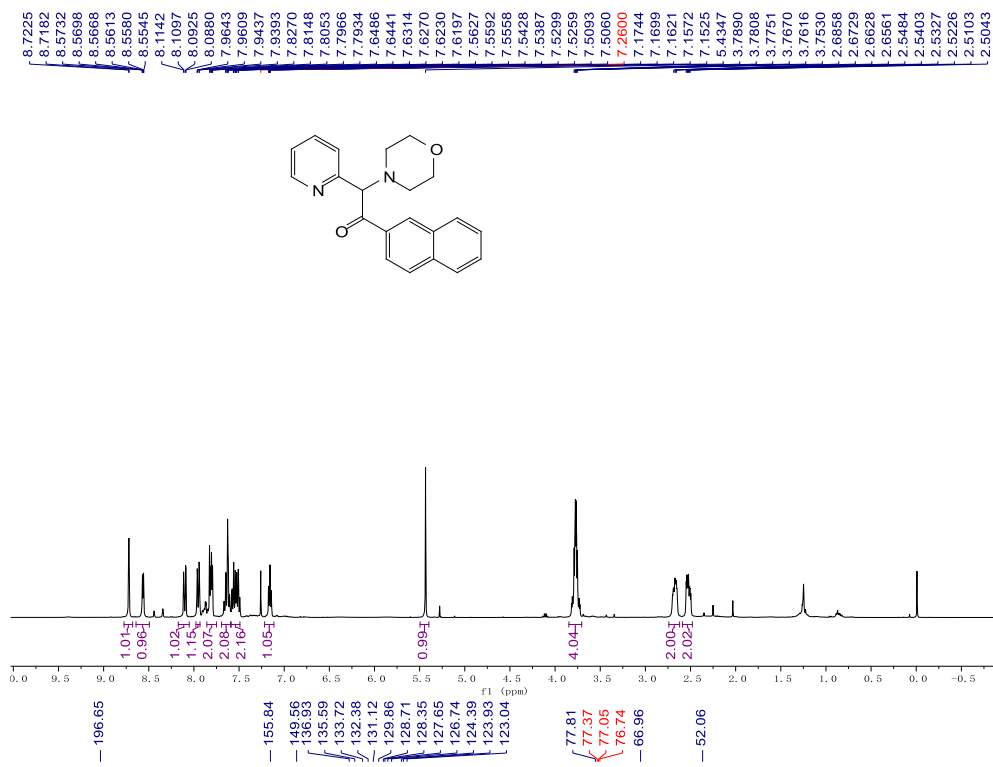
$^1\text{H}$  and  $^{13}\text{C}\{^1\text{H}\}$  NMR spectra of compound **3ao** in  $\text{CDCl}_3$



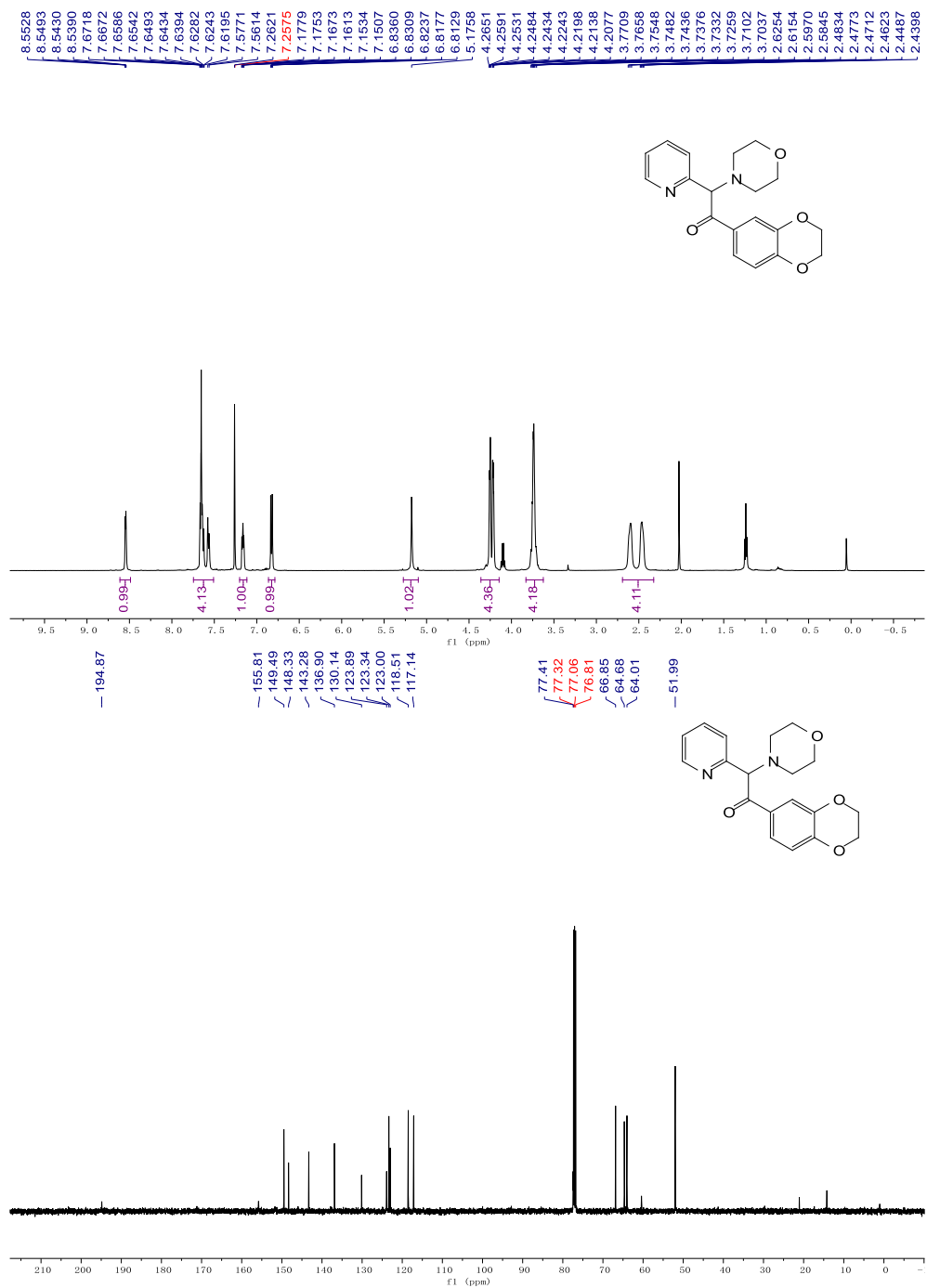
$^1\text{H}$  and  $^{13}\text{C}\{^1\text{H}\}$  NMR spectra of compound **3ap** in  $\text{CDCl}_3$



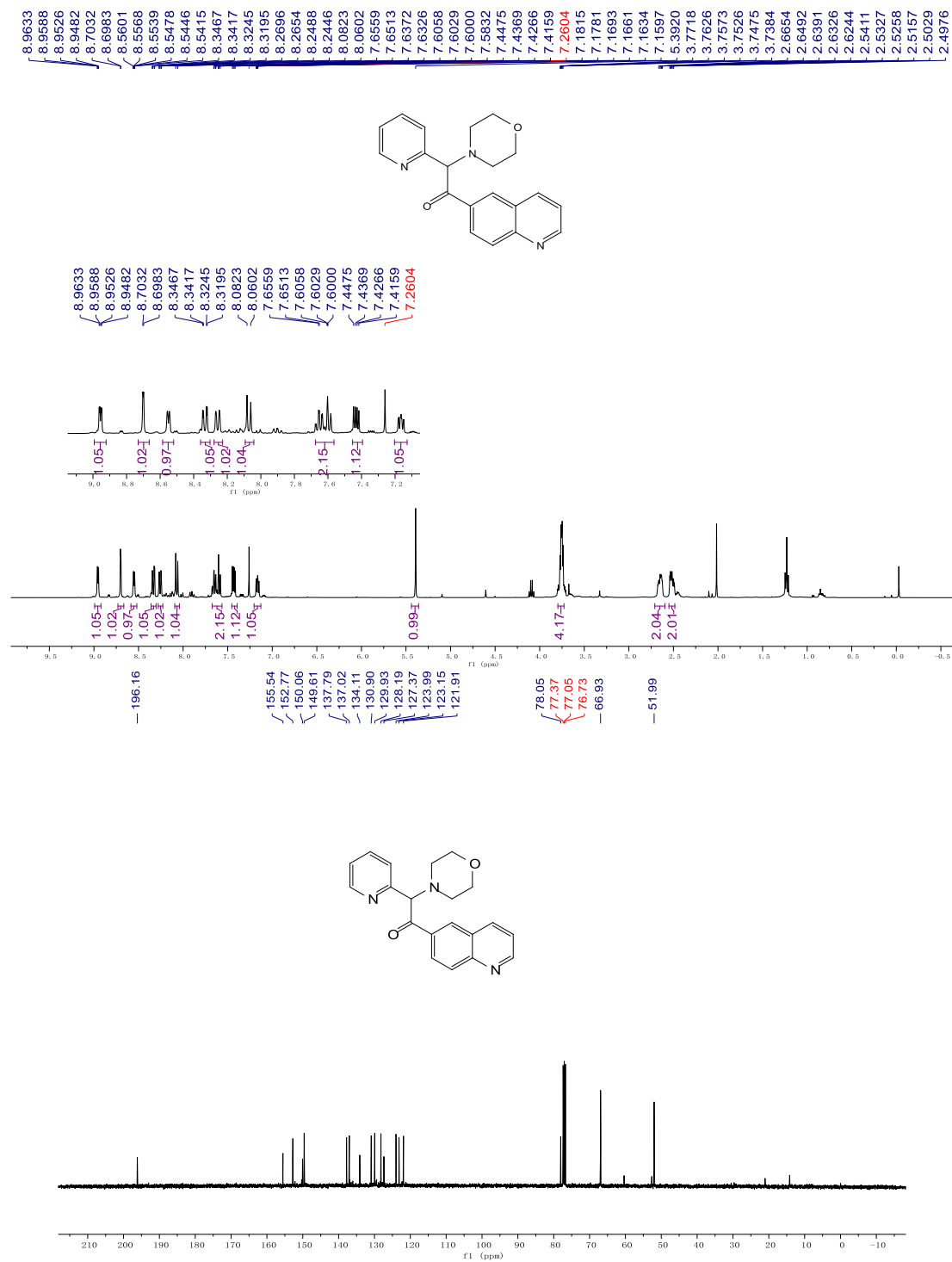
$^1\text{H}$  and  $^{13}\text{C}\{^1\text{H}\}$  NMR spectra of compound **3aq** in  $\text{CDCl}_3$



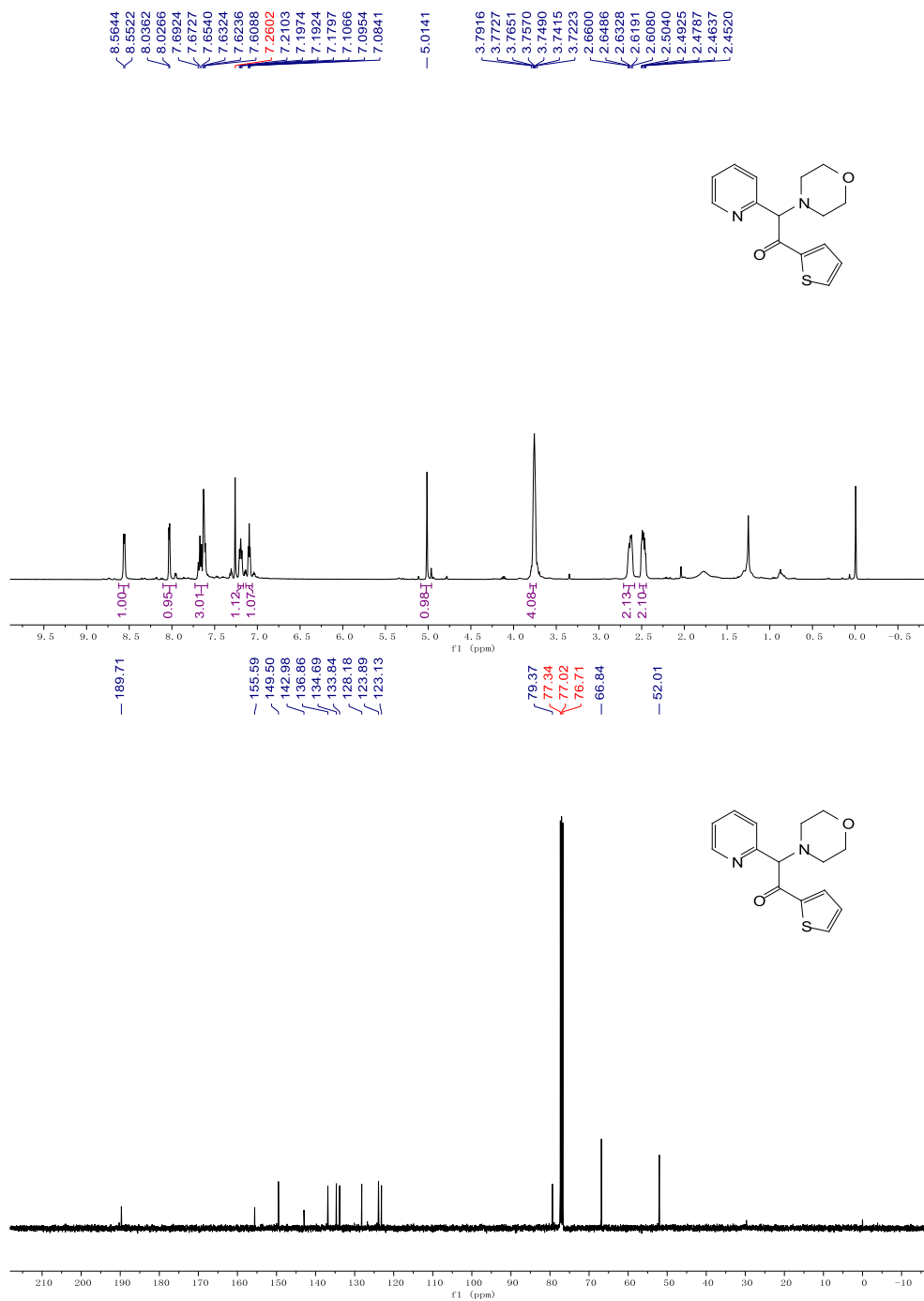
$^1\text{H}$  and  $^{13}\text{C}\{^1\text{H}\}$  NMR spectra of compound **3ar** in  $\text{CDCl}_3$



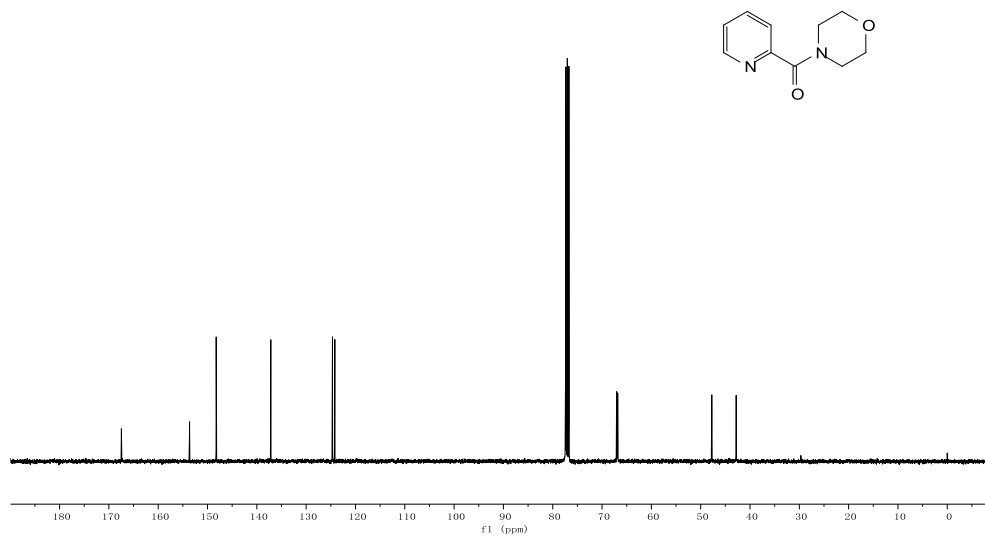
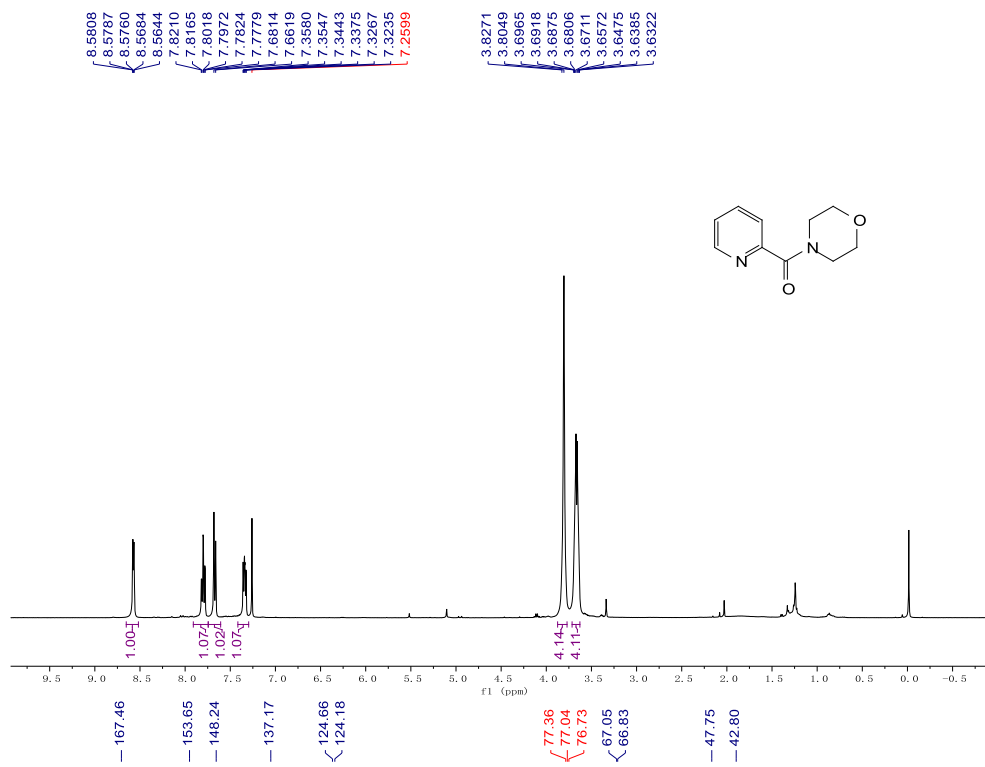
$^1\text{H}$  and  $^{13}\text{C}\{^1\text{H}\}$  NMR spectra of compound **3as** in  $\text{CDCl}_3$



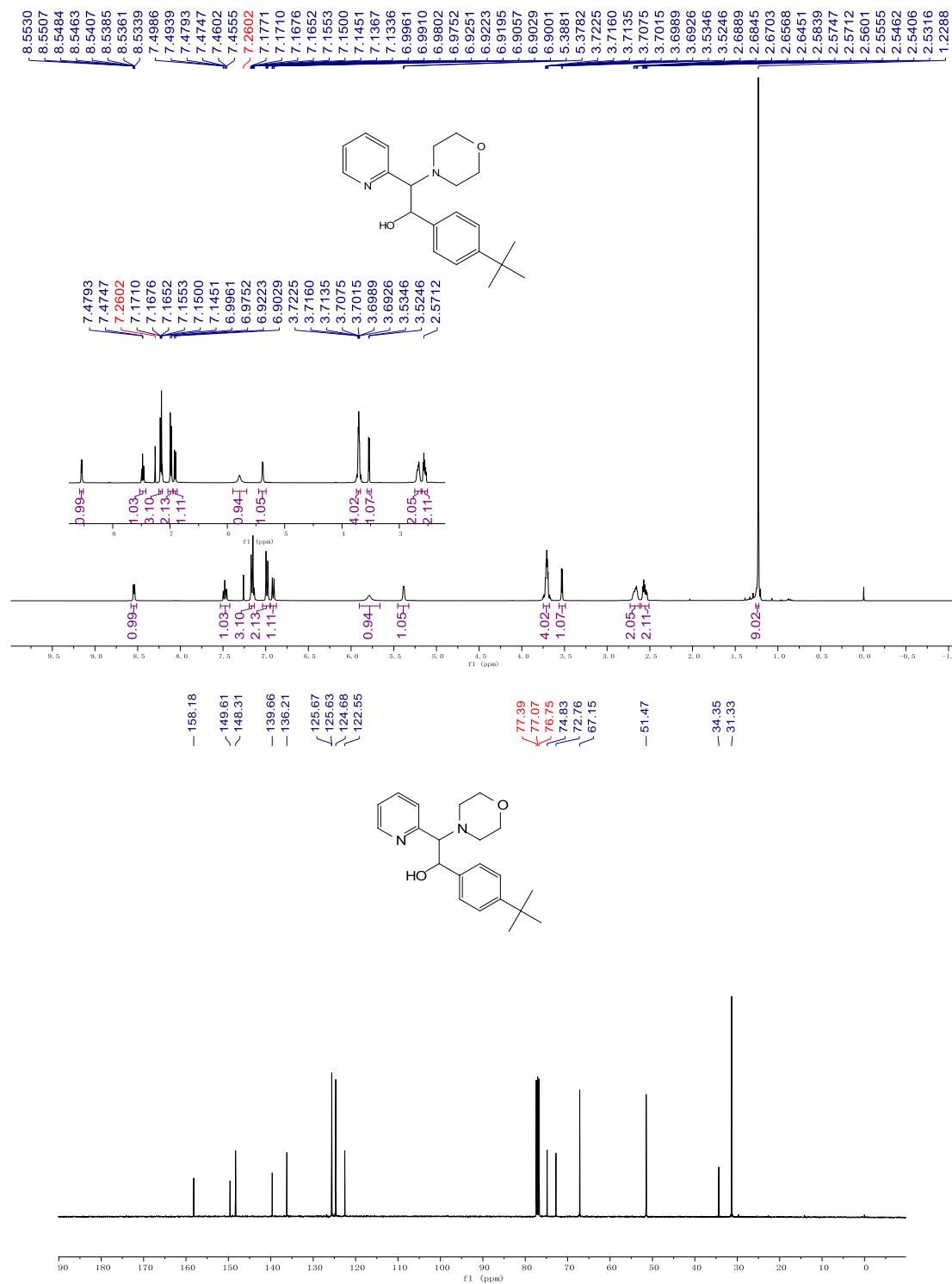
$^1\text{H}$  and  $^{13}\text{C}\{^1\text{H}\}$  NMR spectra of compound **3at** in  $\text{CDCl}_3$



$^1\text{H}$  and  $^{13}\text{C}\{^1\text{H}\}$  NMR spectra of compound **4** in  $\text{CDCl}_3$

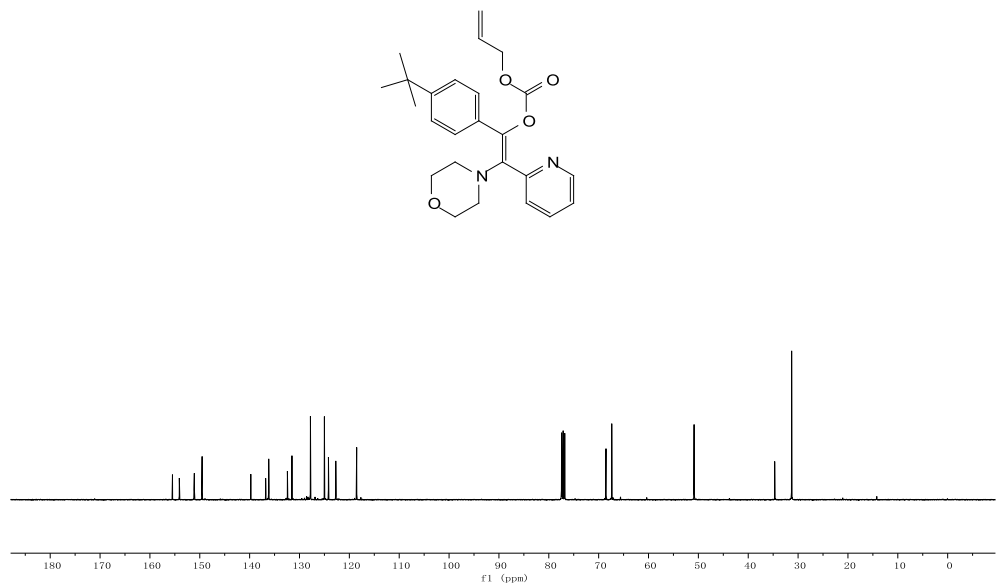
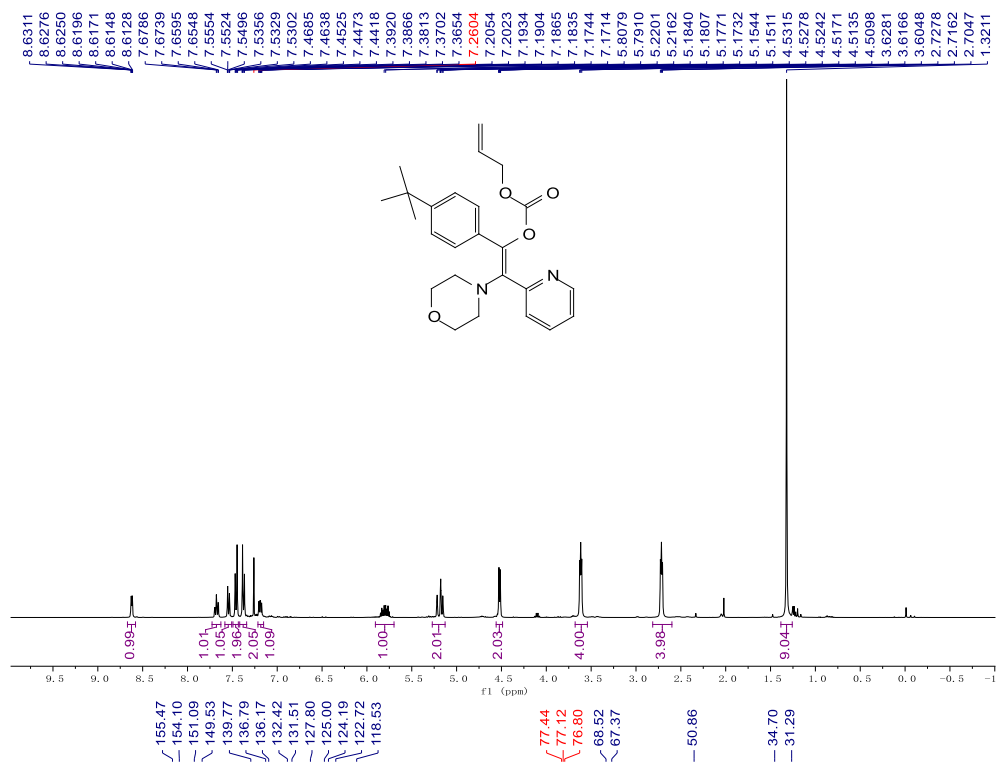


$^1\text{H}$  and  $^{13}\text{C}\{^1\text{H}\}$  NMR spectra of compound **5** in  $\text{CDCl}_3$

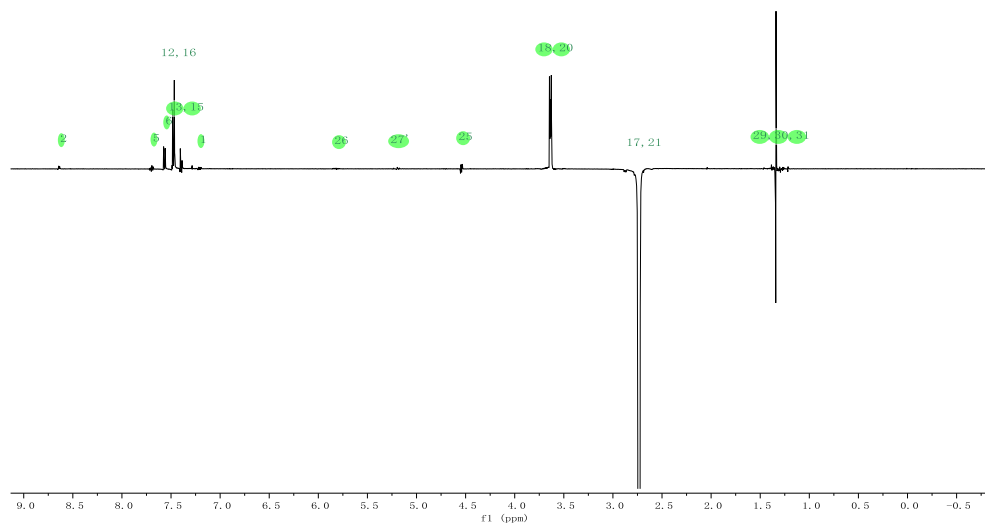
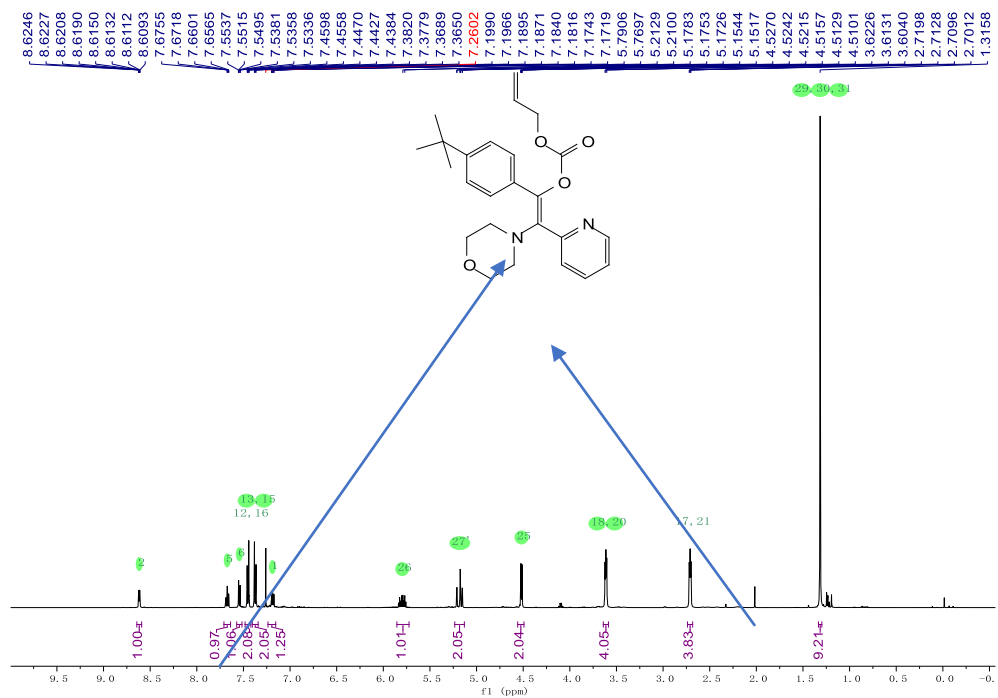




$^1\text{H}$  and  $^{13}\text{C}\{^1\text{H}\}$  NMR spectra of compound **6** in  $\text{CDCl}_3$



1D-NOESY <sup>1</sup>H NMR spectra of compound **6** in CDCl<sub>3</sub>

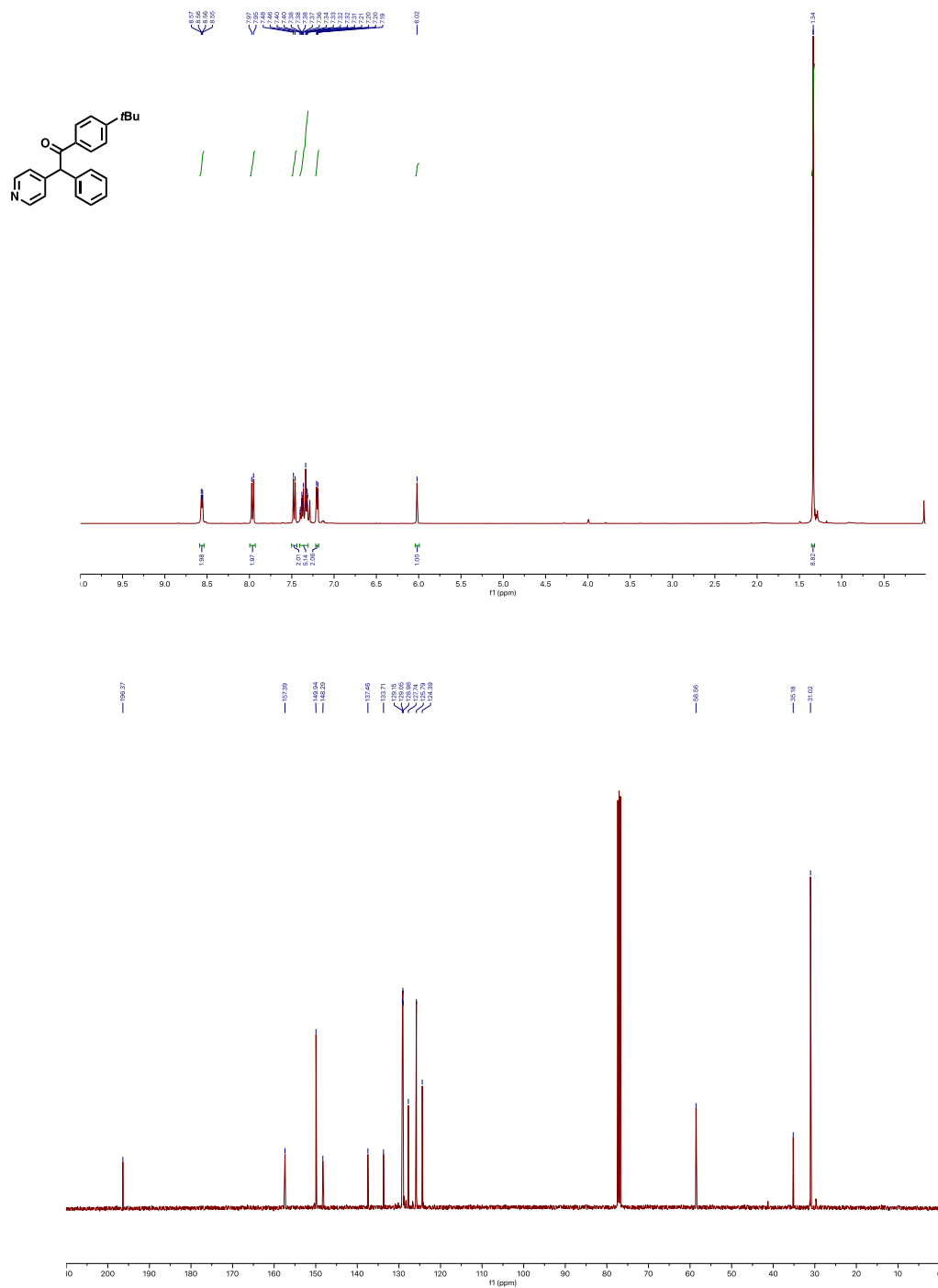




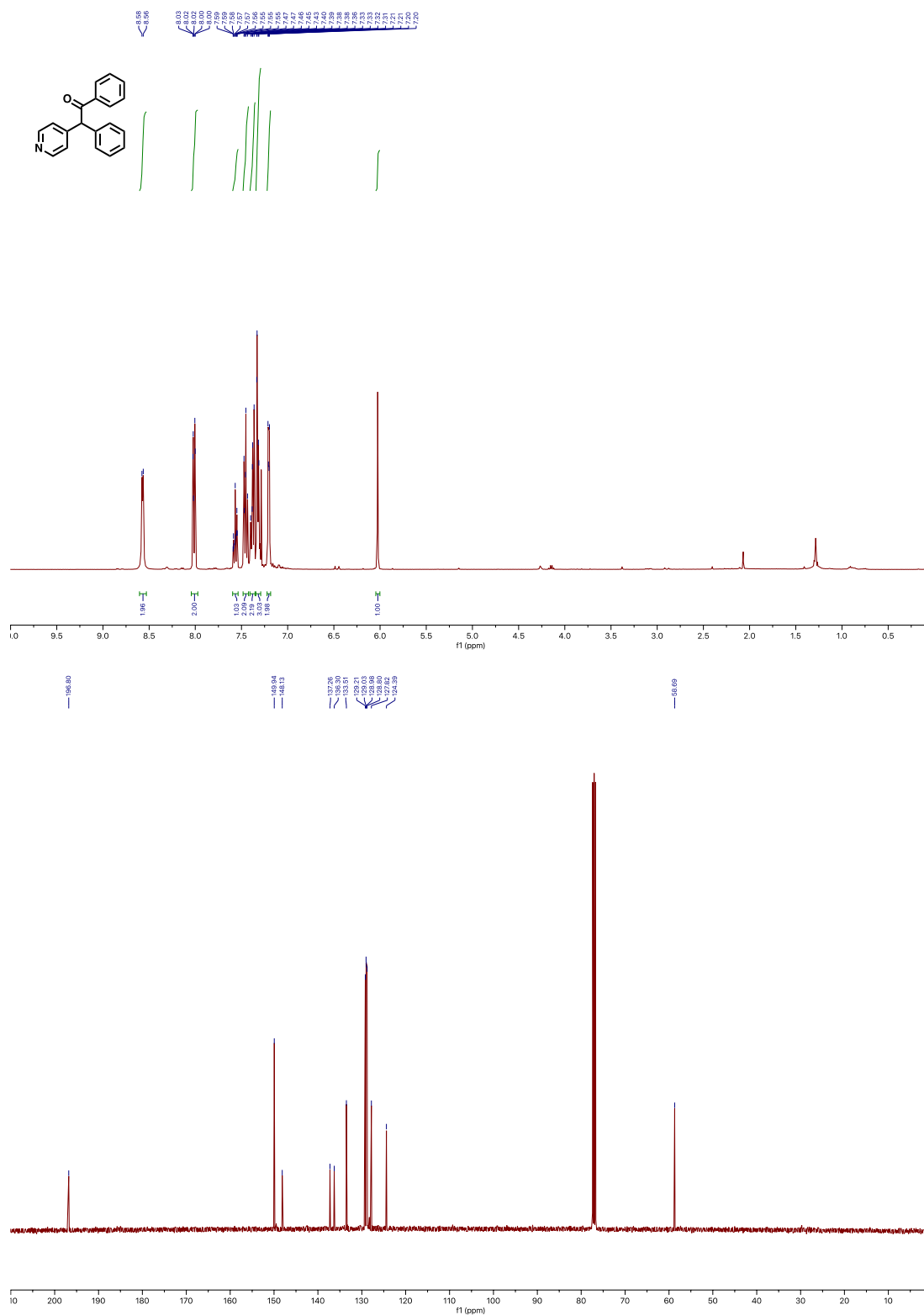
## Appendix B NMR Spectra, IR Spectra and X-Ray Crystallographic Data for Chapter 3

### NMR Spectra

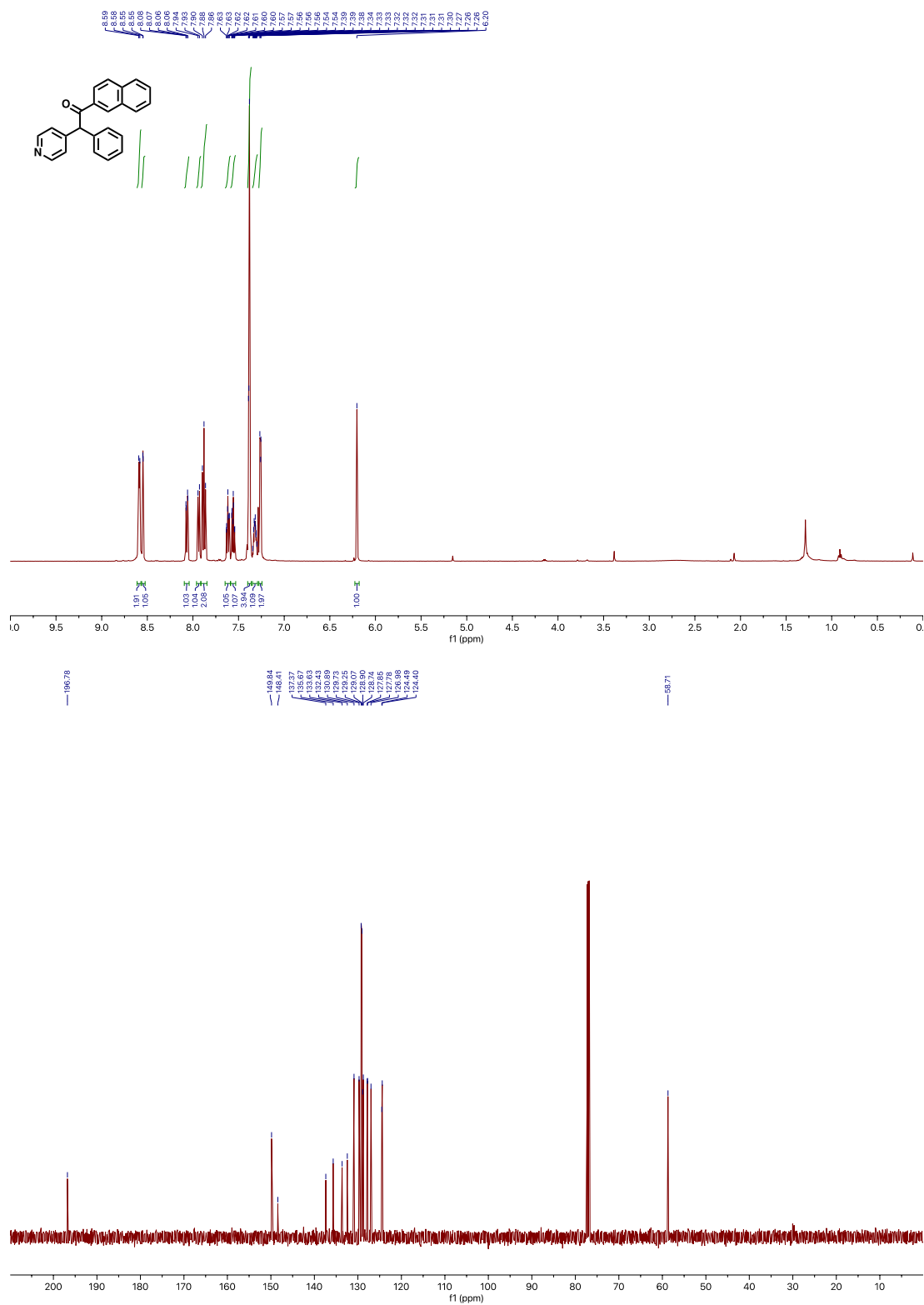
$^1\text{H}$  and  $^{13}\text{C}\{^1\text{H}\}$  NMR spectra of compound **3aa** in  $\text{CDCl}_3$



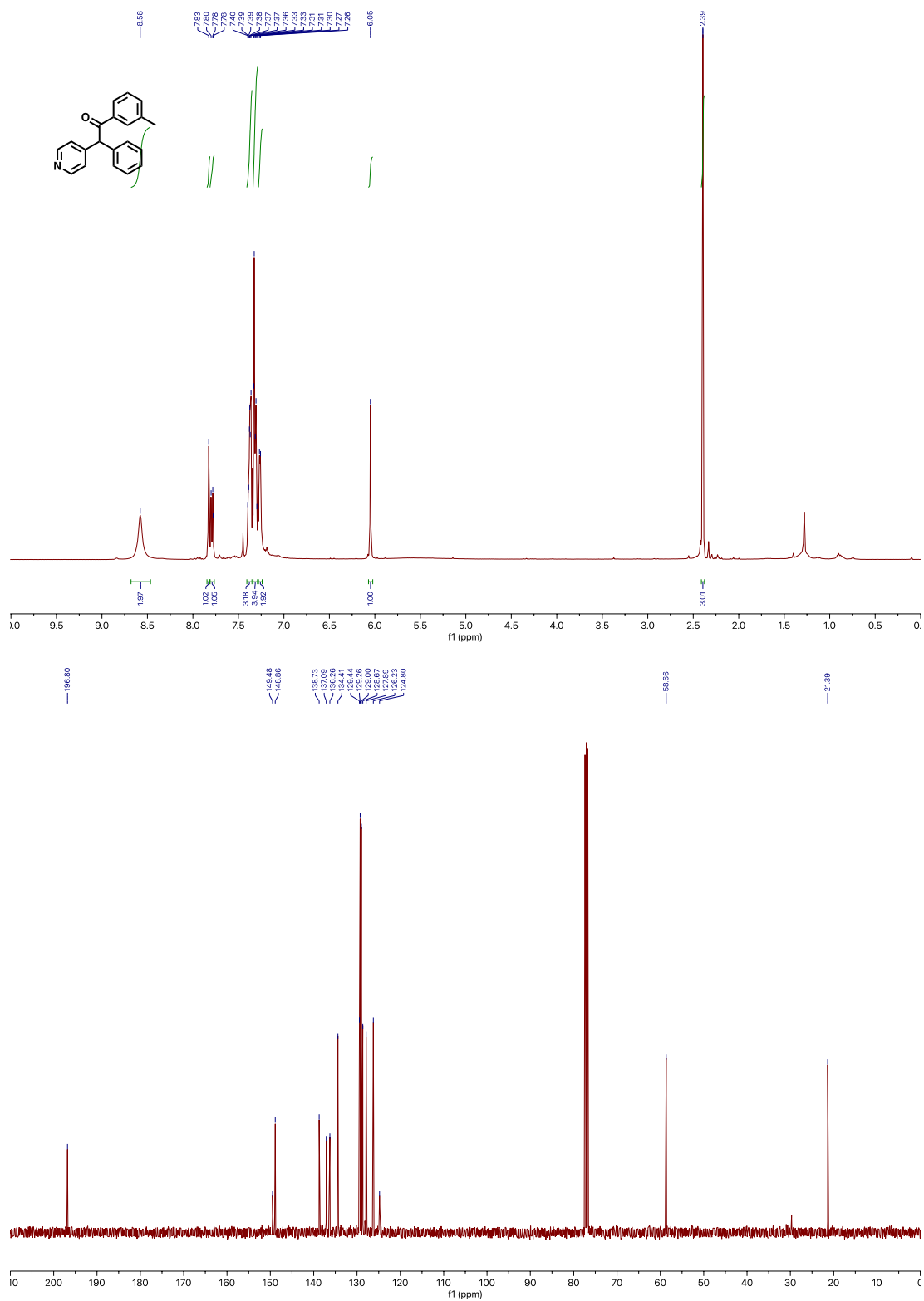
$^1\text{H}$  and  $^{13}\text{C}\{^1\text{H}\}$  NMR spectra of compound **3ab** in  $\text{CDCl}_3$



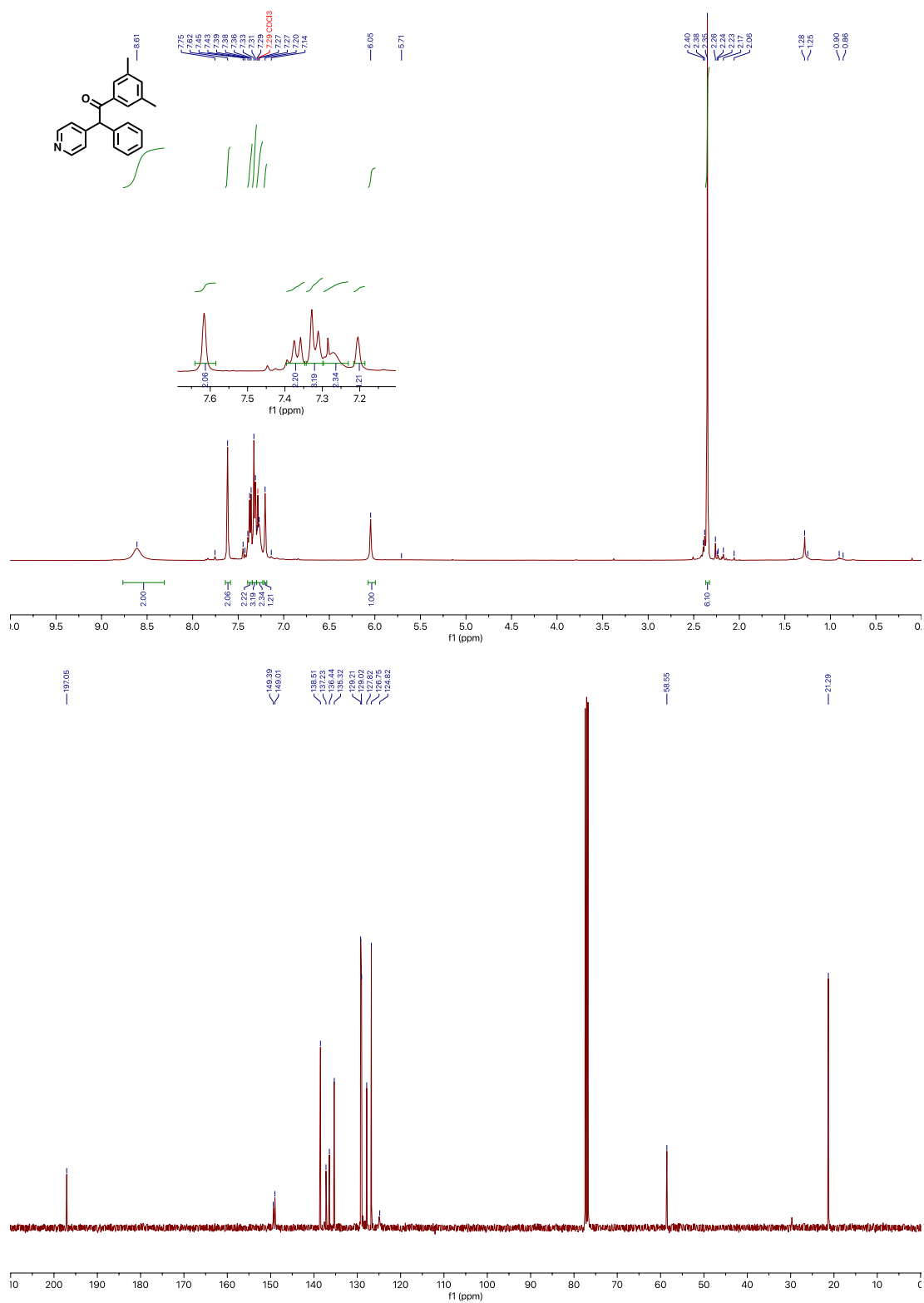
$^1\text{H}$  and  $^{13}\text{C}\{^1\text{H}\}$  NMR spectra of compound **3ac** in  $\text{CDCl}_3$



$^1\text{H}$  and  $^{13}\text{C}\{^1\text{H}\}$  NMR spectra of compound **3ad** in  $\text{CDCl}_3$

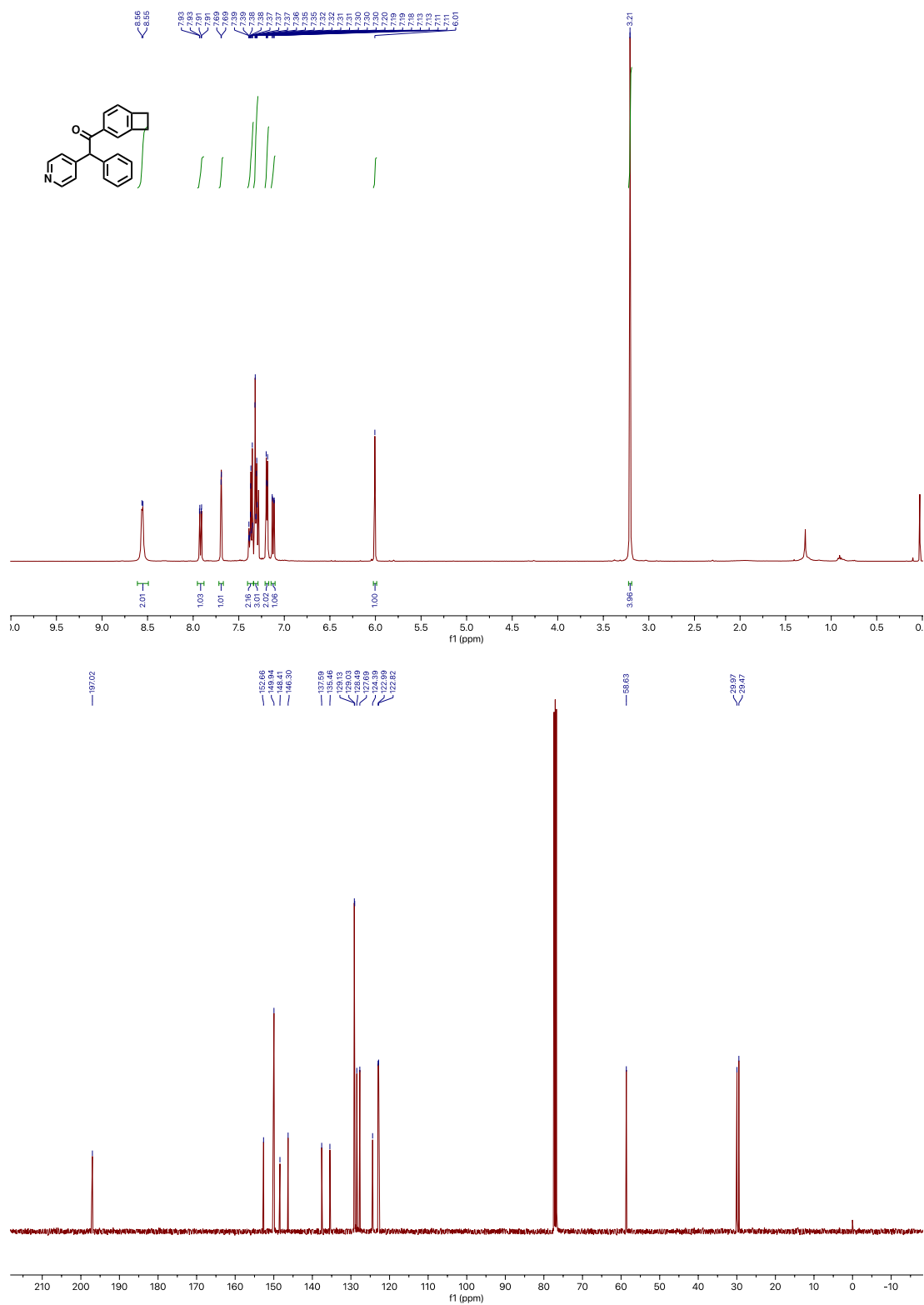


$^1\text{H}$  and  $^{13}\text{C}\{^1\text{H}\}$  NMR spectra of compound **3ae** in  $\text{CDCl}_3$

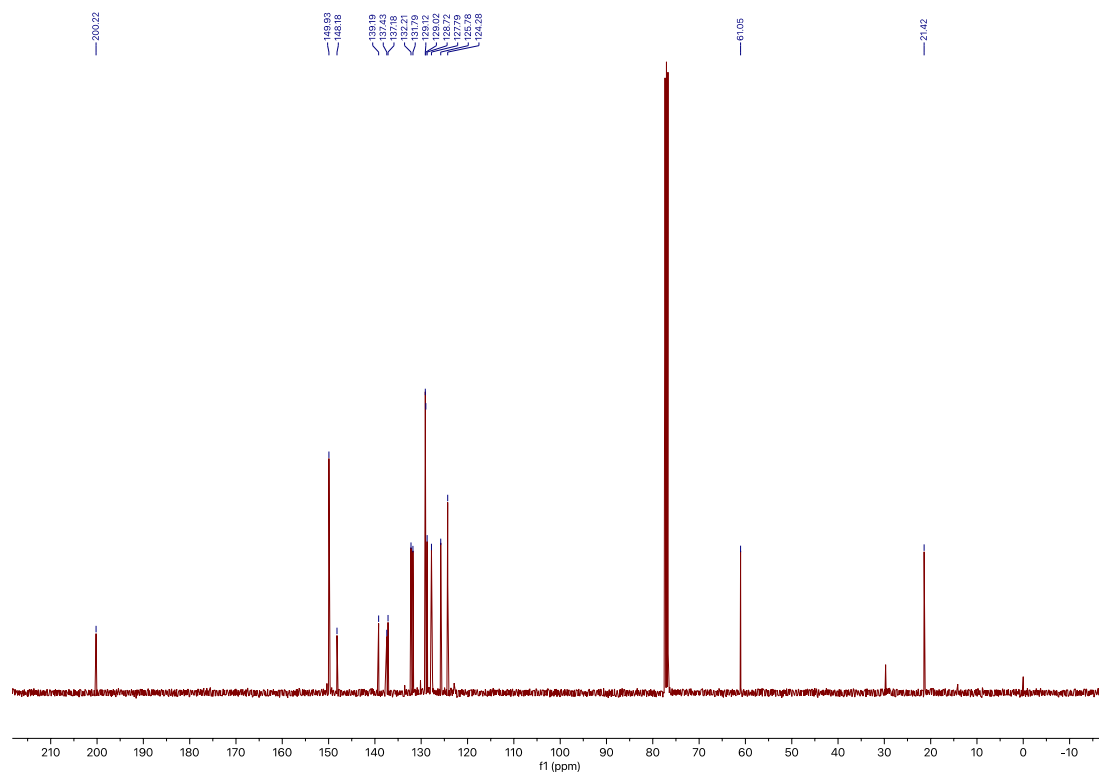
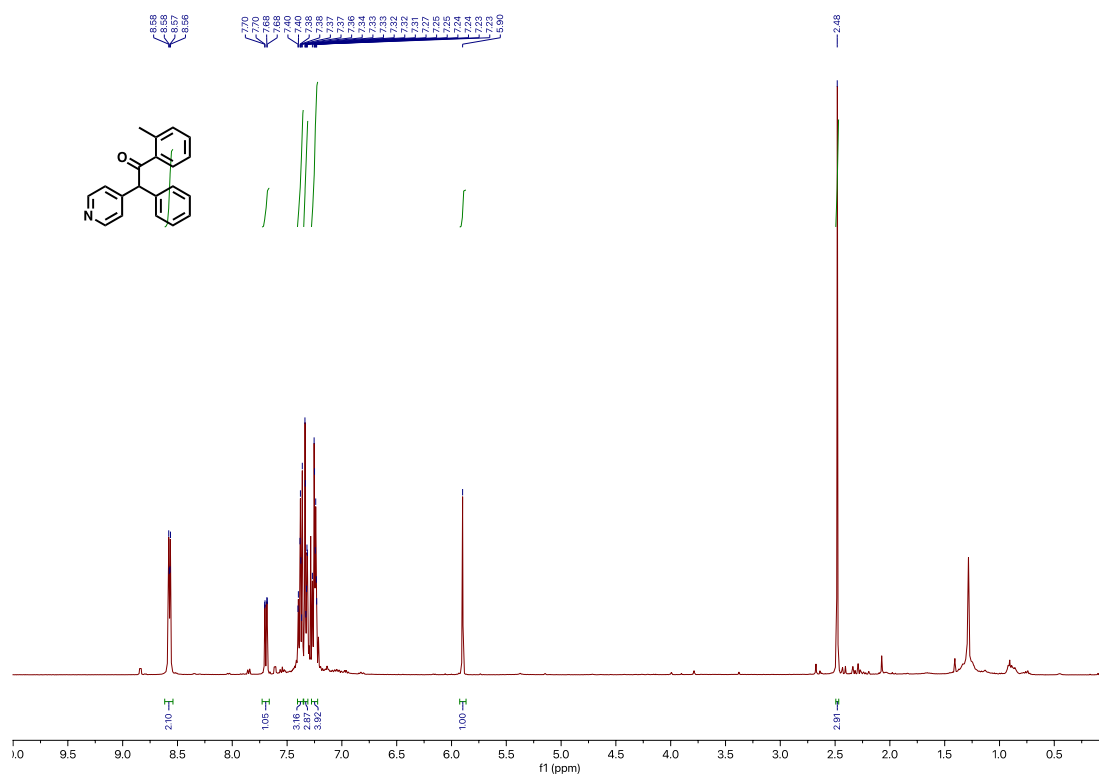




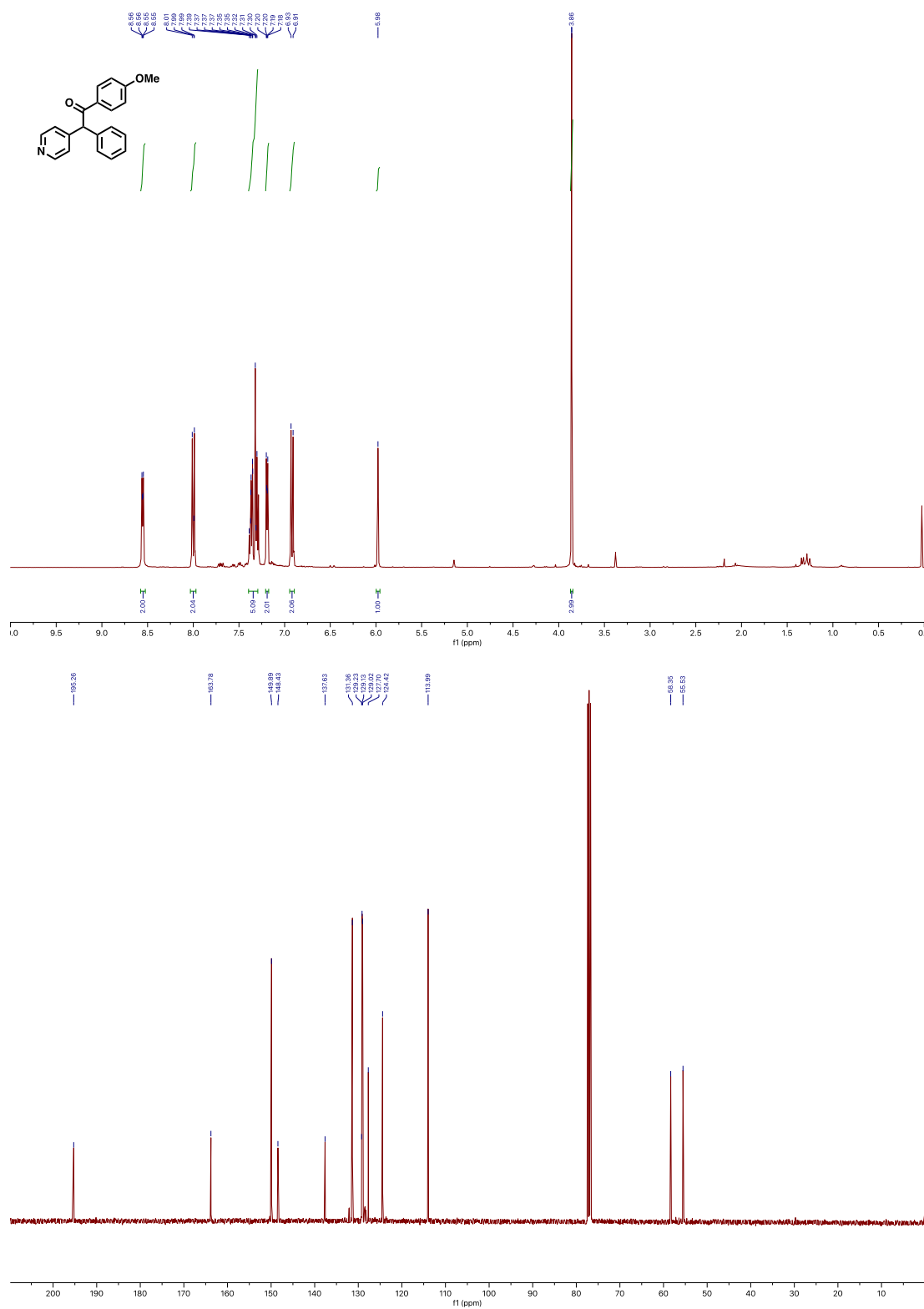
$^1\text{H}$  and  $^{13}\text{C}\{^1\text{H}\}$  NMR spectra of compound **3af** in  $\text{CDCl}_3$



$^1\text{H}$  and  $^{13}\text{C}\{^1\text{H}\}$  NMR spectra of compound **3ag** in  $\text{CDCl}_3$

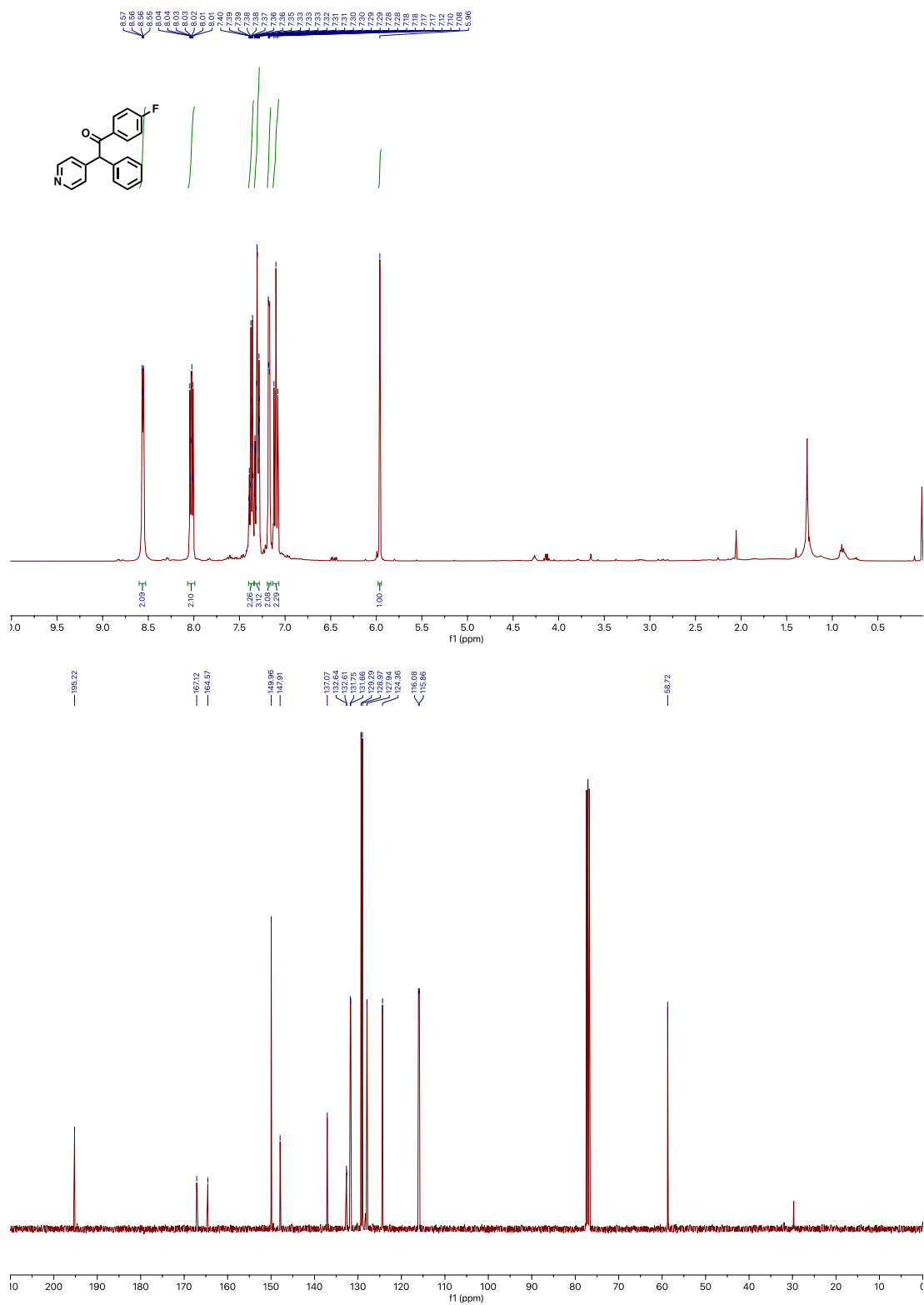


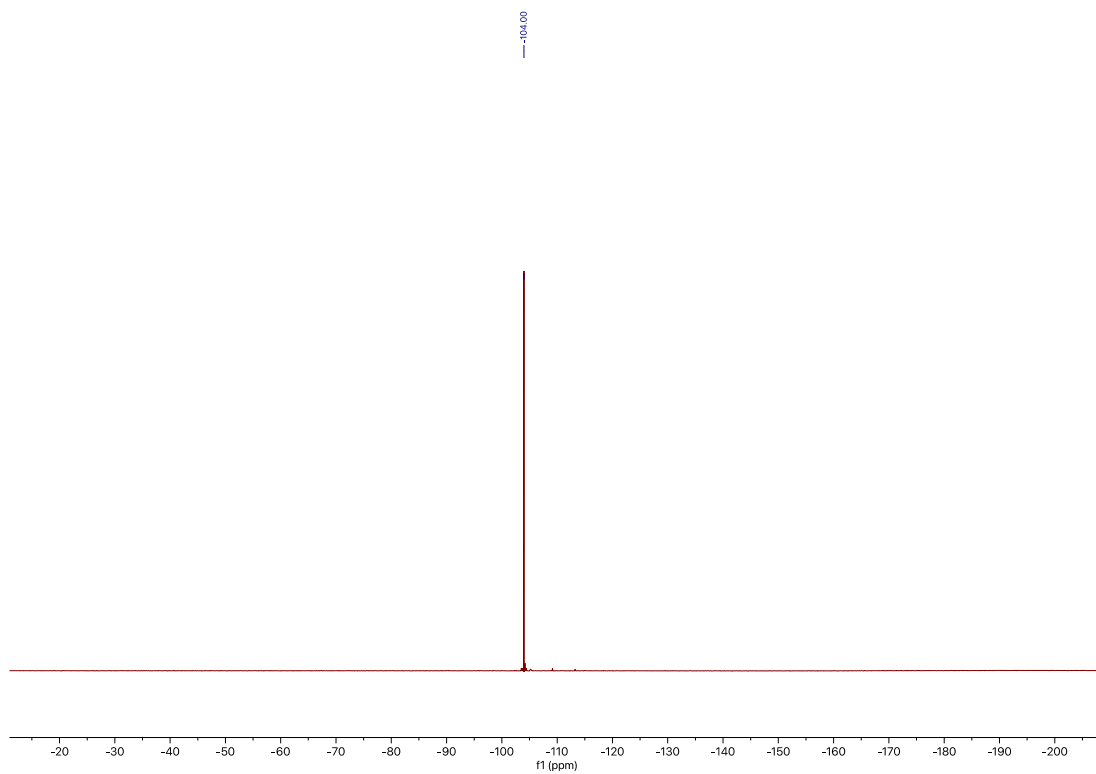
$^1\text{H}$  and  $^{13}\text{C}\{^1\text{H}\}$  NMR spectra of compound **3ah** in  $\text{CDCl}_3$



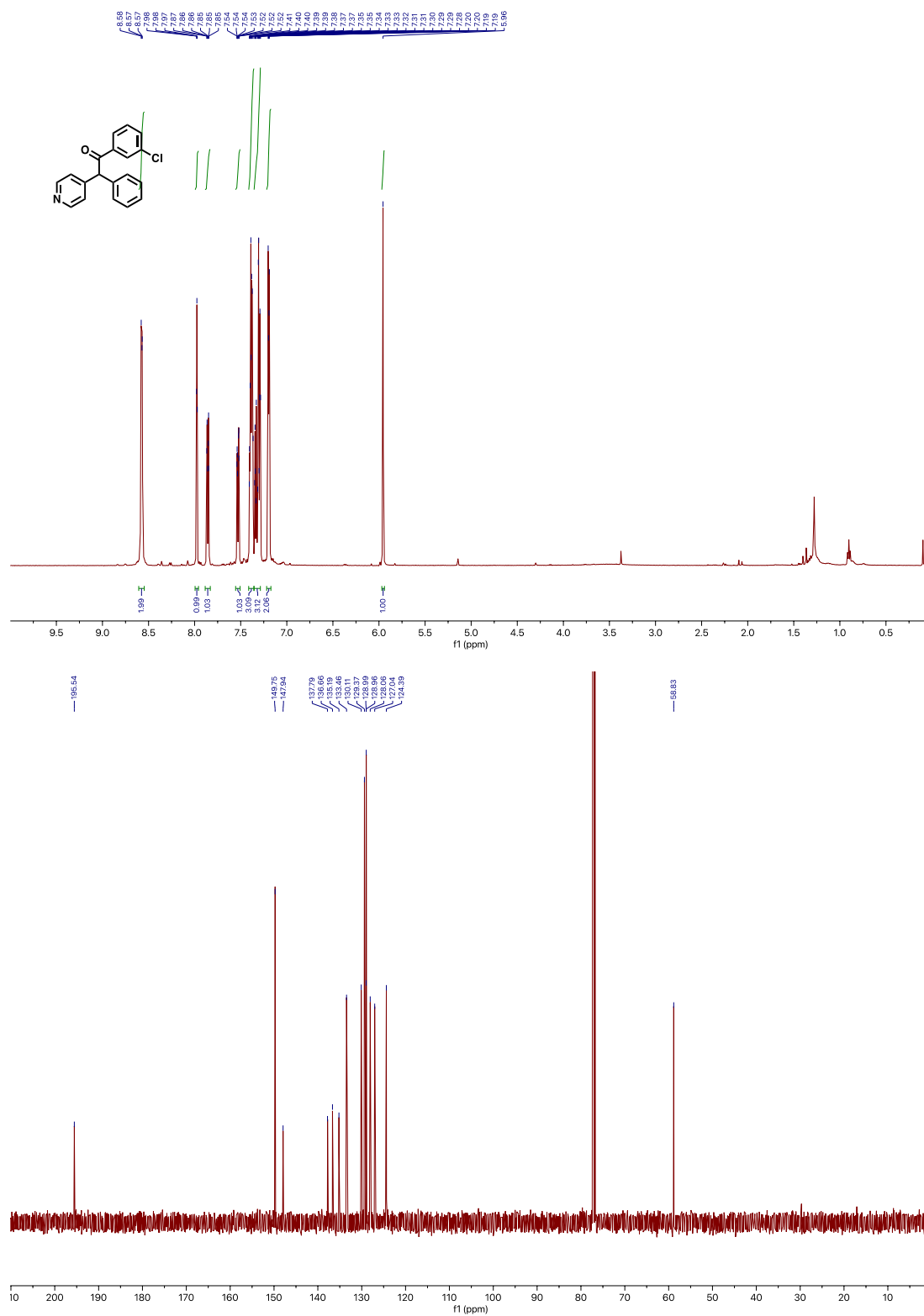


$^1\text{H}$ ,  $^{13}\text{C}\{^1\text{H}\}$  and  $^{19}\text{F}$  NMR spectra of compound **3aj** in  $\text{CDCl}_3$



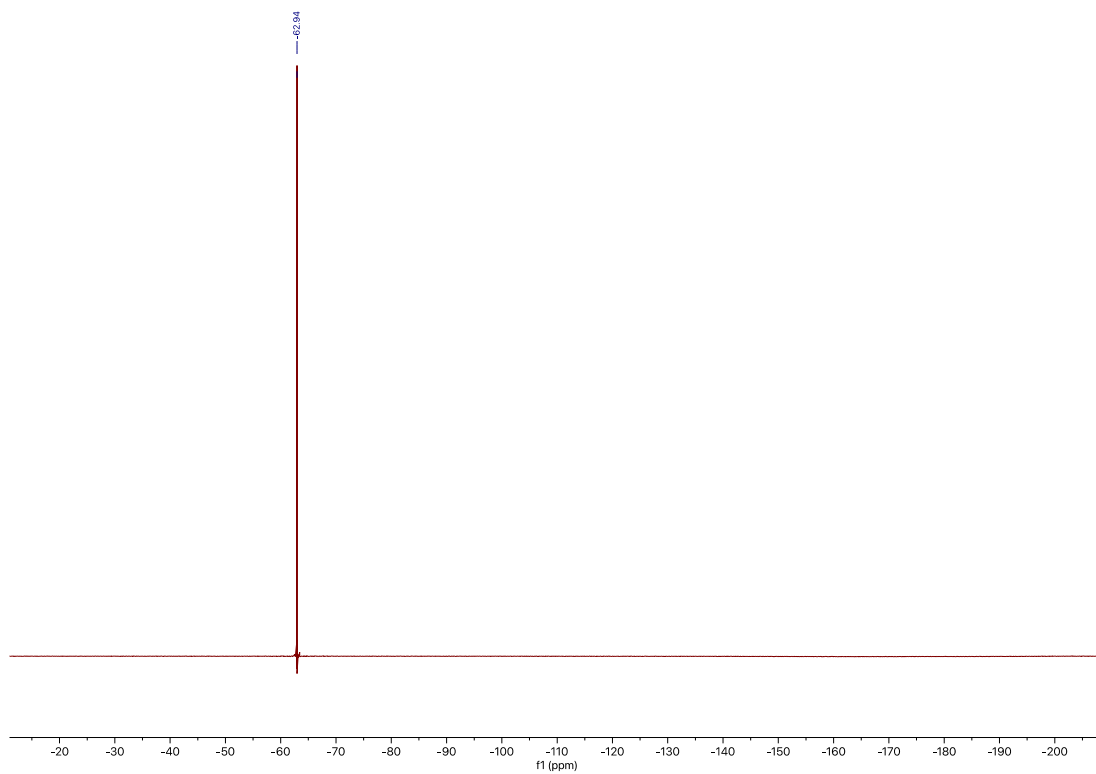


$^1\text{H}$  and  $^{13}\text{C}\{^1\text{H}\}$  NMR spectra of compound **3ak** in  $\text{CDCl}_3$

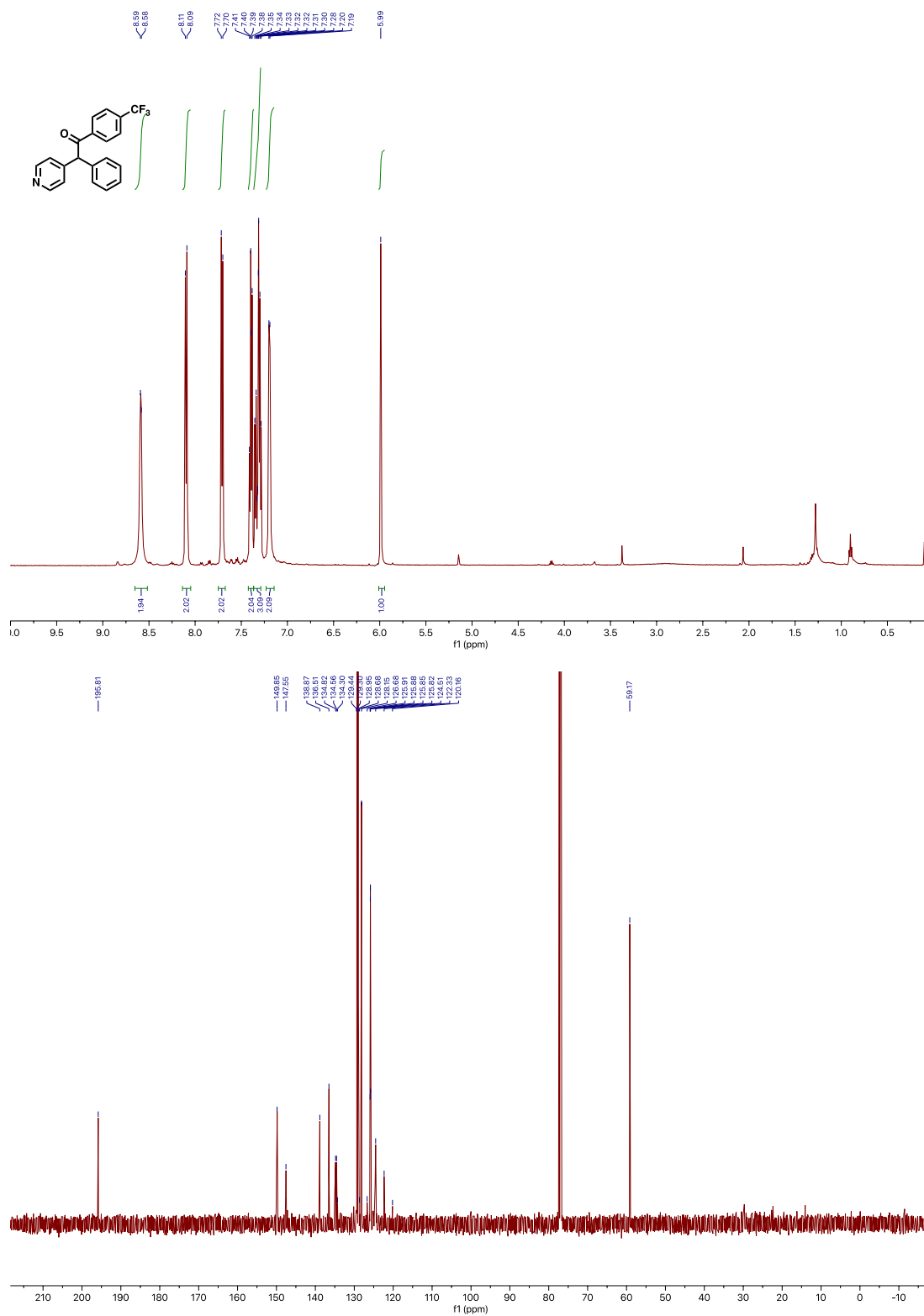


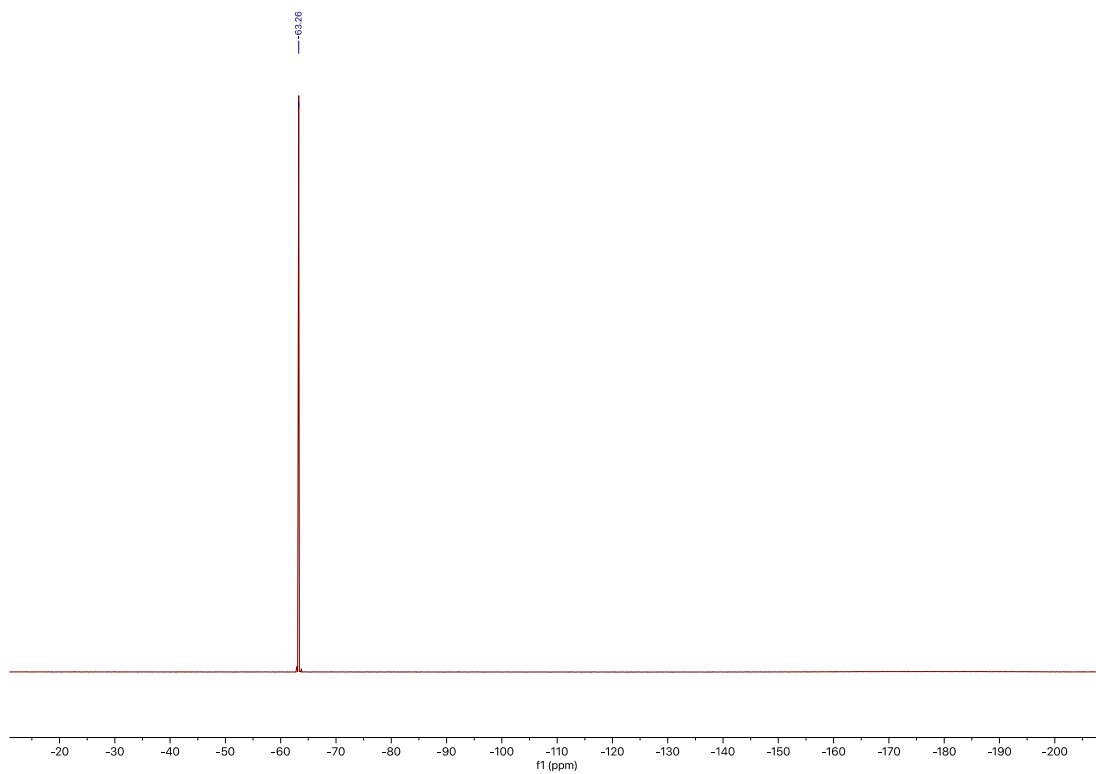




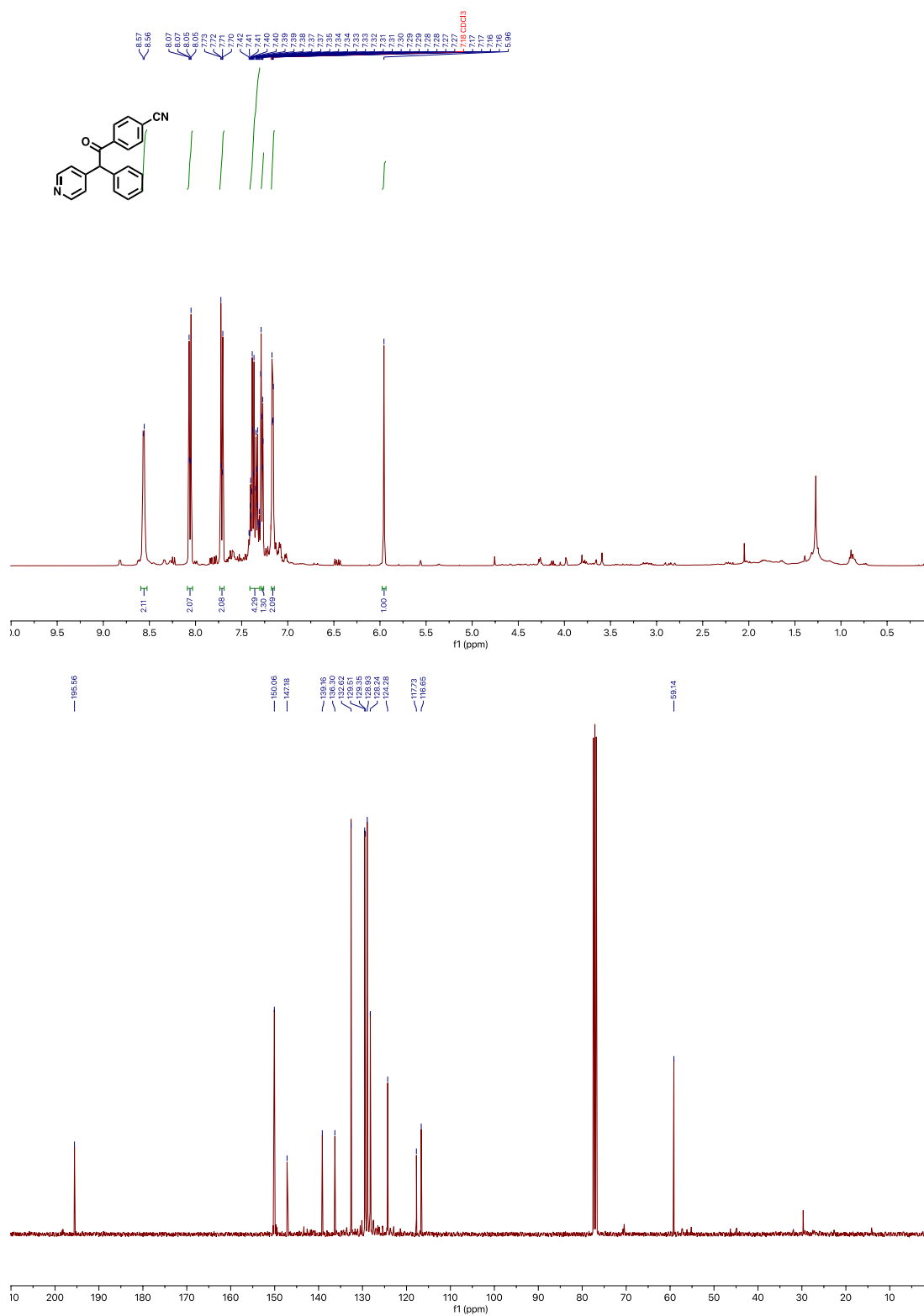


$^1\text{H}$ ,  $^{13}\text{C}\{^1\text{H}\}$  and  $^{19}\text{F}\{^1\text{H}\}$  NMR spectra of compound **3am** in  $\text{CDCl}_3$

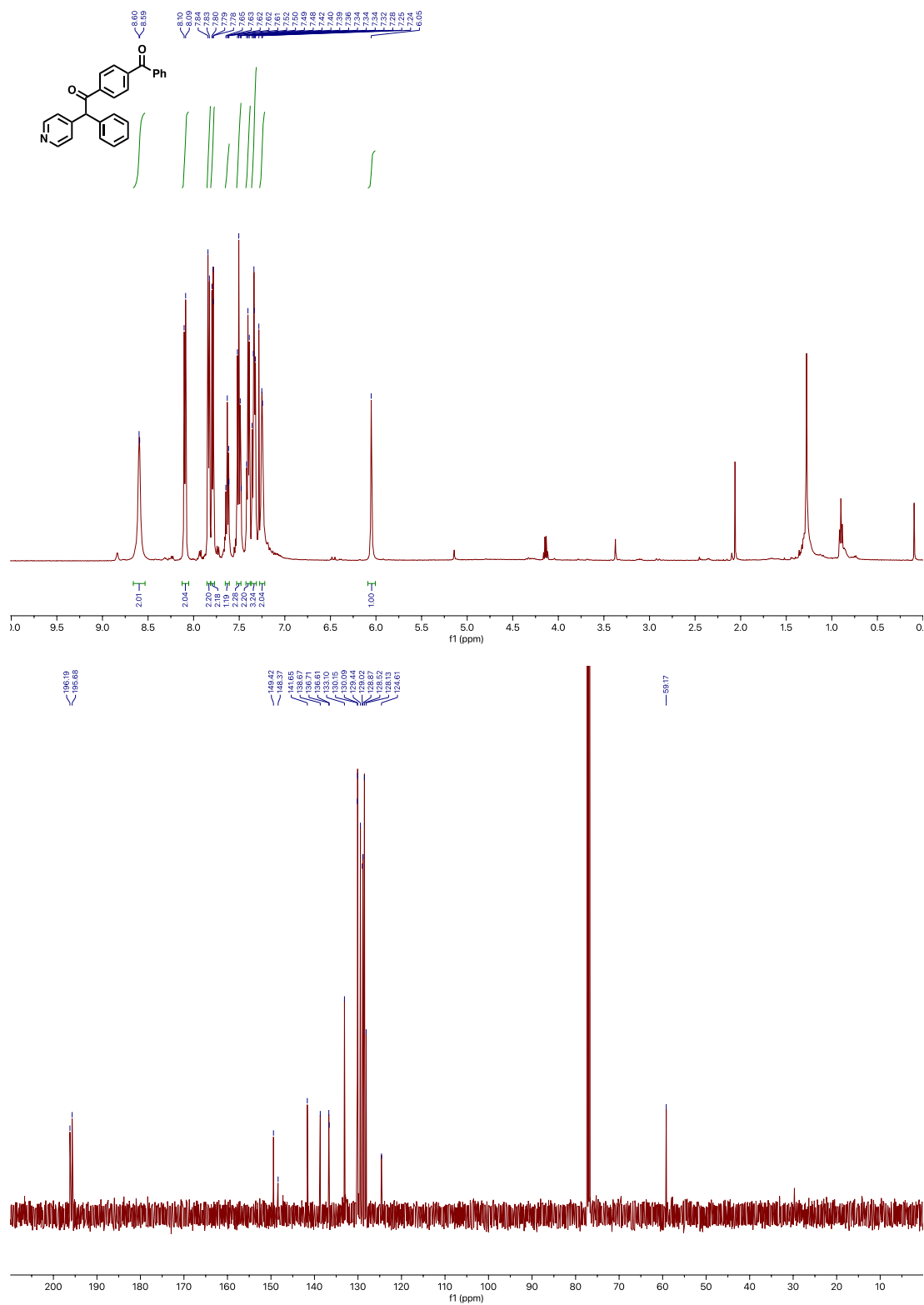




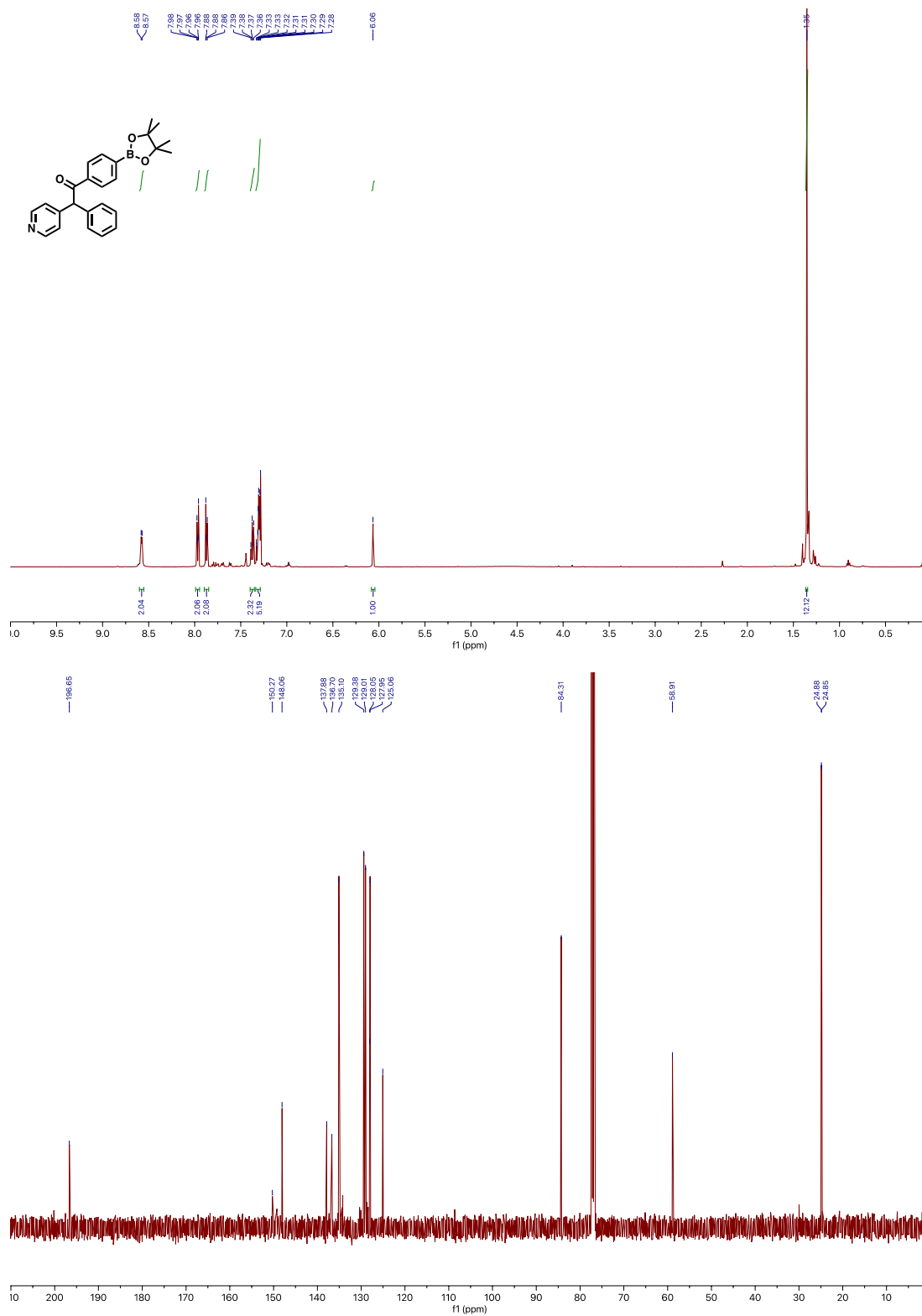
$^1\text{H}$  and  $^{13}\text{C}\{^1\text{H}\}$  NMR spectra of compound **3an** in  $\text{CDCl}_3$



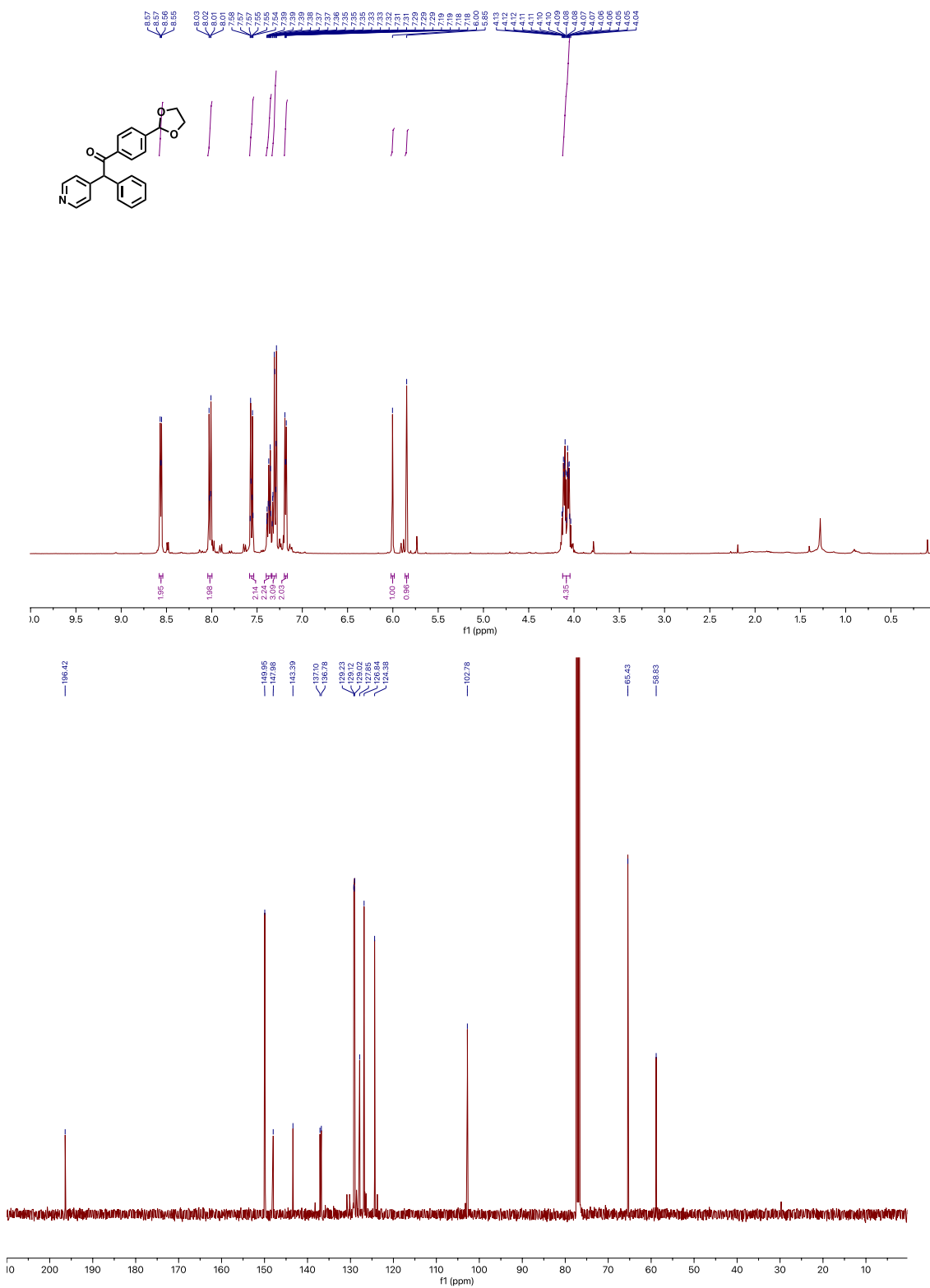
$^1\text{H}$ ,  $^{13}\text{C}\{^1\text{H}\}$  and  $^{19}\text{F}\{^1\text{H}\}$  NMR spectra of compound **3ao** in  $\text{CDCl}_3$



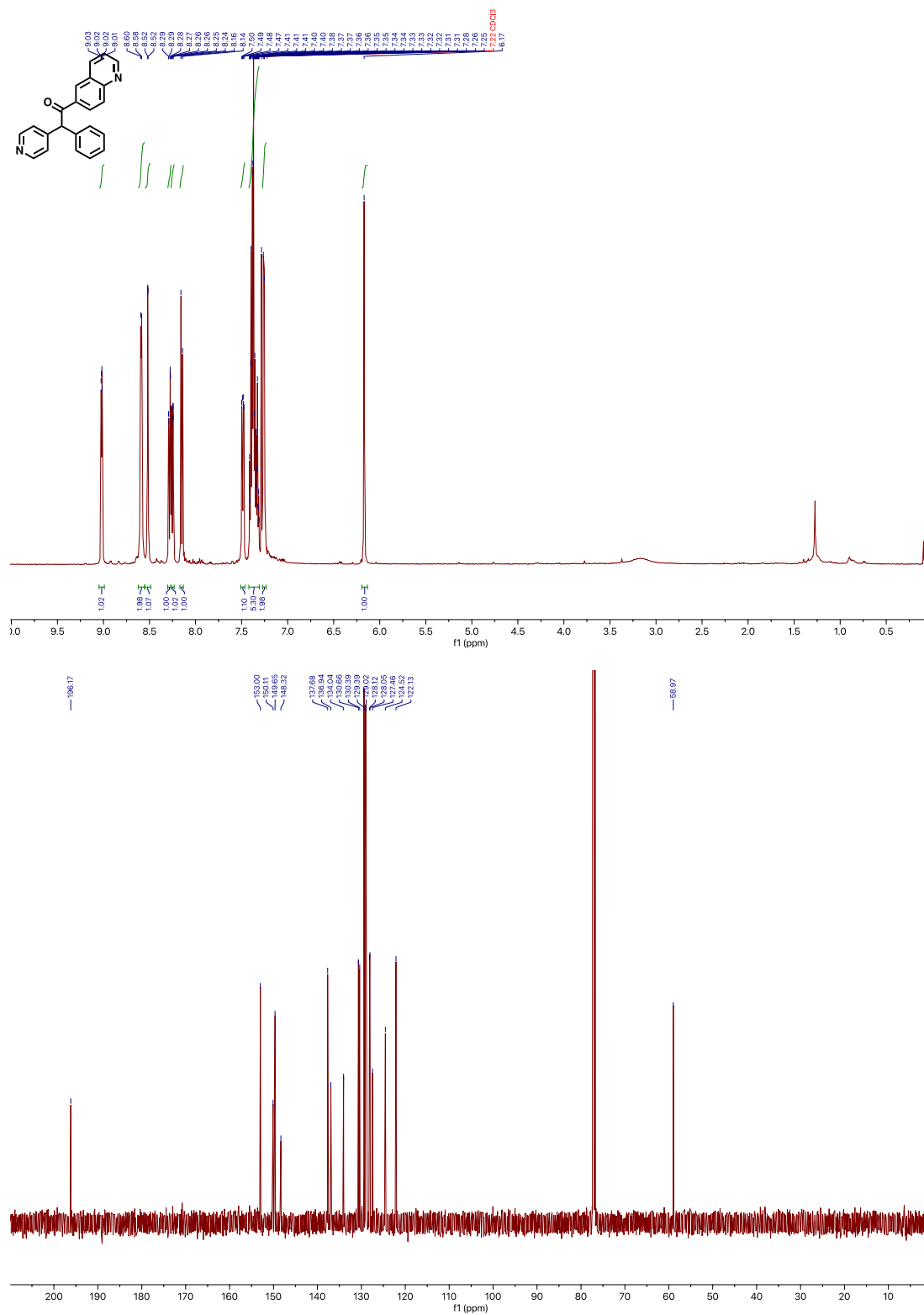
$^1\text{H}$  and  $^{13}\text{C}\{^1\text{H}\}$  NMR spectra of compound **3ap** in  $\text{CDCl}_3$



$^1\text{H}$  and  $^{13}\text{C}\{^1\text{H}\}$  NMR spectra of compound **3aq** in  $\text{CDCl}_3$

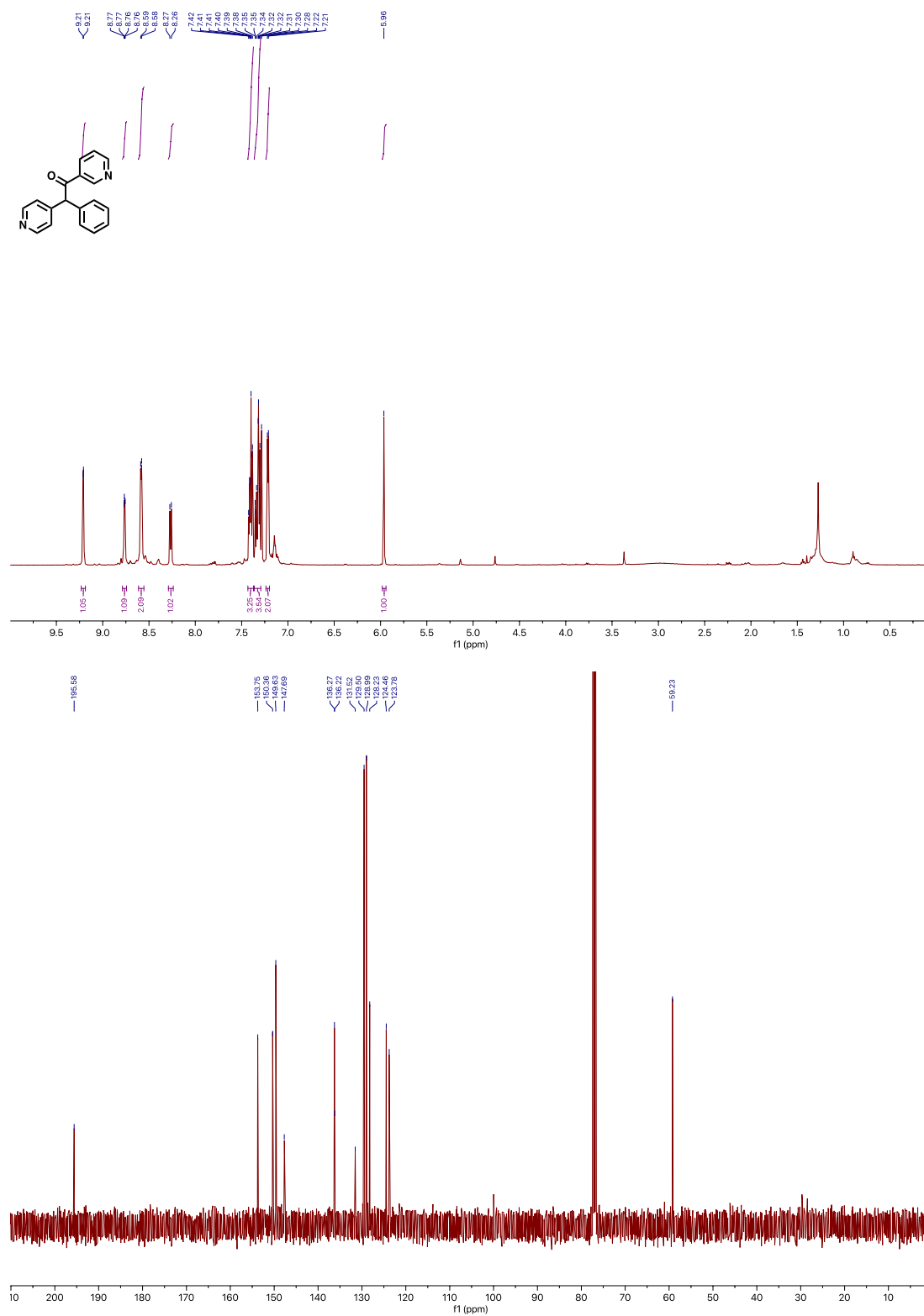


$^1\text{H}$  and  $^{13}\text{C}\{^1\text{H}\}$  NMR spectra of compound **3ar** in  $\text{CDCl}_3$

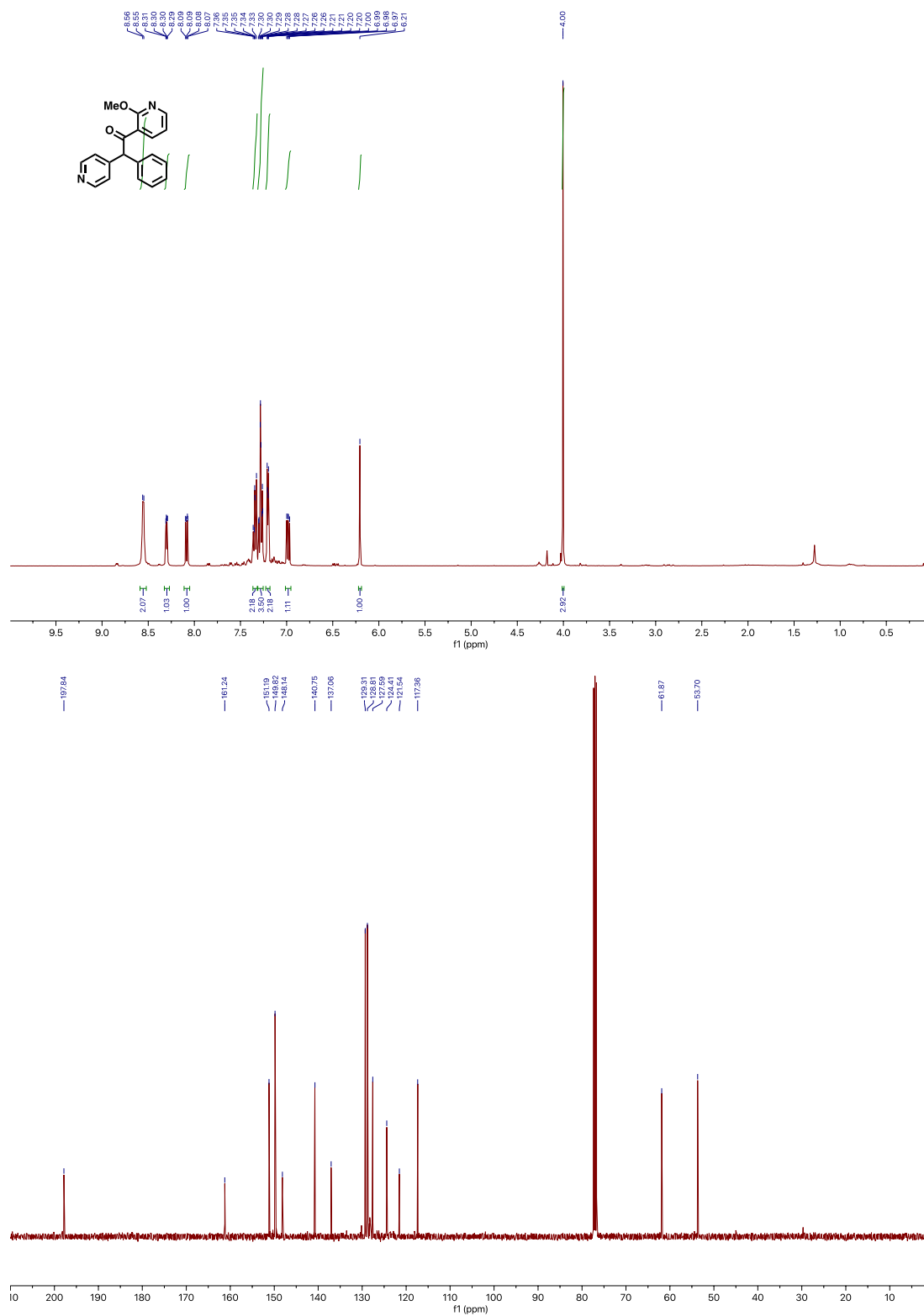




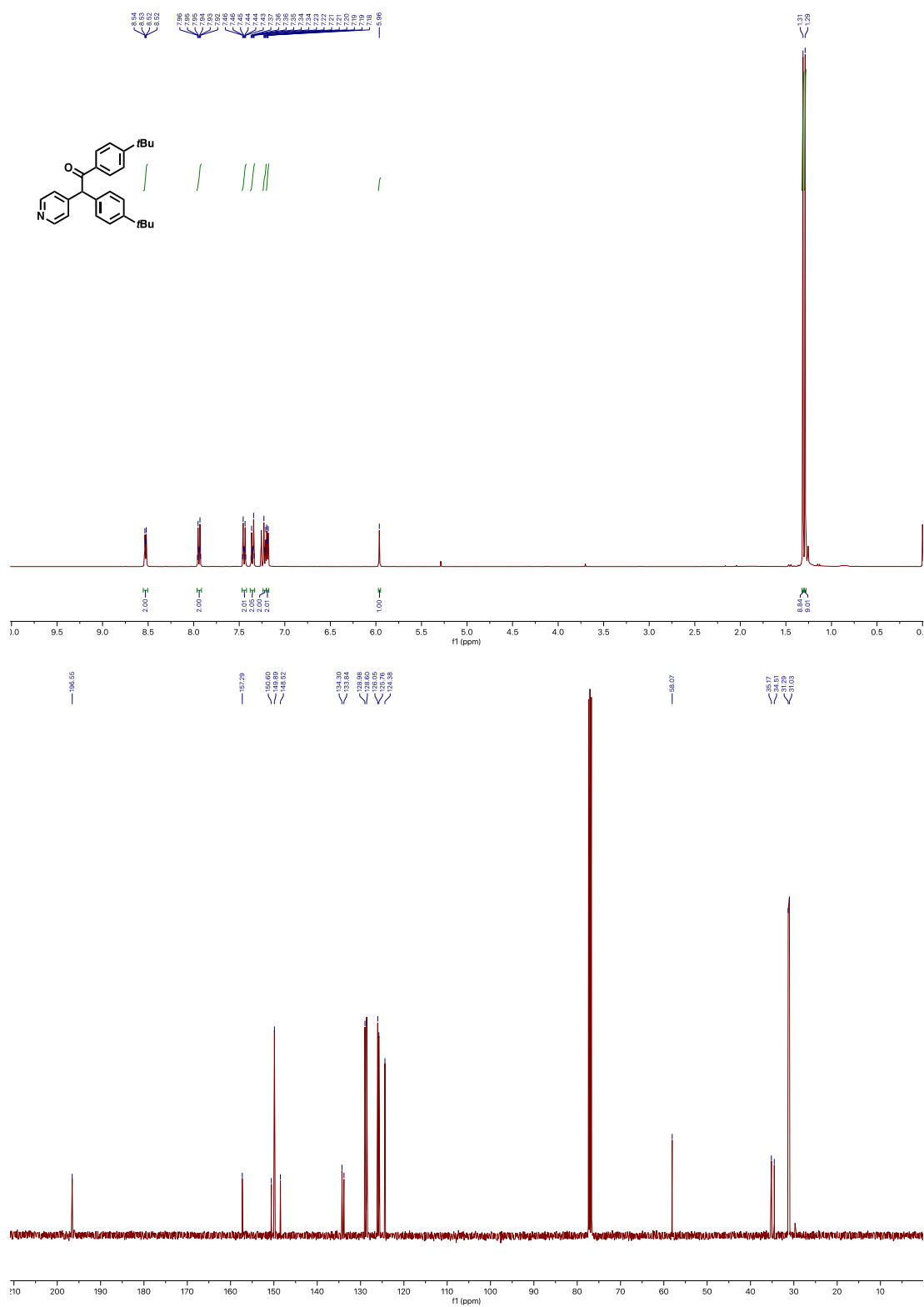
$^1\text{H}$  and  $^{13}\text{C}\{^1\text{H}\}$  NMR spectra of compound **3as** in  $\text{CDCl}_3$



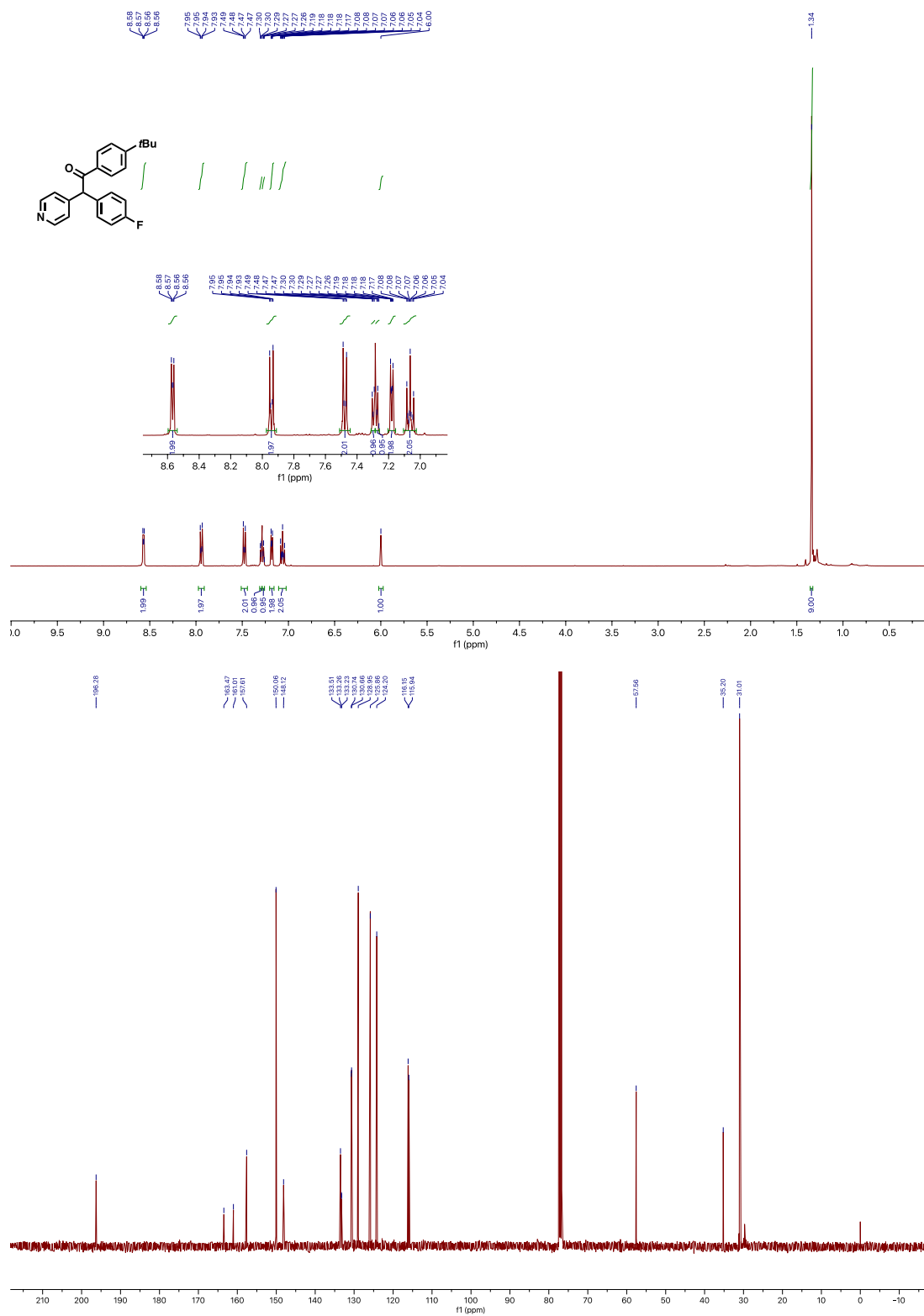
$^1\text{H}$  and  $^{13}\text{C}\{^1\text{H}\}$  NMR spectra of compound **3at** in  $\text{CDCl}_3$

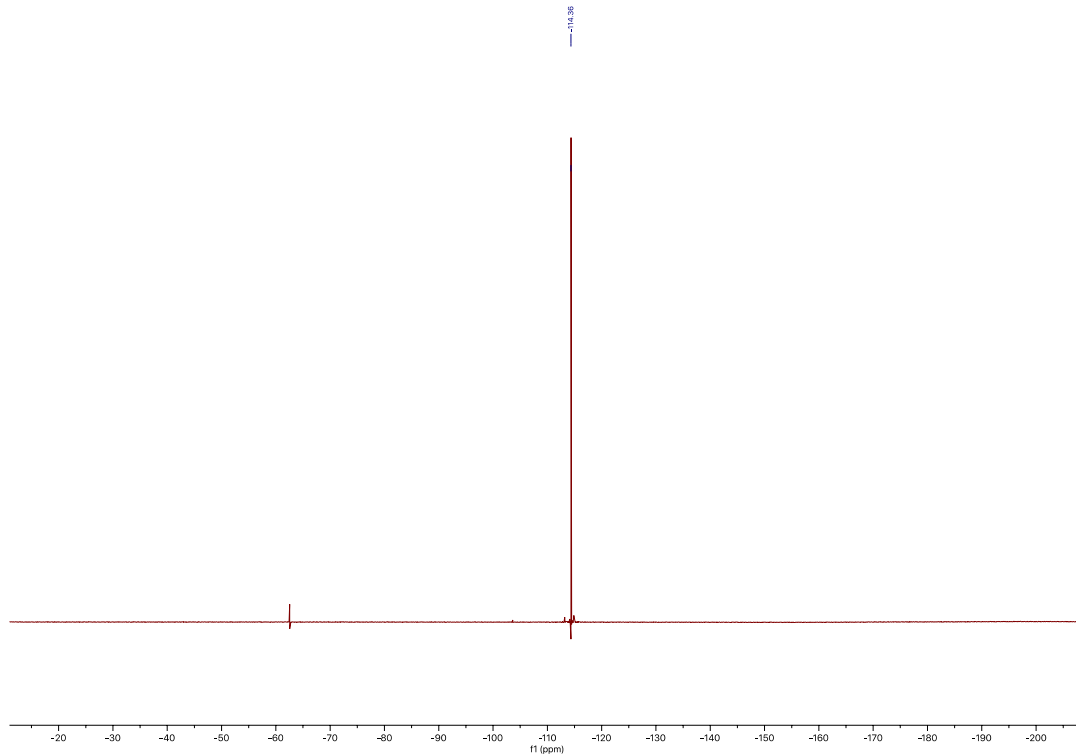


$^1\text{H}$  and  $^{13}\text{C}\{^1\text{H}\}$  NMR spectra of compound **3ba** in  $\text{CDCl}_3$

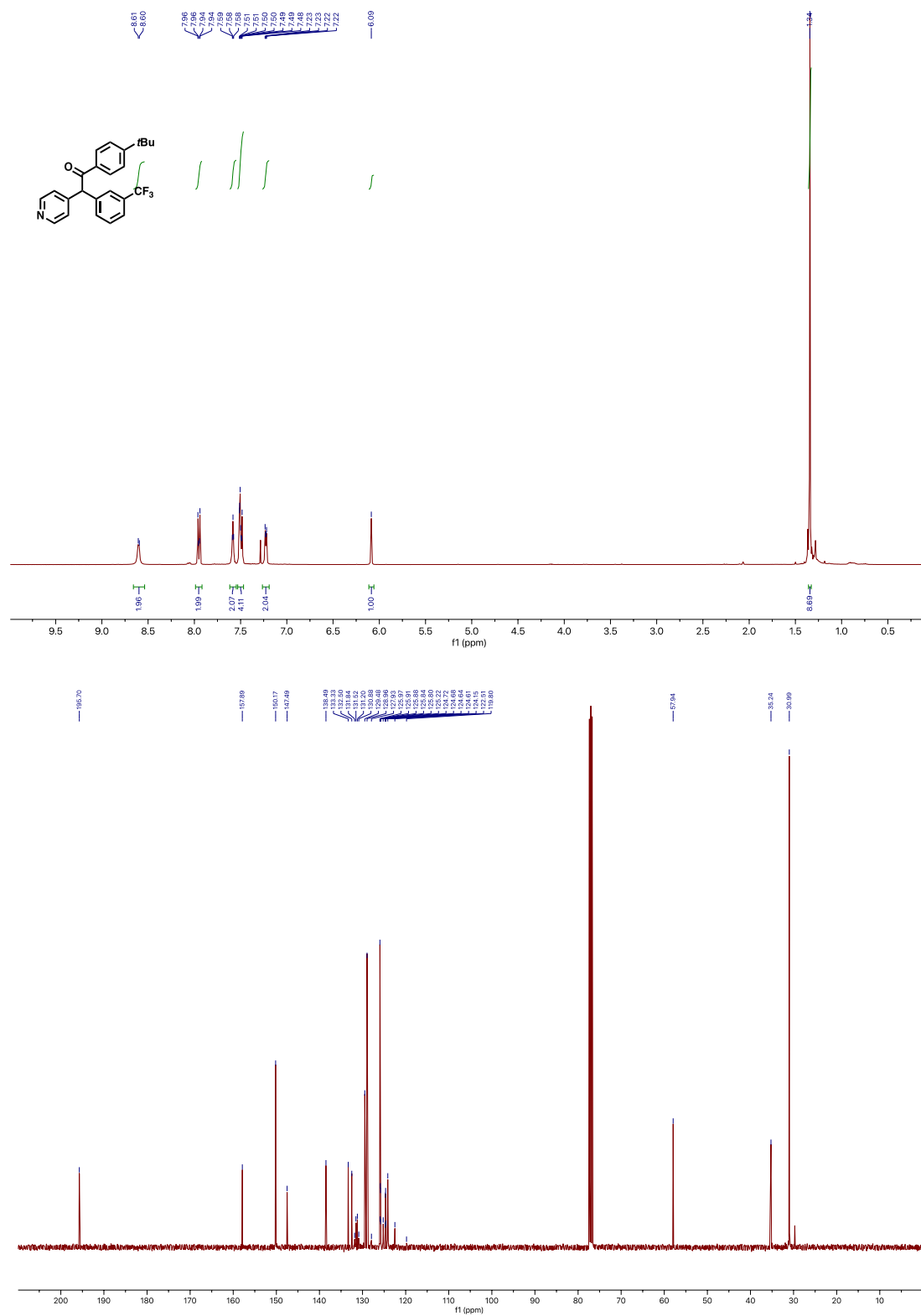


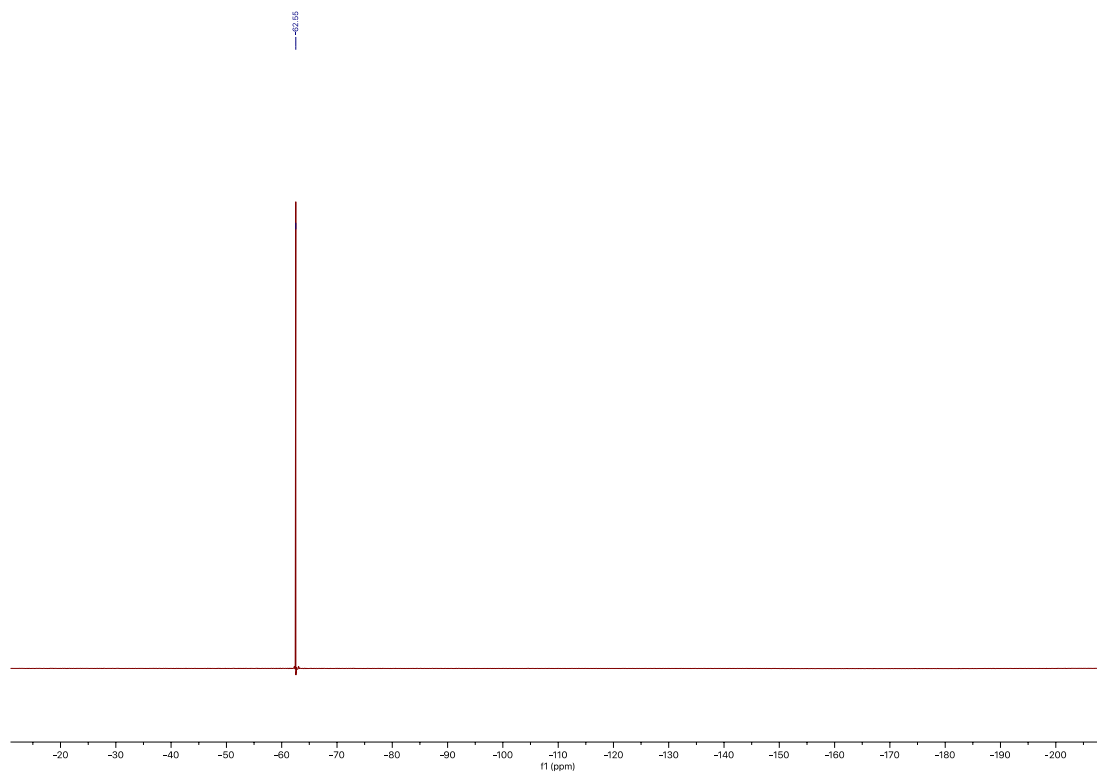
$^1\text{H}$ ,  $^{13}\text{C}\{^1\text{H}\}$  and  $^{19}\text{F}\{^1\text{H}\}$  NMR spectra of compound **3ca** in  $\text{CDCl}_3$



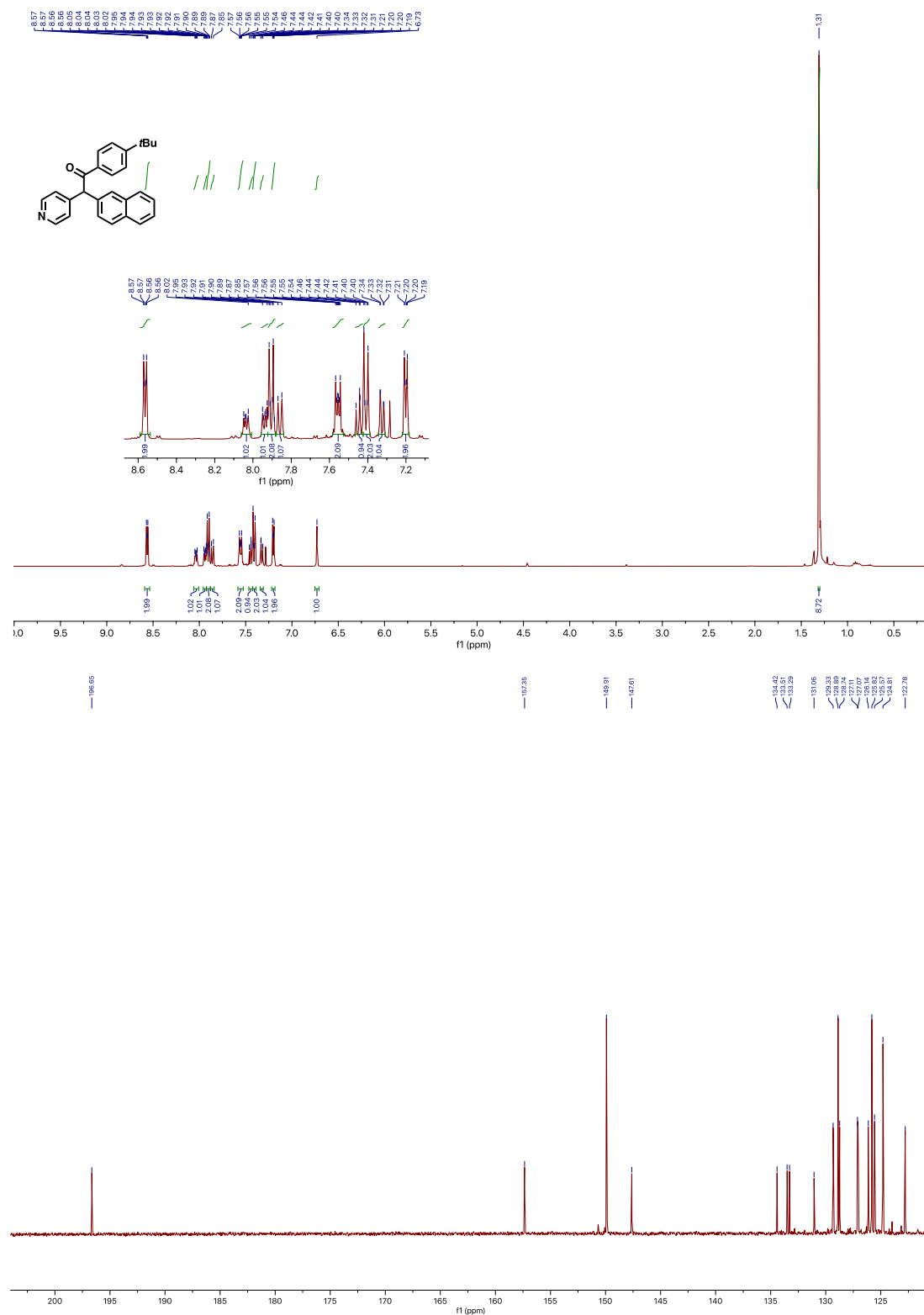


$^1\text{H}$ ,  $^{13}\text{C}\{^1\text{H}\}$  and  $^{19}\text{F}\{^1\text{H}\}$  NMR spectra of compound **3da** in  $\text{CDCl}_3$



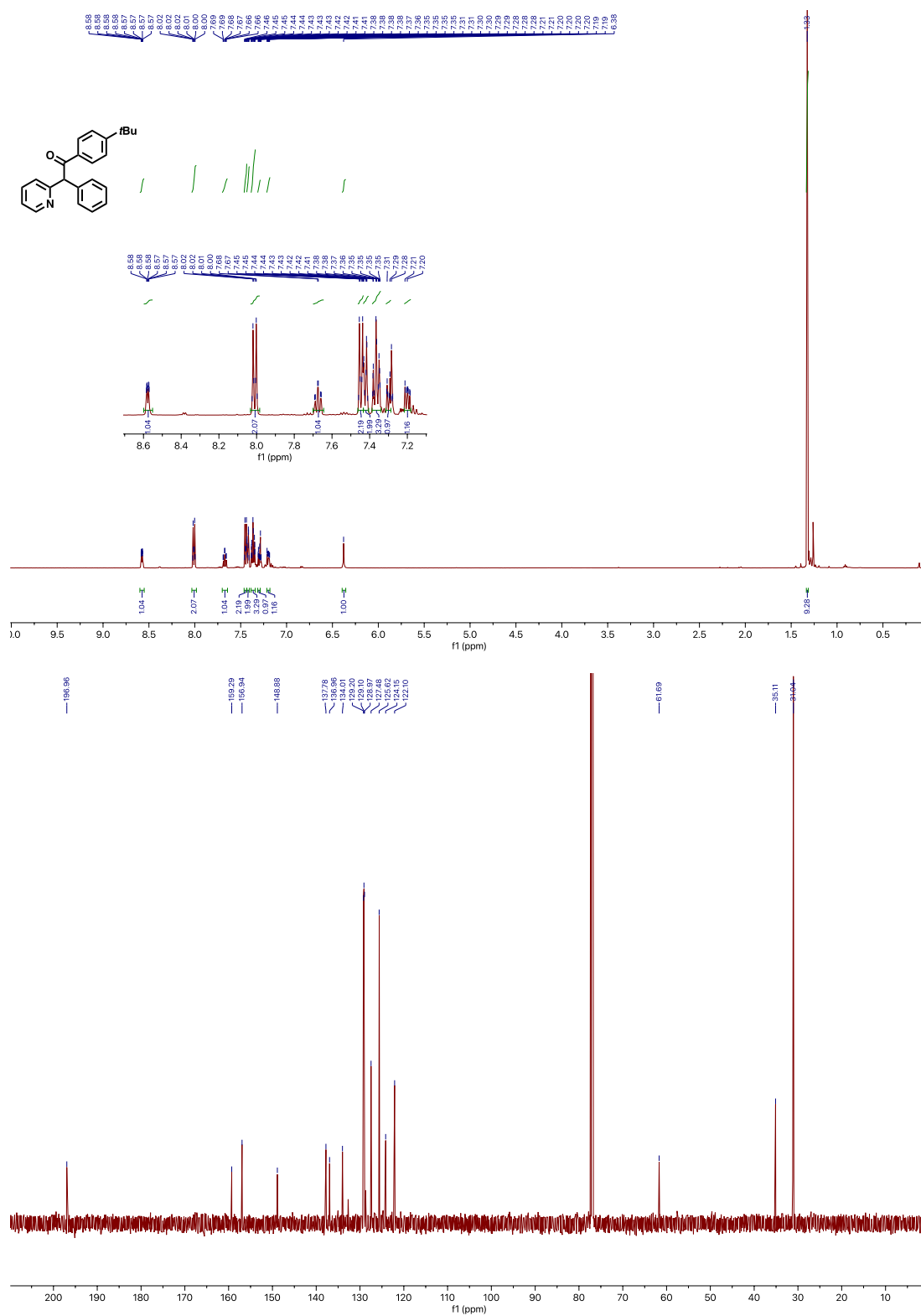


$^1\text{H}$  and  $^{13}\text{C}\{^1\text{H}\}$  NMR spectra of compound **3ea** in  $\text{CDCl}_3$

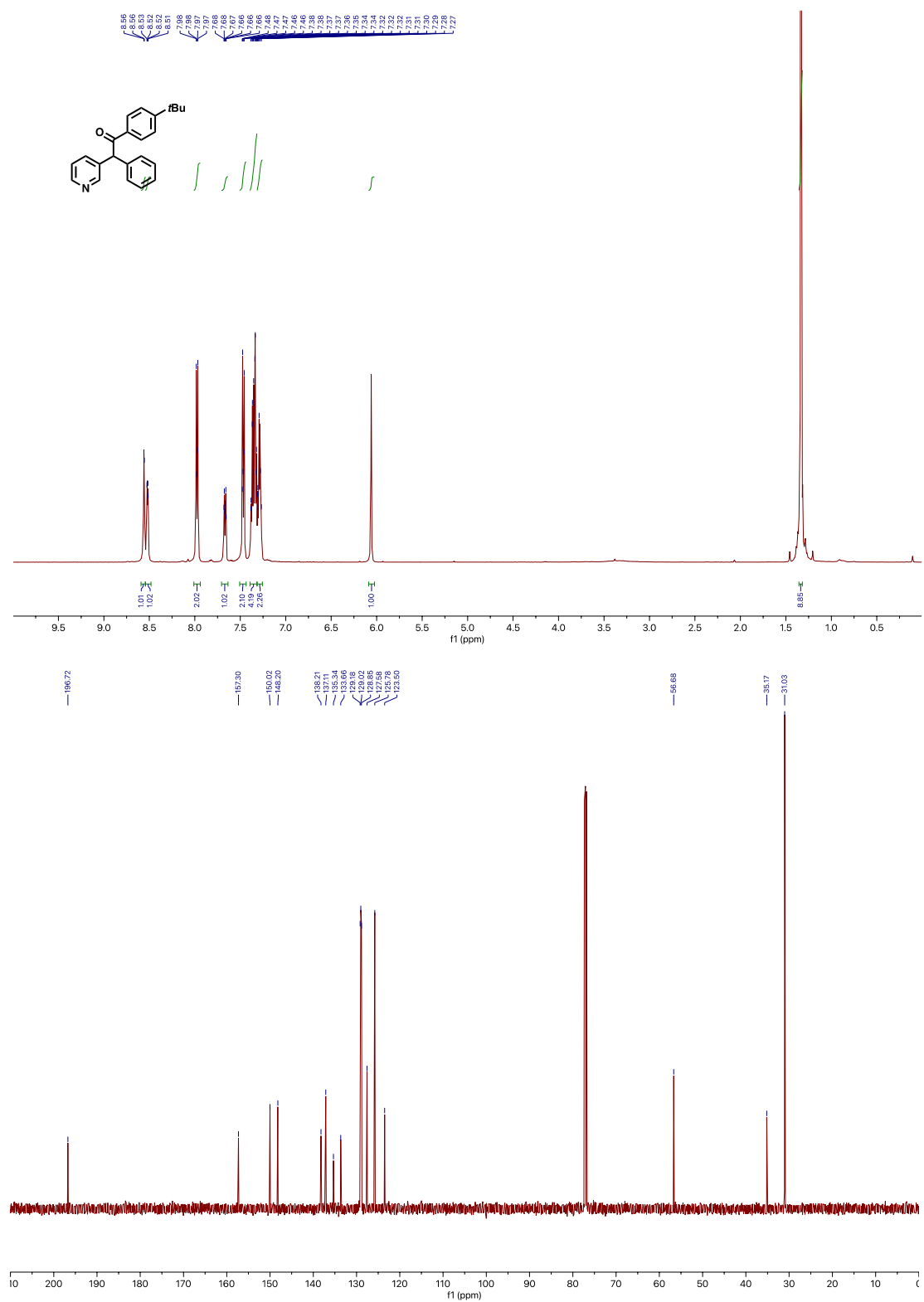




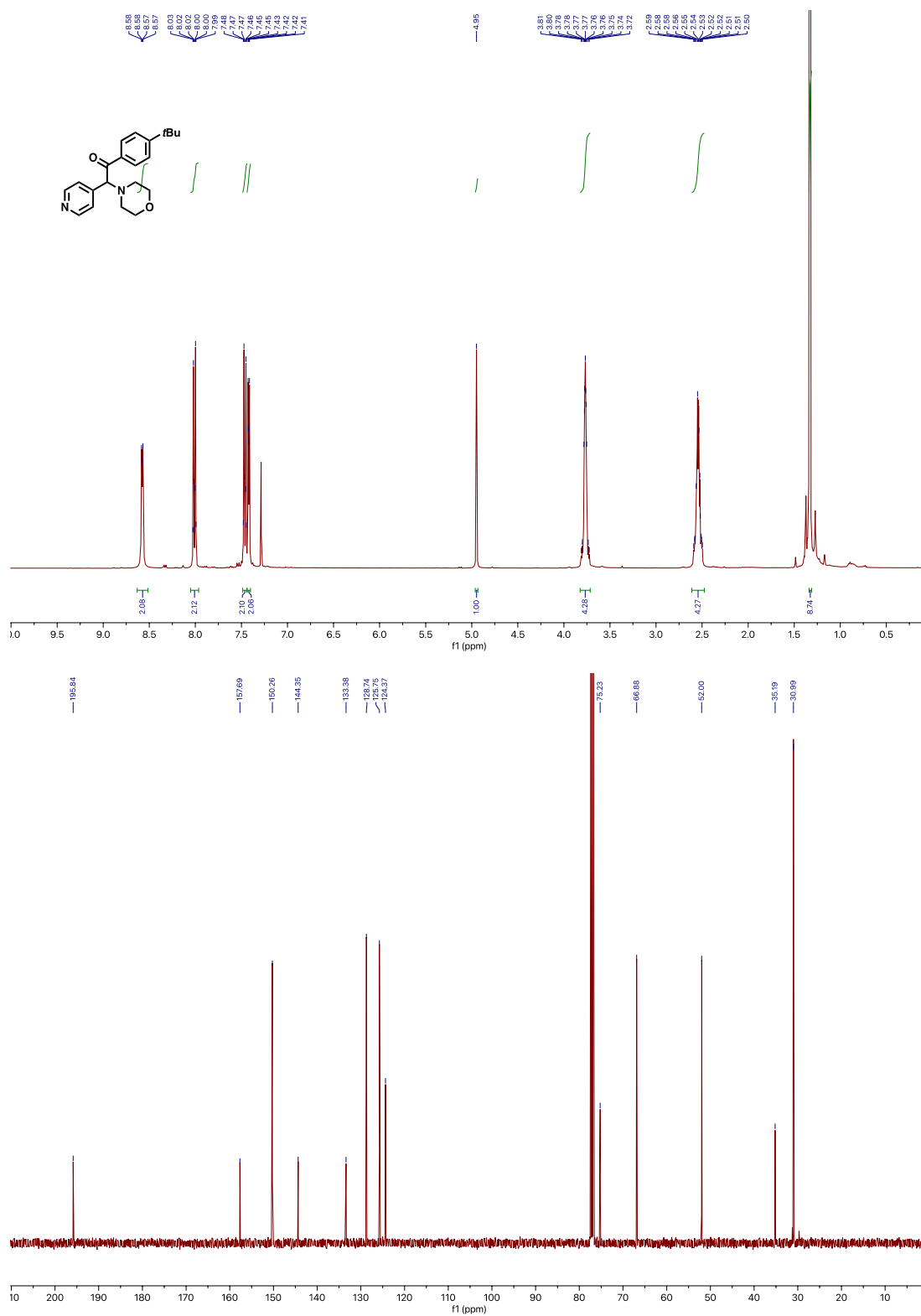
$^1\text{H}$  and  $^{13}\text{C}\{^1\text{H}\}$  NMR spectra of compound **3ga** in  $\text{CDCl}_3$



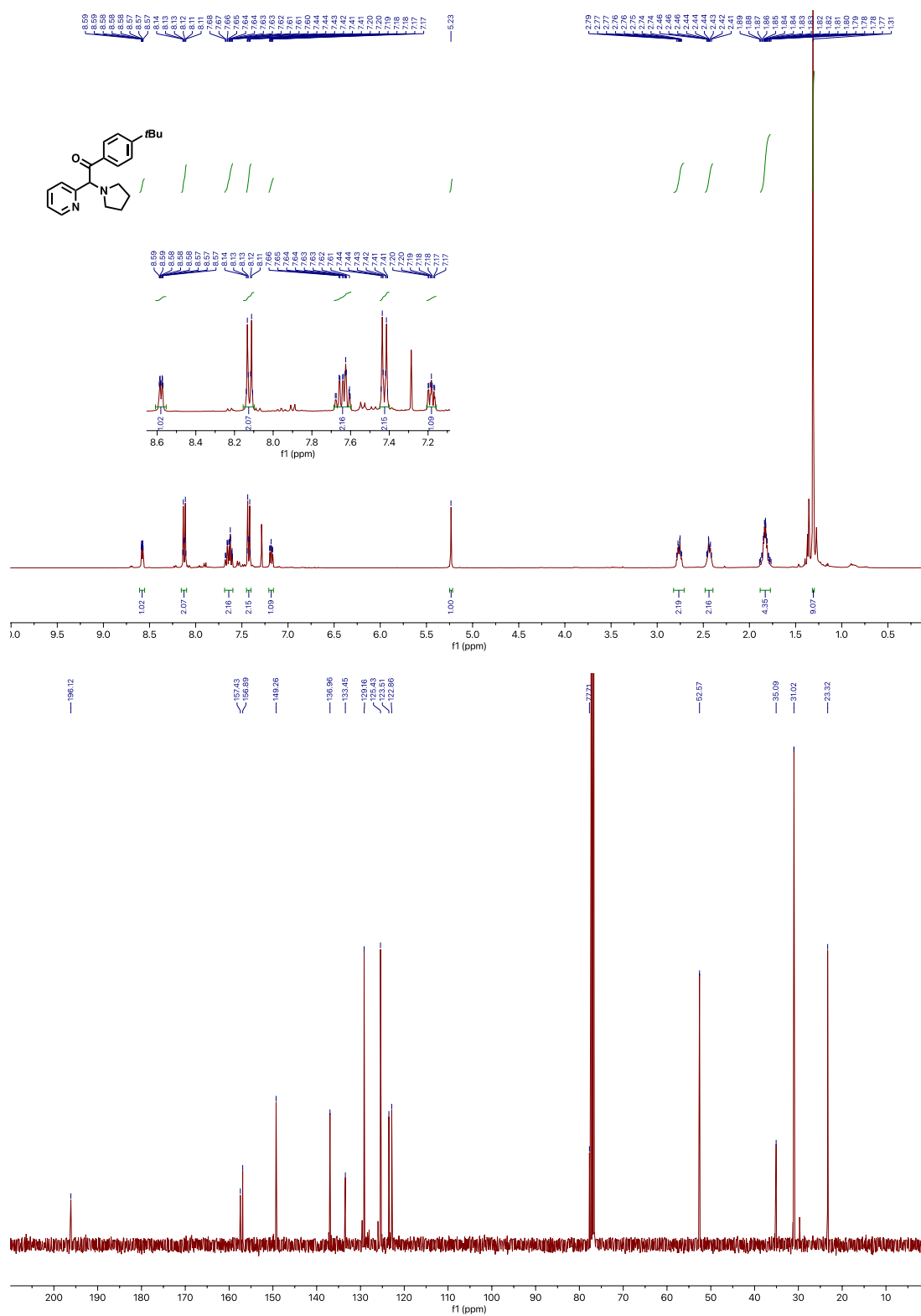
$^1\text{H}$  and  $^{13}\text{C}\{^1\text{H}\}$  NMR spectra of compound **3ha** in  $\text{CDCl}_3$



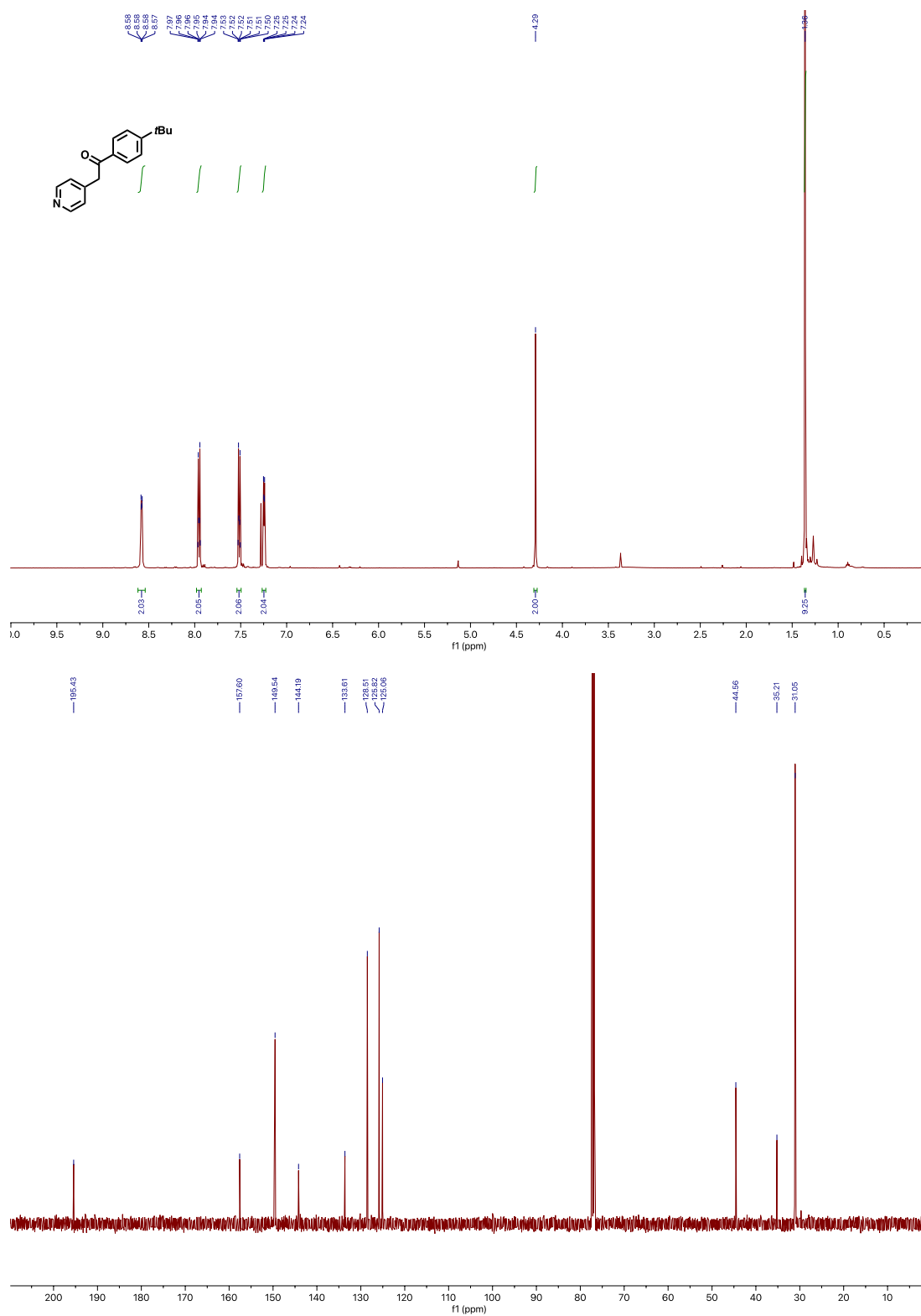
$^1\text{H}$  and  $^{13}\text{C}\{^1\text{H}\}$  NMR spectra of compound **3ia** in  $\text{CDCl}_3$



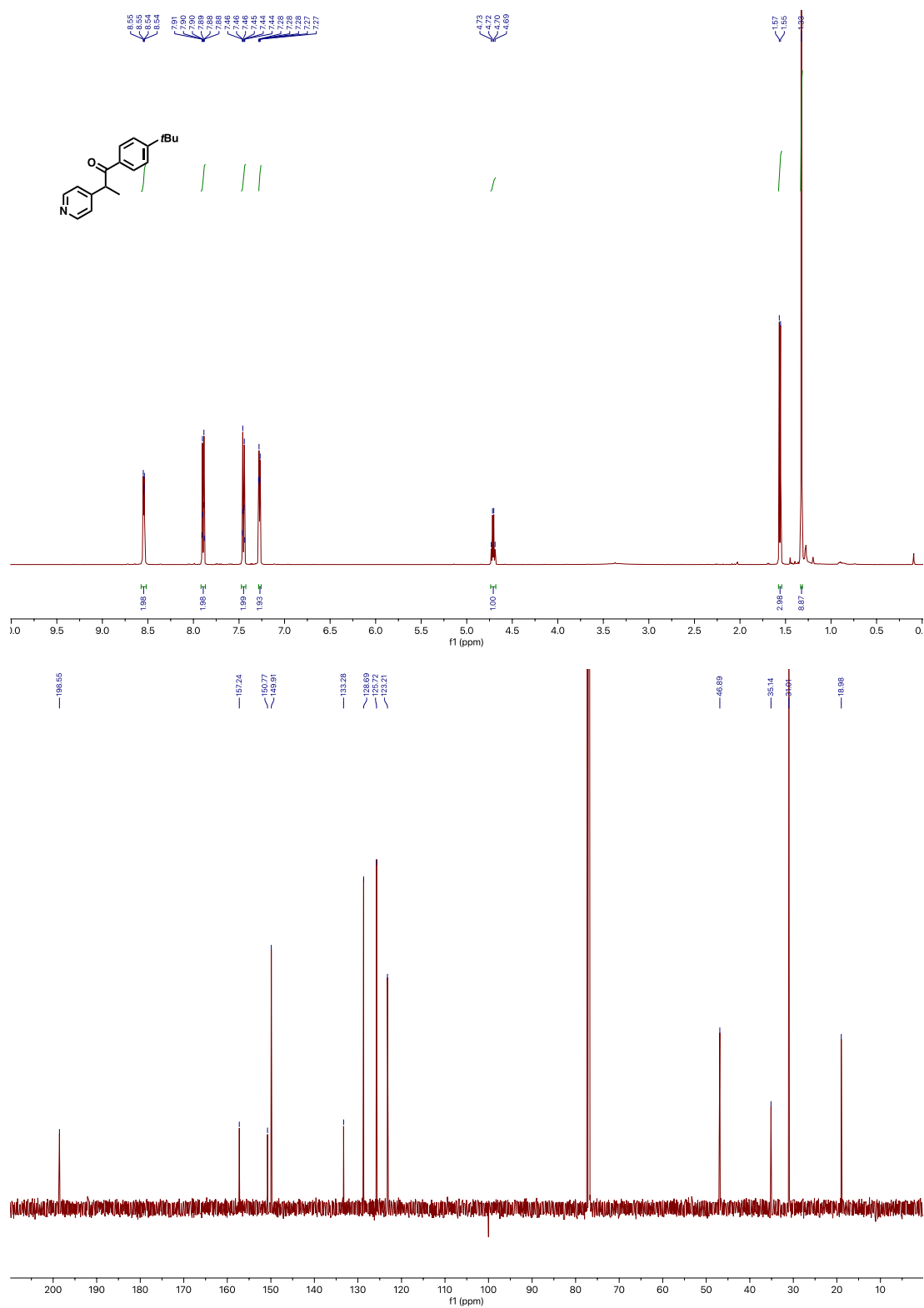
$^1\text{H}$  and  $^{13}\text{C}\{^1\text{H}\}$  NMR spectra of compound **3ja** in  $\text{CDCl}_3$



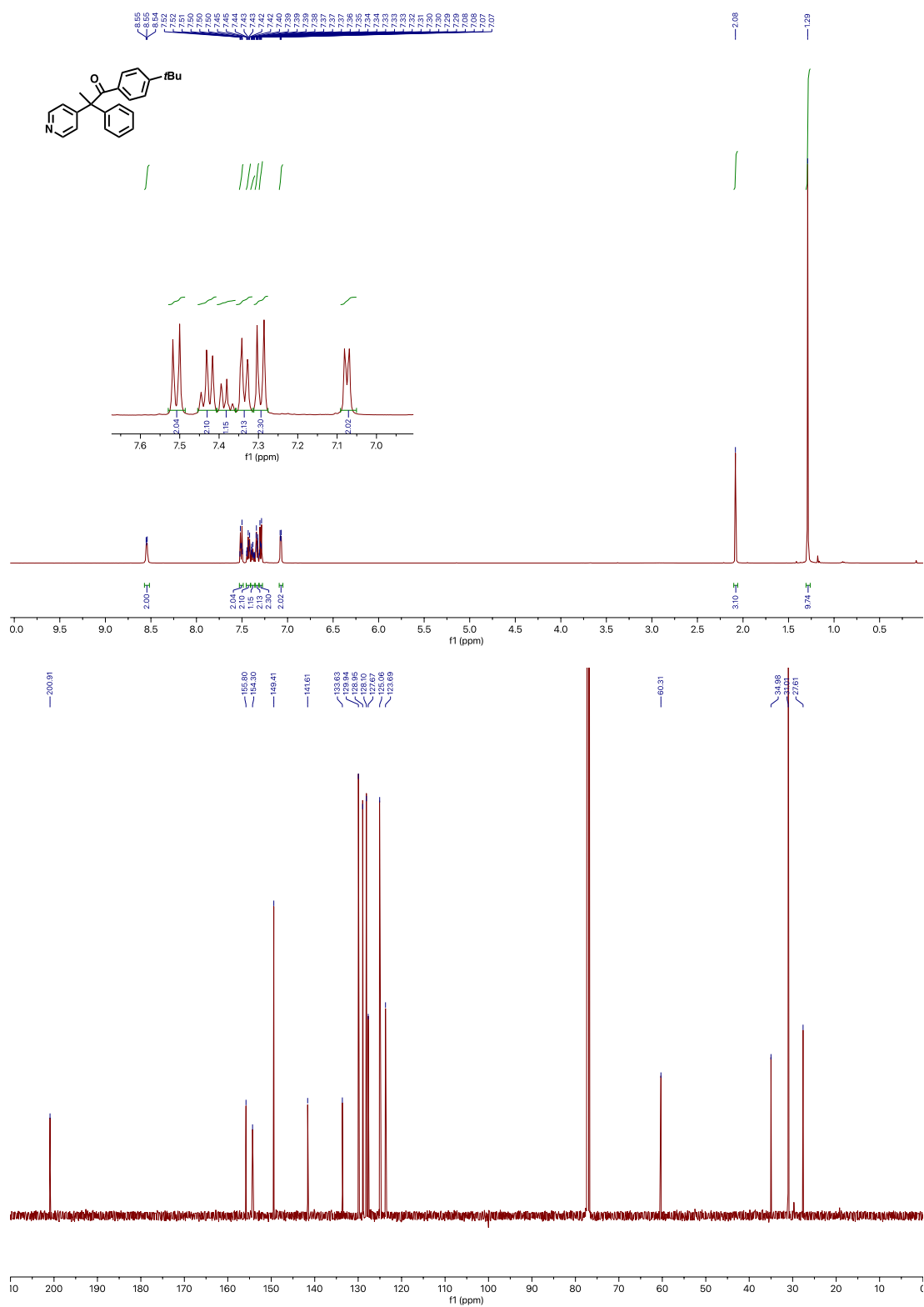
$^1\text{H}$  and  $^{13}\text{C}\{^1\text{H}\}$  NMR spectra of compound **3ka** in  $\text{CDCl}_3$



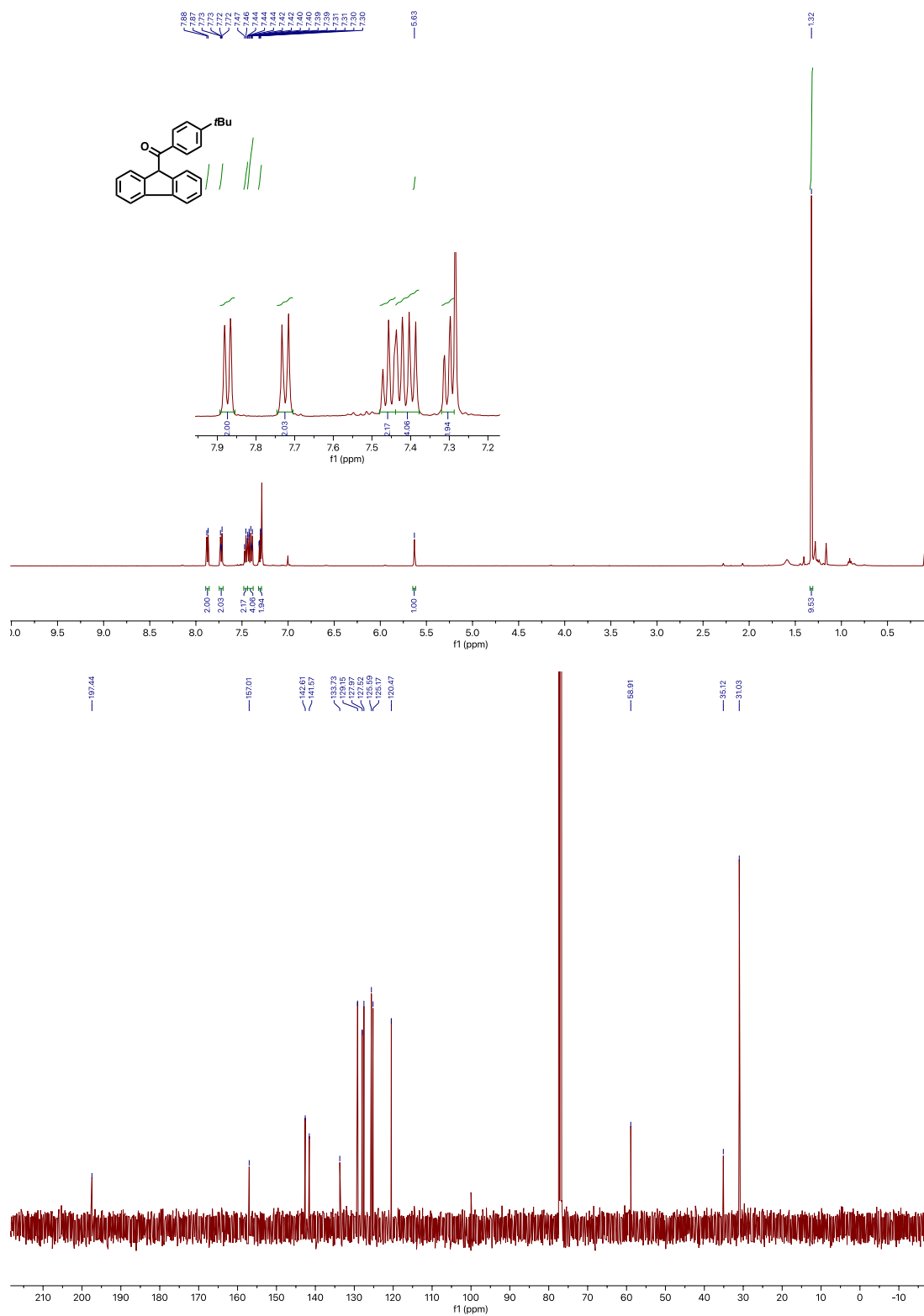
$^1\text{H}$  and  $^{13}\text{C}\{^1\text{H}\}$  NMR spectra of compound **3la** in  $\text{CDCl}_3$



$^1\text{H}$  and  $^{13}\text{C}\{^1\text{H}\}$  NMR spectra of compound **3ma** in  $\text{CDCl}_3$

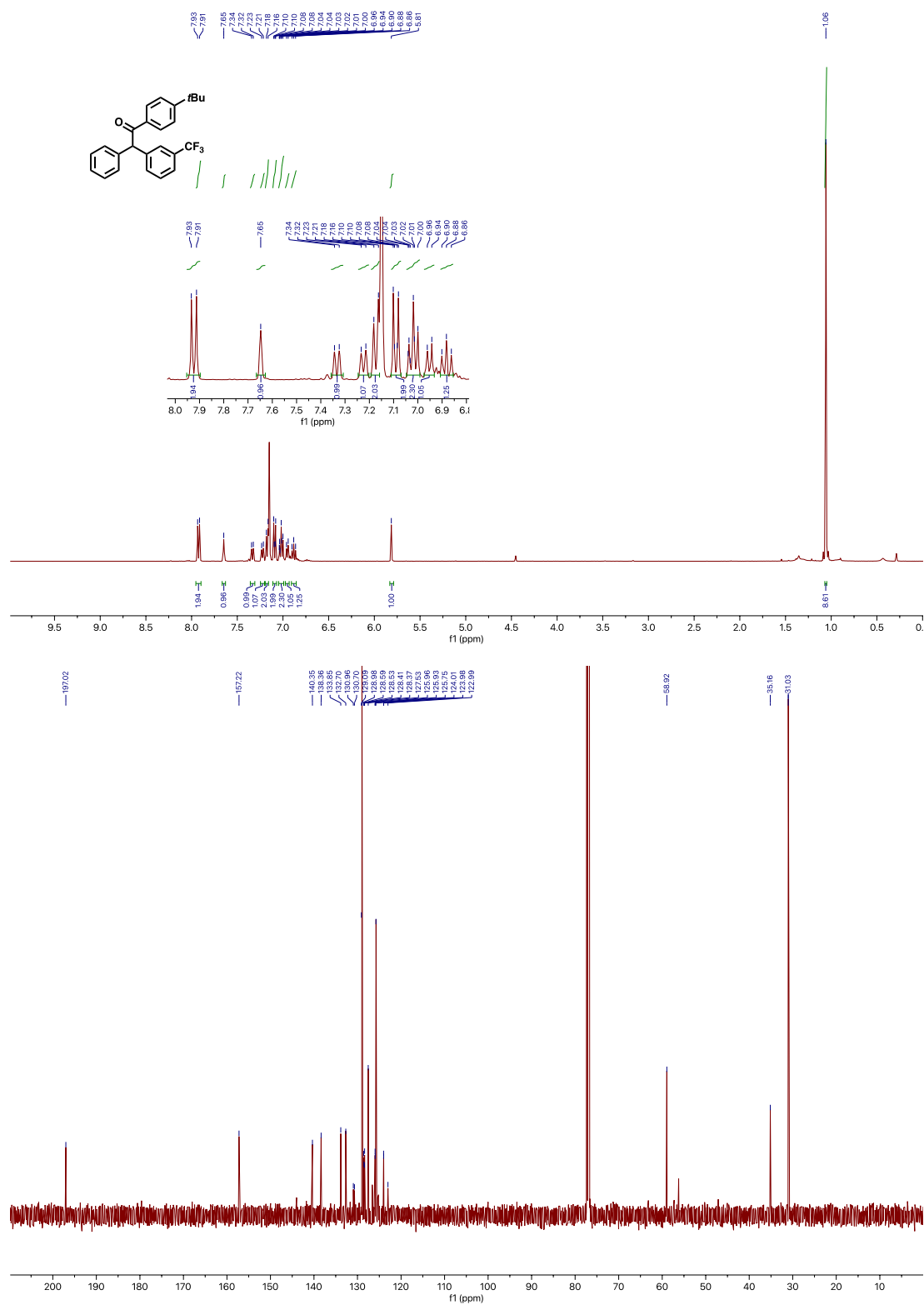


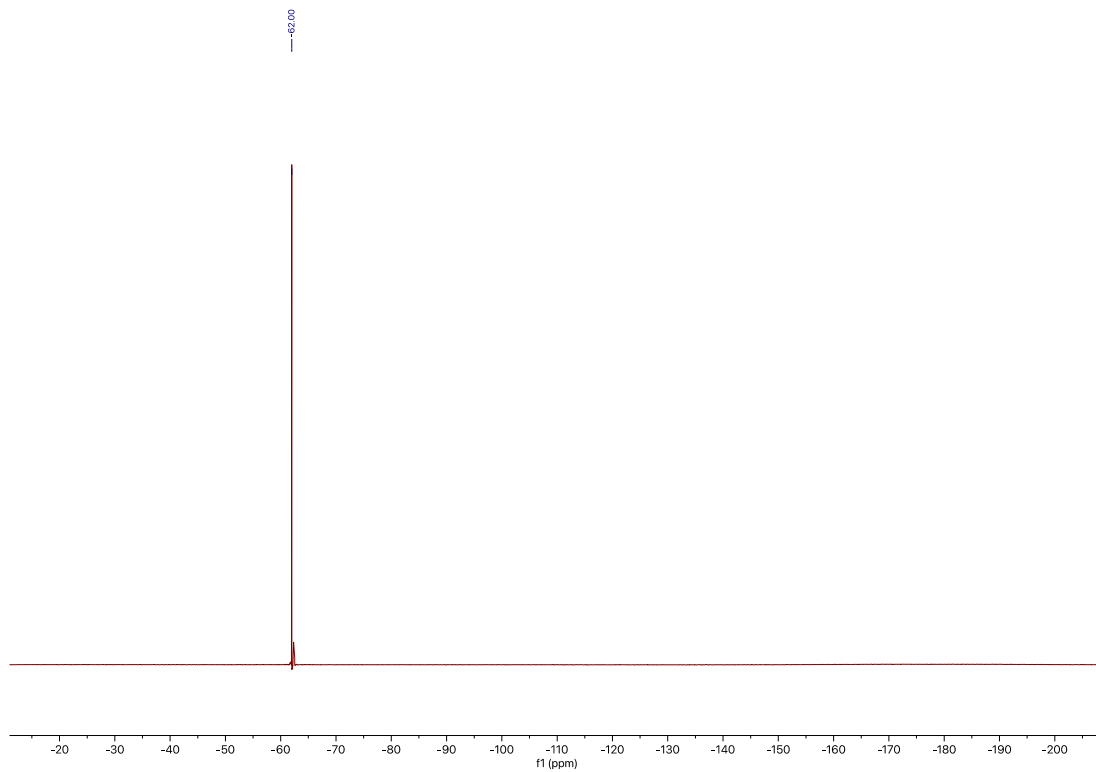
$^1\text{H}$  and  $^{13}\text{C}\{^1\text{H}\}$  NMR spectra of compound **3na** in  $\text{CDCl}_3$





$^1\text{H}$ ,  $^{13}\text{C}\{^1\text{H}\}$  and  $^{19}\text{F}\{^1\text{H}\}$  NMR spectra of compound **30a** in  $\text{CDCl}_3$

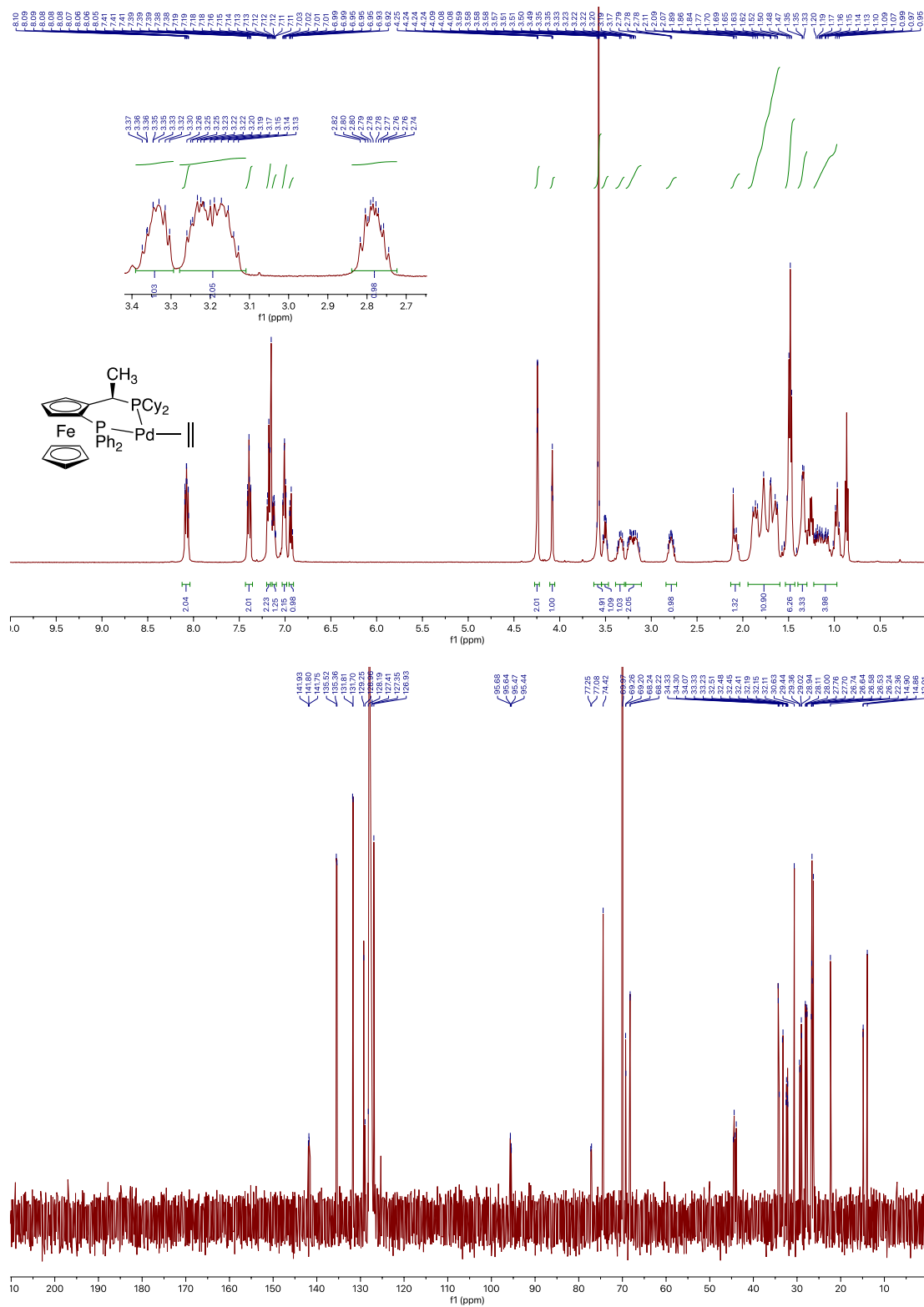


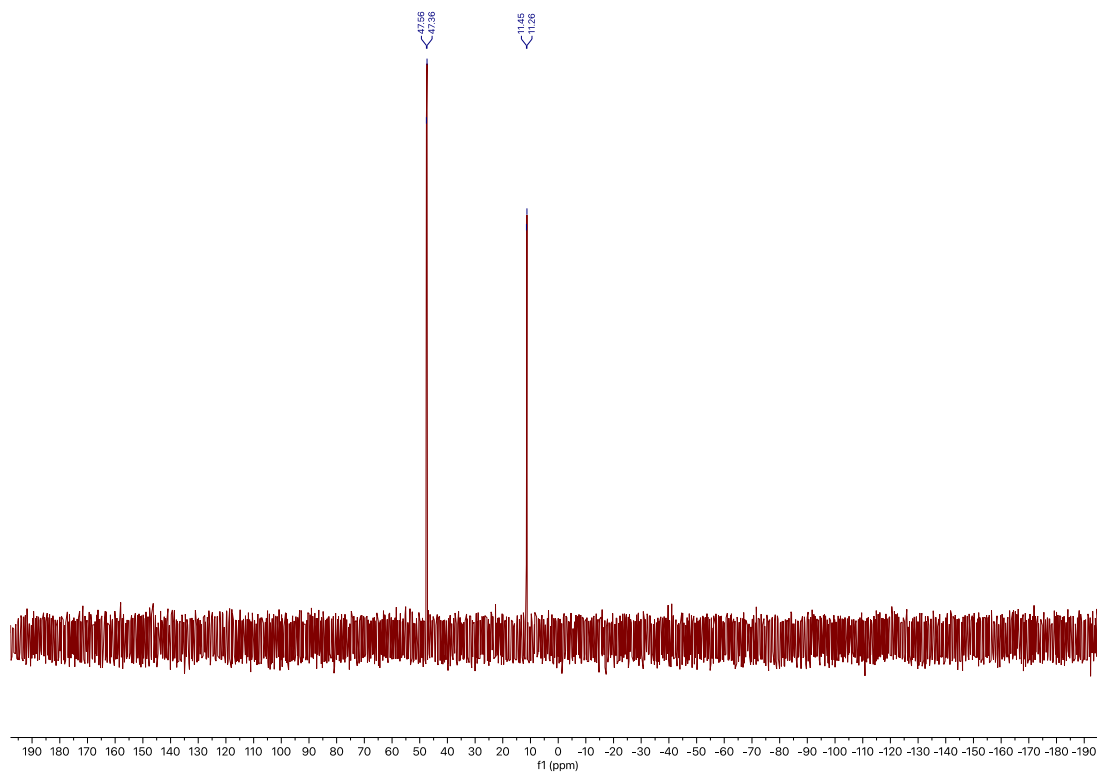




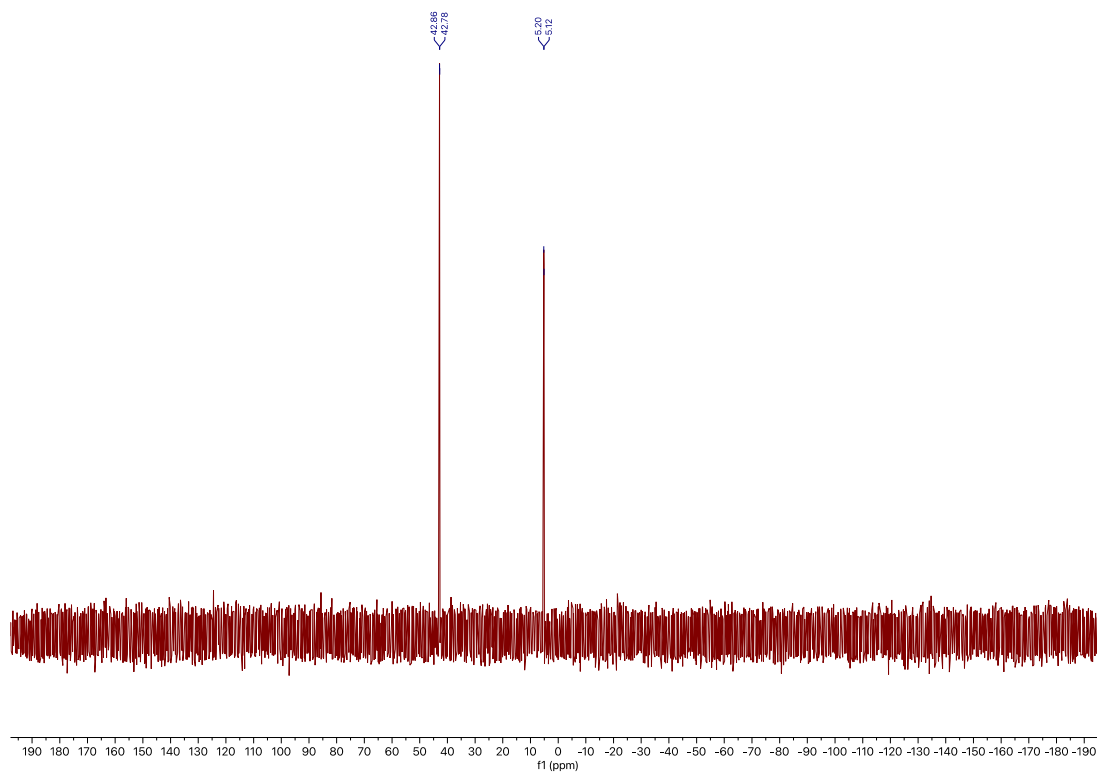


$^1\text{H}$ ,  $^{13}\text{C}\{^1\text{H}\}$  and  $^{31}\text{P}\{^1\text{H}\}$  NMR spectra of compound **4** in  $\text{C}_6\text{D}_6$



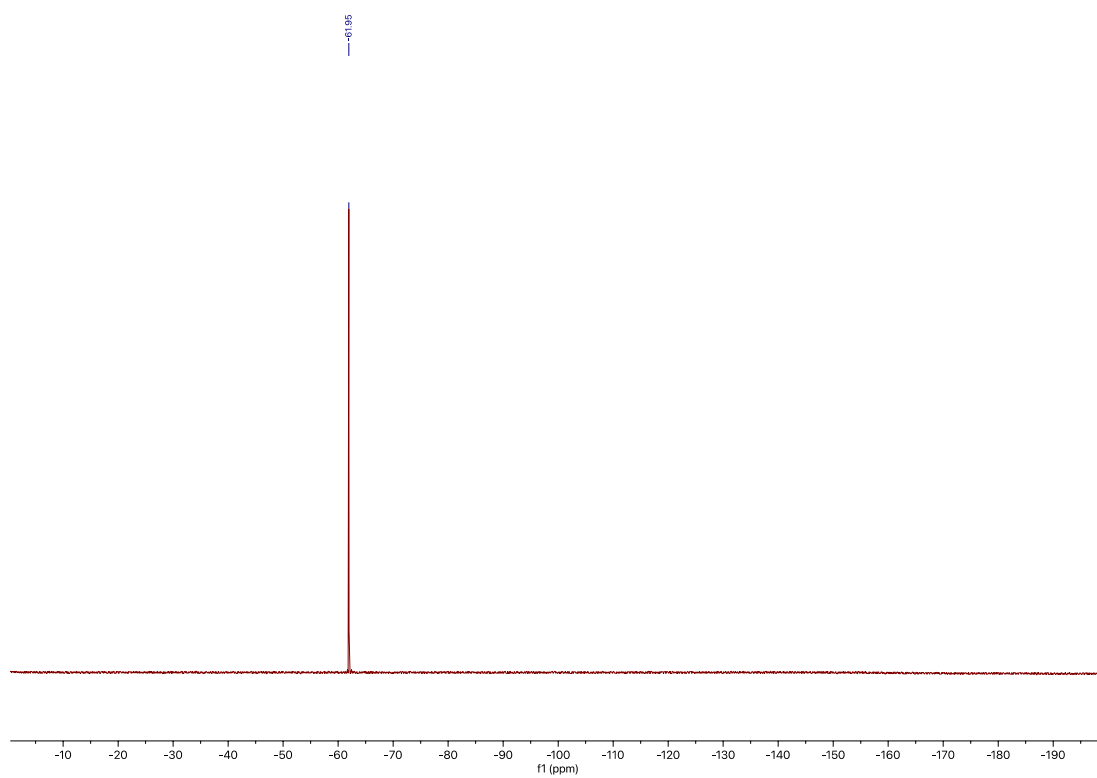






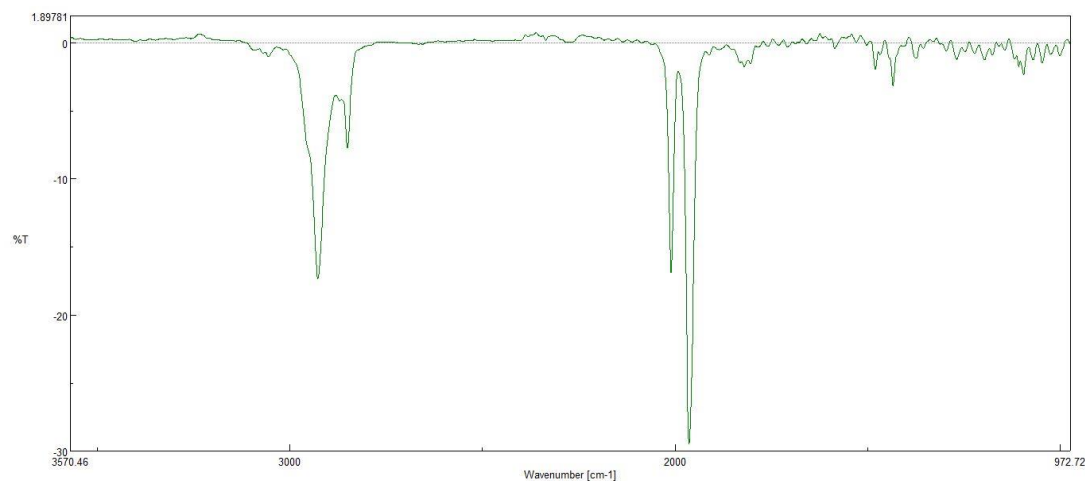






## IR Spectrum

Solution Phase IR of **5** in 1,4-Dioxane-d<sub>8</sub> at Room Temperature under CO



## X-Ray Crystallographic Data

(Josiphos)Pd(C<sub>2</sub>H<sub>4</sub>) (**4**)

Compound **4**•pentane, C<sub>43</sub>H<sub>60</sub>FeP<sub>2</sub>Pd, crystallizes in the tetragonal space group P4<sub>3</sub> (systematic absences 00l: l≠3) with a=16.84223(8)Å, c=13.46917(11)Å, V=3820.68(5)Å<sup>3</sup>, Z=4, and d<sub>calc</sub>=1.393 g/cm<sup>3</sup>. X-ray intensity data were collected on a Rigaku XtaLAB Synergy-S diffractometer [1] equipped with an HPC area detector (HyPix-6000HE) and employing confocal multilayer optic-monochromated Cu-Kα radiation (λ=1.54184 Å) at a temperature of 100K. Preliminary indexing was performed from a series of sixty 0.5° rotation frames with exposures of 1.25 sec. for θ = ±47.31° and 5 sec. for θ = 113.255°. A total of 4878 frames (49 runs) were collected employing ω scans with a crystal to

detector distance of 34.0 mm, rotation widths of 0.5° and exposures of 2 sec. for  $\theta = 47.06^\circ$  and 8 sec. for  $\theta = 90.00$  and  $113.25^\circ$ .

Rotation frames were integrated using CrysAlisPro [2], producing a listing of unaveraged  $F^2$  and  $\sigma(F^2)$  values. A total of 63949 reflections were measured over the ranges  $5.248 \leq 2\theta \leq 148.978^\circ$ ,  $-21 \leq h \leq 21$ ,  $-19 \leq k \leq 21$ ,  $-16 \leq l \leq 16$  yielding 7361 unique reflections ( $R_{\text{int}} = 0.0673$ ). The intensity data were corrected for Lorentz and polarization effects and for absorption using SCALE3 ABSPACK [3] (minimum and maximum transmission 0.6779, 1.0000). The structure was solved by direct methods - ShelXT (Sheldrick, 2015) [4]. Refinement was by full-matrix least squares based on  $F^2$  using SHELXL-2018 [5]. All reflections were used during refinement. The weighting scheme used was  $w=1/[\sigma^2(F_o^2) + (0.0525P)^2 + 1.8873P]$  where  $P = (F_o^2 + 2F_c^2)/3$ . Non-hydrogen atoms were refined anisotropically and hydrogen atoms were refined using a riding model. Refinement converged to  $R1=0.0322$  and  $wR2=0.0856$  for 7116 observed reflections for which  $F > 4\sigma(F)$  and  $R1=0.0334$  and  $wR2=0.0862$  and  $GOF = 1.092$  for all 7361 unique, non-zero reflections and 446 variables. The maximum  $\Delta/\sigma$  in the final cycle of least squares was 0.001 and the two most prominent peaks in the final difference Fourier were +0.35 and -0.84  $e/\text{\AA}^3$ .

Table 1. lists cell information, data collection parameters, and refinement data. Final positional and equivalent isotropic thermal parameters are given in Tables 2. and 3. Anisotropic thermal parameters are in Table 4. Tables 5. and 6. list bond distances and bond angles. Figure 1. is an ORTEP representation of the molecule with 50% probability thermal ellipsoids displayed.

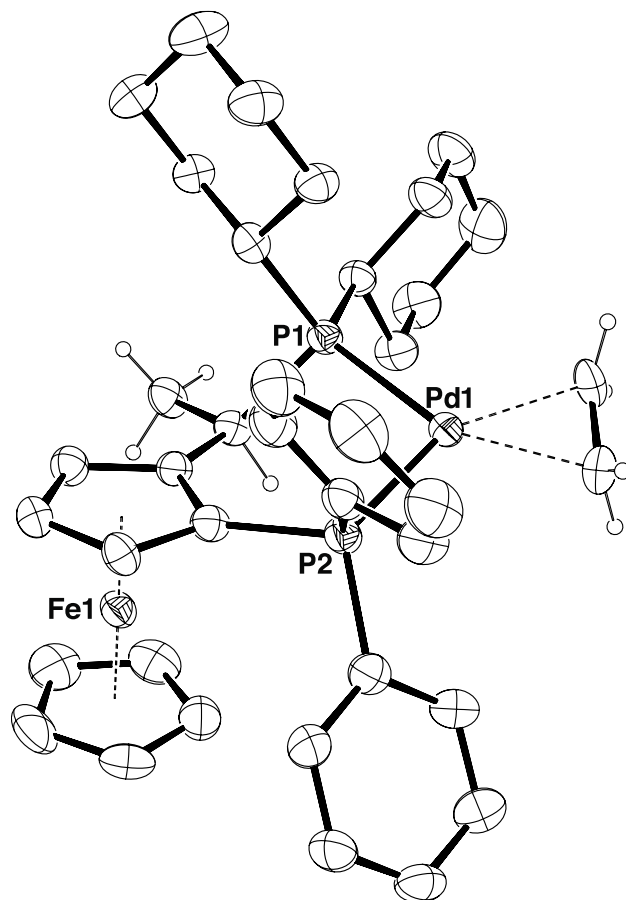


Figure 1. ORTEP drawing of the title compound with 50% thermal ellipsoids.

**Table 1. Summary of Structure Determination of Compound 4**

Empirical formula	$C_{43}H_{60}FeP_2Pd$
Formula weight	801.10
Diffractometer	Rigaku XtaLAB Synergy-S
Temperature/K	100(2)
Crystal system	tetragonal
Space group	$P4_3$
a	16.84223(8)Å

c	13.46917(11)Å
Volume	3820.68(5)Å <sup>3</sup>
Z	4
d <sub>calc</sub>	1.393 g/cm <sup>3</sup>
μ	7.838 mm <sup>-1</sup>
F(000)	1680.0
Crystal size, mm	0.37 × 0.02 × 0.02
2θ range for data collection	5.248 - 148.978°
Index ranges	-21 ≤ h ≤ 21, -19 ≤ k ≤ 21, -16 ≤ l ≤ 16
Reflections collected	63949
Independent reflections	7361[R(int) = 0.0673]
Data/restraints/parameters	7361/77/446
Goodness-of-fit on F <sup>2</sup>	1.092
Final R indexes [I ≥ 2σ (I)]	R <sub>1</sub> = 0.0322, wR <sub>2</sub> = 0.0856
Final R indexes [all data]	R <sub>1</sub> = 0.0334, wR <sub>2</sub> = 0.0862
Largest diff. peak/hole	0.35/-0.84 eÅ <sup>-3</sup>
Flack parameter	-0.016(3)

**Table 2 . Refined Positional Parameters for Compound 4**

Atom	x	y	z	U(eq)
Pd1	0.36914(2)	0.84936(2)	0.40869(2)	0.02508(10)
Fe1	0.52488(4)	1.08179(4)	0.54709(6)	0.02710(17)
P1	0.48851(7)	0.81115(7)	0.47853(10)	0.0244(2)
P2	0.35416(7)	0.96577(7)	0.49374(10)	0.0268(3)
C1	0.4403(3)	0.9957(3)	0.5662(4)	0.0265(10)
C2	0.5195(3)	0.9606(3)	0.5585(4)	0.0247(9)
C3	0.5656(3)	0.9927(3)	0.6370(4)	0.0295(10)
C4	0.5186(3)	1.0465(3)	0.6932(4)	0.0303(10)
C5	0.4424(3)	1.0489(3)	0.6498(4)	0.0284(10)
C6	0.5078(4)	1.1333(3)	0.4113(5)	0.0417(12)
C7	0.5850(4)	1.1030(3)	0.4181(5)	0.0434(13)
C8	0.6240(3)	1.1403(4)	0.4979(6)	0.0488(16)
C9	0.5697(4)	1.1954(3)	0.5412(6)	0.0505(16)
C10	0.4973(4)	1.1902(3)	0.4862(5)	0.0443(14)
C11	0.5505(3)	0.9041(3)	0.4804(4)	0.0260(9)
C12	0.6409(3)	0.8944(3)	0.4881(5)	0.0327(11)
C13	0.5517(3)	0.7412(3)	0.4062(4)	0.0287(9)
C14	0.5673(3)	0.7741(3)	0.3018(4)	0.0352(11)
C15	0.6217(4)	0.7184(4)	0.2443(5)	0.0459(14)
C16	0.5875(5)	0.6350(4)	0.2381(6)	0.0574(18)

C17	0.5670(4)	0.6022(3)	0.3398(5)	0.0465(15)
C18	0.5128(3)	0.6584(3)	0.3987(5)	0.0366(12)
C19	0.4918(3)	0.7750(3)	0.6098(4)	0.0280(10)
C20	0.5687(3)	0.7340(3)	0.6396(4)	0.0306(10)
C21	0.5674(3)	0.7063(4)	0.7471(5)	0.0390(12)
C22	0.4969(4)	0.6521(4)	0.7668(5)	0.0470(15)
C23	0.4191(3)	0.6949(4)	0.7408(5)	0.0427(13)
C24	0.4195(3)	0.7227(3)	0.6336(4)	0.0321(11)
C25	0.2791(3)	0.9519(3)	0.5907(4)	0.0310(10)
C26	0.2982(3)	0.9245(3)	0.6848(5)	0.0375(12)
C27	0.2389(4)	0.9099(4)	0.7550(5)	0.0449(14)
C28	0.1600(4)	0.9219(4)	0.7300(6)	0.0478(15)
C29	0.1394(3)	0.9468(4)	0.6357(6)	0.0502(16)
C30	0.1983(3)	0.9623(3)	0.5672(5)	0.0380(12)
C31	0.3169(3)	1.0563(3)	0.4326(4)	0.0314(11)
C32	0.3049(3)	1.1280(3)	0.4803(5)	0.0402(12)
C33	0.2770(4)	1.1935(3)	0.4306(5)	0.0436(14)
C34	0.2581(3)	1.1889(3)	0.3312(5)	0.0393(13)
C35	0.2692(3)	1.1173(4)	0.2822(5)	0.0404(12)
C36	0.2984(3)	1.0523(3)	0.3325(5)	0.0349(11)
C37	0.2766(4)	0.8325(4)	0.3028(6)	0.0503(16)
C38	0.3250(4)	0.7652(3)	0.3040(5)	0.0430(14)
C39	0.8568(5)	0.2142(5)	0.4870(7)	0.0683(19)
C40	0.8631(7)	0.1564(5)	0.5723(8)	0.095(3)



C41	0.8511(8)	0.0718(5)	0.5304(10)	0.121(4)
C42	0.8414(10)	0.0114(7)	0.6068(12)	0.146(4)
C43	0.9034(17)	0.0131(19)	0.6893(17)	0.152(6)
C43'	0.8927(19)	-0.0624(13)	0.597(2)	0.150(6)

**Table 3 . Positional Parameters for Hydrogens in Compound 4**

Atom	<i>x</i>	<i>y</i>	<i>z</i>	U(eq)
H3	0.619575	0.980152	0.650087	0.035
H4	0.535515	1.075676	0.749747	0.036
H5	0.399309	1.080498	0.672314	0.034
H6	0.46895	1.117851	0.363867	0.05
H7	0.607434	1.063768	0.375838	0.052
H8	0.676906	1.130555	0.519147	0.059
H9	0.579812	1.229256	0.596222	0.061
H10	0.450432	1.220002	0.498295	0.053
H11	0.540736	0.930755	0.415238	0.031
H12a	0.654691	0.874561	0.554302	0.049
H12b	0.666525	0.945892	0.477216	0.049
H12c	0.659118	0.85657	0.437768	0.049
H13	0.603806	0.735436	0.44113	0.034
H14a	0.516334	0.78002	0.265872	0.042
H14b	0.592267	0.82717	0.306832	0.042
H15a	0.629678	0.739365	0.176415	0.055
H15b	0.674165	0.716258	0.277435	0.055
H16a	0.539026	0.635868	0.19649	0.069
H16b	0.626546	0.599491	0.205694	0.069

H17a	0.616624	0.593324	0.377637	0.056
H17b	0.540184	0.550284	0.331922	0.056
H18a	0.503881	0.636769	0.466143	0.044
H18b	0.460731	0.662893	0.365143	0.044
H19	0.487156	0.823128	0.652845	0.034
H20a	0.577587	0.687647	0.595705	0.037
H20b	0.613604	0.771188	0.630092	0.037
H21a	0.617173	0.677423	0.762107	0.047
H21b	0.564425	0.752994	0.791521	0.047
H22a	0.496265	0.636524	0.837678	0.056
H22b	0.501835	0.603323	0.726339	0.056
H23a	0.373813	0.658347	0.751414	0.051
H23b	0.412056	0.74114	0.785281	0.051
H24a	0.370397	0.753145	0.620264	0.038
H24b	0.419777	0.675844	0.589215	0.038
H26	0.352266	0.915491	0.701696	0.045
H27	0.252633	0.89188	0.819625	0.054
H28	0.119687	0.912837	0.778057	0.057
H29	0.085157	0.953155	0.618181	0.06
H30	0.184036	0.980422	0.502777	0.046
H32	0.316313	1.132062	0.549195	0.048
H33	0.270651	1.242349	0.46501	0.052
H34	0.237873	1.233894	0.296863	0.047
H35	0.256614	1.113099	0.213678	0.048

H36	0.306005	1.003782	0.297792	0.042
H37a	0.282(5)	0.865(4)	0.247(4)	0.067
H37b	0.227(2)	0.834(5)	0.333(6)	0.067
H38a	0.355(4)	0.758(4)	0.247(4)	0.057
H38b	0.307(4)	0.719(3)	0.335(5)	0.057
H39a	0.864234	0.268415	0.511659	0.102
H39b	0.897816	0.202119	0.437623	0.102
H39c	0.804266	0.209502	0.456274	0.102
H40a	0.822059	0.168231	0.622795	0.114
H40b	0.915964	0.16082	0.604073	0.114
H41a	0.803546	0.071638	0.487196	0.146
H41b	0.897453	0.057817	0.488702	0.146
H42a	0.843014	-0.041468	0.574668	0.176
H42b	0.788234	0.017712	0.637004	0.176
H42a'	0.785108	-0.005422	0.607166	0.176
H42b'	0.852599	0.036149	0.671941	0.176
H43a	0.892195	-0.029374	0.737019	0.229
H43b	0.956284	0.00524	0.66072	0.229
H43c	0.901381	0.064552	0.723196	0.229
H43a'	0.881162	-0.098597	0.6524	0.225
H43b'	0.881112	-0.088944	0.534201	0.225
H43c'	0.948836	-0.04723	0.599199	0.225

**Table 4 . Refined Thermal Parameters (U's) for Compound 4**

Atom	U <sub>11</sub>	U <sub>22</sub>	U <sub>33</sub>	U <sub>23</sub>	U <sub>13</sub>	U <sub>12</sub>
Pd1	0.02446(16)	0.02160(16)	0.02917(17)	0.00015(13)	-0.00317(14)	-0.00101(12)
Fe1	0.0273(4)	0.0236(3)	0.0304(4)	-0.0011(3)	-0.0008(3)	-0.0038(3)
P1	0.0226(5)	0.0221(5)	0.0287(6)	-0.0010(4)	-0.0004(4)	0.0013(4)
P2	0.0235(5)	0.0231(5)	0.0340(7)	-0.0020(5)	-0.0022(5)	0.0011(4)
C1	0.021(2)	0.025(2)	0.033(3)	0.0023(19)	0.0013(18)	-0.0010(16)
C2	0.020(2)	0.024(2)	0.030(2)	0.0023(18)	-0.0013(18)	-0.0006(16)
C3	0.027(2)	0.029(2)	0.032(3)	-0.001(2)	-0.0011(19)	-0.0013(17)
C4	0.033(2)	0.028(2)	0.030(3)	-0.0044(19)	-0.003(2)	-0.0019(19)
C5	0.027(2)	0.027(2)	0.031(3)	-0.007(2)	0.003(2)	-0.0016(17)
C6	0.052(3)	0.039(3)	0.034(3)	0.009(3)	-0.005(3)	-0.015(2)
C7	0.048(3)	0.038(3)	0.044(3)	0.005(3)	0.016(3)	-0.007(2)
C8	0.034(3)	0.049(3)	0.064(5)	0.017(3)	0.003(3)	-0.015(2)
C9	0.066(4)	0.033(3)	0.052(4)	0.000(3)	0.000(3)	-0.025(3)
C10	0.053(3)	0.027(2)	0.052(4)	0.012(2)	0.005(3)	0.001(2)
C11	0.024(2)	0.024(2)	0.030(2)	0.0008(19)	0.0031(19)	-0.0002(16)
C12	0.022(2)	0.031(2)	0.046(3)	-0.002(2)	0.001(2)	-0.0041(18)
C13	0.029(2)	0.025(2)	0.032(2)	-0.002(2)	-0.001(2)	0.0022(16)
C14	0.042(3)	0.033(3)	0.030(3)	-0.003(2)	0.006(2)	0.007(2)
C15	0.052(3)	0.050(3)	0.036(3)	-0.005(3)	0.010(3)	0.008(3)
C16	0.064(4)	0.054(4)	0.054(4)	-0.023(3)	0.000(3)	0.012(3)

C17	0.053(3)	0.030(3)	0.056(4)	-0.013(3)	0.002(3)	0.006(2)
C18	0.037(2)	0.026(2)	0.047(3)	-0.005(2)	0.002(2)	0.0031(19)
C19	0.024(2)	0.028(2)	0.031(3)	-0.0032(19)	0.0023(19)	-0.0006(18)
C20	0.029(2)	0.031(2)	0.032(3)	0.003(2)	0.0020(19)	0.0017(18)
C21	0.036(3)	0.046(3)	0.035(3)	0.008(2)	-0.002(2)	0.008(2)
C22	0.039(3)	0.054(3)	0.047(4)	0.021(3)	0.006(3)	0.008(3)
C23	0.035(3)	0.042(3)	0.050(4)	0.010(3)	0.006(3)	0.001(2)
C24	0.027(2)	0.034(2)	0.035(3)	0.007(2)	0.003(2)	-0.0021(19)
C25	0.024(2)	0.026(2)	0.042(3)	-0.002(2)	-0.002(2)	-0.0008(18)
C26	0.030(2)	0.036(3)	0.047(3)	0.000(2)	0.001(2)	-0.004(2)
C27	0.040(3)	0.050(3)	0.045(3)	0.002(3)	0.007(3)	-0.011(3)
C28	0.035(3)	0.053(3)	0.055(4)	-0.002(3)	0.016(3)	-0.011(3)
C29	0.029(3)	0.051(3)	0.071(5)	0.002(3)	0.004(3)	-0.005(2)
C30	0.028(2)	0.037(3)	0.049(4)	0.003(2)	0.004(2)	0.001(2)
C31	0.023(2)	0.031(2)	0.040(3)	0.000(2)	0.001(2)	0.0018(18)
C32	0.042(3)	0.034(3)	0.045(3)	-0.003(2)	-0.011(3)	0.006(2)
C33	0.043(3)	0.029(2)	0.060(4)	-0.004(2)	-0.008(3)	0.006(2)
C34	0.029(2)	0.031(3)	0.058(4)	0.010(3)	0.000(2)	0.005(2)
C35	0.038(3)	0.044(3)	0.039(3)	0.006(2)	0.005(2)	0.008(2)
C36	0.036(3)	0.030(2)	0.039(3)	0.005(2)	0.007(2)	0.004(2)
C37	0.048(3)	0.045(3)	0.058(4)	0.002(3)	-0.030(3)	-0.010(3)
C38	0.056(3)	0.034(3)	0.040(3)	-0.011(2)	-0.016(3)	-0.012(2)
C39	0.058(4)	0.072(4)	0.074(5)	-0.014(4)	0.011(4)	0.003(4)
C40	0.093(6)	0.087(5)	0.106(7)	0.006(4)	0.034(5)	0.004(5)

C41	0.135(8)	0.086(5)	0.144(9)	-0.006(5)	0.055(7)	0.011(6)
C42	0.161(10)	0.120(7)	0.158(11)	0.015(7)	0.057(8)	0.024(8)
C43	0.149(13)	0.136(11)	0.172(13)	0.019(11)	0.049(10)	0.028(11)
C43'	0.152(13)	0.128(10)	0.169(14)	0.019(10)	0.041(11)	0.032(10)

**Table 5 . Bond Distances in Compound 4, Å**

Pd1-P1	2.3110(12)	Pd1-P2	2.2848(12)	Pd1-C37	2.132(6)
Pd1-C38	2.133(5)	Fe1-C1	2.048(5)	Fe1-C2	2.048(4)
Fe1-C3	2.047(5)	Fe1-C4	2.058(6)	Fe1-C5	2.038(5)
Fe1-C6	2.045(6)	Fe1-C7	2.043(6)	Fe1-C8	2.049(6)
Fe1-C9	2.059(5)	Fe1-C10	2.054(5)	P1-C11	1.882(5)
P1-C13	1.863(5)	P1-C19	1.871(5)	P2-C1	1.820(5)
P2-C25	1.832(6)	P2-C31	1.843(5)	C1-C2	1.462(6)
C1-C5	1.439(7)	C2-C3	1.419(7)	C2-C11	1.512(7)
C3-C4	1.421(7)	C4-C5	1.411(7)	C6-C7	1.401(9)
C6-C10	1.404(9)	C7-C8	1.408(10)	C8-C9	1.428(10)
C9-C10	1.429(10)	C11-C12	1.534(6)	C13-C14	1.535(8)
C13-C18	1.543(6)	C14-C15	1.523(8)	C15-C16	1.521(10)
C16-C17	1.516(11)	C17-C18	1.536(7)	C19-C20	1.522(7)
C19-C24	1.536(6)	C20-C21	1.522(7)	C21-C22	1.520(8)
C22-C23	1.535(8)	C23-C24	1.519(8)	C25-C26	1.387(8)
C25-C30	1.408(7)	C26-C27	1.398(8)	C27-C28	1.386(9)
C28-C29	1.382(10)	C29-C30	1.380(9)	C31-C32	1.383(7)
C31-C36	1.386(8)	C32-C33	1.374(8)	C33-C34	1.379(10)
C34-C35	1.387(9)	C35-C36	1.379(8)	C37-C38	1.396(10)
C39-C40	1.509(10)	C40-C41	1.547(10)	C41-C42	1.456(10)



C42-C43 1.525(13) C42-C43' 1.518(12)

**Table 6 . Bond Angles in Compound 4, °**

P2-Pd1-P1	97.52(4)	C37-Pd1-P1	150.6(2)	C37-Pd1-P2	111.6(2)
C37-Pd1-C38	38.2(3)	C38-Pd1-P1	112.79(18)	C38-Pd1-P2	149.67(18)
C1-Fe1-C2	41.83(17)	C1-Fe1-C4	68.9(2)	C1-Fe1-C8	161.4(3)
C1-Fe1-C9	156.6(2)	C1-Fe1-C10	121.5(2)	C2-Fe1-C4	68.8(2)
C2-Fe1-C8	122.7(2)	C2-Fe1-C9	160.9(2)	C2-Fe1-C10	154.9(2)
C3-Fe1-C1	68.91(19)	C3-Fe1-C2	40.56(19)	C3-Fe1-C4	40.5(2)
C3-Fe1-C8	105.7(2)	C3-Fe1-C9	125.5(3)	C3-Fe1-C10	164.4(2)
C4-Fe1-C9	108.9(3)	C5-Fe1-C1	41.26(19)	C5-Fe1-C2	69.37(19)
C5-Fe1-C3	68.08(19)	C5-Fe1-C4	40.3(2)	C5-Fe1-C6	128.8(2)
C5-Fe1-C7	164.4(2)	C5-Fe1-C8	155.0(3)	C5-Fe1-C9	121.9(2)
C5-Fe1-C10	111.0(2)	C6-Fe1-C1	108.3(2)	C6-Fe1-C2	118.9(2)
C6-Fe1-C3	152.6(2)	C6-Fe1-C4	166.1(2)	C6-Fe1-C8	67.8(3)
C6-Fe1-C9	67.9(3)	C6-Fe1-C10	40.0(3)	C7-Fe1-C1	125.1(2)
C7-Fe1-C2	105.1(2)	C7-Fe1-C3	117.7(2)	C7-Fe1-C4	152.8(2)
C7-Fe1-C6	40.1(3)	C7-Fe1-C8	40.2(3)	C7-Fe1-C9	67.8(3)
C7-Fe1-C10	67.5(2)	C8-Fe1-C4	119.3(3)	C8-Fe1-C9	40.7(3)
C8-Fe1-C10	68.1(3)	C10-Fe1-C4	128.8(2)	C10-Fe1-C9	40.7(3)
C11-P1-Pd1	104.88(15)	C13-P1-Pd1	117.41(17)	C13-P1-C11	102.5(2)
C13-P1-C19	105.7(2)	C19-P1-Pd1	120.08(15)	C19-P1-C11	104.0(2)
C1-P2-Pd1	114.76(16)	C1-P2-C25	101.7(2)	C1-P2-C31	106.3(2)

C25-P2-Pd1	108.94(16)	C25-P2-C31	100.9(2)	C31-P2-Pd1	121.56(18)
P2-C1-Fe1	133.1(3)	C2-C1-Fe1	69.1(2)	C2-C1-P2	125.2(4)
C5-C1-Fe1	69.0(3)	C5-C1-P2	127.7(3)	C5-C1-C2	106.5(4)
C1-C2-Fe1	69.1(2)	C1-C2-C11	128.2(4)	C3-C2-Fe1	69.7(3)
C3-C2-C1	107.0(4)	C3-C2-C11	124.7(4)	C11-C2-Fe1	124.1(3)
C2-C3-Fe1	69.8(3)	C2-C3-C4	109.6(4)	C4-C3-Fe1	70.2(3)
C3-C4-Fe1	69.3(3)	C5-C4-Fe1	69.1(3)	C5-C4-C3	107.7(4)
C1-C5-Fe1	69.8(3)	C4-C5-Fe1	70.6(3)	C4-C5-C1	109.2(4)
C7-C6-Fe1	69.9(4)	C7-C6-C10	108.5(6)	C10-C6-Fe1	70.3(4)
C6-C7-Fe1	70.0(4)	C6-C7-C8	108.7(6)	C8-C7-Fe1	70.1(4)
C7-C8-Fe1	69.6(3)	C7-C8-C9	107.7(6)	C9-C8-Fe1	70.1(3)
C8-C9-Fe1	69.3(3)	C8-C9-C10	107.1(6)	C10-C9-Fe1	69.5(3)
C6-C10-Fe1	69.6(3)	C6-C10-C9	107.9(6)	C9-C10-Fe1	69.9(3)
C2-C11-P1	110.0(3)	C2-C11-C12	111.3(4)	C12-C11-P1	117.6(3)
C14-C13-P1	110.4(3)	C14-C13-C18	109.8(5)	C18-C13-P1	111.3(3)
C15-C14-C13	110.2(4)	C16-C15-C14	111.7(5)	C17-C16-C15	111.9(6)
C16-C17-C18	112.2(5)	C17-C18-C13	109.8(5)	C20-C19-P1	115.0(3)
C20-C19-C24	111.1(4)	C24-C19-P1	111.1(3)	C21-C20-C19	112.2(4)
C22-C21-C20	111.2(5)	C21-C22-C23	110.2(5)	C24-C23-C22	110.9(5)
C23-C24-C19	112.3(4)	C26-C25-P2	122.2(4)	C26-C25-C30	118.1(5)
C30-C25-P2	119.4(4)	C25-C26-C27	120.7(5)	C28-C27-C26	119.7(6)
C29-C28-C27	120.5(6)	C30-C29-C28	119.5(6)	C29-C30-C25	121.4(6)
C32-C31-P2	124.4(5)	C32-C31-C36	117.5(5)	C36-C31-P2	118.1(4)
C33-C32-C31	121.7(6)	C32-C33-C34	120.5(5)	C33-C34-C35	118.6(5)

C36-C35-C34 120.4(6)	C35-C36-C31 121.3(5)	C38-C37-Pd1 70.9(3)
C37-C38-Pd1 70.9(3)	C39-C40-C41 107.9(8)	C42-C41-C40 113.6(9)
C41-C42-C43 115.2(12)	C41-C42-C43' 116.7(12)	

This report has been created with Olex2 [6], compiled on 2018.05.29 svn.r3508 for OlexSys.

### (Josiphos)Pd(CO)<sub>2</sub> (5)

Compound 5•3/2benzene, C<sub>47</sub>H<sub>53</sub>FeO<sub>2</sub>P<sub>2</sub>Pd, crystallizes in the orthorhombic space group P2<sub>1</sub>2<sub>1</sub>2 (systematic absences h00: h=odd and 0k0: k=odd) with a=69.6935(7)Å, b=12.6585(2)Å, c=9.33880(10)Å, V=8238.83(18)Å<sup>3</sup>, Z=8, and d<sub>calc</sub>=1.409 g/cm<sup>3</sup>. X-ray intensity data were collected on a Rigaku XtaLAB Synergy-S diffractometer [1] equipped with an HPC area detector (HyPix-6000HE) and employing confocal multilayer optic-monochromated Cu-Kα radiation (λ=1.54184 Å) at a temperature of 100K. Preliminary indexing was performed from a series of sixty 0.5° rotation frames with exposures of 15 seconds for θ = ±47.311° and 60 seconds for θ = 113.25°. A total of 2226 frames (22 runs) were collected employing ω scans with a crystal to detector distance of 34.0 mm, rotation widths of 0.5° and exposures of 20 seconds for θ = ±47.061° and 60 seconds for θ = 112.205° and -90°.

Rotation frames were integrated using CrysAlisPro [2], producing a listing of unaveraged F<sup>2</sup> and σ(F<sup>2</sup>) values. A total of 62377 reflections were measured over the ranges 7.098 ≤ 2θ ≤ 149.002°, -60 ≤ h ≤ 82, -15 ≤ k ≤ 14, -11 ≤ l ≤ 11 yielding 15848 unique reflections (R<sub>int</sub> = 0.0671). The intensity data were corrected for Lorentz and polarization effects and for absorption using SCALE3 ABSPACK [3] (minimum and maximum transmission 0.5480, 1.0000). The structure was solved by direct methods - SHELXT [4]. Refinement was by full-matrix least squares based on F<sup>2</sup> using SHELXL [5]. All reflections were used during refinement. The

weighting scheme used was  $w=1/[\sigma^2(F_o^2) + (0.0260P)^2 + 17.6113P]$  where  $P = (F_o^2 + 2F_c^2)/3$ . Non-hydrogen atoms were refined anisotropically and hydrogen atoms were refined using a riding model. Refinement converged to  $R1=0.0420$  and  $wR2=0.0890$  for 13731 observed reflections for which  $F > 4\sigma(F)$  and  $R1=0.0541$  and  $wR2=0.0951$  and  $GOF = 1.023$  for all 15848 unique, non-zero reflections and 957 variables. The maximum  $\Delta/\sigma$  in the final cycle of least squares was 0.001 and the two most prominent peaks in the final difference Fourier were +0.79 and -0.99 e/Å<sup>3</sup>.

Table 1. lists cell information, data collection parameters, and refinement data. Final positional and equivalent isotropic thermal parameters are given in Tables 2. and 3. Anisotropic thermal parameters are in Table 4. Tables 5. and 6. list bond distances and bond angles. Figure 1. is an ORTEP representation of the molecule with 50% probability thermal ellipsoids displayed.

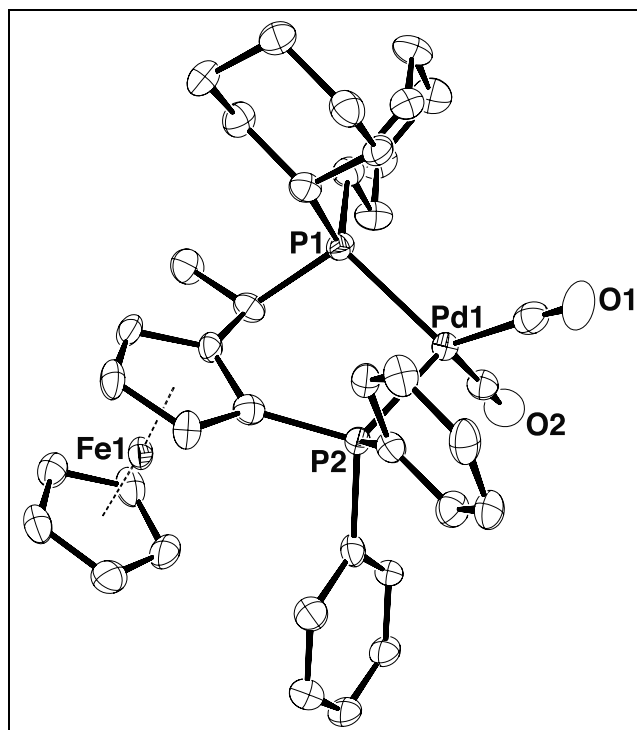


Figure 1. ORTEP drawing of the title compound with 50% thermal ellipsoids.

**Table 1. Summary of Structure Determination of Compound 5•3/2benzene**

Empirical formula	C <sub>47</sub> H <sub>53</sub> FeO <sub>2</sub> P <sub>2</sub> Pd
Formula weight	874.08
Diffractometer	Rigaku XtaLAB Synergy-S (HyPix-6000HE)
Temperature/K	100
Crystal system	orthorhombic
Space group	P2 <sub>1</sub> 2 <sub>1</sub> 2
a	69.6935(7)Å
b	12.6585(2)Å
c	9.33880(10)Å
Volume	8238.83(18)Å <sup>3</sup>
Z	8
d <sub>calc</sub>	1.409 g/cm <sup>3</sup>
μ	7.363 mm <sup>-1</sup>
F(000)	3624.0
Crystal size, mm	0.24 × 0.05 × 0.02
2θ range for data collection	7.098 - 149.002°
Index ranges	-60 ≤ h ≤ 82, -15 ≤ k ≤ 14, -11 ≤ l ≤ 11
Reflections collected	62377
Independent reflections	15848[R(int) = 0.0671]
Data/restraints/parameters	15848/0/957
Goodness-of-fit on F <sup>2</sup>	1.023
Final R indexes [I ≥ 2σ (I)]	R <sub>1</sub> = 0.0420, wR <sub>2</sub> = 0.0890
Final R indexes [all data]	R <sub>1</sub> = 0.0541, wR <sub>2</sub> = 0.0951

Largest diff. peak/hole      0.79/-0.99 eÅ<sup>-3</sup>  
Flack parameter                -0.007(3)

**Table 2 . Refined Positional Parameters for Compound 5•3/2benzene**

Atom	x	y	z	U(eq)
Pd1	0.44331(2)	0.50553(4)	0.38524(5)	0.02189(10)
Fe1	0.43402(2)	0.72934(9)	0.85622(11)	0.0240(2)
P1	0.44842(2)	0.41339(14)	0.60575(18)	0.0221(3)
P2	0.42563(2)	0.64307(14)	0.49668(17)	0.0203(3)
O1	0.41127(8)	0.4094(5)	0.1950(6)	0.0469(16)
O2	0.48106(7)	0.5765(5)	0.2407(6)	0.0430(14)
C1	0.42405(9)	0.6371(6)	0.6895(7)	0.0246(15)
C2	0.43687(9)	0.5772(6)	0.7827(7)	0.0226(14)
C3	0.42891(9)	0.5784(6)	0.9223(7)	0.0276(15)
C4	0.41162(9)	0.6362(6)	0.9215(7)	0.0287(15)
C5	0.40858(9)	0.6728(6)	0.7792(7)	0.0274(16)
C6	0.44942(11)	0.8561(6)	0.7791(8)	0.0362(18)
C7	0.46104(9)	0.7920(7)	0.8714(8)	0.0329(16)
C8	0.45210(9)	0.7894(7)	1.0094(7)	0.0315(16)
C9	0.43514(10)	0.8504(6)	1.0018(8)	0.0325(17)
C10	0.43346(11)	0.8929(6)	0.8587(8)	0.0363(18)
C11	0.45494(9)	0.5207(6)	0.7377(7)	0.0257(15)
C12	0.46754(10)	0.4908(7)	0.8678(8)	0.0352(16)

C13	0.46841(9)	0.3167(6)	0.6247(8)	0.0278(15)
C14	0.48683(9)	0.3657(6)	0.5607(9)	0.0321(16)
C15	0.50377(9)	0.2913(7)	0.5782(9)	0.0391(18)
C16	0.49987(11)	0.1852(6)	0.5077(9)	0.0408(18)
C17	0.48155(10)	0.1364(6)	0.5639(10)	0.0365(18)
C18	0.46434(9)	0.2108(6)	0.5511(7)	0.0294(15)
C19	0.42690(9)	0.3500(6)	0.6869(7)	0.0258(15)
C20	0.43049(9)	0.2873(7)	0.8257(7)	0.0300(16)
C21	0.41160(9)	0.2503(6)	0.8921(8)	0.0316(16)
C22	0.40005(10)	0.1841(6)	0.7842(8)	0.0326(17)
C23	0.39639(10)	0.2465(6)	0.6461(8)	0.0313(16)
C24	0.41516(9)	0.2845(6)	0.5815(7)	0.0257(14)
C25	0.40028(9)	0.6292(6)	0.4437(7)	0.0245(14)
C26	0.38878(9)	0.5541(6)	0.5120(7)	0.0254(15)
C27	0.37044(9)	0.5328(6)	0.4620(7)	0.0292(16)
C28	0.36354(10)	0.5857(7)	0.3425(7)	0.0322(17)
C29	0.37491(10)	0.6608(7)	0.2746(8)	0.0324(17)
C30	0.39318(10)	0.6802(6)	0.3240(7)	0.0294(16)
C31	0.43035(9)	0.7824(6)	0.4582(6)	0.0235(14)
C32	0.4182(1)	0.8640(6)	0.5041(8)	0.0295(16)
C33	0.42262(11)	0.9678(6)	0.4776(8)	0.0363(18)
C34	0.43909(9)	0.9938(6)	0.4028(7)	0.0323(15)
C35	0.4512(1)	0.9151(6)	0.3560(7)	0.0281(15)
C36	0.44696(8)	0.8107(5)	0.3839(7)	0.0233(13)
C37	0.42358(10)	0.4404(6)	0.2605(8)	0.0317(17)



C38	0.46741(10)	0.5492(6)	0.2954(8)	0.0296(16)
Pd1'	0.30842(2)	0.70814(4)	0.07274(5)	0.02329(11)
Fe1'	0.26625(2)	0.79628(11)	-0.37060(11)	0.0309(3)
P1'	0.32413(2)	0.69168(14)	-0.15540(16)	0.0205(3)
P2'	0.28551(2)	0.82997(15)	-0.01652(17)	0.0224(4)
O1'	0.33169(8)	0.8310(5)	0.3026(6)	0.0464(16)
O2'	0.29375(10)	0.5087(6)	0.2253(6)	0.065(2)
C1'	0.28428(9)	0.8434(6)	-0.2088(7)	0.0240(15)
C2'	0.29446(8)	0.7806(6)	-0.3160(6)	0.0214(14)
C3'	0.29267(9)	0.8342(6)	-0.4509(7)	0.0264(15)
C4'	0.28156(10)	0.9254(6)	-0.4299(7)	0.0325(17)
C5'	0.27625(10)	0.9320(6)	-0.2840(7)	0.0297(16)
C6'	0.24488(14)	0.7030(14)	-0.2921(11)	0.081(5)
C7'	0.25498(13)	0.6452(9)	-0.3917(13)	0.066(3)
C8'	0.25405(11)	0.6977(9)	-0.5189(10)	0.049(2)
C9'	0.24338(12)	0.7903(10)	-0.5069(11)	0.060(3)
C10'	0.23716(11)	0.7946(12)	-0.3560(14)	0.088(5)
C11'	0.30467(9)	0.6769(6)	-0.2940(7)	0.0237(14)
C12'	0.31026(10)	0.6263(6)	-0.4369(7)	0.0299(15)
C13'	0.33914(9)	0.5709(6)	-0.1760(7)	0.0242(14)
C14'	0.32751(9)	0.4714(5)	-0.1478(8)	0.0277(15)
C15'	0.33991(11)	0.3727(6)	-0.1565(9)	0.0353(17)
C16'	0.35664(11)	0.3777(6)	-0.0507(9)	0.0357(18)
C17'	0.36846(9)	0.4776(6)	-0.0771(8)	0.0311(16)
C18'	0.35610(9)	0.5773(6)	-0.0704(8)	0.0261(14)

C19'	0.33888(9)	0.8022(6)	-0.2281(7)	0.0233(14)
C20'	0.35287(9)	0.7745(6)	-0.3492(7)	0.0257(15)
C21'	0.36222(9)	0.8733(6)	-0.4117(7)	0.0278(15)
C22'	0.37234(10)	0.9371(6)	-0.2967(8)	0.0287(16)
C23'	0.35863(10)	0.9645(6)	-0.1753(7)	0.0267(15)
C24'	0.34923(9)	0.8658(5)	-0.1121(7)	0.0244(14)
C25'	0.29394(9)	0.9613(6)	0.0348(7)	0.0252(15)
C26'	0.30603(9)	1.0195(6)	-0.0521(7)	0.0300(16)
C27'	0.31401(10)	1.1132(7)	-0.0064(10)	0.041(2)
C28'	0.30995(11)	1.1514(6)	0.130(1)	0.044(2)
C29'	0.29795(10)	1.0942(7)	0.2191(9)	0.040(2)
C30'	0.29021(9)	0.9997(8)	0.1731(7)	0.0346(17)
C31'	0.26021(9)	0.8310(6)	0.0388(7)	0.0261(15)
C32'	0.24897(9)	0.9239(6)	0.0405(7)	0.0276(15)
C33'	0.22976(9)	0.9195(6)	0.0761(8)	0.0321(16)
C34'	0.22146(9)	0.8229(7)	0.1106(8)	0.0341(17)
C35'	0.23222(9)	0.7328(6)	0.1122(8)	0.0343(17)
C36'	0.25166(9)	0.7366(6)	0.0782(7)	0.0273(15)
C37'	0.32363(9)	0.7880(7)	0.2145(8)	0.0333(17)
C38'	0.29922(11)	0.5780(7)	0.1582(8)	0.0387(19)
C39	0.45617(11)	0.1211(7)	1.0677(9)	0.0392(18)
C40	0.45747(12)	0.2155(8)	1.1360(8)	0.044(2)
C41	0.47450(13)	0.2733(7)	1.1345(9)	0.046(2)
C42	0.49008(13)	0.2330(7)	1.0648(9)	0.047(2)
C43	0.48865(12)	0.1378(8)	0.9942(11)	0.052(2)

C44	0.47175(12)	0.0813(7)	0.9969(10)	0.048(2)
C45	0.32222(11)	1.1444(7)	0.5776(8)	0.0422(19)
C46	0.30719(11)	1.2165(8)	0.5727(8)	0.045(2)
C47	0.30957(12)	1.3141(7)	0.5112(9)	0.047(2)
C48	0.32730(11)	1.3405(7)	0.4542(9)	0.042(2)
C49	0.34240(11)	1.2706(8)	0.4619(9)	0.044(2)
C50	0.33987(11)	1.1725(8)	0.5223(9)	0.045(2)
C51	0.37100(12)	0.9622(7)	0.2167(9)	0.042(2)
C52	0.35723(11)	1.0386(7)	0.1983(9)	0.0385(19)
C53	0.36267(11)	1.1427(7)	0.1814(8)	0.0394(19)
C54	0.38178(12)	1.1698(9)	0.1828(10)	0.054(3)
C55	0.39546(14)	1.0955(11)	0.2041(12)	0.073(4)
C56	0.38991(12)	0.9904(10)	0.2182(10)	0.058(3)

**Table 3 . Positional Parameters for Hydrogens in Compound 5•3/2benzene**

Atom	<i>x</i>	<i>y</i>	<i>z</i>	U(eq)
H3	0.434394	0.545339	1.003925	0.033
H4	0.403485	0.648494	1.001409	0.034
H5	0.398001	0.714251	0.748367	0.033
H6	0.45199	0.87127	0.681388	0.043
H7	0.473266	0.755792	0.844237	0.04
H8	0.456734	0.753126	1.091498	0.038
H9	0.425879	0.862328	1.08191	0.039
H10	0.422876	0.938843	0.822148	0.044
H11	0.462556	0.573626	0.682113	0.031
H12a	0.460287	0.444189	0.931707	0.053
H12b	0.471205	0.555049	0.919611	0.053
H12c	0.479105	0.454322	0.834473	0.053
H13	0.4706	0.303368	0.728991	0.033
H14a	0.484798	0.3806	0.457768	0.039
H14b	0.489634	0.433377	0.609503	0.039
H15a	0.506357	0.280497	0.681377	0.047
H15b	0.515313	0.323586	0.534596	0.047
H16a	0.498828	0.194944	0.402822	0.049
H16b	0.510749	0.136916	0.526604	0.049
H17a	0.483355	0.116948	0.66568	0.044
H17b	0.478839	0.070775	0.509764	0.044

H18a	0.452959	0.177499	0.595597	0.035
H18b	0.461444	0.223217	0.448686	0.035
H19	0.418337	0.409802	0.715453	0.031
H20a	0.438635	0.225183	0.804291	0.036
H20b	0.43744	0.332379	0.895064	0.036
H21a	0.403945	0.31244	0.921749	0.038
H21b	0.414303	0.207409	0.978407	0.038
H22a	0.407216	0.118711	0.761232	0.039
H22b	0.38763	0.163536	0.827437	0.039
H23a	0.389597	0.201124	0.576287	0.038
H23b	0.388097	0.308075	0.667433	0.038
H24a	0.412391	0.327614	0.495561	0.031
H24b	0.422811	0.222585	0.550895	0.031
H26	0.39355	0.517312	0.593219	0.031
H27	0.362629	0.482273	0.509418	0.035
H28	0.351057	0.570564	0.307036	0.039
H29	0.37008	0.698559	0.194407	0.039
H30	0.401064	0.729589	0.274838	0.035
H32	0.406739	0.847064	0.554182	0.035
H33	0.414324	1.022113	0.510845	0.044
H34	0.442034	1.065737	0.383808	0.039
H35	0.462489	0.932742	0.30426	0.034
H36	0.45549	0.757039	0.3521	0.028
H3'	0.298082	0.811831	-0.539209	0.032
H4'	0.278145	0.974725	-0.502125	0.039

H5'	0.268627	0.986161	-0.242542	0.036
H6'	0.243334	0.683969	-0.194364	0.098
H7'	0.261445	0.580272	-0.374714	0.079
H8'	0.259942	0.674118	-0.604907	0.058
H9'	0.240673	0.840137	-0.580258	0.072
H10'	0.22959	0.847672	-0.311493	0.105
H11'	0.294948	0.628459	-0.250531	0.028
H12d	0.319001	0.673425	-0.48869	0.045
H12e	0.298706	0.614445	-0.494541	0.045
H12f	0.316658	0.558618	-0.419099	0.045
H13'	0.344267	0.568274	-0.275981	0.029
H14c	0.31702	0.466366	-0.218939	0.033
H14d	0.321639	0.475888	-0.051459	0.033
H15c	0.344983	0.365197	-0.255007	0.042
H15d	0.331948	0.309826	-0.135334	0.042
H16c	0.351642	0.378058	0.048486	0.043
H16d	0.364877	0.31462	-0.062573	0.043
H17c	0.374619	0.472969	-0.17239	0.037
H17d	0.378742	0.482303	-0.004204	0.037
H18c	0.364092	0.639594	-0.093722	0.031
H18d	0.35112	0.586393	0.028141	0.031
H19'	0.329463	0.852412	-0.271615	0.028
H20c	0.362963	0.726879	-0.311828	0.031
H20d	0.345883	0.736606	-0.425802	0.031
H21c	0.3716	0.852433	-0.486051	0.033

H21d	0.35227	0.917615	-0.457718	0.033
H22c	0.377488	1.002933	-0.339069	0.034
H22d	0.38326	0.89588	-0.258267	0.034
H23c	0.348538	1.012583	-0.211746	0.032
H23d	0.365753	1.002143	-0.099071	0.032
H24c	0.339918	0.886941	-0.03732	0.029
H24d	0.359163	0.821166	-0.066605	0.029
H26'	0.308901	0.994326	-0.145484	0.036
H27'	0.322288	1.151743	-0.068092	0.049
H28'	0.315376	1.216161	0.161676	0.052
H29'	0.295026	1.120098	0.312034	0.047
H30'	0.282263	0.960086	0.235915	0.042
H32'	0.254671	0.989784	0.016893	0.033
H33'	0.22225	0.982089	0.077047	0.039
H34'	0.208189	0.819585	0.133218	0.041
H35'	0.226423	0.66726	0.136471	0.041
H36'	0.259129	0.673943	0.082169	0.033
H39	0.444459	0.082795	1.069044	0.047
H40	0.446621	0.242481	1.18553	0.053
H41	0.475246	0.339827	1.18129	0.055
H42	0.501884	0.270521	1.064928	0.056
H43	0.499392	0.110923	0.943299	0.062
H44	0.470929	0.014966	0.949754	0.058
H45	0.320358	1.076433	0.61854	0.051
H46	0.295108	1.197961	0.612439	0.053

H47	0.299216	1.362801	0.507776	0.056
H48	0.329046	1.40731	0.409586	0.051
H49	0.354613	1.290223	0.425344	0.052
H50	0.350274	1.124021	0.525941	0.054
H51	0.367401	0.890279	0.228369	0.051
H52	0.344029	1.019912	0.197136	0.046
H53	0.353185	1.195739	0.16877	0.047
H54	0.385418	1.241361	0.168648	0.064
H55	0.408615	1.11473	0.20931	0.088
H56	0.399442	0.937347	0.229105	0.07



**Table 4 . Refined Thermal Parameters (U's) for Compound 5•3/2benzene**

Atom	U <sub>11</sub>	U <sub>22</sub>	U <sub>33</sub>	U <sub>23</sub>	U <sub>13</sub>	U <sub>12</sub>
Pd1	0.0245(2)	0.0219(2)	0.0193(2)	0.0000(2)	0.00050(17)	0.0001(2)
Fe1	0.0276(5)	0.0268(6)	0.0176(5)	-0.0036(4)	0.0013(4)	-0.0054(4)
P1	0.0224(7)	0.0228(8)	0.0210(8)	0.0016(7)	-0.0035(6)	-0.0025(6)
P2	0.0234(8)	0.0204(9)	0.0171(8)	0.0001(7)	-0.0003(6)	-0.0010(7)
O1	0.052(3)	0.062(4)	0.027(3)	0.000(3)	-0.010(2)	-0.022(3)
O2	0.036(3)	0.043(4)	0.050(4)	0.002(3)	0.015(3)	-0.007(3)
C1	0.023(3)	0.023(4)	0.028(4)	-0.001(3)	-0.003(3)	-0.004(3)
C2	0.028(3)	0.024(4)	0.016(3)	-0.002(3)	-0.002(2)	-0.008(3)
C3	0.038(4)	0.029(4)	0.016(3)	0.004(3)	0.001(3)	-0.010(3)
C4	0.030(3)	0.039(4)	0.018(3)	-0.005(3)	0.007(3)	-0.009(3)
C5	0.025(3)	0.037(4)	0.020(3)	-0.003(3)	0.001(3)	-0.001(3)
C6	0.052(5)	0.031(4)	0.025(4)	0.003(3)	-0.002(3)	-0.018(4)
C7	0.029(3)	0.040(4)	0.030(4)	-0.010(4)	0.005(3)	-0.013(3)
C8	0.033(3)	0.036(4)	0.025(3)	0.000(4)	-0.003(3)	-0.003(3)
C9	0.034(4)	0.036(4)	0.027(4)	-0.011(3)	0.005(3)	-0.006(3)
C10	0.046(4)	0.028(4)	0.036(4)	-0.002(3)	-0.009(3)	-0.004(3)
C11	0.023(3)	0.023(4)	0.031(4)	-0.004(3)	-0.001(3)	-0.002(3)
C12	0.036(3)	0.037(4)	0.033(4)	-0.003(4)	-0.015(3)	0.002(3)
C13	0.026(3)	0.028(4)	0.029(3)	0.003(3)	-0.004(3)	-0.004(3)
C14	0.024(3)	0.027(4)	0.045(4)	0.003(4)	-0.004(3)	-0.003(3)
C15	0.025(3)	0.043(5)	0.049(4)	0.008(4)	-0.005(3)	0.001(3)

C16	0.029(3)	0.040(5)	0.053(5)	0.000(4)	0.002(4)	0.005(4)
C17	0.032(4)	0.024(4)	0.053(5)	-0.003(4)	-0.005(3)	0.004(3)
C18	0.025(3)	0.030(4)	0.033(4)	0.003(3)	-0.001(3)	-0.002(3)
C19	0.026(3)	0.023(4)	0.029(4)	0.000(3)	-0.001(3)	0.001(3)
C20	0.028(3)	0.034(4)	0.027(3)	0.001(3)	-0.007(3)	-0.001(3)
C21	0.037(4)	0.035(4)	0.023(3)	0.007(3)	0.001(3)	-0.001(3)
C22	0.036(4)	0.030(4)	0.032(4)	0.005(3)	0.006(3)	-0.009(3)
C23	0.031(4)	0.030(4)	0.033(4)	-0.005(3)	0.000(3)	-0.005(3)
C24	0.030(3)	0.025(4)	0.022(3)	0.004(3)	0.002(2)	-0.007(3)
C25	0.028(3)	0.022(4)	0.023(3)	-0.003(3)	-0.002(3)	0.000(3)
C26	0.029(3)	0.028(4)	0.019(3)	-0.001(3)	0.001(3)	-0.001(3)
C27	0.022(3)	0.036(4)	0.029(4)	-0.006(3)	0.002(3)	-0.004(3)
C28	0.027(3)	0.046(5)	0.024(4)	-0.007(3)	-0.006(3)	0.004(3)
C29	0.040(4)	0.035(4)	0.022(3)	-0.003(3)	-0.009(3)	0.002(3)
C30	0.030(3)	0.031(4)	0.027(4)	0.000(3)	-0.003(3)	-0.006(3)
C31	0.026(3)	0.026(4)	0.019(3)	-0.005(3)	-0.001(2)	-0.004(3)
C32	0.029(3)	0.030(4)	0.030(4)	0.000(3)	0.003(3)	-0.003(3)
C33	0.050(4)	0.025(4)	0.034(4)	-0.001(3)	0.002(3)	0.005(3)
C34	0.046(4)	0.021(3)	0.030(4)	0.006(3)	0.000(3)	-0.010(3)
C35	0.032(3)	0.026(4)	0.026(4)	0.004(3)	0.000(3)	-0.008(3)
C36	0.028(3)	0.019(3)	0.023(3)	0.000(3)	-0.001(2)	0.003(3)
C37	0.033(4)	0.031(4)	0.030(4)	0.006(3)	0.008(3)	0.004(3)
C38	0.032(4)	0.027(4)	0.030(4)	-0.001(3)	-0.001(3)	0.005(3)
Pd1'	0.0228(2)	0.0277(3)	0.0194(2)	0.0006(2)	0.00118(17)	0.0003(2)
Fe1'	0.0210(5)	0.0510(8)	0.0207(5)	-0.0022(6)	-0.0019(4)	0.0002(5)

P1'	0.0215(7)	0.0233(9)	0.0166(7)	-0.0027(7)	0.0007(5)	-0.0011(7)
P2'	0.0220(8)	0.0274(10)	0.0177(8)	-0.0005(7)	0.0012(6)	0.0004(7)
O1'	0.048(3)	0.063(4)	0.028(3)	-0.013(3)	-0.011(2)	-0.018(3)
O2'	0.105(5)	0.052(4)	0.039(3)	0.024(3)	-0.004(3)	-0.039(4)
C1'	0.015(3)	0.033(4)	0.024(3)	-0.007(3)	0.003(2)	-0.003(3)
C2'	0.016(3)	0.027(4)	0.022(3)	0.001(3)	-0.002(2)	-0.002(3)
C3'	0.026(3)	0.037(4)	0.017(3)	0.000(3)	0.000(2)	-0.001(3)
C4'	0.041(4)	0.041(5)	0.016(3)	0.009(3)	0.003(3)	0.011(3)
C5'	0.034(4)	0.035(5)	0.019(3)	-0.005(3)	0.001(3)	0.012(3)
C6'	0.042(6)	0.156(14)	0.046(6)	0.001(8)	-0.010(4)	-0.052(8)
C7'	0.048(5)	0.071(7)	0.078(8)	0.006(7)	-0.023(5)	-0.026(5)
C8'	0.036(4)	0.066(7)	0.044(5)	-0.008(5)	-0.008(3)	-0.005(4)
C9'	0.047(5)	0.077(8)	0.057(6)	-0.014(6)	-0.035(4)	0.013(5)
C10'	0.013(4)	0.137(12)	0.113(10)	-0.083(10)	0.001(5)	0.003(5)
C11'	0.024(3)	0.021(4)	0.026(3)	0.004(3)	-0.001(2)	0.002(3)
C12'	0.032(3)	0.033(4)	0.025(3)	-0.007(3)	-0.006(3)	0.004(3)
C13'	0.028(3)	0.019(4)	0.025(3)	0.000(3)	-0.001(3)	-0.002(3)
C14'	0.030(3)	0.019(4)	0.034(4)	-0.005(3)	-0.003(3)	0.001(3)
C15'	0.042(4)	0.025(4)	0.039(4)	0.000(3)	-0.003(3)	-0.002(3)
C16'	0.041(4)	0.026(4)	0.040(4)	0.006(3)	-0.002(3)	0.005(3)
C17'	0.029(3)	0.031(4)	0.033(4)	0.004(3)	-0.001(3)	0.003(3)
C18'	0.029(3)	0.024(4)	0.025(3)	-0.001(3)	-0.002(3)	-0.001(3)
C19'	0.023(3)	0.024(4)	0.023(3)	-0.001(3)	0.001(2)	0.001(3)
C20'	0.027(3)	0.026(4)	0.025(3)	-0.005(3)	0.001(2)	0.001(3)
C21'	0.029(3)	0.034(4)	0.021(3)	-0.004(3)	0.007(3)	-0.003(3)

C22'	0.028(3)	0.028(4)	0.030(4)	-0.005(3)	0.003(3)	-0.006(3)
C23'	0.030(3)	0.023(4)	0.027(3)	-0.006(3)	0.002(3)	-0.006(3)
C24'	0.021(3)	0.029(4)	0.023(3)	-0.003(3)	0.003(3)	-0.002(3)
C25'	0.022(3)	0.036(4)	0.017(3)	-0.002(3)	-0.001(2)	0.005(3)
C26'	0.025(3)	0.034(4)	0.031(3)	0.000(3)	-0.001(3)	-0.003(3)
C27'	0.030(4)	0.039(5)	0.054(5)	0.007(4)	0.000(3)	-0.001(3)
C28'	0.030(4)	0.032(4)	0.069(6)	-0.018(4)	-0.010(4)	0.004(3)
C29'	0.028(4)	0.051(6)	0.039(5)	-0.015(4)	-0.006(3)	0.005(4)
C30'	0.029(3)	0.048(5)	0.026(3)	-0.005(4)	-0.001(3)	0.004(4)
C31'	0.023(3)	0.031(4)	0.025(3)	0.000(3)	-0.003(2)	0.000(3)
C32'	0.030(3)	0.028(4)	0.026(4)	0.003(3)	0.000(3)	0.002(3)
C33'	0.025(3)	0.036(4)	0.036(4)	0.004(4)	0.000(3)	0.006(3)
C34'	0.023(3)	0.049(5)	0.030(4)	0.002(4)	0.005(3)	0.006(3)
C35'	0.030(3)	0.038(5)	0.035(4)	0.001(4)	0.003(3)	-0.007(3)
C36'	0.025(3)	0.030(4)	0.026(3)	0.000(3)	0.002(3)	-0.001(3)
C37'	0.027(3)	0.044(5)	0.029(4)	0.007(4)	0.009(3)	0.007(4)
C38'	0.042(4)	0.047(5)	0.027(4)	0.000(4)	-0.004(3)	-0.002(4)
C39	0.043(4)	0.040(5)	0.034(4)	0.007(4)	0.002(3)	0.001(4)
C40	0.051(5)	0.050(5)	0.031(4)	0.000(4)	0.000(3)	0.020(4)
C41	0.073(6)	0.031(5)	0.034(4)	0.005(4)	-0.013(4)	0.008(4)
C42	0.059(5)	0.036(5)	0.045(5)	-0.005(4)	0.000(4)	-0.007(4)
C43	0.046(5)	0.046(6)	0.064(6)	-0.013(5)	0.015(4)	-0.002(4)
C44	0.051(5)	0.031(5)	0.062(6)	-0.016(4)	0.012(4)	-0.011(4)
C45	0.046(4)	0.051(5)	0.029(4)	0.006(4)	-0.001(3)	-0.005(4)
C46	0.031(4)	0.066(6)	0.037(4)	-0.017(4)	-0.001(3)	-0.002(4)

C47	0.037(4)	0.049(6)	0.054(5)	-0.024(4)	-0.015(4)	0.004(4)
C48	0.048(5)	0.035(5)	0.044(5)	-0.011(4)	-0.015(4)	0.000(4)
C49	0.039(4)	0.049(6)	0.042(5)	-0.013(4)	0.008(3)	0.003(4)
C50	0.039(4)	0.053(6)	0.043(5)	-0.002(4)	0.001(3)	0.011(4)
C51	0.051(5)	0.042(5)	0.034(4)	0.002(4)	-0.005(4)	0.007(4)
C52	0.037(4)	0.038(5)	0.040(4)	-0.003(4)	-0.001(3)	-0.006(4)
C53	0.036(4)	0.046(5)	0.036(4)	-0.002(4)	0.005(3)	0.002(4)
C54	0.046(5)	0.053(6)	0.062(6)	0.029(5)	-0.003(4)	-0.010(4)
C55	0.041(5)	0.10(1)	0.079(8)	0.057(7)	0.002(5)	-0.008(6)
C56	0.048(5)	0.077(8)	0.050(5)	0.022(6)	0.007(4)	0.022(5)

**Table 5 . Bond Distances in Compound 5•3/2benzene, Å**

Pd1-P1	2.3931(17)	Pd1-P2	2.3735(18)	Pd1-C37	1.982(8)
Pd1-C38	1.957(7)	Fe1-C1	2.066(7)	Fe1-C2	2.054(7)
Fe1-C3	2.039(7)	Fe1-C4	2.049(7)	Fe1-C5	2.042(7)
Fe1-C6	2.060(8)	Fe1-C7	2.049(7)	Fe1-C8	2.053(7)
Fe1-C9	2.050(7)	Fe1-C10	2.070(8)	P1-C11	1.890(7)
P1-C13	1.863(7)	P1-C19	1.862(7)	P2-C1	1.806(7)
P2-C25	1.843(6)	P2-C31	1.830(8)	O1-C37	1.124(9)
O2-C38	1.134(9)	C1-C2	1.459(9)	C1-C5	1.438(9)
C2-C3	1.416(9)	C2-C11	1.508(9)	C3-C4	1.410(10)
C4-C5	1.423(10)	C6-C7	1.434(11)	C6-C10	1.416(11)
C7-C8	1.432(9)	C8-C9	1.414(10)	C9-C10	1.445(11)
C11-C12	1.546(9)	C13-C14	1.546(9)	C13-C18	1.533(10)
C14-C15	1.519(10)	C15-C16	1.520(11)	C16-C17	1.513(11)
C17-C18	1.530(10)	C19-C20	1.540(10)	C19-C24	1.525(9)
C20-C21	1.529(9)	C21-C22	1.538(10)	C22-C23	1.534(10)
C23-C24	1.519(9)	C25-C26	1.398(10)	C25-C30	1.383(10)
C26-C27	1.387(9)	C27-C28	1.387(10)	C28-C29	1.391(11)
C29-C30	1.377(10)	C31-C32	1.402(10)	C31-C36	1.396(9)
C32-C33	1.373(11)	C33-C34	1.383(10)	C34-C35	1.377(10)
C35-C36	1.380(9)	Pd1'-P1'	2.4046(15)	Pd1'-P2'	2.3712(18)
Pd1'-C37'	1.975(8)	Pd1'-C38'	1.940(9)	Fe1'-C1'	2.054(6)

Fe1'-C2'	2.040(6)	Fe1'-C3'	2.045(6)	Fe1'-C4'	2.028(8)
Fe1'-C5'	2.023(8)	Fe1'-C6'	2.037(11)	Fe1'-C7'	2.077(11)
Fe1'-C8'	2.049(9)	Fe1'-C9'	2.041(7)	Fe1'-C10'	2.032(8)
P1'-C11'	1.884(6)	P1'-C13'	1.862(7)	P1'-C19'	1.864(7)
P2'-C1'	1.805(7)	P2'-C25'	1.827(8)	P2'-C31'	1.838(6)
O1'-C37'	1.135(9)	O2'-C38'	1.143(10)	C1'-C2'	1.463(9)
C1'-C5'	1.437(10)	C2'-C3'	1.436(9)	C2'-C11'	1.507(9)
C3'-C4'	1.403(10)	C4'-C5'	1.414(9)	C6'-C7'	1.377(17)
C6'-C10'	1.41(2)	C7'-C8'	1.363(14)	C8'-C9'	1.393(14)
C9'-C10'	1.475(15)	C11'-C12'	1.531(9)	C13'-C14'	1.521(9)
C13'-C18'	1.542(9)	C14'-C15'	1.521(10)	C15'-C16'	1.530(10)
C16'-C17'	1.529(10)	C17'-C18'	1.529(9)	C19'-C20'	1.534(8)
C19'-C24'	1.530(9)	C20'-C21'	1.526(10)	C21'-C22'	1.518(9)
C22'-C23'	1.523(9)	C23'-C24'	1.529(9)	C25'-C26'	1.383(9)
C25'-C30'	1.404(9)	C26'-C27'	1.377(11)	C27'-C28'	1.392(12)
C28'-C29'	1.384(12)	C29'-C30'	1.381(12)	C31'-C32'	1.412(10)
C31'-C36'	1.385(10)	C32'-C33'	1.381(9)	C33'-C34'	1.390(11)
C34'-C35'	1.365(10)	C35'-C36'	1.392(9)	C39-C40	1.357(12)
C39-C44	1.367(11)	C40-C41	1.395(12)	C41-C42	1.365(12)
C42-C43	1.377(12)	C43-C44	1.378(12)	C45-C46	1.390(12)
C45-C50	1.381(11)	C46-C47	1.372(13)	C47-C48	1.387(12)
C48-C49	1.377(12)	C49-C50	1.376(13)	C51-C52	1.374(11)
C51-C56	1.365(12)	C52-C53	1.380(12)	C53-C54	1.376(11)
C54-C55	1.354(14)	C55-C56	1.392(17)		

**Table 6 . Bond Angles in Compound 5•3/2benzene, °**

P2-Pd1-P1	93.29(6)	C37-Pd1-P1	114.0(2)	C37-Pd1-P2	101.7(2)
C38-Pd1-P1	112.3(2)	C38-Pd1-P2	115.3(2)	C38-Pd1-C37	117.4(3)
C1-Fe1-C10	124.6(3)	C2-Fe1-C1	41.5(3)	C2-Fe1-C6	124.3(3)
C2-Fe1-C10	160.5(3)	C3-Fe1-C1	68.9(3)	C3-Fe1-C2	40.5(3)
C3-Fe1-C4	40.4(3)	C3-Fe1-C5	68.1(3)	C3-Fe1-C6	157.9(3)
C3-Fe1-C7	120.1(3)	C3-Fe1-C8	104.1(3)	C3-Fe1-C9	120.4(3)
C3-Fe1-C10	158.5(3)	C4-Fe1-C1	69.1(3)	C4-Fe1-C2	68.5(3)
C4-Fe1-C6	161.6(3)	C4-Fe1-C8	118.3(3)	C4-Fe1-C9	105.2(3)
C4-Fe1-C10	123.9(3)	C5-Fe1-C1	41.0(3)	C5-Fe1-C2	68.8(3)
C5-Fe1-C4	40.7(3)	C5-Fe1-C6	127.0(3)	C5-Fe1-C7	163.3(3)
C5-Fe1-C8	155.2(3)	C5-Fe1-C9	121.9(3)	C5-Fe1-C10	109.8(3)
C6-Fe1-C1	110.6(3)	C6-Fe1-C10	40.1(3)	C7-Fe1-C1	125.4(3)
C7-Fe1-C2	107.3(3)	C7-Fe1-C4	154.5(3)	C7-Fe1-C6	40.8(3)
C7-Fe1-C8	40.9(3)	C7-Fe1-C9	68.2(3)	C7-Fe1-C10	68.2(3)
C8-Fe1-C1	160.2(3)	C8-Fe1-C2	121.4(3)	C8-Fe1-C6	68.6(3)
C8-Fe1-C10	68.5(3)	C9-Fe1-C1	159.2(3)	C9-Fe1-C2	156.8(3)
C9-Fe1-C6	68.2(3)	C9-Fe1-C8	40.3(3)	C9-Fe1-C10	41.0(3)
C11-P1-Pd1	104.3(2)	C13-P1-Pd1	120.9(2)	C13-P1-C11	103.3(3)
C19-P1-Pd1	116.2(2)	C19-P1-C11	103.8(3)	C19-P1-C13	106.3(3)
C1-P2-Pd1	116.0(3)	C1-P2-C25	101.9(3)	C1-P2-C31	104.3(3)
C25-P2-Pd1	108.1(2)	C31-P2-Pd1	121.8(2)	C31-P2-C25	102.2(3)
P2-C1-Fe1	135.0(4)	C2-C1-Fe1	68.8(4)	C2-C1-P2	125.4(5)
C5-C1-Fe1	68.6(4)	C5-C1-P2	127.8(5)	C5-C1-C2	105.9(6)



C1-C2-Fe1	69.7(4)	C1-C2-C11	126.2(6)	C3-C2-Fe1	69.2(4)
C3-C2-C1	107.7(6)	C3-C2-C11	126.0(6)	C11-C2-Fe1	128.2(5)
C2-C3-Fe1	70.3(4)	C4-C3-Fe1	70.2(4)	C4-C3-C2	109.6(6)
C3-C4-Fe1	69.4(4)	C3-C4-C5	107.5(6)	C5-C4-Fe1	69.4(4)
C1-C5-Fe1	70.4(4)	C4-C5-Fe1	69.9(4)	C4-C5-C1	109.3(6)
C7-C6-Fe1	69.1(4)	C10-C6-Fe1	70.3(4)	C10-C6-C7	108.3(7)
C6-C7-Fe1	70.0(4)	C8-C7-Fe1	69.7(4)	C8-C7-C6	107.9(7)
C7-C8-Fe1	69.4(4)	C9-C8-Fe1	69.7(4)	C9-C8-C7	107.8(7)
C8-C9-Fe1	69.9(4)	C8-C9-C10	108.5(6)	C10-C9-Fe1	70.2(4)
C6-C10-Fe1	69.6(5)	C6-C10-C9	107.4(7)	C9-C10-Fe1	68.7(4)
C2-C11-P1	108.8(4)	C2-C11-C12	111.8(6)	C12-C11-P1	118.2(5)
C14-C13-P1	108.7(5)	C18-C13-P1	113.2(4)	C18-C13-C14	109.3(6)
C15-C14-C13	110.8(6)	C14-C15-C16	111.2(6)	C17-C16-C15	111.2(6)
C16-C17-C18	112.5(6)	C17-C18-C13	111.0(5)	C20-C19-P1	115.7(5)
C24-C19-P1	113.8(5)	C24-C19-C20	110.5(6)	C21-C20-C19	111.1(5)
C20-C21-C22	110.6(6)	C23-C22-C21	110.9(6)	C24-C23-C22	110.7(6)
C23-C24-C19	112.2(6)	C26-C25-P2	119.5(5)	C30-C25-P2	121.0(5)
C30-C25-C26	118.8(6)	C27-C26-C25	120.4(7)	C28-C27-C26	119.8(7)
C27-C28-C29	119.9(6)	C30-C29-C28	119.8(7)	C29-C30-C25	121.2(7)
C32-C31-P2	122.7(5)	C36-C31-P2	119.6(5)	C36-C31-C32	117.7(7)
C33-C32-C31	121.0(7)	C32-C33-C34	120.3(7)	C35-C34-C33	119.8(7)
C34-C35-C36	120.1(6)	C35-C36-C31	121.1(6)	O1-C37-Pd1	173.9(7)
O2-C38-Pd1	177.9(7)	P2'-Pd1'-P1'	92.96(6)	C37'-Pd1'-P1'	113.22(19)
C37'-Pd1'-P2'	105.3(2)	C38'-Pd1'-P1'	116.2(3)	C38'-Pd1'-P2'	118.3(2)
C38'-Pd1'-C37'	109.7(3)	C1'-Fe1'-C7'	124.6(4)	C2'-Fe1'-C1'	41.9(3)

C2'-Fe1'-C3'	41.2(2)	C2'-Fe1'-C7'	107.3(4)	C2'-Fe1'-C8'	120.6(3)
C2'-Fe1'-C9'	154.8(3)	C3'-Fe1'-C1'	69.6(3)	C3'-Fe1'-C7'	121.5(4)
C3'-Fe1'-C8'	105.6(3)	C4'-Fe1'-C1'	69.2(3)	C4'-Fe1'-C2'	68.9(3)
C4'-Fe1'-C3'	40.3(3)	C4'-Fe1'-C6'	161.7(5)	C4'-Fe1'-C7'	156.2(4)
C4'-Fe1'-C8'	121.6(3)	C4'-Fe1'-C9'	105.7(4)	C4'-Fe1'-C10'	123.5(5)
C5'-Fe1'-C1'	41.3(3)	C5'-Fe1'-C2'	69.6(3)	C5'-Fe1'-C3'	68.7(3)
C5'-Fe1'-C4'	40.9(3)	C5'-Fe1'-C6'	126.9(5)	C5'-Fe1'-C7'	161.9(4)
C5'-Fe1'-C8'	158.5(4)	C5'-Fe1'-C9'	123.3(4)	C5'-Fe1'-C10'	109.0(4)
C6'-Fe1'-C1'	110.5(3)	C6'-Fe1'-C2'	123.9(5)	C6'-Fe1'-C3'	157.9(6)
C6'-Fe1'-C7'	39.1(5)	C6'-Fe1'-C8'	65.6(4)	C6'-Fe1'-C9'	68.4(5)
C8'-Fe1'-C1'	158.1(4)	C8'-Fe1'-C7'	38.6(4)	C9'-Fe1'-C1'	161.3(4)
C9'-Fe1'-C3'	118.9(4)	C9'-Fe1'-C7'	67.2(5)	C9'-Fe1'-C8'	39.8(4)
C10'-Fe1'-C1'	124.3(4)	C10'-Fe1'-C2'	160.6(5)	C10'-Fe1'-C3'	157.7(5)
C10'-Fe1'-C6'	40.6(6)	C10'-Fe1'-C7'	67.6(5)	C10'-Fe1'-C8'	68.0(4)
C10'-Fe1'-C9'	42.5(4)	C11'-P1'-Pd1'	106.8(2)	C13'-P1'-Pd1'	114.7(2)
C13'-P1'-C11'	104.6(3)	C13'-P1'-C19'	105.6(3)	C19'-P1'-Pd1'	120.6(2)
C19'-P1'-C11'	102.8(3)	C1'-P2'-Pd1'	116.3(2)	C1'-P2'-C25'	101.0(3)
C1'-P2'-C31'	103.5(3)	C25'-P2'-Pd1'	106.4(2)	C25'-P2'-C31'	103.2(3)
C31'-P2'-Pd1'	123.5(2)	P2'-C1'-Fe1'	137.2(4)	C2'-C1'-Fe1'	68.6(3)
C2'-C1'-P2'	127.4(5)	C5'-C1'-Fe1'	68.2(4)	C5'-C1'-P2'	125.3(5)
C5'-C1'-C2'	106.1(6)	C1'-C2'-Fe1'	69.6(3)	C1'-C2'-C11'	127.5(6)
C3'-C2'-Fe1'	69.6(3)	C3'-C2'-C1'	107.6(6)	C3'-C2'-C11'	124.9(6)
C11'-C2'-Fe1'	125.0(5)	C2'-C3'-Fe1'	69.2(3)	C4'-C3'-Fe1'	69.2(4)
C4'-C3'-C2'	108.3(6)	C3'-C4'-Fe1'	70.5(4)	C3'-C4'-C5'	109.2(6)
C5'-C4'-Fe1'	69.4(5)	C1'-C5'-Fe1'	70.5(4)	C4'-C5'-Fe1'	69.8(5)

C4'-C5'-C1'	108.8(6)	C7'-C6'-Fe1'	72.0(6)	C7'-C6'-C10'	110.2(10)
C10'-C6'-Fe1'	69.5(7)	C6'-C7'-Fe1'	68.9(7)	C8'-C7'-Fe1'	69.6(6)
C8'-C7'-C6'	107.8(11)	C7'-C8'-Fe1'	71.8(6)	C7'-C8'-C9'	111.5(9)
C9'-C8'-Fe1'	69.8(5)	C8'-C9'-Fe1'	70.4(5)	C8'-C9'-C10'	105.4(10)
C10'-C9'-Fe1'	68.4(4)	C6'-C10'-Fe1'	69.9(5)	C6'-C10'-C9'	105.2(9)
C9'-C10'-Fe1'	69.1(5)	C2'-C11'-P1'	110.3(5)	C2'-C11'-C12'	111.4(5)
C12'-C11'-P1'	117.2(4)	C14'-C13'-P1'	111.3(4)	C14'-C13'-C18'	109.9(6)
C18'-C13'-P1'	108.7(5)	C13'-C14'-C15'	111.6(6)	C14'-C15'-C16'	111.4(6)
C17'-C16'-C15'	110.0(6)	C16'-C17'-C18'	111.9(5)	C17'-C18'-C13'	111.3(6)
C20'-C19'-P1'	116.6(5)	C24'-C19'-P1'	113.4(4)	C24'-C19'-C20'	110.0(5)
C21'-C20'-C19'	111.5(6)	C22'-C21'-C20'	111.3(6)	C21'-C22'-C23'	110.9(5)
C22'-C23'-C24'	111.7(6)	C23'-C24'-C19'	111.0(6)	C26'-C25'-P2'	121.8(5)
C26'-C25'-C30'	117.9(7)	C30'-C25'-P2'	119.8(6)	C27'-C26'-C25'	121.6(7)
C26'-C27'-C28'	120.0(8)	C29'-C28'-C27'	119.4(8)	C30'-C29'-C28'	120.1(8)
C29'-C30'-C25'	120.9(8)	C32'-C31'-P2'	122.8(5)	C36'-C31'-P2'	118.8(5)
C36'-C31'-C32'	118.5(6)	C33'-C32'-C31'	120.4(7)	C32'-C33'-C34'	119.6(7)
C35'-C34'-C33'	120.6(6)	C34'-C35'-C36'	120.2(7)	C31'-C36'-C35'	120.6(7)
O1'-C37'-Pd1'	175.7(7)	O2'-C38'-Pd1'	170.8(8)	C40-C39-C44	119.9(8)
C39-C40-C41	120.9(8)	C42-C41-C40	119.0(8)	C41-C42-C43	119.9(8)
C42-C43-C44	120.5(8)	C39-C44-C43	119.7(8)	C50-C45-C46	119.3(8)
C47-C46-C45	120.9(8)	C46-C47-C48	119.1(8)	C49-C48-C47	120.4(9)
C50-C49-C48	120.3(8)	C49-C50-C45	120.0(8)	C56-C51-C52	119.4(9)
C51-C52-C53	119.7(8)	C54-C53-C52	120.2(9)	C55-C54-C53	120.6(10)
C54-C55-C56	118.8(9)	C51-C56-C55	121.2(9)		

This report has been created with Olex2 [6], compiled on 2021.08.20 svn.r13c46975 for OlexSys.

(Josiphos)Pd(Br)(4-C<sub>6</sub>H<sub>4</sub>-CF<sub>3</sub>) (**6m'**)

Compound **6m'**, C<sub>42.79</sub>H<sub>47.88</sub>Br<sub>1.03</sub>F<sub>2.91</sub>FeP<sub>2</sub>Pd, crystallizes in the orthorhombic space group P2<sub>1</sub>2<sub>1</sub>2<sub>1</sub> (systematic absences h00: h=odd, 0k0: k=odd, and 00l: l=odd) with a=9.5489(3)Å, b=15.6393(5)Å, c=25.5458(10)Å, V=3815.0(2)Å<sup>3</sup>, Z=4, and d<sub>calc</sub>=1.609 g/cm<sup>3</sup>. X-ray intensity data were collected on a Rigaku XtaLAB Synergy-S diffractometer [1] equipped with an HPC area detector (Dectris Pilatus3 R 200K) and employing confocal multilayer optic-monochromated Mo-Kα radiation (λ=0.71073 Å) at a temperature of 100K. Preliminary indexing was performed from a series of thirty 0.5° rotation frames with exposures of 0.25 seconds. A total of 618 frames (7 runs) were collected employing ω scans with a crystal to detector distance of 34.0 mm, rotation widths of 0.5° and exposures of 3 seconds.

Rotation frames were integrated using CrysAlisPro [2], producing a listing of unaveraged F<sup>2</sup> and σ(F<sup>2</sup>) values. A total of 40064 reflections were measured over the ranges 4.998 ≤ 2θ ≤ 56.56°, -12 ≤ h ≤ 12, -20 ≤ k ≤ 19, -34 ≤ l ≤ 34 yielding 9435 unique reflections (R<sub>int</sub> = 0.0500). The intensity data were corrected for Lorentz and polarization effects and for absorption using SCALE3 ABSPACK [3] (minimum and maximum transmission 0.8286, 1.0000). The structure was solved by direct methods - SHELXT [4]. The PhCF<sub>3</sub> is disordered with 3% Br<sup>-</sup> ion. Refinement was by full-matrix least squares based on F<sup>2</sup> using SHELXL [5]. All reflections were used during refinement. The weighting scheme used was w=1/[σ<sup>2</sup>(F<sub>o</sub><sup>2</sup>) + (0.0314P)<sup>2</sup> + 0.4733P] where P = (F<sub>o</sub><sup>2</sup> + 2F<sub>c</sub><sup>2</sup>)/3. Non-hydrogen atoms were refined anisotropically and hydrogen atoms were refined using a riding model. Refinement converged to R1=0.0299 and wR2=0.0632 for 8612 observed reflections for which F > 4σ(F) and R1=0.0354 and wR2=0.0646 and GOF =1.037 for all 9435 unique, non-zero reflections and 497 variables. The maximum Δ/σ in the final cycle

of least squares was 0.001 and the two most prominent peaks in the final difference Fourier were +0.90 and -0.43 e/Å<sup>3</sup>.

Table 1. lists cell information, data collection parameters, and refinement data. Final positional and equivalent isotropic thermal parameters are given in Tables 2. and 3. Anisotropic thermal parameters are in Table 4. Tables 5. and 6. list bond distances and bond angles. Figure 1. is an ORTEP representation of the molecule with 50% probability thermal ellipsoids displayed.

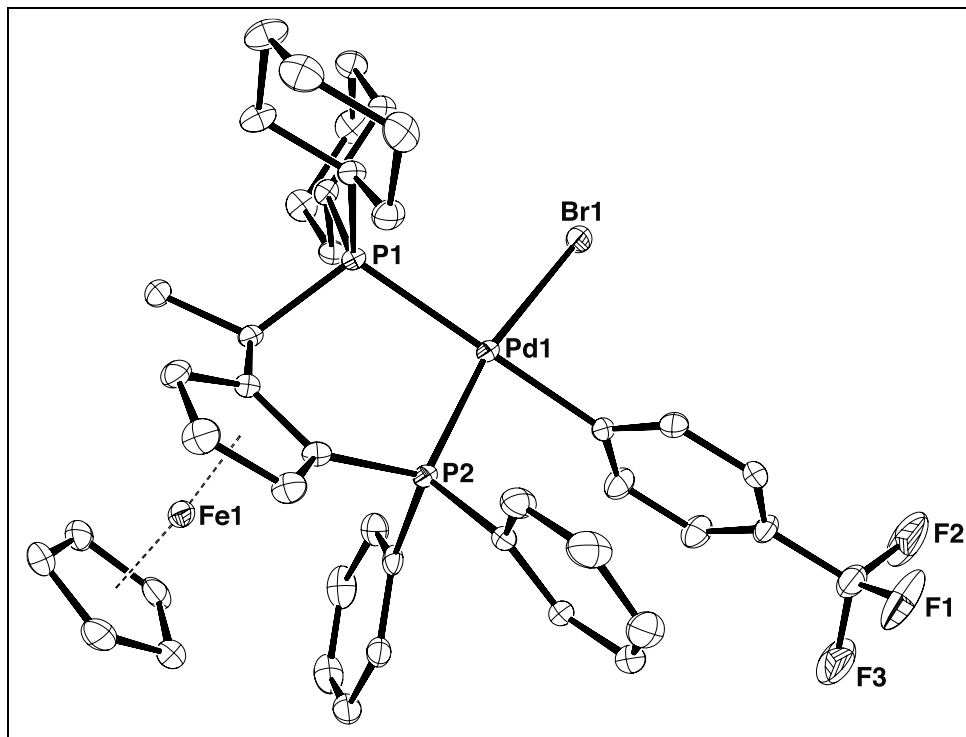


Figure 1. ORTEP drawing of the title compound with 50% thermal ellipsoids.

**Table 1. Summary of Structure Determination of Compound 6m'**

Empirical formula	C <sub>42.79</sub> H <sub>47.88</sub> Br <sub>1.03</sub> F <sub>2.91</sub> FeP <sub>2</sub> Pd
Formula weight	923.96
Diffractometer	Rigaku XtaLAB Synergy-S (Dectris Pilatus3 R 200K)
Temperature/K	100
Crystal system	orthorhombic
Space group	P2 <sub>1</sub> 2 <sub>1</sub> 2 <sub>1</sub>
a	9.5489(3)Å
b	15.6393(5)Å
c	25.5458(10)Å
Volume	3815.0(2)Å <sup>3</sup>
Z	4
d <sub>calc</sub>	1.609 g/cm <sup>3</sup>
μ	2.059 mm <sup>-1</sup>
F(000)	1875.0
Crystal size, mm	0.22 × 0.19 × 0.15
2θ range for data collection	4.998 - 56.56°
Index ranges	-12 ≤ h ≤ 12, -20 ≤ k ≤ 19, -34 ≤ l ≤ 34
Reflections collected	40064
Independent reflections	9435[R(int) = 0.0500]
Data/restraints/parameters	9435/48/497
Goodness-of-fit on F <sup>2</sup>	1.037
Final R indexes [I ≥ 2σ (I)]	R <sub>1</sub> = 0.0299, wR <sub>2</sub> = 0.0632
Final R indexes [all data]	R <sub>1</sub> = 0.0354, wR <sub>2</sub> = 0.0646

Largest diff. peak/hole	0.90/-0.43 eÅ <sup>-3</sup>
Flack parameter	0.003(4)

**Table 2 . Refined Positional Parameters for Compound 6m'**

Atom	x	y	z	U(eq)
Pd1	0.33476(3)	0.40953(2)	0.68212(2)	0.01374(7)
Br1	0.14213(4)	0.47709(2)	0.73235(2)	0.02213(10)
Br2*	0.168(3)	0.4377(16)	0.6034(9)	0.024(3)
Fe1	0.75474(6)	0.20015(3)	0.63906(2)	0.01601(12)
P1	0.4241(1)	0.32773(6)	0.75319(4)	0.01272(19)
P2	0.49118(10)	0.36154(6)	0.62312(4)	0.01315(19)
F1	0.1834(4)	0.7040(2)	0.48478(15)	0.0533(8)
F1*	0.101(5)	0.7215(16)	0.5134(17)	0.0568(13)
F2	-0.0211(4)	0.6795(3)	0.51129(17)	0.0607(9)
F2*	-0.040(3)	0.628(3)	0.489(2)	0.0590(13)
F3	0.0741(5)	0.5991(2)	0.45456(15)	0.0586(9)
F3*	0.166(5)	0.624(3)	0.4548(13)	0.0560(13)
C1	0.6475(4)	0.3131(2)	0.65092(15)	0.0151(7)
C2	0.6467(4)	0.2617(2)	0.69771(15)	0.0152(7)
C3	0.7898(4)	0.2478(3)	0.71228(17)	0.0191(8)
C4	0.8773(4)	0.2897(3)	0.67548(18)	0.0242(9)
C5	0.7912(4)	0.3289(3)	0.63704(17)	0.0198(8)
C6	0.6452(4)	0.1064(2)	0.59960(17)	0.0228(9)
C7	0.7174(5)	0.0709(2)	0.64274(18)	0.0262(10)
C8	0.8624(5)	0.0868(3)	0.63592(18)	0.0302(10)
C9	0.8801(5)	0.1336(3)	0.58825(19)	0.0284(10)



C10	0.7442(4)	0.1452(2)	0.56599(17)	0.0224(9)
C11	0.5191(4)	0.2321(2)	0.72630(15)	0.0141(7)
C12	0.5497(4)	0.1583(2)	0.76462(17)	0.0189(8)
C13	0.5459(4)	0.3898(2)	0.79510(16)	0.0149(8)
C14	0.6252(4)	0.3396(2)	0.83667(16)	0.0195(8)
C15	0.7096(4)	0.3990(3)	0.87259(17)	0.0257(9)
C16	0.8079(5)	0.4552(3)	0.84109(19)	0.0269(10)
C17	0.7287(5)	0.5061(2)	0.79941(18)	0.0240(9)
C18	0.6466(4)	0.4468(2)	0.76349(16)	0.0198(8)
C19	0.2998(4)	0.2768(2)	0.79933(16)	0.0140(8)
C20	0.1888(4)	0.2278(2)	0.76801(17)	0.0185(8)
C21	0.0952(4)	0.1759(2)	0.80454(18)	0.0227(9)
C22	0.0244(4)	0.2343(3)	0.84443(19)	0.0269(10)
C23	0.1319(4)	0.2866(2)	0.87499(17)	0.0211(9)
C24	0.2296(4)	0.3372(2)	0.83923(16)	0.0163(8)
C25	0.5587(4)	0.4440(2)	0.57945(16)	0.0167(8)
C26	0.6639(5)	0.4992(2)	0.59730(17)	0.0229(8)
C27	0.7097(5)	0.5659(3)	0.56536(19)	0.0321(11)
C28	0.6505(5)	0.5796(2)	0.51676(19)	0.0335(11)
C29	0.5437(5)	0.5274(3)	0.49972(18)	0.028(1)
C30	0.4970(4)	0.4598(2)	0.53093(16)	0.0193(8)
C31	0.4165(4)	0.2792(2)	0.58090(16)	0.0159(8)
C32	0.4750(4)	0.2589(2)	0.53289(16)	0.0177(8)
C33	0.4257(5)	0.1907(3)	0.50361(18)	0.0244(9)
C34	0.3177(5)	0.1408(2)	0.52271(19)	0.028(1)

C35	0.2574(4)	0.1602(3)	0.5703(2)	0.0276(10)
C36	0.3048(4)	0.2304(2)	0.59951(18)	0.0207(9)
C37	0.2599(4)	0.4812(2)	0.62129(16)	0.0165(8)
C38	0.1571(8)	0.4534(4)	0.5876(2)	0.0227(13)
C39	0.1029(4)	0.5033(3)	0.54786(19)	0.0229(9)
C40	0.1557(4)	0.5862(2)	0.54113(16)	0.0195(8)
C41	0.2591(4)	0.6165(2)	0.57426(17)	0.0178(8)
C42	0.3101(4)	0.5652(2)	0.61352(16)	0.0189(9)
C43	0.0977(5)	0.6414(3)	0.49850(18)	0.0248(10)

**Table 3 . Positional Parameters for Hydrogens in Compound 6m'**

Atom	<i>x</i>	<i>y</i>	<i>z</i>	U(eq)
H3	0.820833	0.215917	0.741703	0.023
H4	0.976773	0.291248	0.676384	0.029
H5	0.822844	0.360116	0.607397	0.024
H6	0.546874	0.104442	0.594116	0.027
H7	0.675984	0.041476	0.671352	0.031
H8	0.935105	0.069514	0.65898	0.036
H9	0.966218	0.153279	0.574044	0.034
H10	0.723898	0.173946	0.53413	0.027
H11	0.455866	0.207564	0.698953	0.017
H12a	0.603421	0.179996	0.794484	0.028
H12b	0.604029	0.113905	0.746658	0.028
H12c	0.461223	0.133908	0.777073	0.028
H13	0.485076	0.430449	0.815017	0.018
H14a	0.689615	0.298734	0.819409	0.023
H14b	0.557892	0.306268	0.857947	0.023
H15a	0.644493	0.435398	0.892914	0.031
H15b	0.764557	0.364252	0.897637	0.031
H16a	0.879594	0.419096	0.823962	0.032
H16b	0.856535	0.495324	0.864935	0.032
H17a	0.66357	0.546476	0.816645	0.029
H17b	0.796155	0.5398	0.77842	0.029

H18a	0.712554	0.410269	0.743617	0.024
H18b	0.592449	0.481232	0.738065	0.024
H19	0.353976	0.233495	0.819849	0.017
H20a	0.130901	0.268669	0.747865	0.022
H20b	0.235452	0.188913	0.742863	0.022
H21a	0.152119	0.132469	0.823043	0.027
H21b	0.022939	0.145656	0.783795	0.027
H22a	-0.031164	0.199221	0.869124	0.032
H22b	-0.040529	0.273462	0.826074	0.032
H23a	0.082124	0.326757	0.898477	0.025
H23b	0.188325	0.247637	0.897071	0.025
H24a	0.302343	0.365992	0.860488	0.02
H24b	0.175642	0.381685	0.820432	0.02
H26	0.703764	0.491286	0.631019	0.027
H27	0.782639	0.602443	0.577194	0.039
H28	0.683255	0.62485	0.495171	0.04
H29	0.50161	0.537303	0.46658	0.034
H30	0.422625	0.424434	0.519033	0.023
H32	0.550299	0.292394	0.519789	0.021
H33	0.466121	0.178197	0.470499	0.029
H34	0.284952	0.093288	0.503062	0.034
H35	0.183297	0.125751	0.583337	0.033
H36	0.261138	0.24466	0.631766	0.025
H38	0.121612	0.397057	0.591842	0.027
H39	0.031449	0.481896	0.525562	0.027

H41	0.294807	0.672703	0.569852	0.021
H42	0.380941	0.586743	0.636031	0.023

**Table 4 . Refined Thermal Parameters (U's) for Compound 6m'**

Atom	U <sub>11</sub>	U <sub>22</sub>	U <sub>33</sub>	U <sub>23</sub>	U <sub>13</sub>	U <sub>12</sub>
Pd1	0.01652(13)	0.01507(12)	0.00964(13)	0.00069(11)	-0.00084(11)	0.00346(11)
Br1	0.0259(2)	0.02430(19)	0.0162(2)	0.00235(16)	0.00398(17)	0.01111(16)
Br2*	0.027(5)	0.023(6)	0.022(7)	0.006(5)	0.006(6)	-0.002(5)
Fe1	0.0127(3)	0.0216(3)	0.0138(3)	0.0018(2)	0.0005(2)	0.0041(2)
P1	0.0143(5)	0.0138(4)	0.0101(5)	0.0006(4)	-0.0004(4)	0.0005(3)
P2	0.0146(5)	0.0148(4)	0.0101(5)	0.0010(4)	-0.0008(4)	0.0014(4)
F1	0.0605(19)	0.0531(16)	0.0463(18)	0.0349(15)	-0.0125(16)	-0.0060(16)
F1*	0.062(3)	0.061(2)	0.048(3)	0.034(2)	-0.005(2)	0.013(2)
F2	0.0620(19)	0.071(2)	0.050(2)	0.0329(17)	0.0034(17)	0.0323(17)
F2*	0.075(3)	0.059(2)	0.043(2)	0.024(2)	-0.011(2)	0.019(2)
F3	0.089(2)	0.0487(17)	0.0376(18)	0.0138(16)	-0.0239(17)	0.0062(18)
F3*	0.075(3)	0.051(2)	0.042(2)	0.025(2)	-0.018(2)	0.001(2)
C1	0.0155(18)	0.0176(16)	0.0123(18)	-0.0013(14)	-0.0010(15)	-0.0007(15)
C2	0.0182(18)	0.0158(16)	0.0117(18)	-0.0009(14)	0.0003(15)	0.0034(14)
C3	0.0172(19)	0.026(2)	0.014(2)	0.0011(16)	-0.0020(15)	0.0031(15)
C4	0.0175(19)	0.031(2)	0.024(2)	0.0005(19)	0.0002(17)	-0.0008(16)
C5	0.0163(18)	0.0254(19)	0.018(2)	-0.0002(17)	-0.0013(16)	-0.0014(15)
C6	0.024(2)	0.0171(18)	0.027(2)	-0.0053(16)	0.0037(18)	0.0051(16)
C7	0.039(2)	0.0184(19)	0.021(2)	0.0036(17)	0.0071(19)	0.0100(17)
C8	0.031(2)	0.034(2)	0.026(2)	-0.002(2)	0.0012(19)	0.020(2)
C9	0.022(2)	0.039(2)	0.024(2)	-0.002(2)	0.0069(18)	0.0109(18)

C10	0.024(2)	0.025(2)	0.019(2)	-0.0007(17)	0.0028(18)	0.0084(17)
C11	0.0155(17)	0.0169(16)	0.0100(18)	-0.0009(15)	-0.0017(15)	0.0025(14)
C12	0.023(2)	0.0176(17)	0.016(2)	0.0039(16)	0.0040(17)	0.0026(15)
C13	0.0161(18)	0.0166(17)	0.0122(19)	0.0000(15)	0.0008(15)	-0.0013(14)
C14	0.0200(19)	0.0237(18)	0.015(2)	0.0022(16)	-0.0013(16)	-0.0067(15)
C15	0.024(2)	0.035(2)	0.018(2)	-0.0013(19)	-0.0063(17)	-0.0076(18)
C16	0.023(2)	0.028(2)	0.029(2)	-0.0082(19)	-0.0006(18)	-0.0078(17)
C17	0.026(2)	0.0158(17)	0.030(2)	0.0009(17)	0.0029(19)	-0.0058(16)
C18	0.025(2)	0.0171(16)	0.017(2)	0.0017(15)	0.0009(18)	-0.0029(15)
C19	0.0136(17)	0.0139(16)	0.0144(19)	0.0015(14)	-0.0013(14)	-0.0022(13)
C20	0.021(2)	0.0177(17)	0.016(2)	-0.0044(16)	-0.0046(17)	0.0006(15)
C21	0.0184(19)	0.0217(19)	0.028(3)	-0.0010(17)	0.0000(18)	-0.0048(15)
C22	0.020(2)	0.031(2)	0.030(3)	0.003(2)	0.0058(19)	-0.0052(17)
C23	0.020(2)	0.0243(19)	0.019(2)	-0.0003(17)	0.0059(17)	-0.0016(16)
C24	0.0179(19)	0.0167(17)	0.0144(19)	-0.0013(15)	0.0014(16)	-0.0021(15)
C25	0.025(2)	0.0124(16)	0.013(2)	0.0001(15)	0.0032(16)	0.0034(15)
C26	0.032(2)	0.0173(17)	0.019(2)	-0.0019(16)	0.004(2)	-0.0034(17)
C27	0.048(3)	0.021(2)	0.028(3)	-0.0048(19)	0.008(2)	-0.0132(18)
C28	0.057(3)	0.0163(18)	0.027(2)	0.0050(18)	0.015(2)	-0.004(2)
C29	0.049(3)	0.0188(19)	0.017(2)	0.0005(17)	0.004(2)	0.0085(19)
C30	0.030(2)	0.0165(17)	0.012(2)	0.0008(15)	0.0013(17)	0.0057(16)
C31	0.0140(18)	0.0140(17)	0.020(2)	0.0004(15)	-0.0085(16)	0.0030(14)
C32	0.0201(19)	0.0150(16)	0.018(2)	-0.0009(15)	-0.0039(16)	0.0026(15)
C33	0.032(2)	0.0228(19)	0.019(2)	-0.0071(17)	-0.0113(19)	0.0071(17)
C34	0.028(2)	0.0185(18)	0.037(3)	-0.0069(18)	-0.016(2)	0.0002(17)

C35	0.016(2)	0.023(2)	0.044(3)	0.002(2)	-0.008(2)	-0.0022(17)
C36	0.0145(19)	0.0217(18)	0.026(2)	0.0016(17)	-0.0001(17)	0.0033(15)
C37	0.0198(19)	0.0171(17)	0.0127(19)	0.0008(16)	0.0004(16)	0.0077(16)
C38	0.026(2)	0.020(3)	0.021(4)	0.006(2)	0.001(3)	-0.004(2)
C39	0.021(2)	0.026(2)	0.022(2)	0.0026(18)	-0.0069(18)	-0.0025(17)
C40	0.022(2)	0.0222(18)	0.0145(19)	0.0056(17)	-0.0013(17)	0.0067(19)
C41	0.024(2)	0.0124(17)	0.017(2)	-0.0015(15)	0.0008(18)	0.0028(15)
C42	0.025(2)	0.0181(17)	0.014(2)	-0.0030(15)	-0.0047(17)	0.0004(15)
C43	0.032(2)	0.024(2)	0.019(2)	0.0067(18)	-0.0018(19)	0.0017(18)



**Table 5 . Bond Distances in Compound 6m', Å**

Pd1-Br1	2.4792(5)	Pd1-Br2*	2.60(2)	Pd1-P1	2.3792(10)
Pd1-P2	2.2508(10)	Pd1-C37	2.045(4)	Fe1-C1	2.064(4)
Fe1-C2	2.058(4)	Fe1-C3	2.041(4)	Fe1-C4	2.049(4)
Fe1-C5	2.045(4)	Fe1-C6	2.064(4)	Fe1-C7	2.055(4)
Fe1-C8	2.050(4)	Fe1-C9	2.050(4)	Fe1-C10	2.058(4)
P1-C11	1.879(4)	P1-C13	1.855(4)	P1-C19	1.853(4)
P2-C1	1.819(4)	P2-C25	1.823(4)	P2-C31	1.825(4)
F1-C43	1.323(6)	F1*-C43	1.31(2)	F2-C43	1.322(6)
F2*-C43	1.35(2)	F3-C43	1.323(6)	F3*-C43	1.32(2)
C1-C2	1.441(5)	C1-C5	1.438(5)	C2-C3	1.432(5)
C2-C11	1.494(5)	C3-C4	1.418(6)	C4-C5	1.420(6)
C6-C7	1.413(6)	C6-C10	1.414(6)	C7-C8	1.417(6)
C8-C9	1.430(7)	C9-C10	1.428(6)	C11-C12	1.543(5)
C13-C14	1.523(5)	C13-C18	1.539(5)	C14-C15	1.534(5)
C15-C16	1.518(6)	C16-C17	1.529(6)	C17-C18	1.522(6)
C19-C20	1.533(5)	C19-C24	1.543(5)	C20-C21	1.526(6)
C21-C22	1.526(6)	C22-C23	1.527(6)	C23-C24	1.527(5)
C25-C26	1.401(6)	C25-C30	1.395(6)	C26-C27	1.395(6)
C27-C28	1.381(7)	C28-C29	1.377(7)	C29-C30	1.396(6)
C31-C32	1.385(6)	C31-C36	1.394(6)	C32-C33	1.385(6)
C33-C34	1.382(6)	C34-C35	1.378(7)	C35-C36	1.404(6)

C37-C38 1.376(8)	C37-C42 1.413(5)	C38-C39 1.381(7)
C39-C40 1.401(6)	C40-C41 1.384(6)	C40-C43 1.496(6)
C41-C42 1.373(6)		

**Table 6 . Bond Angles in Compound 6m', °**

Br1-Pd1-Br2*	82.8(6)	P1-Pd1-Br1	95.76(3)	P1-Pd1-Br2*	154.2(6)
P2-Pd1-Br1	168.83(3)	P2-Pd1-Br2*	86.8(6)	P2-Pd1-P1	95.38(3)
C37-Pd1-Br1	84.28(11)	C37-Pd1-P1	179.21(12)	C37-Pd1-P2	84.60(11)
C2-Fe1-C1	40.91(14)	C2-Fe1-C6	115.72(16)	C3-Fe1-C1	68.53(15)
C3-Fe1-C2	40.89(15)	C3-Fe1-C4	40.58(17)	C3-Fe1-C5	68.61(17)
C3-Fe1-C6	142.20(17)	C3-Fe1-C7	110.24(18)	C3-Fe1-C8	105.64(17)
C3-Fe1-C9	132.08(17)	C3-Fe1-C10	172.73(16)	C4-Fe1-C1	68.38(15)
C4-Fe1-C2	68.66(16)	C4-Fe1-C6	175.52(17)	C4-Fe1-C7	138.66(18)
C4-Fe1-C8	108.79(18)	C4-Fe1-C9	107.52(18)	C4-Fe1-C10	136.51(17)
C5-Fe1-C1	40.97(15)	C5-Fe1-C2	69.08(16)	C5-Fe1-C4	40.61(17)
C5-Fe1-C6	140.70(17)	C5-Fe1-C7	178.81(18)	C5-Fe1-C8	139.92(18)
C5-Fe1-C9	112.63(18)	C5-Fe1-C10	113.39(17)	C6-Fe1-C1	115.38(15)
C7-Fe1-C1	138.53(17)	C7-Fe1-C2	109.87(16)	C7-Fe1-C6	40.13(18)
C7-Fe1-C10	67.79(17)	C8-Fe1-C1	173.80(17)	C8-Fe1-C2	133.16(17)
C8-Fe1-C6	67.71(17)	C8-Fe1-C7	40.40(18)	C8-Fe1-C10	68.15(17)
C9-Fe1-C1	144.81(18)	C9-Fe1-C2	172.43(17)	C9-Fe1-C6	68.03(18)
C9-Fe1-C7	68.33(18)	C9-Fe1-C8	40.84(18)	C9-Fe1-C10	40.69(17)
C10-Fe1-C1	117.82(15)	C10-Fe1-C2	146.25(16)	C10-Fe1-C6	40.13(17)
C11-P1-Pd1	108.78(13)	C13-P1-Pd1	112.57(12)	C13-P1-C11	108.96(17)
C19-P1-Pd1	119.15(12)	C19-P1-C11	101.50(16)	C19-P1-C13	105.05(17)
C1-P2-Pd1	114.97(13)	C1-P2-C25	104.07(18)	C1-P2-C31	104.94(16)

C25-P2-Pd1	114.12(12)	C25-P2-C31	106.01(19)	C31-P2-Pd1	111.82(13)
P2-C1-Fe1	134.9(2)	C2-C1-Fe1	69.3(2)	C2-C1-P2	123.5(3)
C5-C1-Fe1	68.8(2)	C5-C1-P2	128.0(3)	C5-C1-C2	107.8(3)
C1-C2-Fe1	69.8(2)	C1-C2-C11	125.6(3)	C3-C2-Fe1	68.9(2)
C3-C2-C1	107.1(3)	C3-C2-C11	127.2(3)	C11-C2-Fe1	128.3(3)
C2-C3-Fe1	70.2(2)	C4-C3-Fe1	70.0(2)	C4-C3-C2	108.7(4)
C3-C4-Fe1	69.4(2)	C3-C4-C5	108.4(3)	C5-C4-Fe1	69.5(2)
C1-C5-Fe1	70.3(2)	C4-C5-Fe1	69.9(2)	C4-C5-C1	107.9(4)
C7-C6-Fe1	69.6(2)	C7-C6-C10	108.4(4)	C10-C6-Fe1	69.7(2)
C6-C7-Fe1	70.3(2)	C6-C7-C8	108.2(4)	C8-C7-Fe1	69.6(2)
C7-C8-Fe1	70.0(2)	C7-C8-C9	108.1(4)	C9-C8-Fe1	69.6(2)
C8-C9-Fe1	69.6(2)	C10-C9-Fe1	70.0(2)	C10-C9-C8	107.2(4)
C6-C10-Fe1	70.2(2)	C6-C10-C9	108.1(4)	C9-C10-Fe1	69.4(3)
C2-C11-P1	109.0(2)	C2-C11-C12	112.8(3)	C12-C11-P1	117.1(3)
C14-C13-P1	116.4(3)	C14-C13-C18	110.7(3)	C18-C13-P1	113.1(3)
C13-C14-C15	111.4(3)	C16-C15-C14	111.0(4)	C15-C16-C17	111.4(3)
C18-C17-C16	110.9(3)	C17-C18-C13	111.0(3)	C20-C19-P1	109.0(3)
C20-C19-C24	110.5(3)	C24-C19-P1	115.8(2)	C21-C20-C19	110.6(3)
C20-C21-C22	110.5(3)	C21-C22-C23	111.4(3)	C24-C23-C22	112.5(4)
C23-C24-C19	110.1(3)	C26-C25-P2	119.4(3)	C30-C25-P2	121.3(3)
C30-C25-C26	118.9(4)	C27-C26-C25	119.7(4)	C28-C27-C26	120.9(4)
C29-C28-C27	119.7(4)	C28-C29-C30	120.3(4)	C25-C30-C29	120.4(4)
C32-C31-P2	121.8(3)	C32-C31-C36	119.0(4)	C36-C31-P2	118.9(3)
C31-C32-C33	121.1(4)	C34-C33-C32	119.8(4)	C35-C34-C33	119.9(4)
C34-C35-C36	120.4(4)	C31-C36-C35	119.5(4)	C38-C37-Pd1	123.5(3)

C38-C37-C42	116.6(4)	C42-C37-Pd1	119.8(3)	C37-C38-C39	123.3(5)
C38-C39-C40	118.6(5)	C39-C40-C43	119.4(4)	C41-C40-C39	119.8(4)
C41-C40-C43	120.8(4)	C42-C41-C40	120.0(4)	C41-C42-C37	121.7(4)
F1-C43-F2*	131.9(19)	F1-C43-F3	104.5(4)	F1-C43-C40	113.0(4)
F1*-C43-F1	50(2)	F1*-C43-F2	61(2)	F1*-C43-F2*	103(3)
F1*-C43-F3	137(2)	F1*-C43-F3*	115(3)	F1*-C43-C40	109(2)
F2-C43-F1	105.3(4)	F2-C43-F2*	44(2)	F2-C43-F3	106.8(4)
F2-C43-C40	113.4(4)	F2*-C43-C40	114(2)	F3-C43-F2*	67(2)
F3-C43-C40	113.0(4)	F3*-C43-F1	68(2)	F3*-C43-F2	136(2)
F3*-C43-F2*	107(3)	F3*-C43-F3	42(2)	F3*-C43-C40	108.4(19)

This report has been created with Olex2 [6], compiled on 2021.08.20 svn.r13c46975 for OlexSys.